

**Synthesis of Tubular and Belt-like aromatics having
Anthracene units**



Dissertation

**Zur Erlangung des Doktorgrades der
Mathematisch-Naturwissenschaftlichen Fakultät der
Christian-Albrechts-Universität zu Kiel**

Vorgelegt von

Ali Reza Mohebbi

geboren in Amol, Iran

Kiel 2009

1. Referent: Prof. Dr. Rainer Herges

2. Koreferent: Prof. Dr. Thisbe K. Lindhorst

Eingereicht am: 17. December 2008

Tag der mündliche Prüfung (Disputation) : 03. February 2009

To best mine:

My dear wife; Sareh

My dear parents

ACKNOWLEDGEMENT

It was my privilege to work under the guidance of **Prof. Dr. Rainer Herges**, an eminent teacher and an excellent human being for my thesis work. I owe a great debt of gratitude for his indispensable guidance, kind cooperation, persistent encouragement and timely advice through out my thesis.

I express sincere thanks to all of colleagues in the lab, Claudia Bornholdt, Catrin Goeschen, Dr. Anke Krüger, Regina Meinschmidt, Eva Mucke, Hannelore Pohl, Jan Bornhöft, Dr. Bengt Buchhein-Stehn, Dr Felix Köhler, Jens Kubitschke, Venkataramana Rajuri, Jens Walther, Dr. Torsten Winkler, Dr. Jan Siegwarth, Hanno Sell, Gaston Schaller, Benjamin Sahlmann, Thore Wendler, Marscha Ried, Dr. Umasish Jana, Anika Gehl, and Steffen Thies who were friendly and helpful during my thesis project work.

I specially thank Gaston Schaller, Dr. Torsten Winkler, Dr. Felix Köhler and Dr. Umasish Jana for helping me in completion of my thesis.

I thank institute members of analytical department for measuring NMR and mass spectra.

I specially thank Dr. Christian Näther for X-ray crystallographic analysis.

Finally, I would like to thank my wife Sareh M. Nasser and my family for their constant encouragement and support through my academic training.

Die vorliegende Arbeit wurde auf Anregung und unter Anleitung von

Herrn Prof. Dr. Rainer Herges

am Otto-Diels-Institut für Organische Chemie

der Christian-Albrechts-Universität zu Kiel

im Zeitraum von

February 2005 bis December 2008

angefetigt.

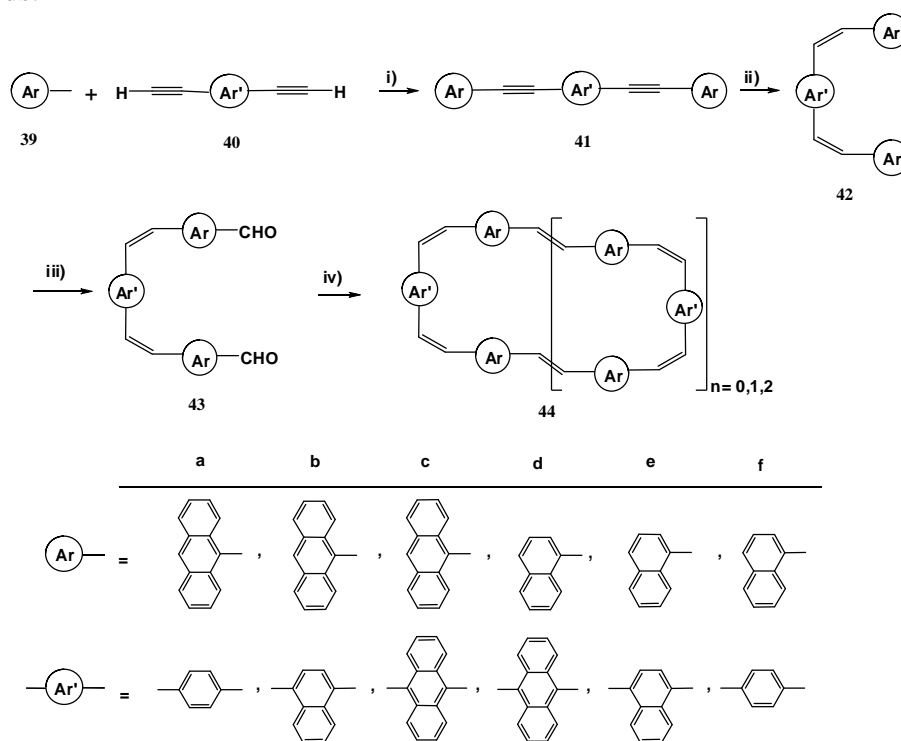
Eidesstattliche Erklärung

Hiermit erkläre ich an Eidesstatt, dass die Vorliegende Dissertation – abgesehen von der wissenschaftlichen Beratung meines Doktorvaters, Prof. Dr. R. Herges- nach Inhalt und Form die eigene Arbeit ist. Ich habe bislang noch keinen Promotionsversuch unternommen.

Ali Reza Mohebbi

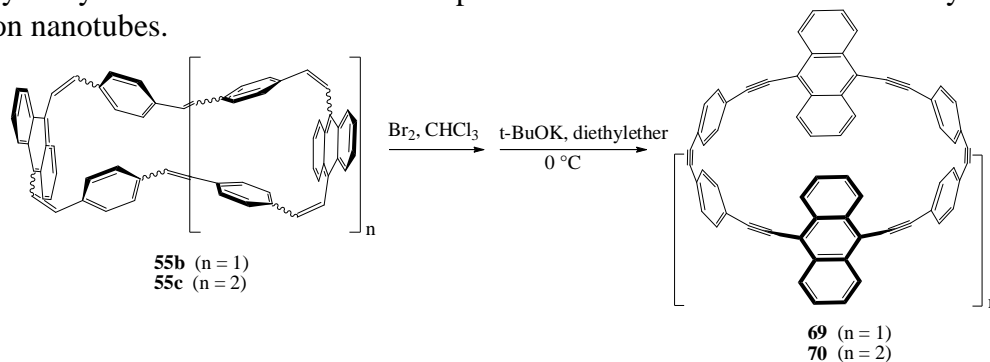
Abstract

The work presented in this thesis was aimed at developing a new strategy to prepare conjugated molecular belts with possible applications as precursors in rational carbon nanotube syntheses. Using the reaction scheme below, the range of the accessible belt oligoarylacetylenes was increased by the introduction of anthracene units. As a first step towards this goal, it was essential to develop and optimize a new synthetic route to cyclic *para*-anthrylethylenes **44**, which in turn can be used as precursors for belt-like aromatic compounds.



Multi-step synthesis of anthracenophanes; reagents and conditions: i) Pd(PPh₃)₂Cl₂, CuI, diisopropylamine; ii) H₂, Pd/C ethylacetate; iii) SnCl₄, Cl₂CHOCH₃, CH₂Cl₂; iv) TiCl₄/Zn, DME, toluene.

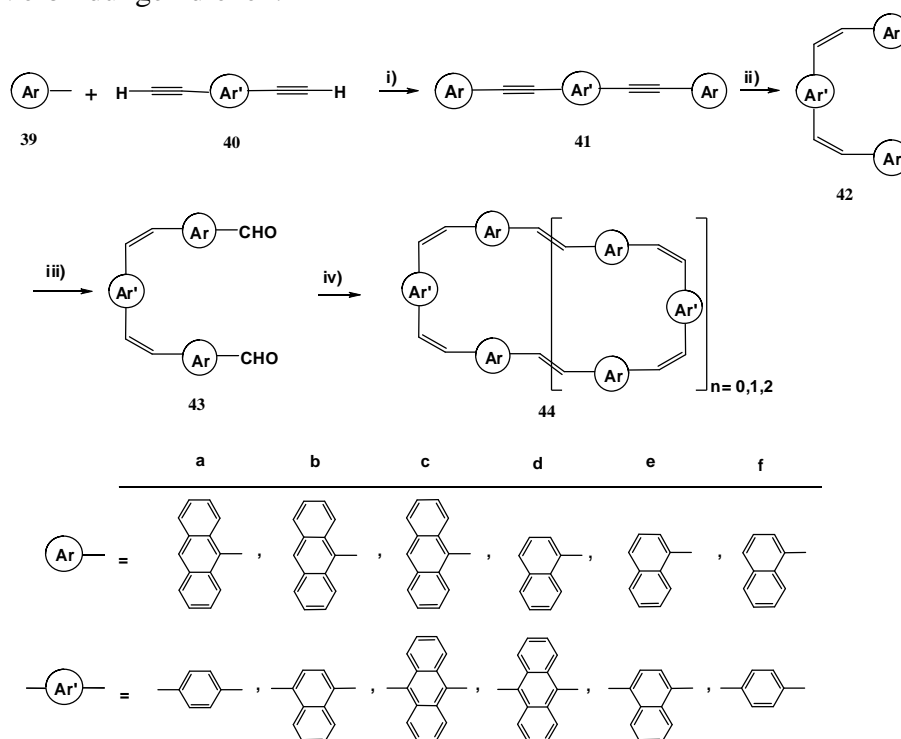
The halogenation and dehydrohalogenation reactions of the corresponding anthracenophanes as a simple and efficient access to belt-shaped aromatic molecules were extensively investigated. The products of these reactions like cyclic [6] and [9]-*para*-anthrylacetylene **69** and **70** could be important intermediates in the rational synthesis of carbon nanotubes.



Synthesis of CPAA's **69** and **70** by bromination and dehydrobromination reactions.

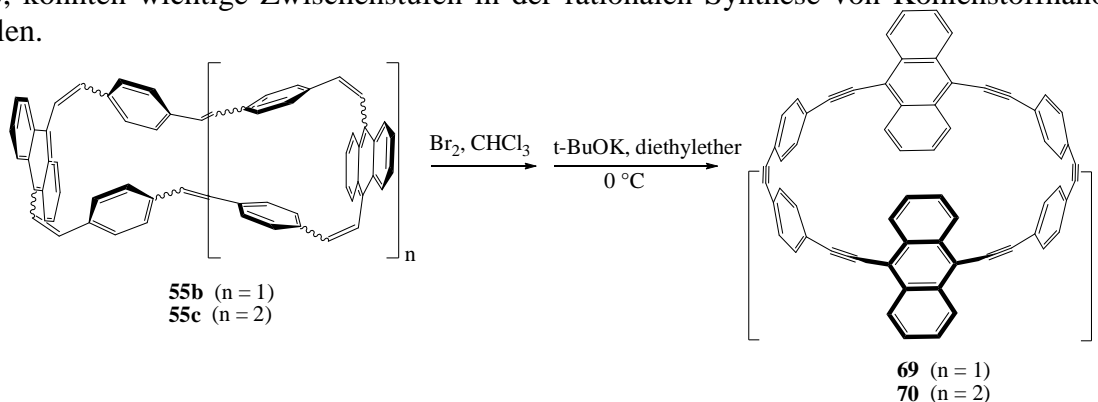
Kurzzusammenfassung

Die vorliegende Arbeit hatte die Entwicklung neuer Strategien zur Darstellung konjugierter molekularer Bänder als Vorstufen in der rationalen Synthese von Kohlenstoffnanoröhren zum Ziel. Unter Verwendung des unten dargestellten Syntheseschemas wurde das Spektrum der zugänglichen Oligoarylacetylene durch die Einführung von Anthraceneinheiten erweitert. Einen wichtigen ersten Schritt in Richtung dieses Ziels stellt die Entwicklung und Optimierung der Synthese von zyklischen *para*-Anthrylethylenen **44** dar, welche ihrerseits als Vorstufen der gürtelartigen aromatischen Verbindungen dienen.



Mehrstufigensynthese der Anthracenophane; Reagenzien und Bedingungen: i) Pd(PPh₃)₂Cl₂, CuI, Diisopropylamin; ii) H₂, Pd/C, Ethylacetat; iii) SnCl₄, Cl₂CHOCH₃, CH₂Cl₂; iv) TiCl₄/Zn, DME, Toluol.

Die Halogenierungs- und Dehalogenierungsreaktionen der entsprechenden Anthracenophane als einfacher und effizienter Zugang zu gürtelförmigen aromatischen Verbindungen wurde ausführlich untersucht. Die Produkte dieser Reaktionen, z.B. zyklisches [6] und [9]-*para*-Anthrylacetylen **69** und **70**, könnten wichtige Zwischenstufen in der rationalen Synthese von Kohlenstoffnanoröhren darstellen.



Synthese von CPAA's **69** und **70** durch Bromierung und Dehydrobromierung.

Contents

Chapter 1: General introduction

1.1. General Purpose of the present study	1
1.2. Recent synthesis challenges toward fully conjugated beltene (Belt-Like and Tubular Aromatics)	3
1.2.1. Introduction	3
1.2.2. Cyclacenes	4
1.2.3. Benzoannulenes	5
1.2.4. Picotubes	6
1.2.5. Cyclic[<i>n</i>]- <i>para</i> -phenylacetylenes.....	7
1.3. Our approach toward synthesis of [<i>n</i>]- <i>para</i> -arylacetylenes	9
1.3.1. Synthesis of [<i>n</i>]- <i>para</i> arylethene	10
1.3.1.1. The Wittig reaction	11
1.3.1.2. The McMurry reaction	12
1.3.2. Bromination and dehydrobromination of cyclophanes	13
1.3.2.1 Degradation of 1,2-dihydrazone system	13
1.3.2.2. Rearrangement reaction	13
1.3.2.3. Cycloelimination reactions	14
1.3.2.4. Ring closure reactions of system containing triple bonds	15
1.3.2.5. Dehydrohalogenation reaction	15
1.4. The target molecules of the present work	16
1.4.1. Cyclic [<i>n</i>]- <i>para</i> -arylethylene	17
1.4.2. Cyclic[<i>n</i>]- <i>para</i> -arylacetylene	18

Chapter 2: Synthesis of anthracenophanes

2.1. Synthesis of cyclic [<i>n</i>]- <i>para</i> -antherylethylene	23
2.1.1. Synthesis of <i>cis</i> -1,2-bis (9-anthryl) ethylene	23
2.1.2. Synthesis of <i>cis</i> -1,2-Bis[10-formyl(9-antheryl)]ethene	26
2.1.2.1. Method (a)	27
2.1.2.2. Methods (b,c)	27
2.1.3. Synthesis of cyclic [<i>n</i>]- <i>para</i> -antrylethylenes	28
2.2. New strategy to synthesis of cyclic [<i>n</i>]- <i>para</i> -anthrylethylenes	31
2.2.1. Synthesis of arylene-ethynylene 41 (a, b, c, d, e, f)	33
2.2.2. Synthesis of arylene-ethenylene by hydrogenation reaction	35
2.2.3. Synthesis of dialdehyde ethenylarenes 43 (a,b,c,d,e,f)	41
2.2.4. Synthesis and properties of cyclophanes 55a, 55b and 55c	43
2.2.4.1. Synthesis	43
2.2.4.2. The effects of concentration	44
2.2.4.3. solvents effects	44
2.2.4.4. Physical properties	45
2.2.4.5. NMR spectra	46
2.2.4.6. UV-Vis spectra	49
2.2.4.7. X-ray analysis of 55a	50
2.2.5. Synthesis and properties of cyclophanes 56b and 56c	54
2.2.5.1 Synthesis	54
2.2.5.2. Physical properties	55
2.2.5.3. NMR spectra	56

2.2.5.4. X-ray analysis of 56b	58
2.2.6. Synthesis and properties of cyclophanes 57a-a , 57b and 57c	59
2.2.6.1 Synthesis	59
2.2.6.2. Physical property	61
2.2.6.3. NMR spectra	63
2.2.6.4. UV-Vis spectra	66
2.2.6.5. X-ray analysis	67
2.2.7. Synthesis and properties of cyclophanes 58b , 58c	69
2.2.7.1. Synthesis	69
2.2.7.2. Physical properties	72
2.2.7.3. NMR spectra	73
2.2.7.4. UV-Vis spectra	74
2.2.8. Anisotropy of current induced density (ACID).....	75
2.2.9. Nucleus independent chemical shift (NICS)	76
2.2.10. Conclusion	77

Chapter 3: The belt-shaped conjugated systems

3.1. Synthesis of cyclic [6]- <i>para</i> -anthrylacetylene: [6]-CPAA	79
3.1.1. Introduction	79
3.1.2. Recent synthesis challenges toward strained cycloalkynes	80
3.1.2.1. Synthesis of [2.2]-tolanophane 60	80
3.1.2.2. Synthesis of [2.4]- <i>meta</i> -cyclophantetrayne 62	82
3.1.2.3. Synthesis of [6]-CPA's 65 and 66 ; and [6]-CPNA's 68	82
3.1.3. Synthesis of cyclic [6] and [9]- <i>para</i> -anthrylacetylene 69 and 70	83

3.1.3.1. Physical properties	84
3.1.3.2. NMR data.....	87
3.1.3.3. UV-Vis and fluorescence spectra.....	89
3.1.3.4. Anisotropy of current induced density (ACID)	91
3.1.4. Synthesis of cyclic [6]- <i>para</i> -anthrylacetylene 72a	92
3.1.4.1. Physical properties	95
3.1.4.2. UV-Vis spectra	95
3.1.5. Conclusion	96
Chapter 4: Summary	98
Chapter 5: Experimental	102
5.1. Apparatus	102
5.2. Common procedure	103
5.3. Synthesis	104
5.3.1. Synthesis of pentachlorocyclopropane	104
5.3.2. Synthesis of tetrachlorocyclopropene	104
5.3.3. Synthesis of 2,3-bis-9-anthrylcyclopropanone 29	104
5.3.4. Synthesis of 1,2- di-9-anthrylacetylen 30	105
5.3.5. Synthesis of 1,4-dibromonaphthalene	105
5.3.6. Synthesis of 9, 10-dibromoanthracene	106
5.3.7. Synthesis of 9-bromoanthracene	106
5.3.8. Synthesis of 1,4-diiodonaphthalene	107
5.3.9. Synthesis of 9,10-diiodoanthracene	107
5.3.10. Synthesis of 1-iodonaphthalene	108

5.3.11. Synthesis of 9-iodoanthracene	108
5.3.12. Synthesis of 1,4-bis(trimethylsilylethynyl)naphthalene	109
5.3.13. Synthesis of 1,4-bis(ethynyl)naphthalene	109
5.3.14. Synthesis of 9,10-bis(trimethylsilylethynyl)anthracene	110
5.3.15. Synthesis of 9,10-bis(ethynyl)anthracene	110
5.3.16. General procedure for the Sonogashira coupling	110
5.3.17. Synthesis of 1,4-bis(9-ethynylantraceny)benzene 41a	111
5.3.18. Synthesis of 1,4-bis(9-ethynylantraceny)naphthalene 41b	111
5.3.19. Synthesis of 9,10-bis(9-ethynylantraceny)anthracene 41c	112
5.3.20. Synthesis of 9,10-bis(1-ethynyl-naphthyl)anthracene 41d	112
5.3.21. Synthesis of 1,4-bis(1-ethynyl-naphthaleny)naphthalene 41e	113
5.3.22. Synthesis of 1,4-bis(1-ethynyl-naphthaleny)benzene 41f	113
5.3.23. Synthesis of 9,10-bis[(1-ethynyl-4-bromo)phenyl]dihydroanthracene-9,10-diol 48a ..	114
5.3.24. Synthesis of 9,10-bis[(1-ethynyl-4-bromo)phenyl]anthracene 48b	114
5.3.25. General procedure for the Hydrogenation reaction	115
5.3.26. Synthesis of (Z)-1,2-di(9-anthryl)ethenes 27	115
5.3.27. Synthesis of (Z,Z)-9,10-bis(4-bromo-styryl)anthracene 50	116
5.3.28. Synthesis of (Z,Z)-1,4-bis(9-ethenyl-antheraceny)benzene 42a	116
5.3.29. Synthesis of (Z,Z)-1,4-bis(9-ethenyl-anthraceny)naphthalene 42b	117
5.3.30. Synthesis of (Z,Z)-9,10-bis(9-ethenyl-anthraceny)anthracene 42c	117
5.3.31. Synthesis of (Z,Z)-9,10-bis(1-ethenyl-naphthyl)anthracene 42d	118
5.3.32. Synthesis of (Z,Z)-1,4-bis(1-ethenyl-naphthyl)naphthalene 42e	118
5.3.33. Synthesis of (Z,Z)-1,4-bis(1-ethenyl-naphthyl)benzene 41f	119

5.3.34. Synthesis of (Z, Z)-9, 10-bis (4-formyl-styryl)anthracene 52	119
5.3.35. General procedure for the formylation reaction	120
5.3.36. Spectral data for (Z)-1,2-bis(10-formyl-9-anthracenyl)ethene 31	120
5.3.37. Spectral data for (Z,Z)-1,4-bis[(9-ethenyl-10-formyl)anthracenyl]benzene 43a	120
5.3.38. Spectral data for (Z,Z)-1,4-bis[(9-ethenyl-10-formyl)anthracenyl]naphthalene 43b ..	121
5.3.39. Spectral data for (Z,Z)-9,10-bis[(9-ethenyl-10-formyl)anthracenyl]anthracene 43c ...	121
5.3.40. Spectral data for (Z,Z)-1,4-bis[(1-ethenyl-4-formyl)naphthyl]naphthalene 43e	121
5.3.41. Spectral data for (Z,Z)-1,4-bis[(1-ethenyl-4-formyl)naphthyl]benzene 43f	121
5.3.42. General procedure for the McMurry coupling	122
5.3.43. Spectral data for compound 38	122
5.3.44. Spectral data for compound 37	122
5.3.45. Spectral data for compound 55a	122
5.3.46. Spectral data for compound 55b	123
5.3.47. Spectral data for compound 55c	123
5.3.48. Spectral data for compound 56b	123
5.3.49. Spectral data for compound 56c	124
5.3.50. Spectral data for compound 56a-b	124
5.3.51. Spectral data for compound 57a-a	124
5.3.52. Spectral data for compound 57b	125
5.3.53. Spectral data for compound 57c	125
5.3.54. Spectral data for compound 57a-b	125
5.3.55. Spectral data for compound 58a-b	125
5.3.56. Spectral data for compound 58b	125

5.3.57. Spectral data for compound 58c	126
5.3.58. General procedure for bromination and dehydrobromination of 55b , 55c and 56b	126
5.3.59. Spectral data for compound 69	126
5.3.60. Spectral data for compound 70	127
5.3.61. Spectral data for compound 72a	127
5.4. Supplementary data	128
5.4.1. Appendix A: X-ray crystallography data of 55a	128
5.4.2. Appendix B: X-ray crystallography data of 57a-a	138
5.4.3. Appendix C: X-ray crystallography data of 55b	151
5.4.4. Appendix C: X-ray crystallography data of 56b	158
6. References	196

Chapter 1: General introduction

1.1. General Purpose of the present study

Tubular aromatic compounds namely carbon nanotubes are generally considered to be key structures in nanotechnology. A number of applications already have been realized (molecular transistors and logic gates,^[1] molecular wires,^[2] tips of AFM and STM microscopes,^[3] molecular flow meters,^[4] flat panel displays.^[5] These compounds are currently only accessible via physical methods e.g. chemical vapor deposition (CVD),^[6] pulsed laser vaporization (PLV),^[7] and arc discharge^[8] under very high temperatures which is not suitable for producing large quantities. Under the drastic conditions, the reactions are uncontrolled and produce a variety of nanotubes which are typically very difficult to separate. With this problem in mind and considering the importance of the synthesis of single-walled carbon nanotubes with specific diameter a rational chemical synthesis to prepare the conjugated molecular belts as precursors in carbon nanotube syntheses would be important. These belt-like compounds because of highly strained curved aromatic structure^[9] and having the same overall cyclic shape could be suitable templates for this purpose.^[10]

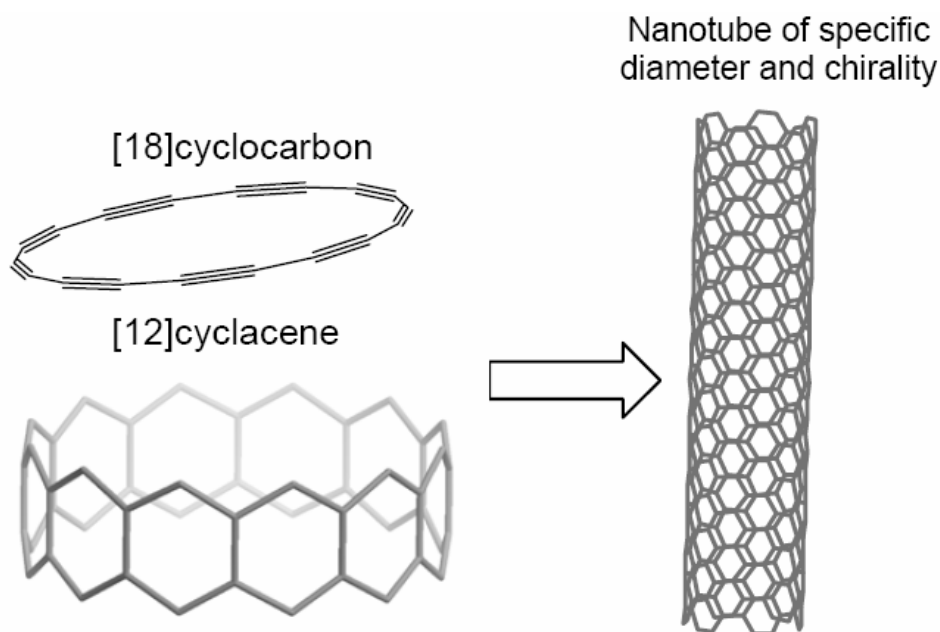


Figure 1-1. Conjugated molecular belts as precursors in carbon nanotube synthesis.

The discovery of fullerenes^[11] in 1985 and related carbon nanotubes^[12] by Iijima in 1991 has prompted a flurry of activity directed toward the synthesis and study of curved, fully conjugated π -systems. In a similar regard, there have been numerous attempts to prepare related belt-like molecules^[13] possessing conjugated π -electron circuits. Various belt- and hoop-shaped compounds, including cyclic[n]carbon,^[14,15] cyclacenes,^[16] cyclic oligoparaphenylenes,^[17] cyclophynes,^[18] ortho-cyclophanes^[19] have been reported. These strained molecules are interesting not only from the synthetic and theoretical point of view, but also as host molecules having well-defined π -electron cavities^[20]. Moreover, strained molecules have always been of special interest in organic chemistry because of their enhanced reactivity and their unusual physical and spectroscopic properties. The only successful preparation of fully conjugated, belt-like compounds has been reported by Herges, Darabi and Gleiter separately. Oda and Darabi^[21] produced cyclic *para*-phenylacetylenes containing six to nine subunits. Herges et al.^[22] isolated a picotube based on four anthracene units. Gleiter^[23] synthesized [6.8]₃cyclacene which is the first double stranded molecular belt.

In this project, the chemical synthesis of buckbelts like **1** with various diameter sizes is the main goal.

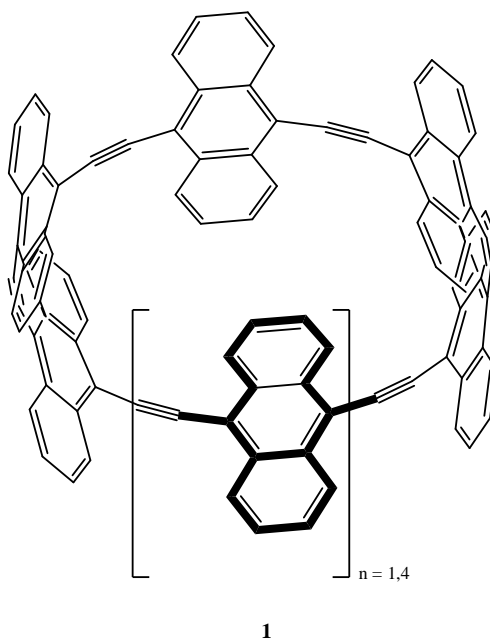


Figure 1-2. Structure of cyclic [6]-*para*-anthrylacetylene, [6]-CPAA.

1.2. Recent synthesis challenges toward fully conjugated beltenees (belt-like and tubular aromatics).

1.2.1. Introduction

Organic π -conjugated systems have become increasingly popular as active materials in optoelectronic devices such as light-emitting diodes,^[24] field-effect transistors^[25] and solar cells.^[26] These, belt-shaped conjugated systems are interesting as attractive synthetic targets because of their architectural beauty and potential applications. The cylindrical cavities of these molecular belts are predicted to act as molecular hosts to cylindrical molecular guests of the diameter of acetylene and fullerenes.^[27] They have also become the subject of recent interest, because they are subunits of carbon nanotubes. The p-orbitals in belt-like aromatics are perpendicular to the surface of a cylinder, in such a way that the inner part of the p-orbitals point towards the axis of the tube. While in classical aromatic systems these orbitals are perpendicular with respect to the ring plane.^[28]

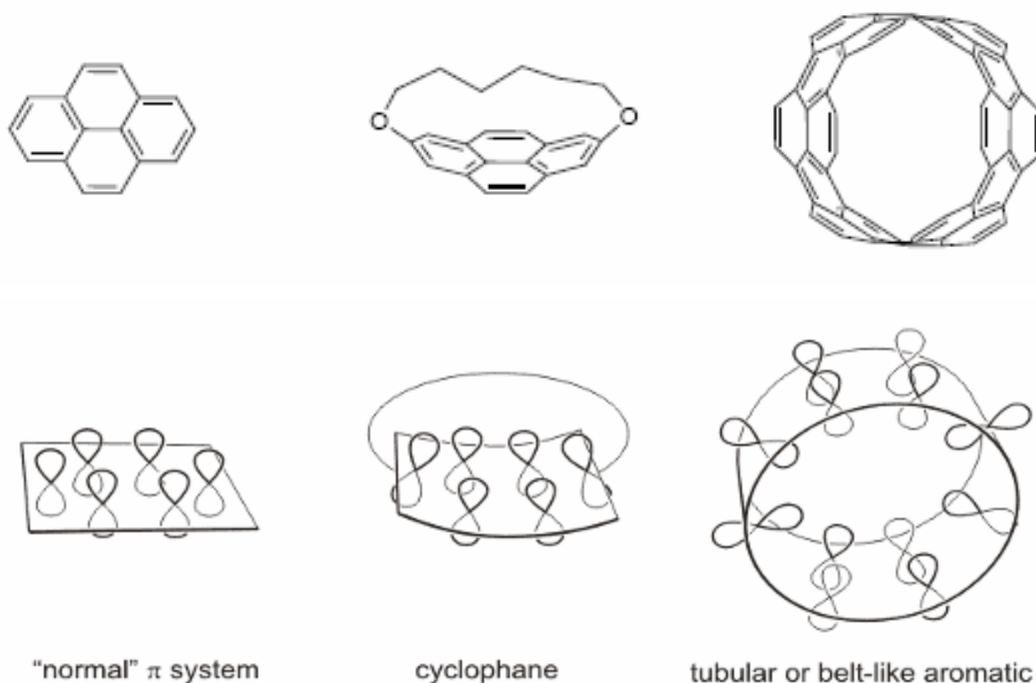


Figure 1-3. The representation of p-orbitals in normal aromatics, cyclophanes and belt-like conjugated systems (Vögtle belt).^[29, 30]

The angle between the p-orbitals and σ -bonds in sp^2 hybridized carbon is 90° but this angle is larger than 90° in a curved system.^[31]

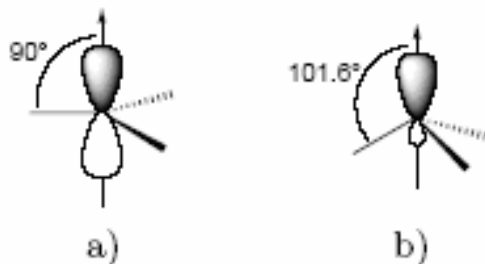
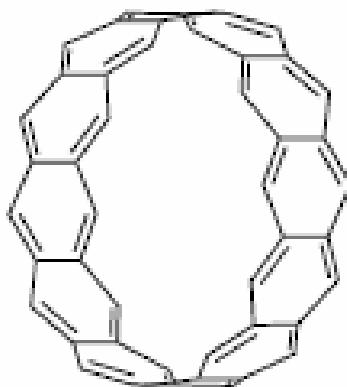


Figure 1-4. Pyramidalization angle θ_p for a) sp^2 -hybridized carbon and b) a nonplanar sp^2 -hybridized carbon in C_{60} fullerene ($\theta_p=11.6^\circ$).

1.2.2. Cyclacenes

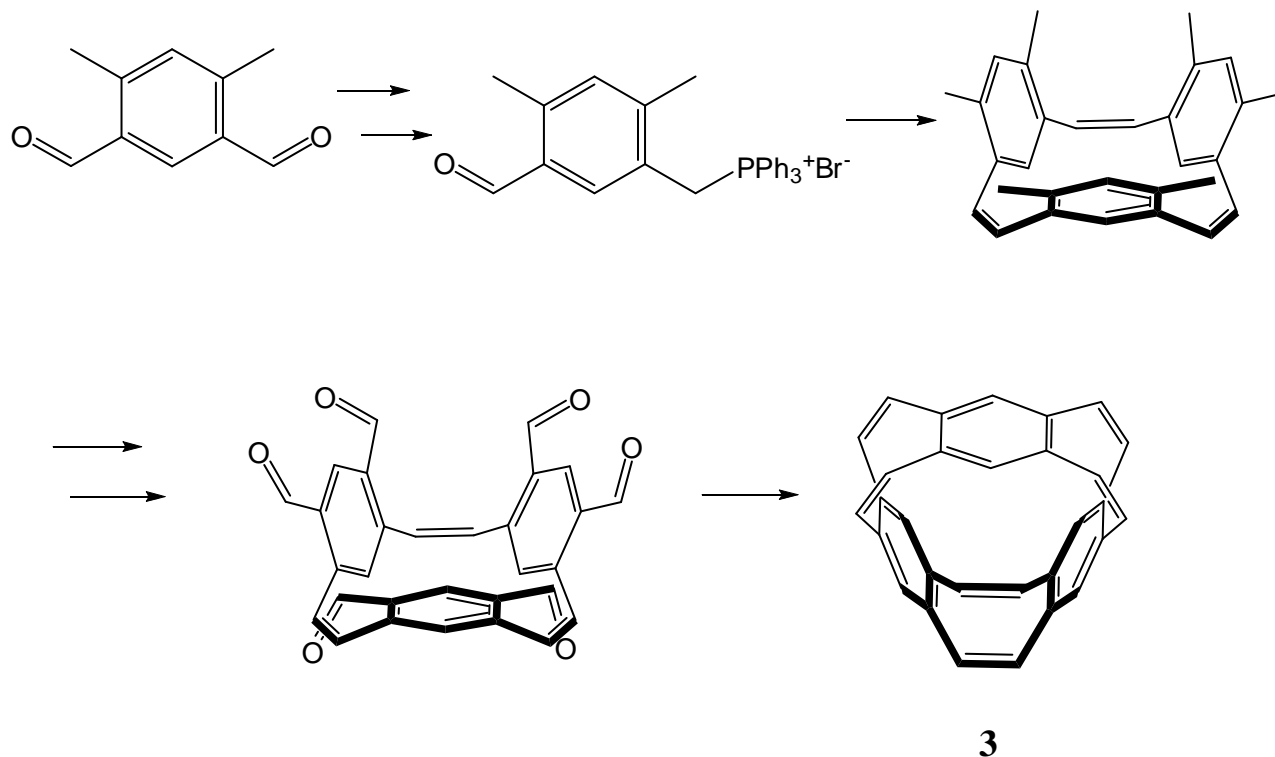
In 1987, Stoddart and et al.^[32, 33] proposed the synthesis of **2** as a major synthetic target for conjugated molecular belts. But unfortunately, synthesis of the desired cyclacene was not achieved. These fully hoop-shaped cyclophanes are of interest with respect to their conjugation, their spectroscopic properties, and their cavities. They are also ideal carbon nanotube precursors, because they are the repeating units found in a zigzag carbon nanotubes.



2

Figure 1-5. Structure of [12]cyclacene.

In another attempt in 2008, Gleiter and et al.^[23] developed a new synthesis strategy for [6.8]₃cyclacene **3** as the first pure hydrocarbon cyclacene by stepwise synthesis. It is the smallest and most strained member of the [6.8]_n series which consisted of annelated six- and eight-membered rings.

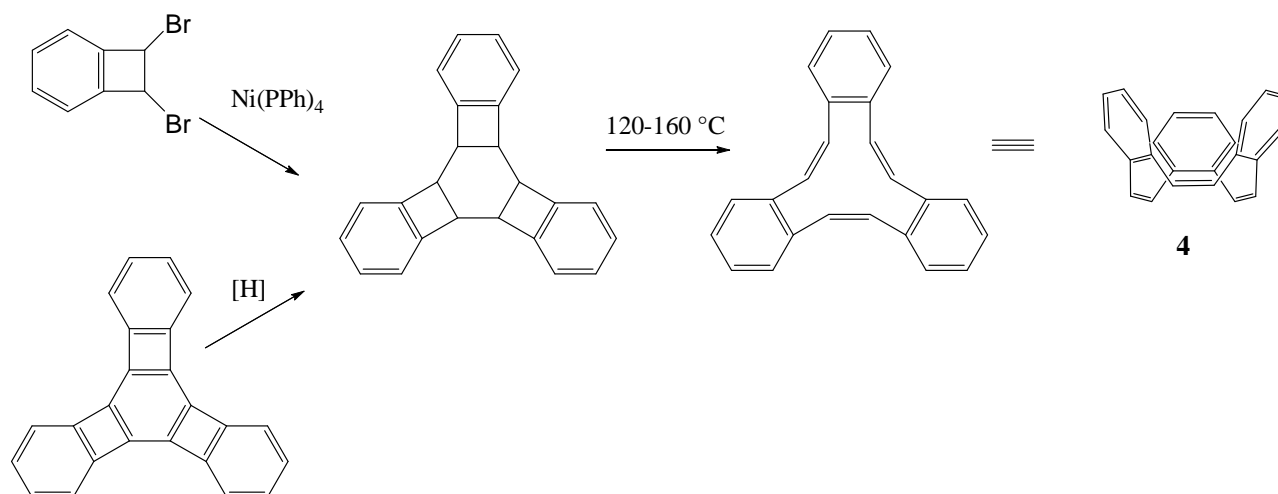


Scheme 1-1. Synthesis strategy of [6.8]₃cyclacene.

1.2.3. Benzoannulenes

Another challenging molecule among fully conjugated belts is all-*Z*-tribenzo[12]-annulene **4** which was synthesized by Lyodo^[34] and Vollhardt.^[35] They applied two different strategies, Nickel-catalyzed cyclization and selective hydrogenation, for producing an intermediate compound and finally by using [2+2+2] cycloreversion they obtained the target molecule. Also, higher rings sizes of benzoannulene with all-*Z*-configuration were synthesized by same group.^[36] Molecular models

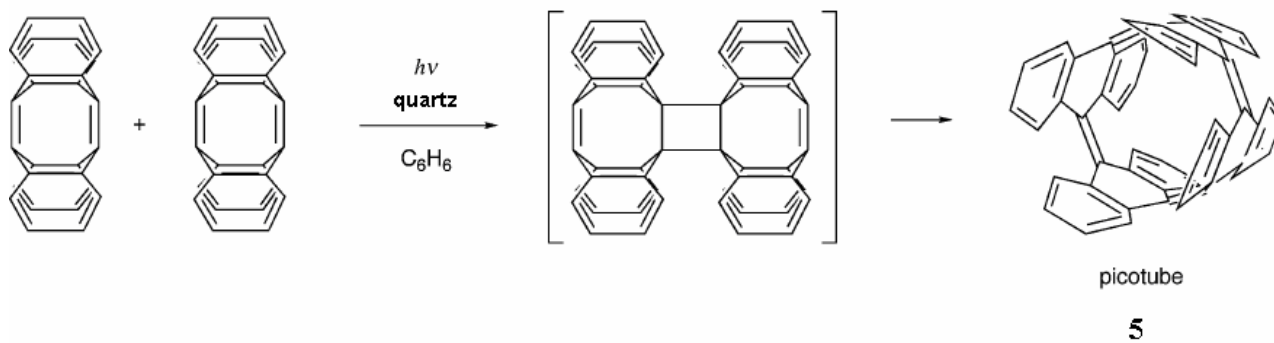
showed a crow-like, rigid structure involving well-defined cavities for complexation with metals.^[37]



Scheme 1-2. Synthesis of *all-Z*-tribenzo[12]annulene.

1.2.4. Picotubes

In another strategy, Herges et al.^[22] synthesized picotube **5** by metathesis reaction of tetrahydrodianthracene (TDDA). Their approach followed a ring-expansion metathesis strategy in which two small belts combine to form larger belts (Scheme 1-3). The so called “picotubes” are small and short substructures of the larger carbon nanotubes. Similarly, Kammermeierphane **6**^[38] was synthesized as a fully conjugated tubular compound (Scheme 1-4).



Scheme 1-3. Synthesis of picotube.

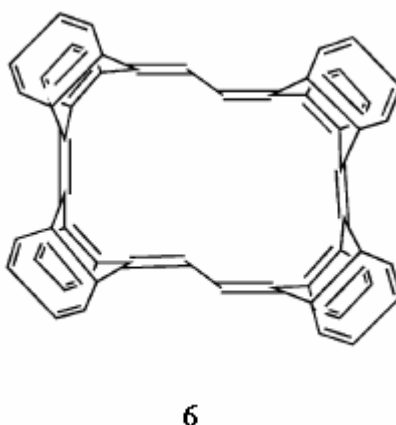
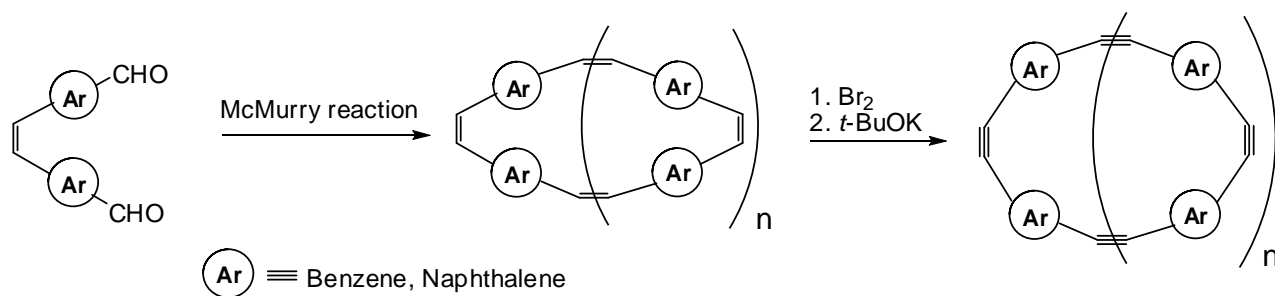


Figure 1-6. Structure of Kammermeierphane.

1.2.5. Cyclic[*n*]-*para*-phenylacetylenes

Kawase et al.^[21, 39] introduced a new strategy for the synthesis of some fully conjugated nanorings (**7** and **8**) with different ring sizes. These compounds were prepared using McMurry coupling, bromination and dehydrobromination of corresponding precursors.



Scheme 1-4. Oda, Kawase, Darabi strategy to synthesize cyclic $[n]$ -*para*-arylacetylene.

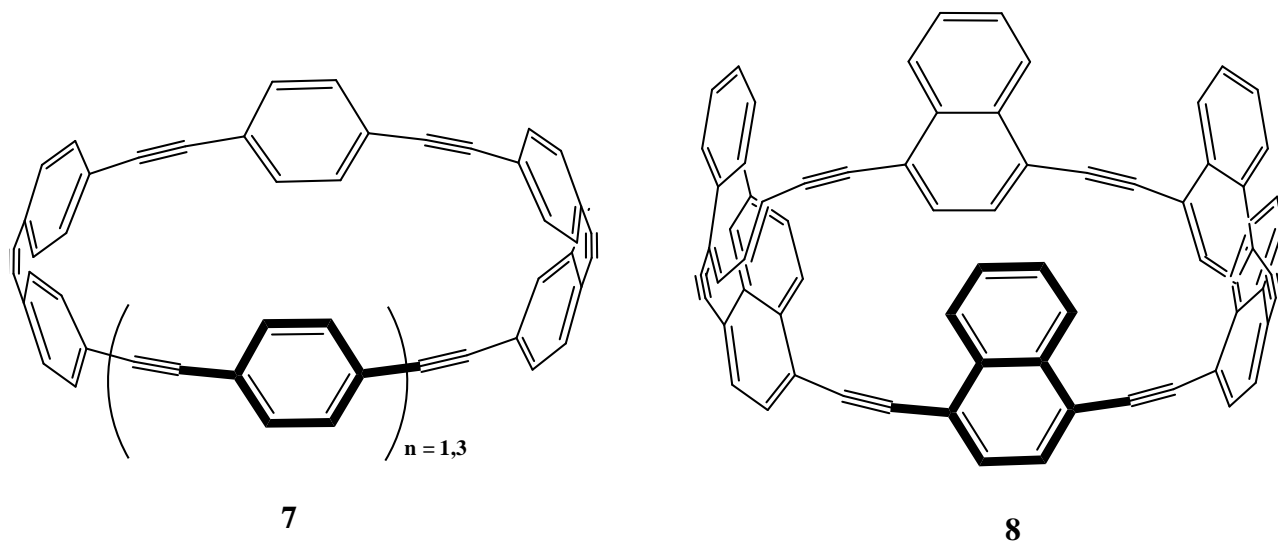


Figure 1-7. Structures of $[n]$ -CPPA **7** and $[n]$ -CPNA **8**.

These molecules have smooth belt-like structures and some of them contain a suitable cavity for inclusion of C_{60} .

They also reported the formation of the ring-in-ring compound **9** and the double-inclusion structure **10** (onion-type) which are complexes between two different sizes of nanorings and fullerene.^[40]

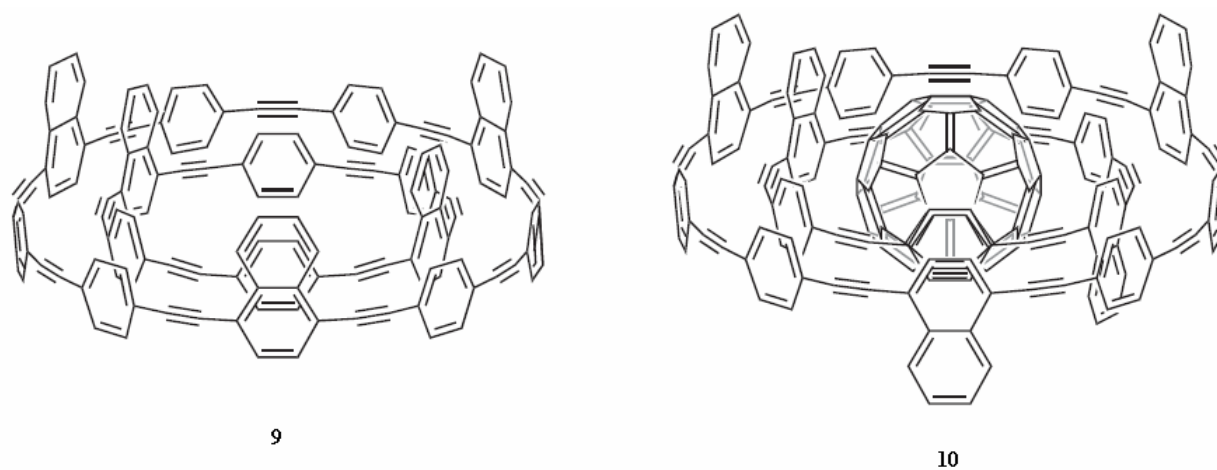


Figure 1-8. A ring-ring complex (9) and an onion-type complex (10).

A concave-convex π - π interaction is supposed in the formation of these complexes.

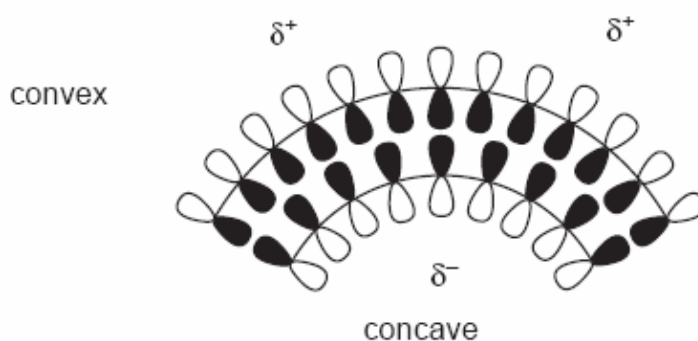


Figure 1-9. Schematic presentation of concave-convex π - π interactions.^[40]

1.3. Our approach toward the synthesis of $[n]$ -*para*-arylacetylene

Respect to the importance of these cyclophanes as the precursor for the belt-like aromatics, we tried to extend the width of the belt in cyclic oligoarylacetylene by introducing anthracene units.

The synthesis of these nanorings can be divided into two steps: 1. Synthesis of $[n]$ -*para*-arylethylene. 2. Synthesis of $[n]$ -*para*-arylacetylene.

1.3.1. Synthesis of $[n]$ -*para*-arylethylene

In general, there are several methods to synthesize 1,2-arylethylene as the main part of the cyclophanes. Figure 10 summarizes four methods for preparing carbon-carbon double bonds. Among these methods, we applied two the most reported methods to build our target molecules: the Wittig reaction and the McMurry coupling.

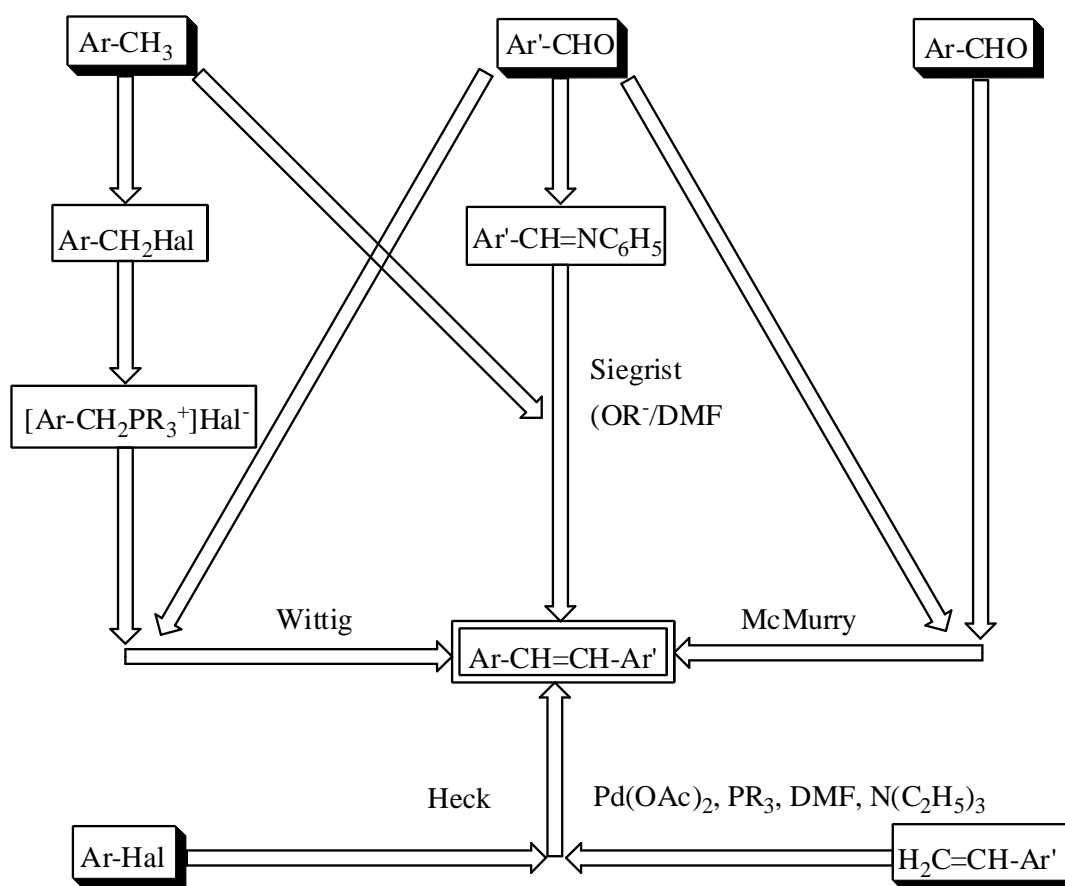
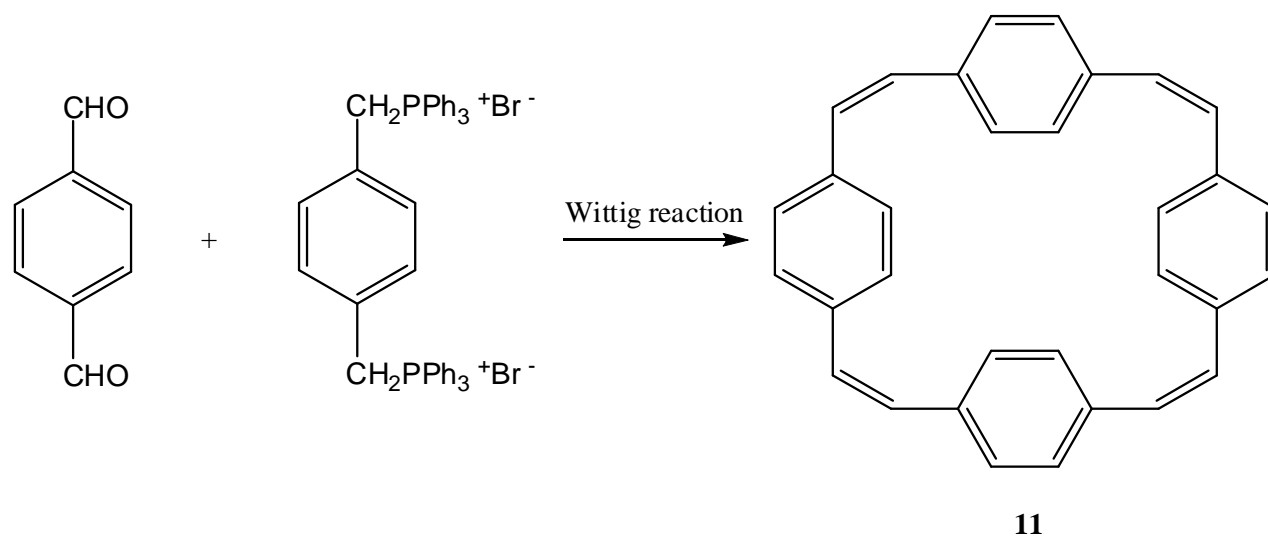


Figure 1-10. The most important synthetic routes to stilbenoid compounds.^[41] Hal=halogen.

1.3.1.1. The Wittig reaction

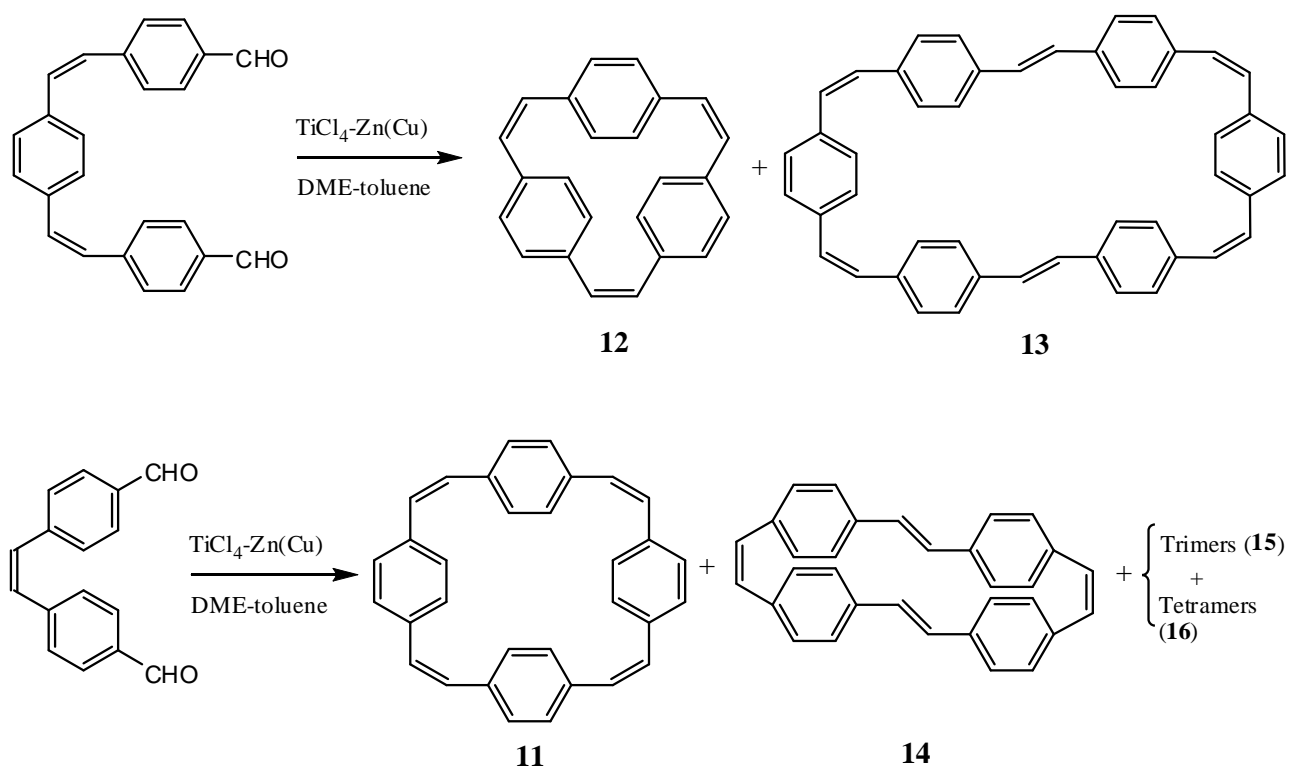
There are several reports for the synthesis of cyclophanes by the Wittig reaction. Wennerström et al. synthesized cyclophane **11** using a one-pot multiple Wittig reaction.^[42, 43] The Wittig reaction has many advantages over other methods for the preparation of large cyclophanes. The reaction conditions are mild enough to allow the variation of the arenes as well as the substituents. Unsaturated bridges are introduced directly, which may be desired for further reactions, for example, photochemical ring closure. The experimental procedure is simple; high dilution techniques, which often are necessary in the synthesis of ring compounds, are not essential.^[44] Starting materials are often easily available. Despite all indicated advantages of the Wittig reaction, the reaction has some inherent limitations. The initial reaction between an ylide and a carbonyl group to form a betain is reversible. Consequently, the reaction progresses toward the favored linear unstrained product instead of the corresponding cyclophanes. Therefore, small cyclophanes with considerable strain energy usually require other methods of preparation.



Scheme 1-5. Synthesis of cyclophane **11** by Wittig reaction.

1.3.1.2. The McMurry reaction

Since 1973, the McMurry reaction was used to produce double bonds from dialdehydes and ketones.^[45,46,47] A number of strained olefins, many unusual molecules, and a variety of complex natural products have all been synthesized using the McMurry coupling as the key synthetic step.^[48] Wennerström et al. were the first to use the McMurry reaction for the synthesis of cyclophane **12**. But, they did not succeed in synthesizing large cyclic oligomers.^[49] Oda and co-workers^[50,51] used a modified McMurry reaction for the improved synthesis of cyclic paracyclophanes. Different sizes of paracyclophanes **11**, **12**, **13**, **14**, **15**, **16** were obtained by this modified reaction.

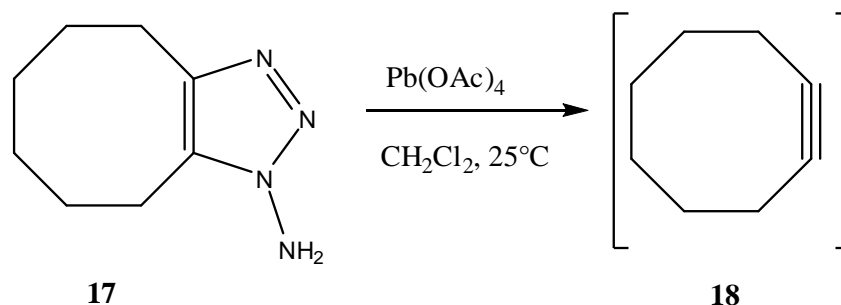
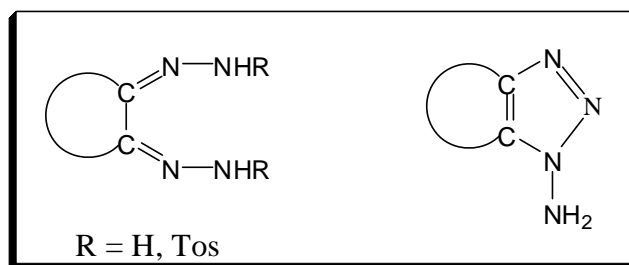


Scheme 1-6. McMurry reaction as the key step for the synthesis of cyclophanes with different ring sizes.

1.3.2. Bromination and dehydrobromination of cyclophanes

1.3.2.1. Degradation of triazole

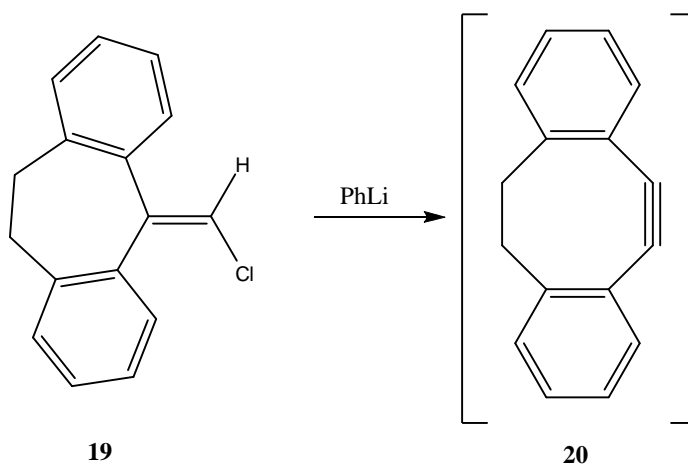
This method has a great advantage for the preparation of sensitive cyclophanes by various oxidizing reagents. The triazole **17** can be oxidized to alkyne **18** by this method.^[52]



1.3.2.2. Rearrangement reactions

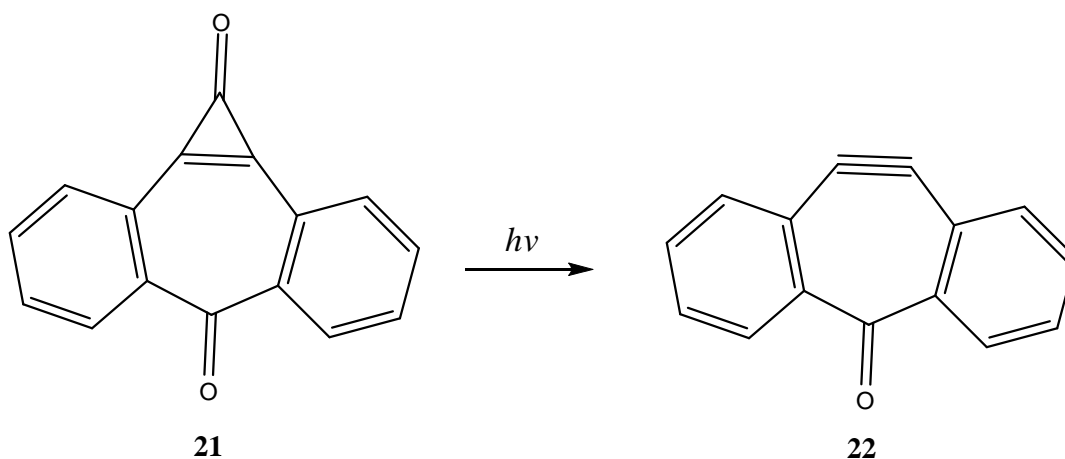
Rearrangements (Fritsch-Buttenberg-Wiechell reaction) of the carbon skeleton starting from 1,1'-dihaloalkenes have been often applied for the generation of strained cyclic alkynes. It is well-known that 1,1'-diaryl-2-haloethylenes undergo rapid rearrangement to diarylacetylene by treatment with a strong base (FBW rearrangement).^[53] The treatment of 9-chloromethylenefluorene **19** with phenyllithium in ether results in the formation of the highly strained diarylacetylene **20** as an intermediate.^[54] In this type of rearrangement, a hydrogen and a halogen and or two halogens are

removed from the same carbon on treatment with a base (α -elimination). It has been argued that a carbene or carbenoid intermediate is involved here.



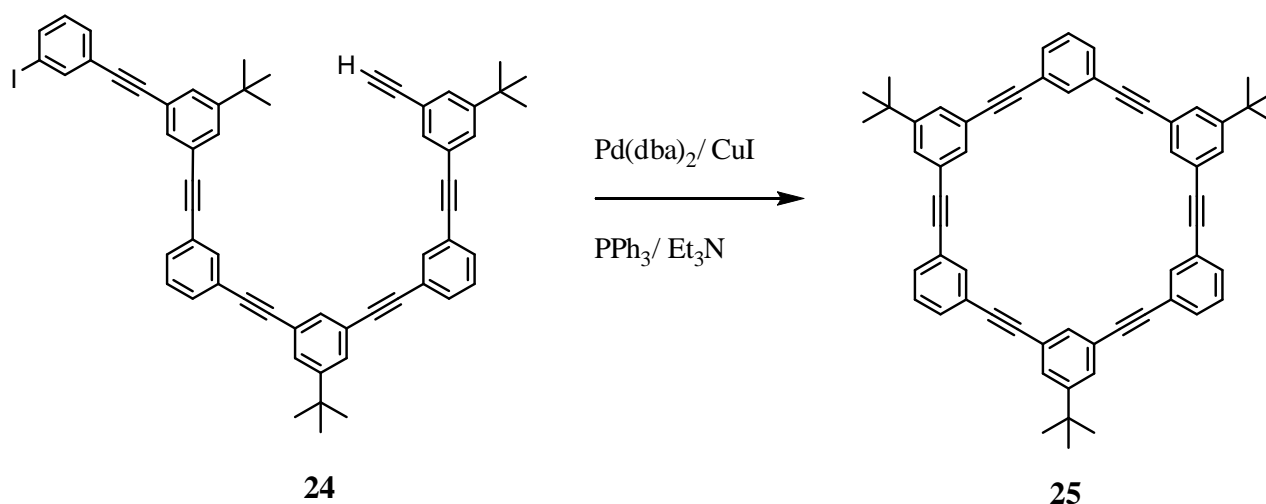
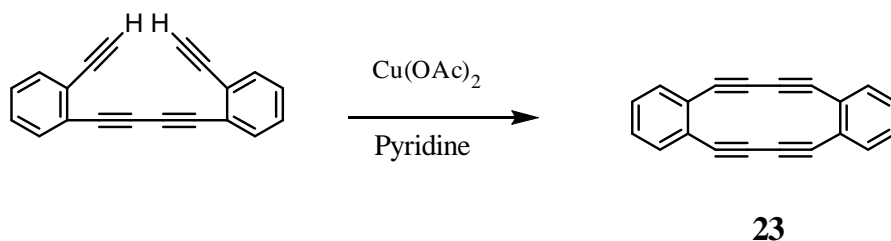
1.3.2.3. Cycloelimination reactions ^[55]

Cyclopropenone systems have proved to be particularly useful for the matrix isolation of short-lived cyclophanes like cycloheptyne. For example, photochemical decarbonylation of **21** leads to alkyne **22**.^[56]



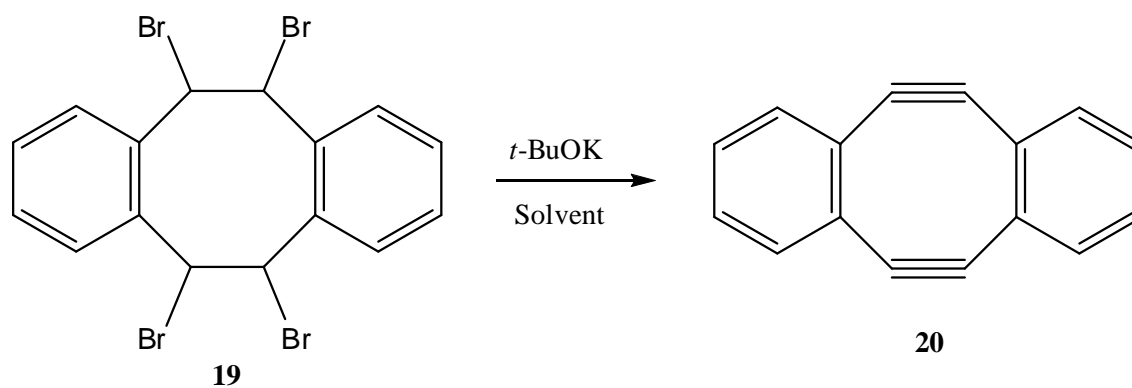
1.3.2.4. Ring closure reactions of systems containing triple bonds

The Glaser coupling of terminal dialkynes is another way to obtain strained compounds such as alkyne **23**.^[57] Less strained cycloalkynes can be generated by the Sonogashira coupling. The cyclic alkyne **24** is formed by the intramolecular coupling of linear phenylacetylene **25**.^[58]



1.3.2.5. Dehydrohalogenation reactions

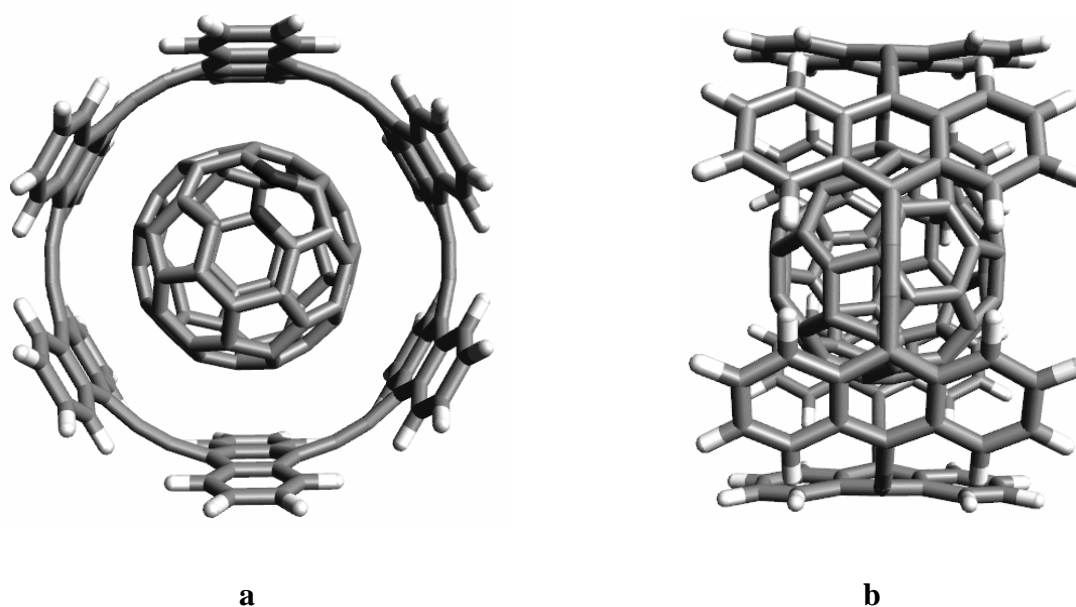
Perhaps the most obvious approach to the synthesis of cycloalkynes is the dehydrohalogenation of the corresponding 1,2-dihalogenocycloalkanes. For example, dibenzocyclooctadiyne **27** was efficiently prepared by dehydrobromination of **26** by treatment with base.^[59] The X-ray structure shows a high deformation for the triple bonds (ca.156°).^[60]



Oda *et al.* used this strategy to synthesize cyclic *para* phenylacetylenes.^[21]

1.4. The target molecules of the present work

Although numerous attempts have been made for the preparation of cyclic $[n]$ -*para*-phenylacetylenes ($[n]$ -CPPA) and cyclic $[n]$ -*para*-naphthylacetylene ($[n]$ -CPNA) but, synthesis of cyclic 9,9'-anthrylacetylene ($[n]$ -CPAA) as a novel member of this class of compounds has remained unknown to date. The present work is aimed at the synthesis of these types of conjugated, curved surface molecules using a new strategy. The main problem in the synthesis of these compounds seems to be the higher strain of the molecular structure in comparison with $[n]$ -CPPA and $[n]$ -CPNA. Despite the expected instability, we are interested in these type of compounds because of: i) their unusual structure ii) their suitable, rigid and deeper cavity as compared to $[n]$ -CPPA and $[n]$ -CPNA which makes the compounds likely to host some interesting compounds, e.g. fullerenes **28**.

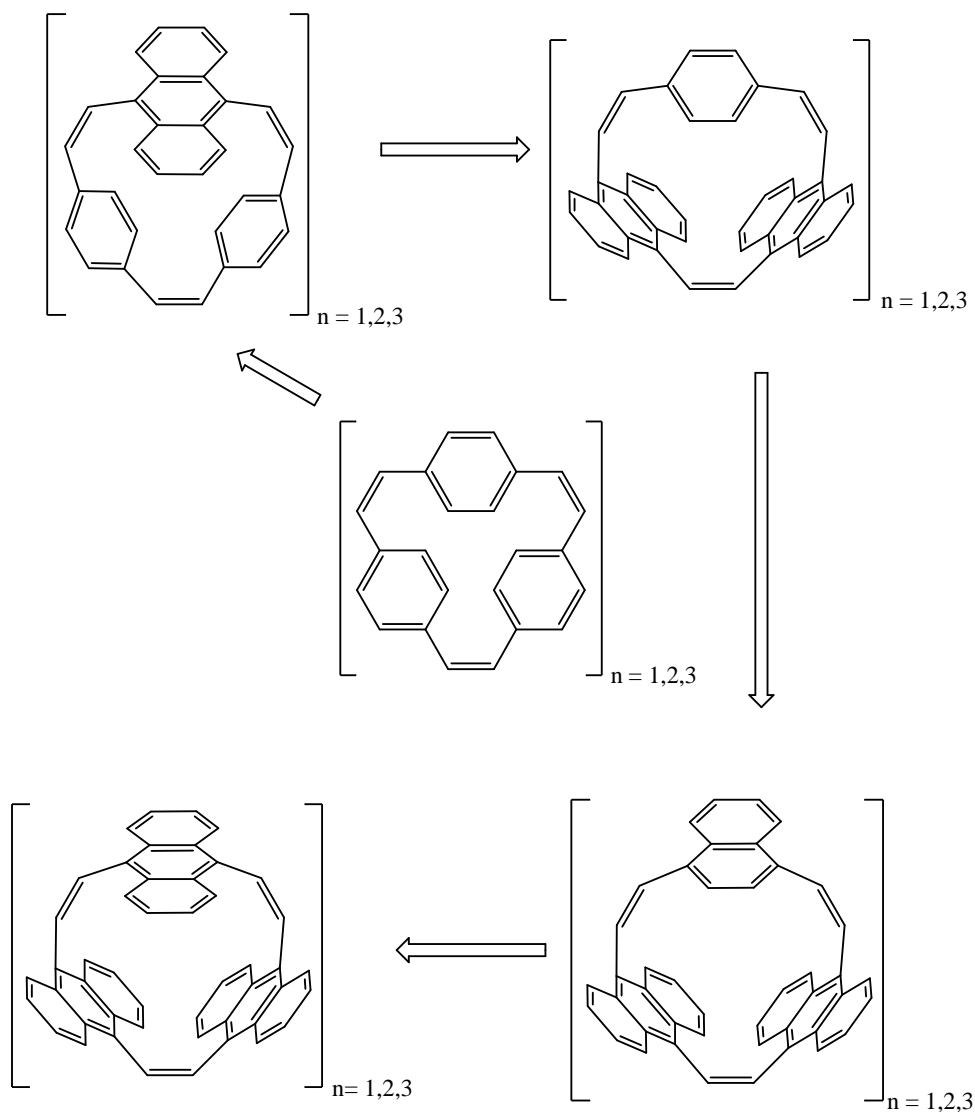


28

Figure 1-11. Semiempirical (PM3) calculated structure of an onion-type complex of [6]-CPAA with C_{60} in two views a) top view. b) side view.

1.4.1. Cyclic [*n*]-*para*-arylethylene

In order to synthesize [*n*]-CPAA, we have to prepare corresponding ethylene bridged cyclophanes. Since, the anthryl-containing [*n*]-CPAA's are expected to suffer from a higher strain and sterical hindrance, we applied a gradual strategy to prepare different cyclophanes by introducing the anthracene units step by step. To the best of our knowledge, all synthesized cyclophanes are unknown.



Scheme 1-7. Synthesis of different *para*-anthrylcyclophanes.

1.4.2. Cyclic[*n*]-*para*-arylacetylene

Figure 12 presents the molecular structures of the cyclic [*n*]-*para*-arylacetylene obtained from the corresponding cyclic [*n*]-*para*-arylethylenes. The curved surface of these molecules causes strain in their frameworks. According to semiempirical and *ab initio* calculations the aryl rings (phenyl, naphthyl and anthryl) are perpendicular with respect to the macrocyclic ring. Hence, the p-orbitals form a fully conjugated aromatic belt.

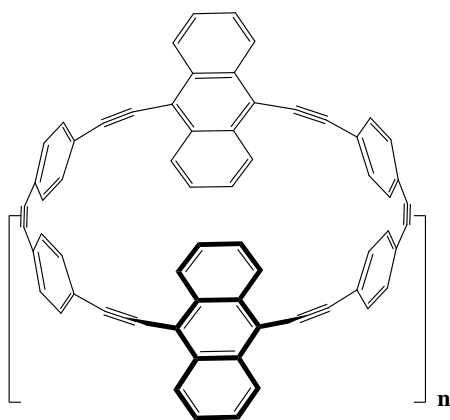
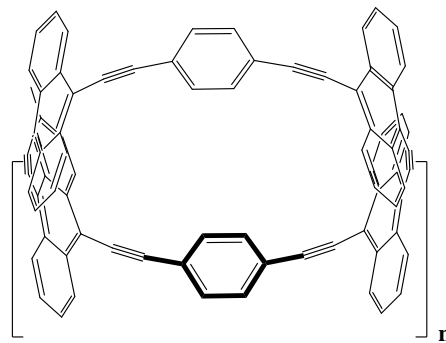
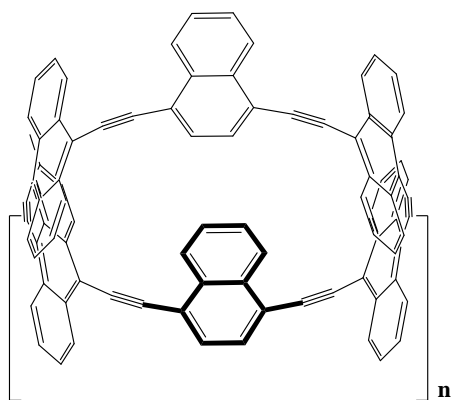
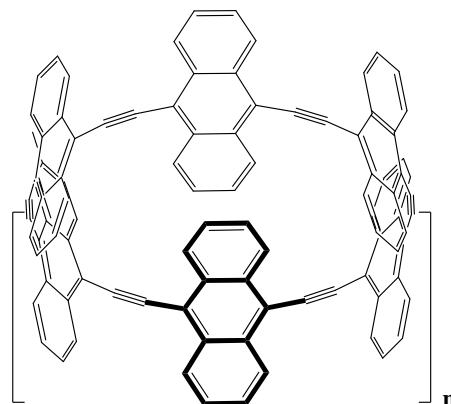
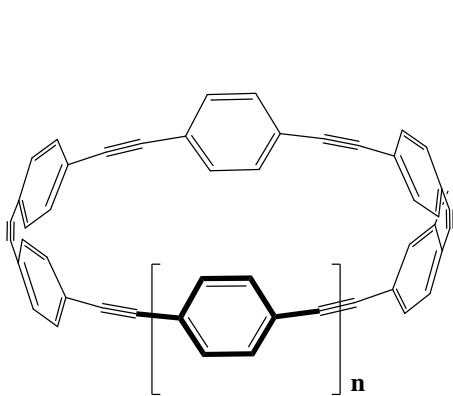
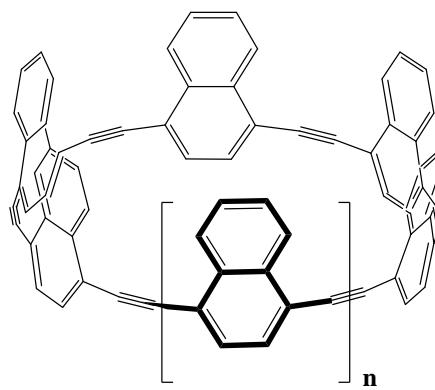
**29** ($n = 1,2$)**30** ($n = 1,2$)**31** ($n = 1,2$)**32** ($n = 1,2$)**33** ($n = 1,4$)**34** ($n = 1,4$)**Figure 1-12:** The dimer and trimer structure of different cyclic[*n*]-*para*-arylacetylene.

Table 1-1 lists the E_{HF} -values (enthalpy of formation) and E_s (strain energy) of desired cyclic[n]-*para*-arylacetylene together with their related acyclic [3]-*para*-arylacetylene as strainless references. For having a rational comparison, we did same calculation for known compounds [n]-CPPA **33** and [n]-CPNA **34**.

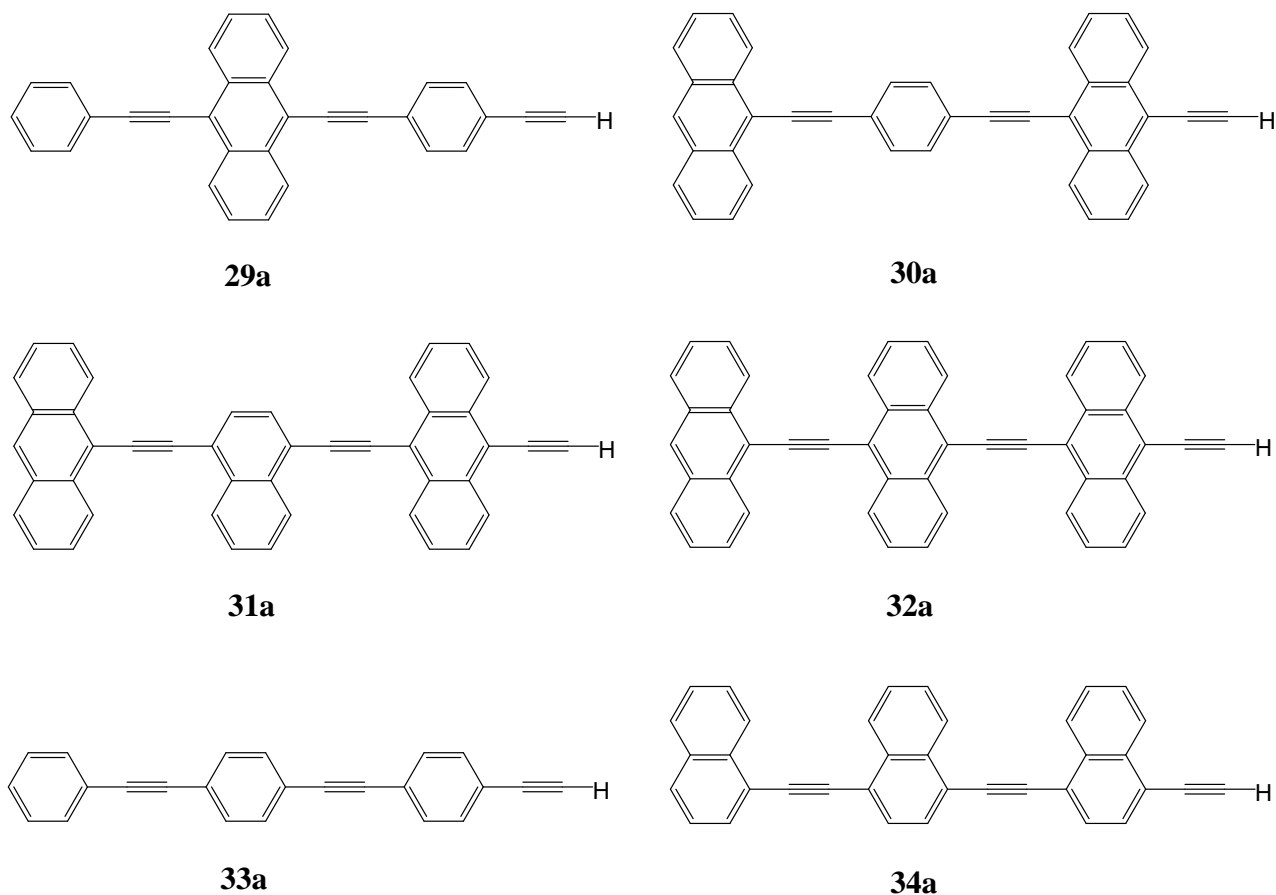


Figure 1-13. Acyclic [3]-*para*-arylacetylene as strainless references.

As shown in table1-1, the strain energy is calculated from the difference in the enthalpies of formation between cyclic[n]-*para*-arylacetylene and their related acyclic compounds. The strain energies ' $E_{s[n]}$ ' are determined using following equation, where ' $E_{\text{HF}[\text{cyclic}]}$ ' represents the heat of formation of the corresponding[n]yne. Because acyclics **29a-34a** have no strain in their frameworks, their heat of formation, $E_{\text{HF}[\text{acyclic}]}$, are used as the standard. To get the equation

isodesmic, we have to consider $2E_{\text{HF}[\text{H}_2]}$ for dimer ($n=1$) and $3E_{\text{HF}[\text{H}_2]}$ for trimer ($n=4$). Since, the standard heat of formation of hydrogen in the semiempirical method is zero, it is neglectable.

$$E_{s[n]} = [E_{\text{HF}[\text{cyclic}]} + 2(n=1) \text{ or } 3(n=4) E_{\text{HF}[\text{H}_2]}] - [E_{\text{HF}[\text{acyclic}]} \cdot 2(n=1) \text{ or } 3(n=4)]$$

According to the calculated data, the strain energies (E_s) as expected, increase with decreasing ring size from the trimer to the dimer. Within the same size of rings, E_s 's slightly increase with increasing number of anthracene units in the structure. In this order, compound **32** has the highest E_s in trimer and also dimer except dimer **34**.

Table 1-1. Standard heat of formation E_{HF} and strain energy E_s (kcal/mol)] of optimized acyclic and cyclic compounds using the PM3 method (for structures see Fig.1-12 and Fig.1-13)

Compound	Dimer		Trimer		Acyclic	
	E_{HF}	E_s	E_{HF}	E_s	E_{HF}	E_s
32	726.27	46.13	1051.81	31.60		
32a					340.07	0
31	684.88	44.00	988.06	26.73		
31a					320.44	0
30	650.94	40.60	940.97	25.46		
30a					305.17	0
29	572.76	42.29	824.15	28.44		
29a					265.24	0
33	491.57	43.80	701.08	29.43		
33a					223.88	0
34	599.81	47.36	856.08	27.42		
34a					276.22	0

Table 1-2 lists the average acetylene bond angles and cavity sizes of cyclic (dimer and trimer) and acyclic compounds **29-34**. The values also show too deviations from planarity in cyclic

compounds. This deviations decrease with increasing ring size from dimer to trimer. The cavity diameters of trimers are about 6 Å bigger than those of dimers.

The theoretical data, on the strain energy could explain some of the experimental results. According to Oda and Kawase, the yield of reaction in the preparation of [6]-CPPA is about 85 %, while the yield of [6]-CPNA in the same approach and similar conditions, is only 2.8 %.^[39] Therefore, the results are in a good agreement with theoretical data. Increasing the strain energy from 43.80 (**33**) to 47.36 (**34**) kcal/mol leads to the decrease of the yields from 85 % to 2.8%, respectively. The higher steric demand of the naphthyl with respect to the phenyl group could also be the cause for the reduced yields.

Table 1-2. Acetylene bond angles and cavity sizes of cyclic and acyclic compounds **29-34**.

Compound	Cavity diameter (nm)	Bond angle (°)
Dimer	13.20	167.45
Trimer	19.60	171.56
Acyclic	-	180

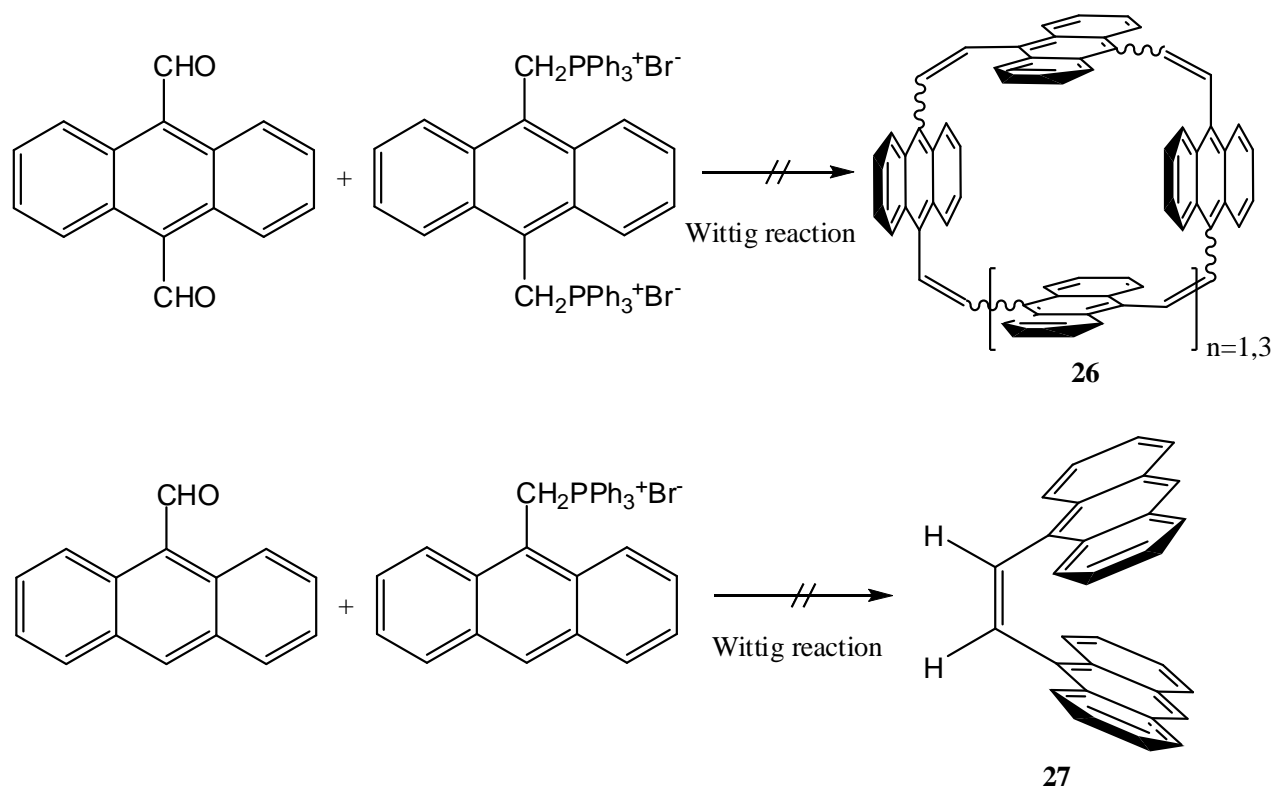
According to the calculated data, the strain energy in our target molecules **32** similar to compound **34** is relatively high. Consequently, difficulties in the synthesis of these belt-like aromatics can be expected.

Chapter 2: Synthesis of anthracenophanes

2.1. Synthesis of cyclic $[n]$ -*para*-anthrylethylenes

2.1.1. Synthesis of *cis*-1,2-bis(9-anthryl)ethylene

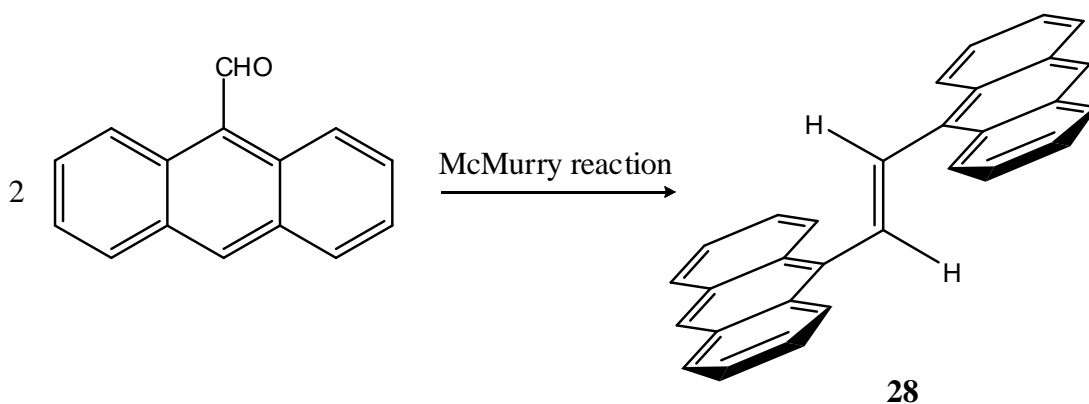
Among the methods for the synthesis of the stilbenoid compounds outlined in Chapter 1, only two methods, the Wittig reaction and the McMurry coupling, are frequently used to synthesize the cyclophanes. Even though the Wittig coupling is a common method for the synthesis of cyclophanes,^[61,62] it is not applicable to the synthesis of cyclophanes with anthracenes as aryl units **26** (Scheme 2-1). The problems are probably due to sterical hindrance in the 9- and 10- positions of anthracene. This could explain why the synthesis of *cis*-1,2-bis(9-anthryl)ethylene **27** which is precursor for the anthracenophanes failed^[63] (Scheme 2-1).



Scheme 2-1. The attempted Wittig reaction for synthesis of anthracenophanes.

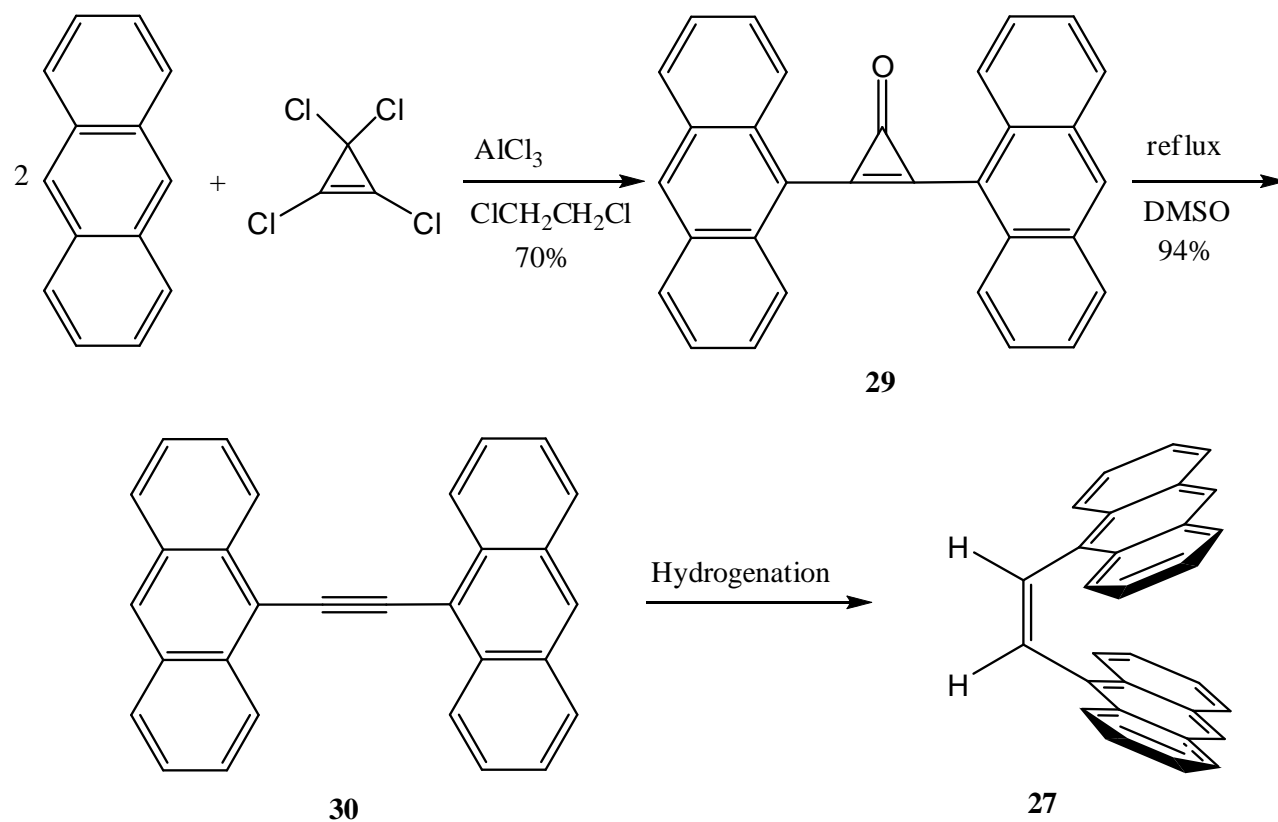
Since, preliminary attempts for the synthesis of anthracenophanes by a simple one-step route of the Wittig coupling were failed, step by step method were applied to synthesize these compounds.

The McMurry coupling reaction has shown remarkable utility for the synthesis of cyclophanes. This method would allow a simple route for the preparation of **27** from commercially available 9-anthraldehyde, however not surprisingly, the *trans*-isomer **28** is the only product observed which could not be used as a precursor for the next steps^[64] (Scheme 2-2).



Scheme 2-2. The McMurry reaction yields exclusively the *trans*-configuration *trans*-1,2-bis (9-anthryl) ethylene.

After the failure of the attempts using the Wittig and the McMurry reactions, we applied indirect methods for the synthesis of the desired cyclophanes. A suitable method was reported by Wadsworth^[65] and Becker^[66] in 1981 who employed Friedel-Crafts reaction, decarbonylation and hydrogenation reactions^[67] to obtain the *cis*-configuration of the double bond in **27** (Scheme 2-3). Even though, they succeeded to obtain the final compound with a good yield, a huge amount of Lindlar catalyst had to be used in the hydrogenation reaction which makes the synthesis quite expensive. To optimize the reaction, we used different catalysts. The results are listed in Table 2-1. Palladium on barium sulfate and palladium on calcium carbonate turned out to be more active catalysts. The amount of catalyst, and reaction time could be reduced while increasing the yield of the reaction, remarkably.



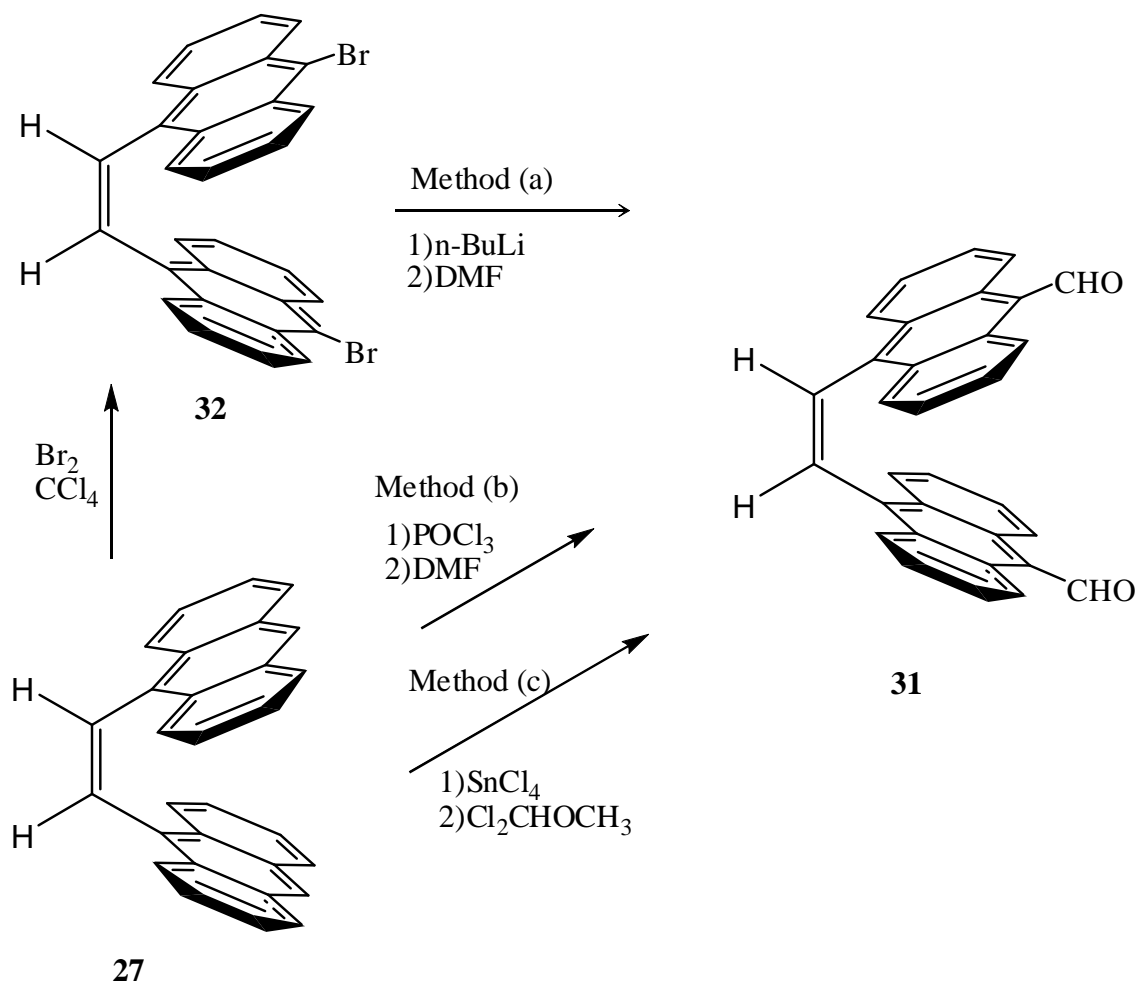
Scheme 2-3. The Wadsworth and Becker method for the synthesis of *cis*-1,2-bis(9-anthryl)ethylene.

Table 2-1. Comparison of hydrogen reaction result of 1,2-di-9-anthrylacetylene **30** in different catalyst.

Catalyst	Cat : start material (mg)	Time (min.)	Yield %
Lindlar cat.	40 : 1	45	72
Pd/CaCO₃	2 : 1	120	98
Pd/BaSO₄	2 : 1	120	98

2.1.2. Synthesis of *cis*-1,2-bis[10-formyl-9-anthryl]ethene

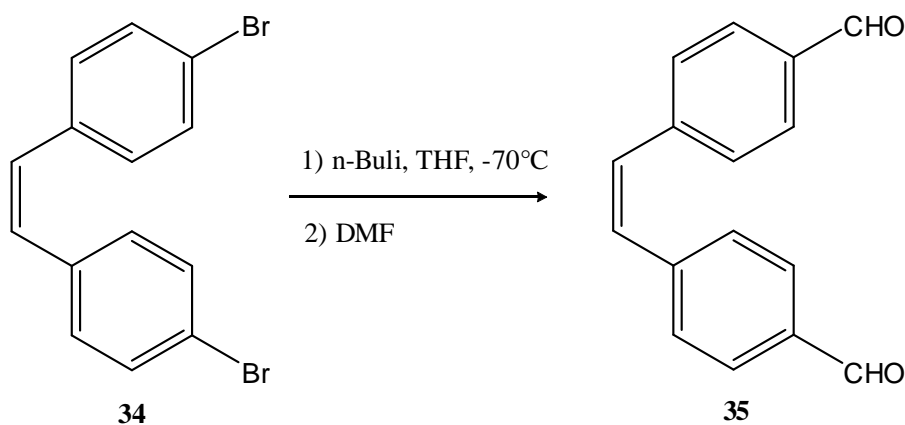
The formylation of aromatic compounds is an important synthetic step in organic chemistry.^[68] Among all the formylation methods, three methods are particularly useful for the formylation of electron- rich arenes, as shown in Scheme 2-4.



Scheme 2-4. The three attempted methods for the synthesis of *cis*-1,2-bis[10-formyl-9-anthryl]ethene.

2.1.2.1. Method (a)

Method (a) has been applied first time by Wennerström et al.^[69] starting from *cis*-4,4'-dibromostilbene **34** (Scheme 2-5). We tried to extend it to synthesize our desired compound (Scheme 2-5).



Scheme 2-5. The Wennerström method for the synthesis of *Z*-4,4'-diformyl-stilbene **35**.

But, all attempts to prepare **32** as a precursor in the formylation reaction failed. Actually, the bromination reaction of compound **27** was not complete and the mixture of the mono brominated compound **33** and the dibrominated compound **34** could not be separated.

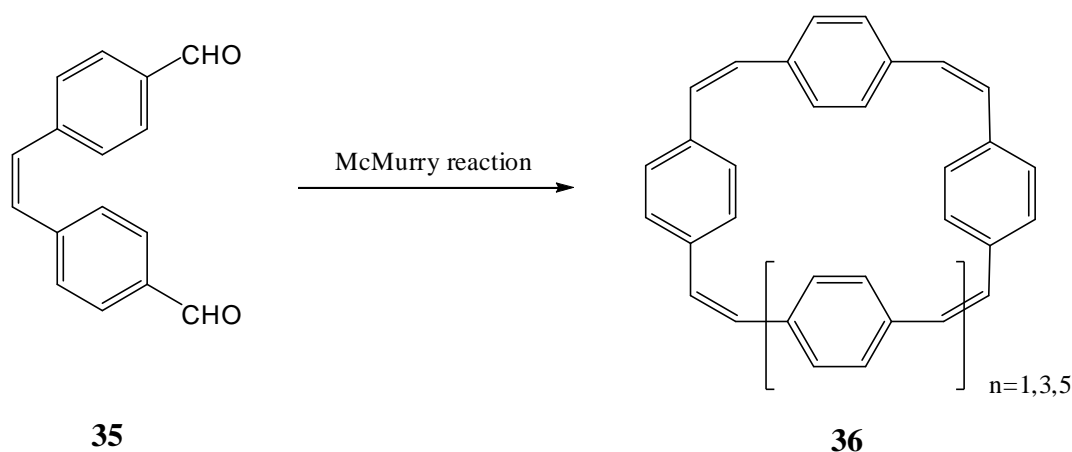
2.1.2.2. Methods (b,c)^[70,71]

Both methods are potentially applicable for the synthesis of our desired compound **31**. But, method (c) due to the simplicity of reaction and also, because of the fairly high yields was selected. This simple procedure involves the reaction of an arene with the Lewis acid SnCl₄ and Cl₂CHOCH₃ at low temperatures and then mixing at room temperature and finally, quenching with cold water. A definitive advantage of this method is the easy work-up that avoids any purification by column

chromatography. The crude products were recrystallized and filtrated with acetone to obtain the pure product. In this reaction, temperature plays an important role. Addition of reagents at room temperature produces a mixture mono and diformylated compounds while, doing the reaction at 0 °C forms compound **31** with a fairly good yield.

2.1.3. Synthesis of cyclic[n]-para-antrylethylenes

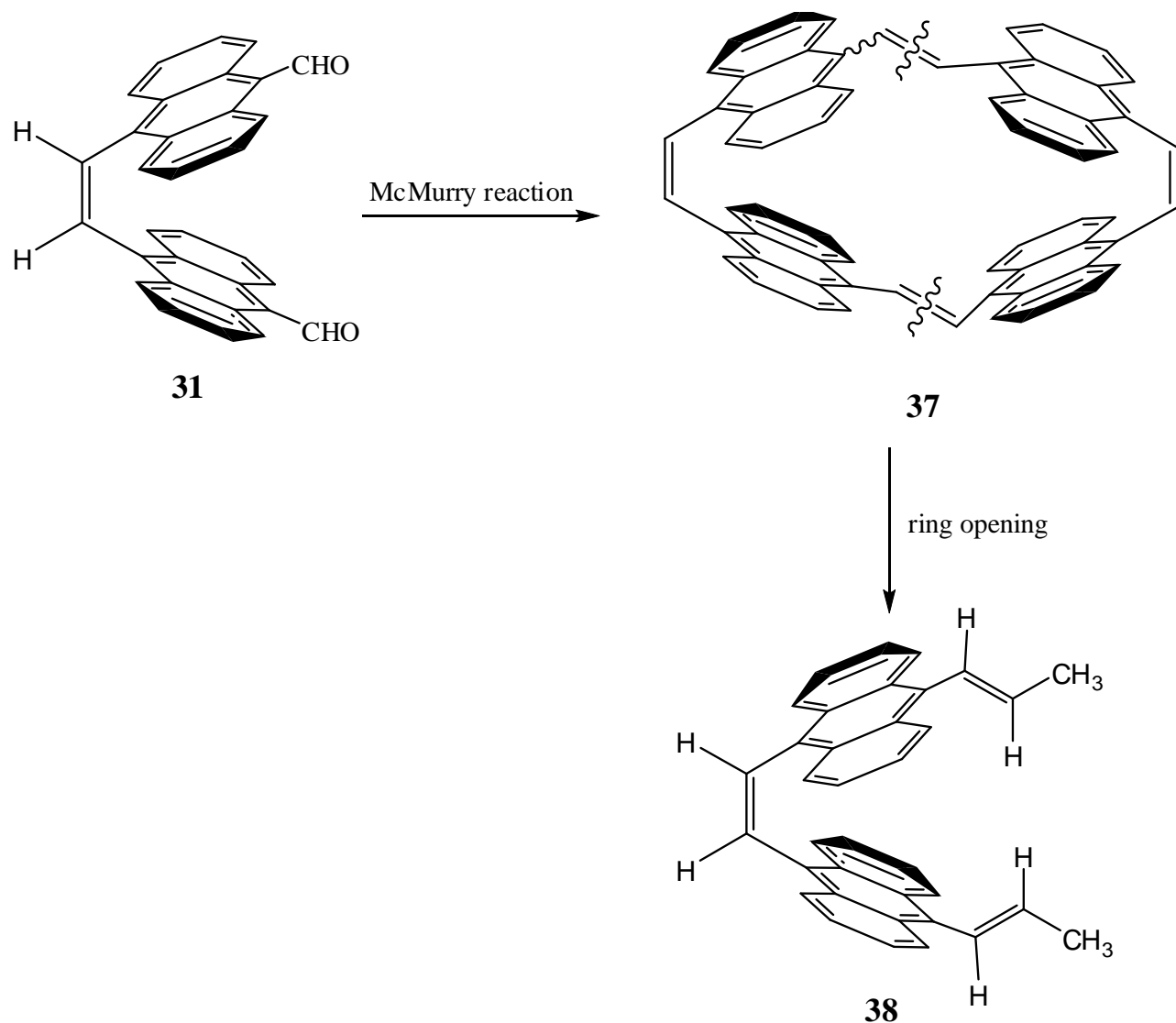
As we discussed in Chapter 1, the McMurry coupling has been successfully used to synthesize some cyclophanes, even strained compounds^[72] (Scheme 2-6). However, the reaction led to a mixture of isomers. Oda *et al.*^[51] performed a detailed study to determine all existing conformers and products in this reaction. They could separate and characterize all possible isomers by column chromatography and were also able to optimize the reaction conditions using some selected solvents to obtain a major isomer.^[50]



Scheme 2-6. The McMurry reaction for synthesis of cyclic [n]-para-phenylethylenes.

Using the same approach and similar conditions, we prepared cyclophane **37** as a minor product (Scheme 2-7). Main product, however, was an insoluble oligo- or polymer, besides the unexpected open ring compound **38**. Probably, the open ring compound **38** is a decomposition product of dimer **37** which was formed due to sterical hindrance between the four opposed anthracenes as shown in

the molecular structure. The methyl groups in structure of **38** derive from the solvent (DME) and were attached by an unknown mechanism.



Scheme 2-7. The McMurry reaction to prepare the cyclic $[n]$ -*para*-antrylethylene.

The structure of compound **38** could be assigned by ¹H- and ¹³C-NMR spectra. The ¹H- NMR shows a doublet for the methyl protons in the aliphatic region (2.21 ppm), a quartet for the *cis*

olefinic protons connected to the methyl group, a singlet for the olefinic protons between two anthracene units, a doublet for the olefinic protons connected to the anthracene units and three multiplets for the anthracene protons.

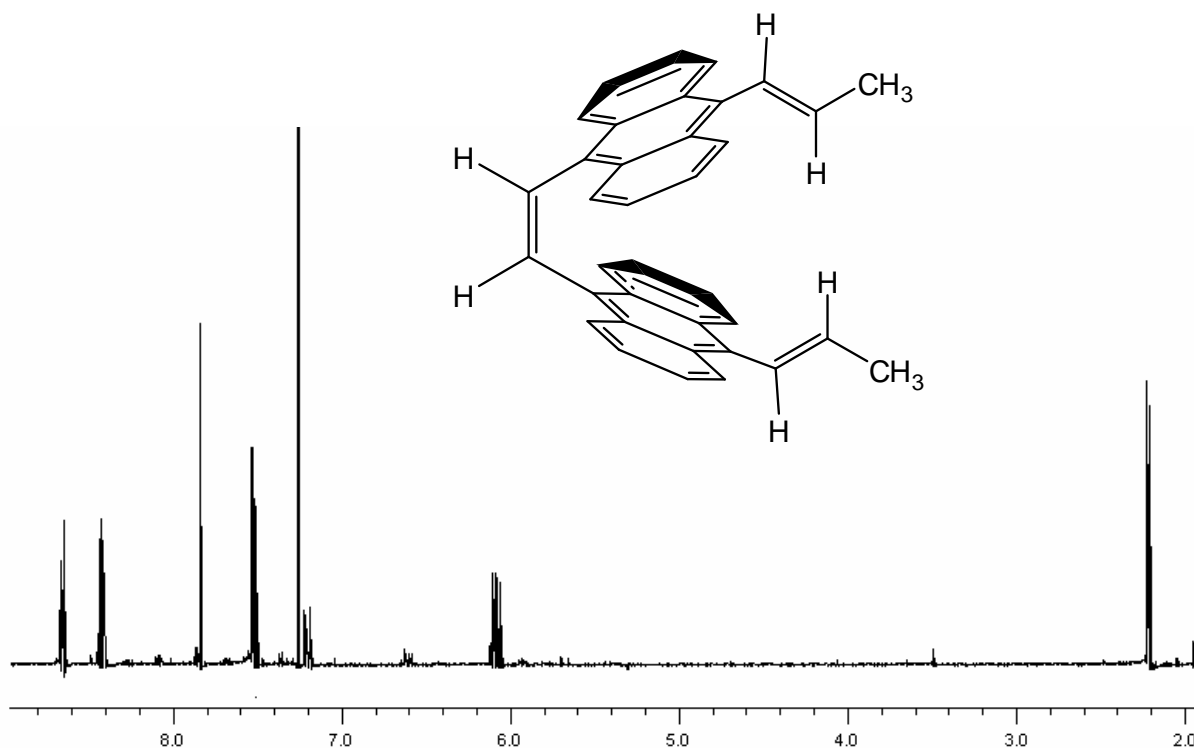


Figure 2-1. ¹H-NMR (500 MHz, CDCl₃/TMS) spectrum of **38**.

Attempts to purify cyclophane **37**(n=1) by flash chromatography and analytical HPLC failed and its identification is only based on MALDI- TOF mass spectrometry.

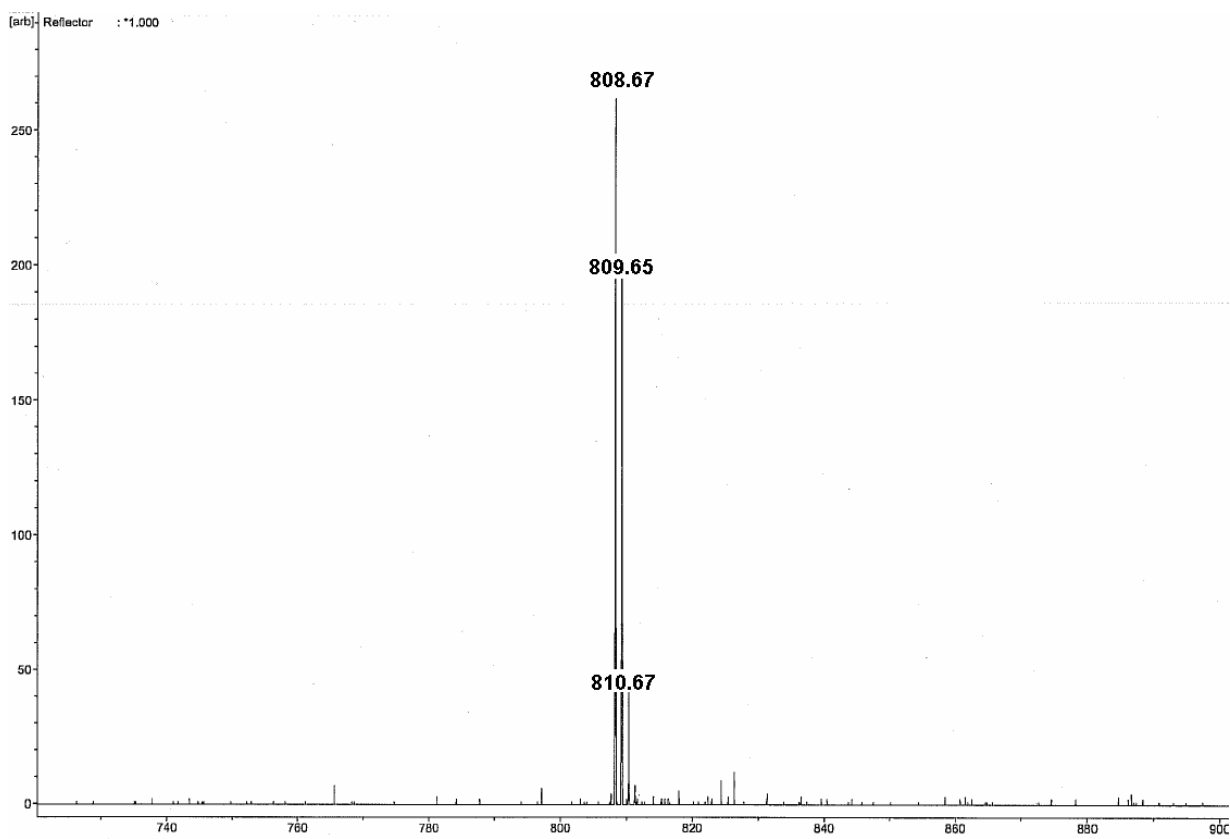
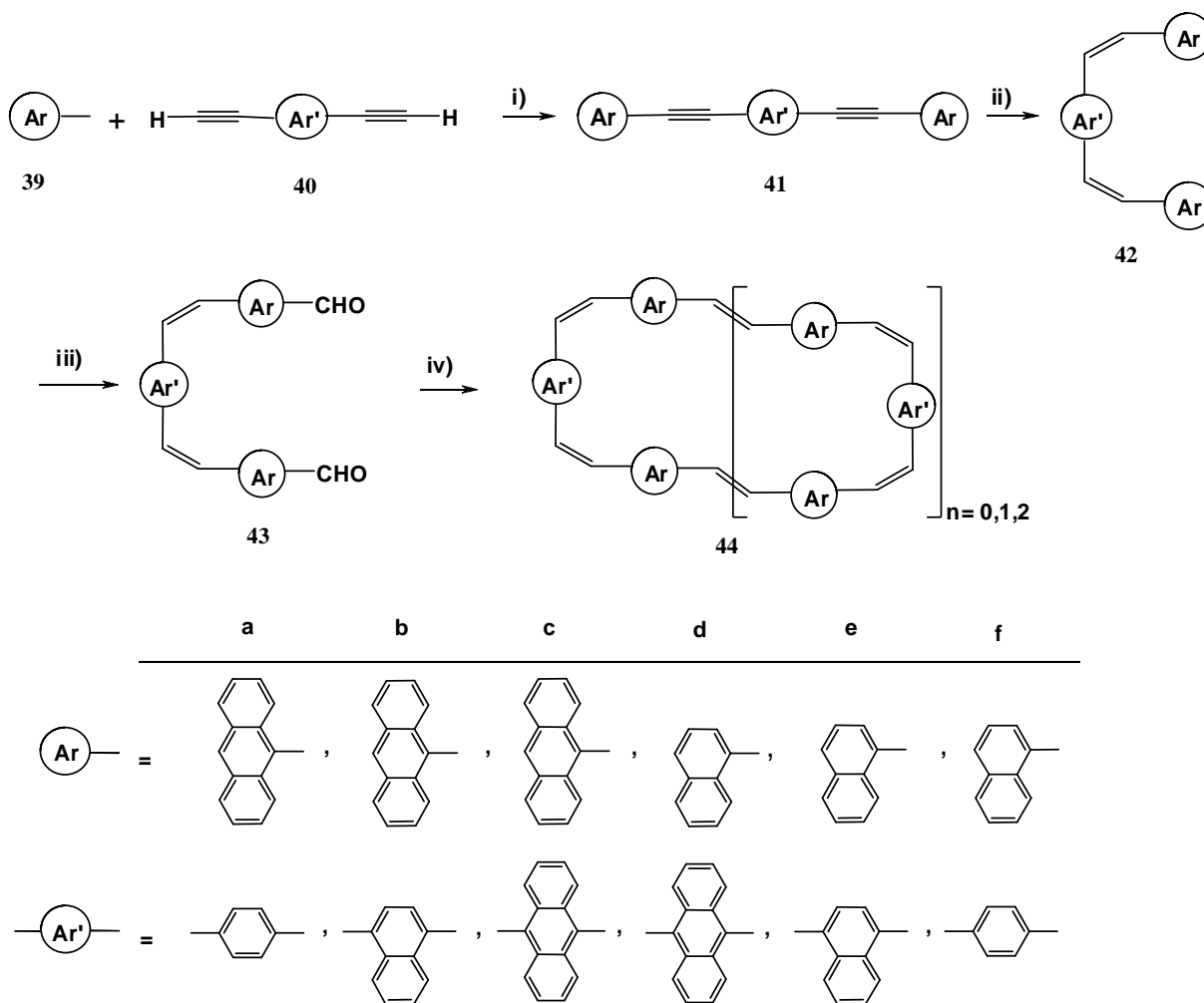


Figure 2-2. MALDI-TOF mass spectrum of **37**.

2.2. New strategy for the synthesis of cyclic [*n*]-*para*-anthrylethylenes

As it is explained in section 2.1., the Oda, Kawase, Darabi method to prepare cyclic *para*-phenyl and *para*-naphthylethylenes failed if anthracene units were used. Therefore it was necessary to develop a new strategy to synthesize the cyclic *para*-anthrylethylenes, which are precursors for the belt-like aromatics (Scheme 2-8). In this route, the employed ethynylarenes **43** contain three instead of two arene units and therefore are stronger bent and therefore better precursors for the anticipated cyclization.

In contrast to previous methods, the new strategy is a multi-step reaction. However, the approach outlined in follow was used to attempt the synthesis of the first cyclic $[n]$ -*para*-arylethylenes containing anthracene units.



Scheme 2-8. Attempted multi-step synthesis of anthracenophanes. Reagents and conditions: i) $\text{Pd}(\text{PPh}_3)_2\text{Cl}_2$, CuI , diisopropylamine; ii) H_2 , Pd/C ethylacetate; iii) SnCl_4 , $\text{Cl}_2\text{CHOCH}_3$, CH_2Cl_2 ; iv) TiCl_4/Zn , DME, toluene.

2.2.1. Synthesis of arylene-ethynylene **41** (a, b, c, d, e, f)

The Sonogashira coupling between terminal alkynes and arylhalide has been widely used to prepare arylene-ethynylene and their derivatives.^[73-75] the arylene-ethynylene structure **45** have been extensively utilized in the molecular design of novel π -conjugated aromatic oligomers and polymers, particularly in the fields of supramolecular chemistry and material science.^[76-78] A wide variety of compounds with phenylene (or naphthylene) units were synthesized.^[79,80] The compounds have been used in molecular machines,^[81,82] and electronic devices.^[83,84]

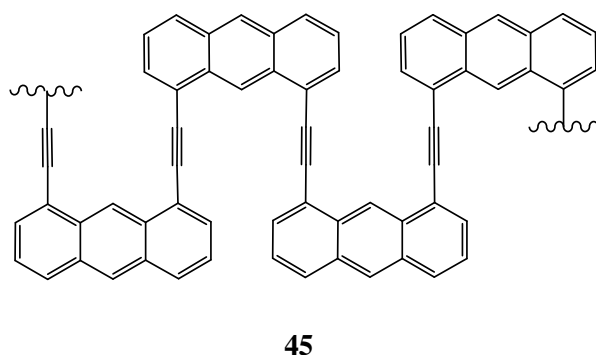
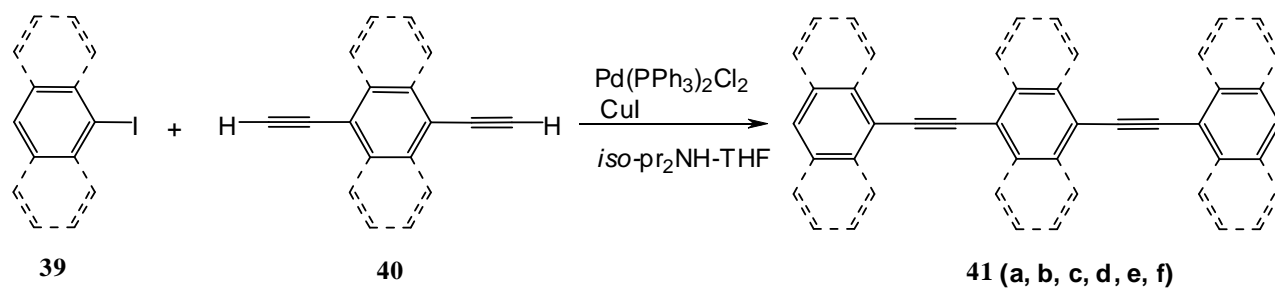


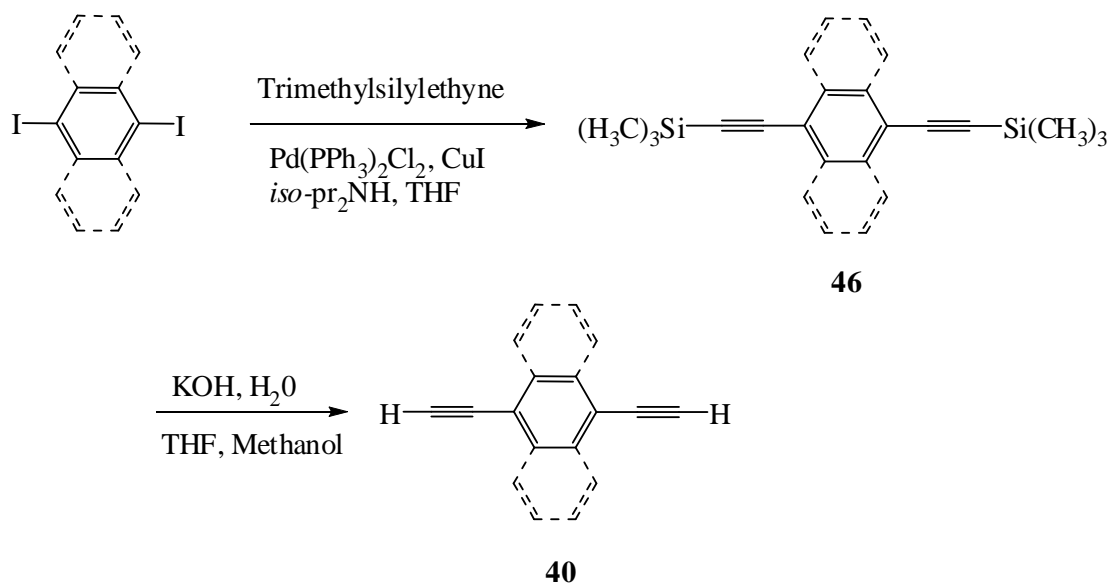
Figure 2-3. Structure of an acyclic 1,8-anthrylene-ethynylene oligomer.

Using the same approach, it was tried to extend the width of the arylene-ethynylene units by introducing anthracene, naphthalene and benzene units as aromatic building blocks. Among the several possible connection sites, the following positions were selected with respect to our target molecules (9,10 for anthracene, 1,4 for naphthalene and 1,4 for benzene). Except arylene-ethynylene **41a**, the other anthrylene-ethynylene precursors for the nanoring synthesis have not yet been described in the literature.



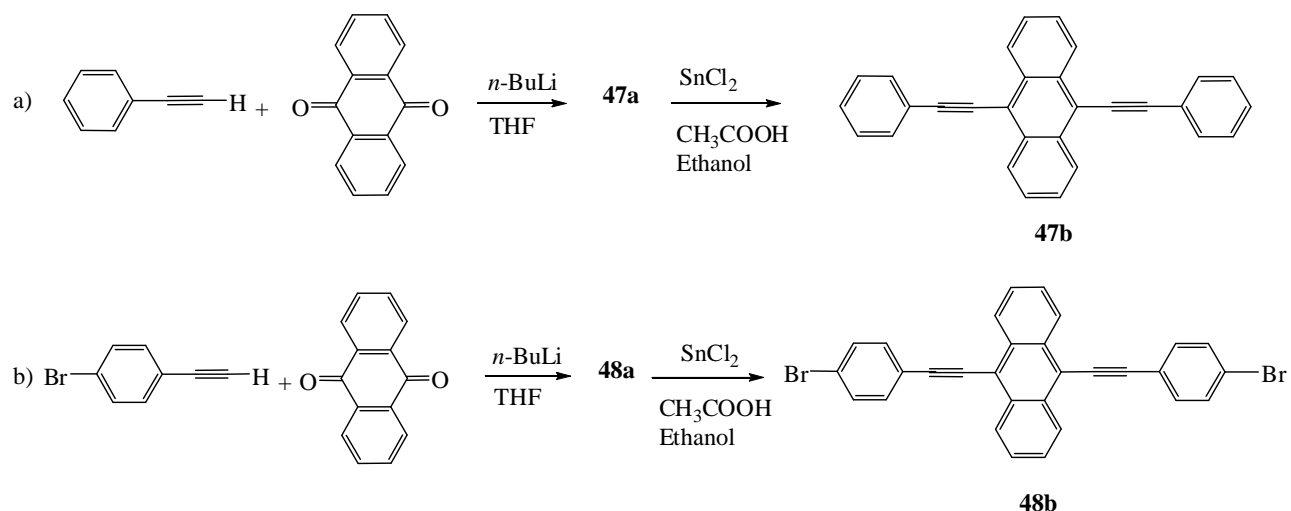
Scheme 2-9. Synthesis of arylene-ethynylene by Sonogashira coupling.

The synthesis of diethynylarenes **40** has been done according to the literature procedure.^[86] To optimize the reaction, $\text{Pd(PPh}_3)_2\text{Cl}_2$, instead of Pd(OAc)_2 , was used as catalyst and the reaction time was reduced significantly from 20 to 4 hours.



Scheme 2-10. Synthesis of diethynylarenes **40**.

The compound **48b** was synthesized by a similar approach as compound **47b**.^[87]



Scheme 2-11. Synthesis of 9,10-bis(phenylethynyl)anthracenes **47b** and **48b** from anthraquinone.

In contrast to reaction (a), 9,10-bis(phenylethynyl)anthracene in reaction (b) has two active positions (the acetylenic hydrogen and the bromine) in reaction with *n*-BuLi. The *n*-BuLi has to be added at low temperatures in reaction b) to avoid metal halogen exchange of the bromine.

2.2.2. Synthesis of 9,10-bis(arylethenyl)anthracenes by hydrogenation reaction

The *syn/syn*-selectivity of the hydrogenation of the triple bonds plays a key role in the synthesis of the desired anthracenophanes. Only one example of such a hydrogenation reaction is known.^[88] Based on a latter dynamic NMR study of *Z,Z*-9,10-bis(styryl)anthracene **49** at both 25 and -10 °C, two isomers the *syn/anti* conformers were found in solution. According to molecular mechanics calculations each of the isomers can have two conformations.^[89] Among the different low energy conformations only the *syn* isomers have a proper orientation to form ring closed products.

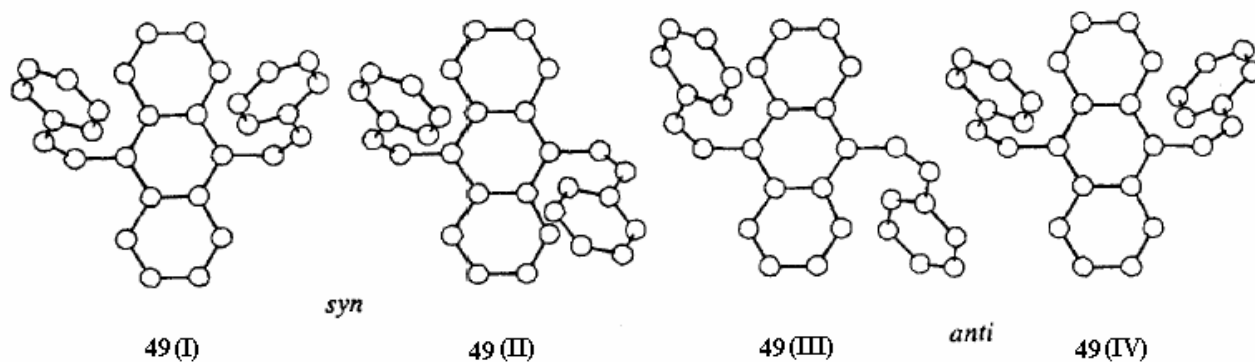
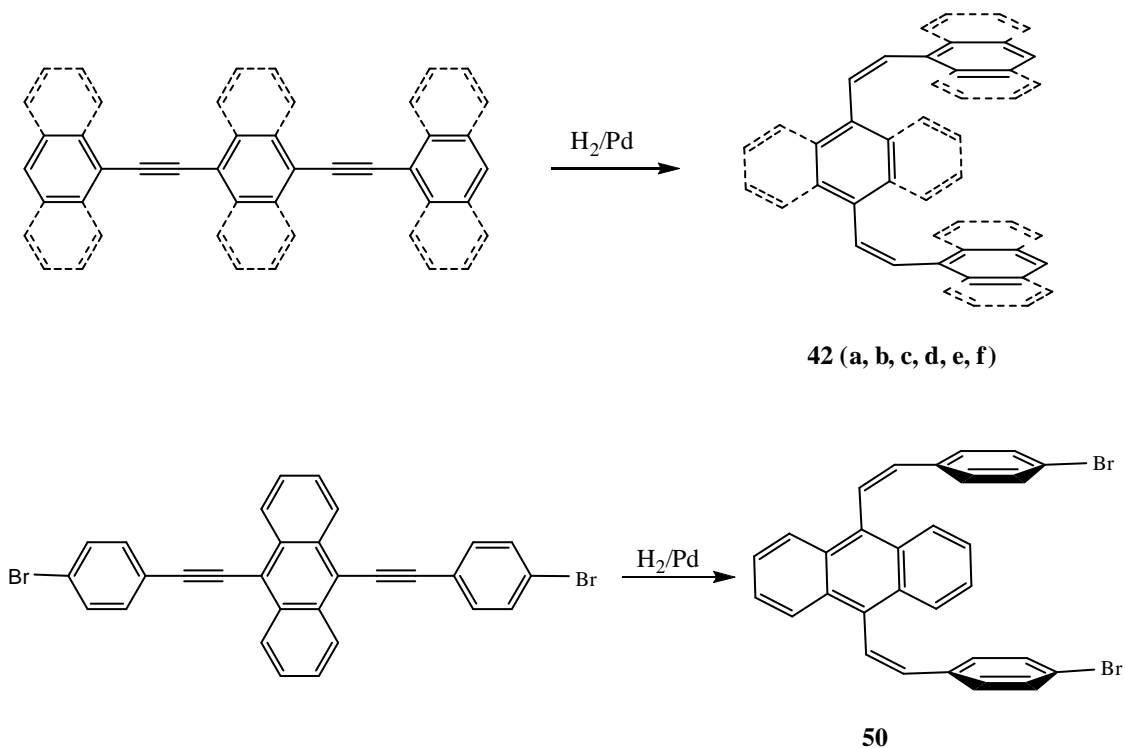


Figure 2-4. The four different (MMP2 calculated) optimized conformations of compound **49**.

The desired aryleno-ethynyls show a different reactivities upon hydrogenation with Pd catalysts depending on their structures. Therefore, the reaction had to be optimized using different Pd-catalysts and solvents. Results are showed in table 2-2.



Scheme 2-12. Synthesis of 9,10-bis(arylethenyl)anthracenes by hydrogenation reaction (Refer to scheme 2-8, page 32 for the clarity).

Table 2-2: Results from hydrogenation reactions of arylene-ethynylenes.

Entry	Catalyst	Ratio cat : start material	Time (min) ^a	Solvent	Temperature (°C)	Yield (%)
41a	Pd/BaSO ₄ , 5%	2 : 1	40	ethylacetate	r.t.	100
41b	Pd/BaSO ₄ , 5%	2.5 : 1	50	toluene	50	100
41c	Pd/BaSO ₄ , 10%	2.5 : 1	60	toluene	50	100
41d	Lindlar cat.	2.5 : 1	50	ethylacetate	r.t.	75
41e	Pd/BaSO ₄ , 5% (reduced)	3 : 1	60	ethylacetate	r.t.	70
41f	Pd/BaSO ₄ , 5% (reduced)	2 : 1	50	ethylacetate	r.t.	50
48	Pd/BaSO ₄ , 5%	2.5 : 1	55	ethylacetate	r.t.	100

^a The reaction time could be variable by changing the amount of catalyst.

The investigation of ¹H-NMR spectra of the products could be interesting. Based on a latter study, Wennerström and Sundahl^[89] have reported a dynamic NMR study of *Z,Z*-9,10-bis(styryl)anthracene **49** at both 25 and -10 °C. The ¹H-NMR spectrum of this compound was more complicated than expected for a single isomer. This intricacy is explained by a slow interconversion of the two isomers (*syn/anti*) at room temperature.

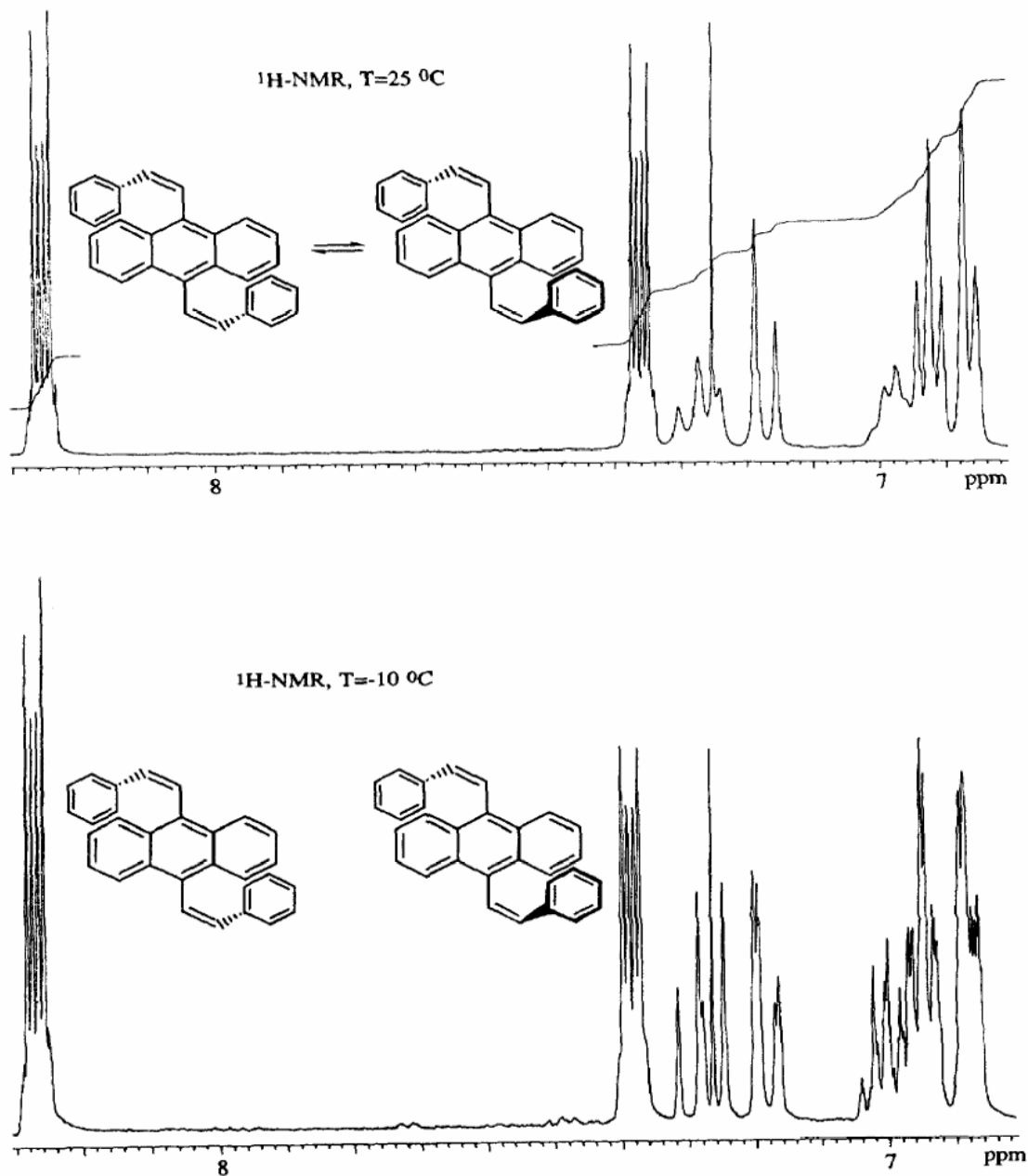


Figure 2-5. $^1\text{H-NMR}$ (CDCl_3 , 400 MHz) spectra of **49** at two different temperatures.^[89]

The $^1\text{H-NMR}$ spectrum of compound **50** at room temperature also shows more signals than expected for a single isomer. It probably concerned to existing two different *syn/anti* isomers with a different ratio (Figure 2-6). Equilibration between *syn/anti* inclines to *syn* isomer **50** with regard to

obtained results of the McMurry reaction (Section 2.2.4). However, the McMurry reaction of the *anti* isomer **50** does not produce any ring compounds.

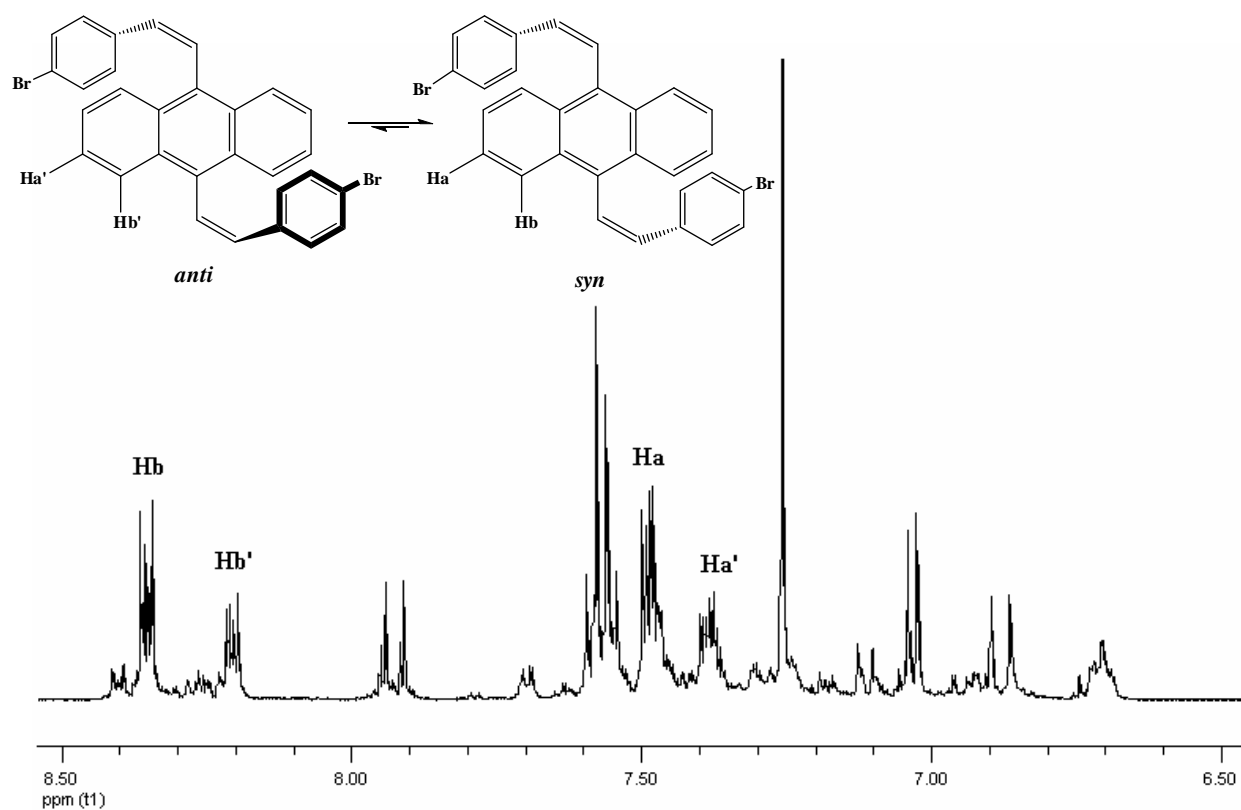


Figure 2-6. ¹H-NMR (500 MHz, CDCl₃/TMS) spectrum of the arylene-ethenylene **50** at room temperature.

Unlike compound **50**, the ¹H-NMR spectra of the compounds **42** (**a**, **b**, **c**, **d**, **e**, **f**) show only the corresponding *syn* isomer. It is probably due to large barrier between *syn/anti* conformers at room temperature. Such restricted rotation and flip around the double bond was also observed in the ¹H-NMR spectrum of *cis*-1,2-bis (9-anthryl) ethylene **27**.^[90]

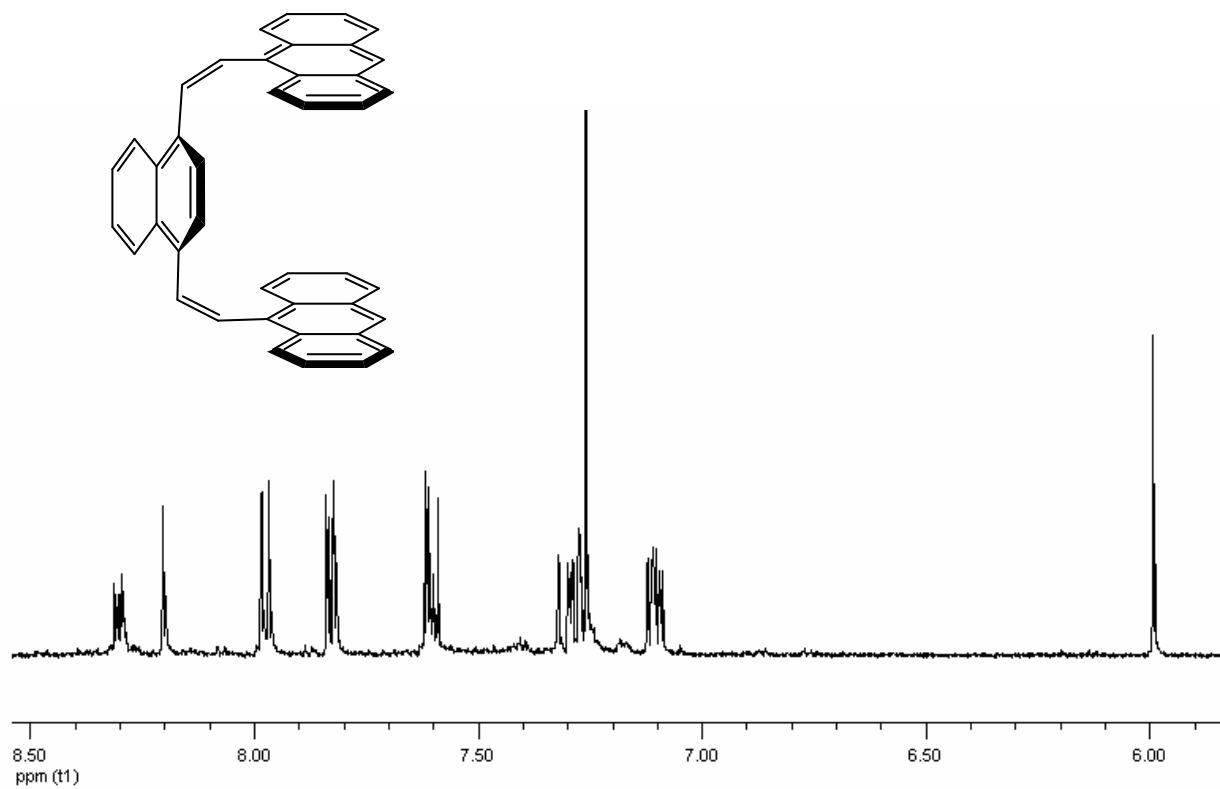
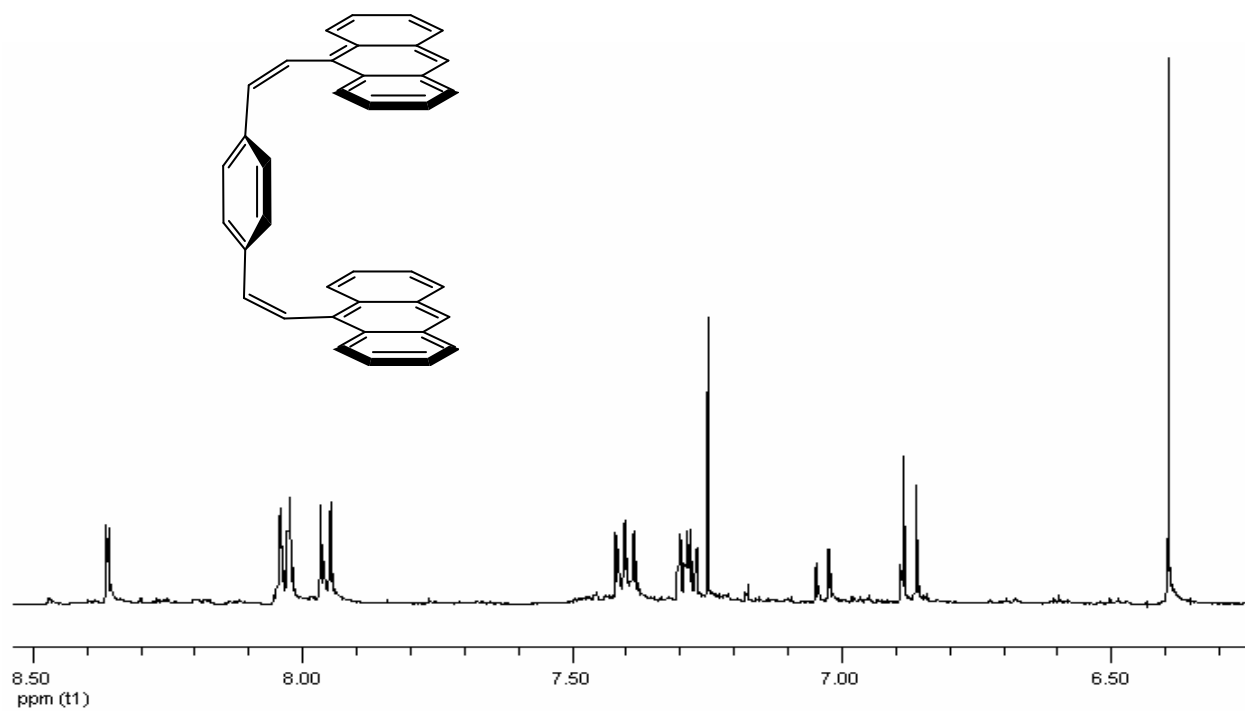
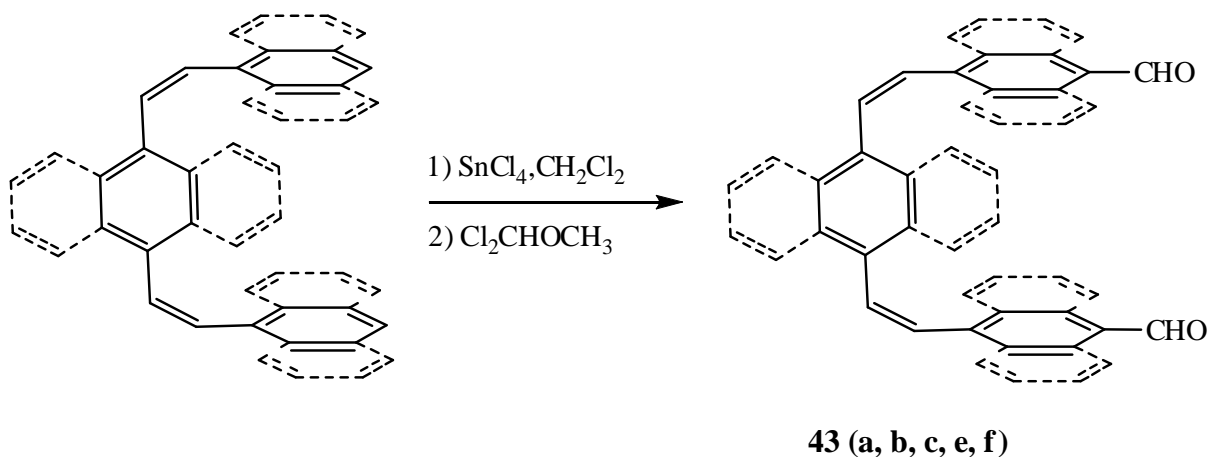


Figure 2-7. ¹H-NMR (500 MHz, CDCl₃/TMS) spectra of the arylene-ethenylene **42a** (top) and **42b** (bottom) at room temperature.

2.2.3. Synthesis of the dialdehyde of ethenylarenes **43** (a, b, c, d, e, f)

Using the same approach and similar conditions as explained in section 2.1.2. for compound **27**, the dialdehyde of ethenylarenes **43**, were also prepared in fairly good yields. Unexpectedly, compound **43d** did not yield any formylated products. The reason for this deviating behavior could not be explained.



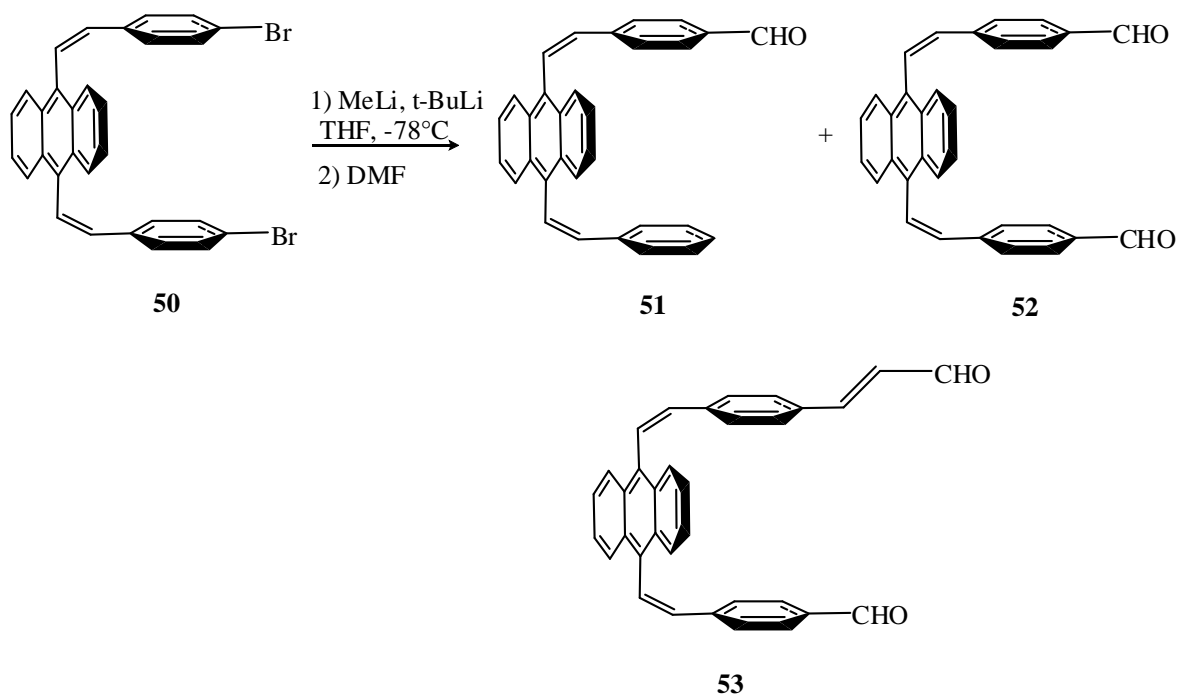
Scheme 2-13. Synthesis of the dialdehyde of ethenylarenes **43** (a, b, c, e, f) (Refer to scheme 2-8, page 32 for the clarity).

The formylation of compound **50** using a similar method already explained for compound **34** (Section 2.1.2.), furnished compound **51** as the main product, besides compound **52** as a minor side product. To improve the yield of the reaction, other alkyllithium reagents such as *sec*- and *tert*-BuLi were used. However, the combination of the both alkyllithium reagents gave better yields. The reaction conditions are listed in table 2-3.

Table 2-3. Formylation reaction of **50** with different alkyllithium reagents.

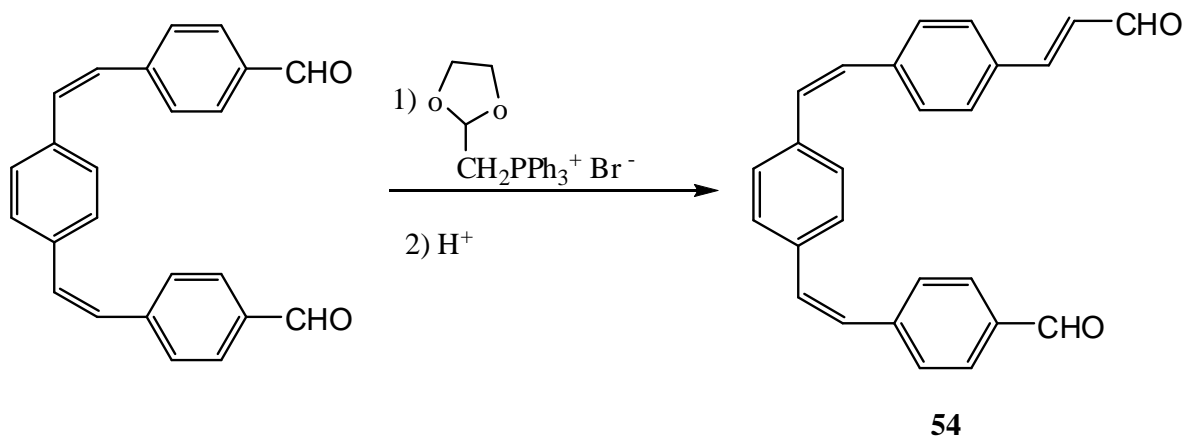
Entry	Reagent	Yield (%)		
		51	52	53
50	<i>n</i> -BuLi	40	5	0
	<i>sec</i> -BuLi	35	8	0
	<i>t</i> -BuLi	20	20	0
	MeLi	28	10	0
	<i>n</i> -BuLi, <i>t</i> -BuLi	20	30	0
	MeLi, <i>t</i> -BuLi	10	55	15

Using the combination of the MeLi and *t*-BuLi reagents improved the yield of the desired compound **52** up to 55% ,besides a small amount of monoformylated compound **51** and the unexpected product **53**.



Scheme 2-14. Improved synthesis of the dialdehyde of ethenylarenes **52** using a mixture of alkyllithium reagents.

Although, the mechanism of formation of compound **53** was not understood, but the similar compound **54** was synthesized by Wittig reaction.^[91]



Scheme 2-15. Synthesis of compound **54** by Wittig reaction.

2.2.4. Synthesis and properties of cyclophanes **55a**, **55b** and **55c**

2.2.4.1. Synthesis

Paracyclophanes **55a**, **55b** and **55c** are they all unknown then cyclophanes were obtained by using the modified McMurry coupling on the preoriented skeleton of *syn*-(*Z,Z*)-9,10-bis(4-formostyryl)anthracene **52**, as shown in figure 2-8 and scheme 2-16.

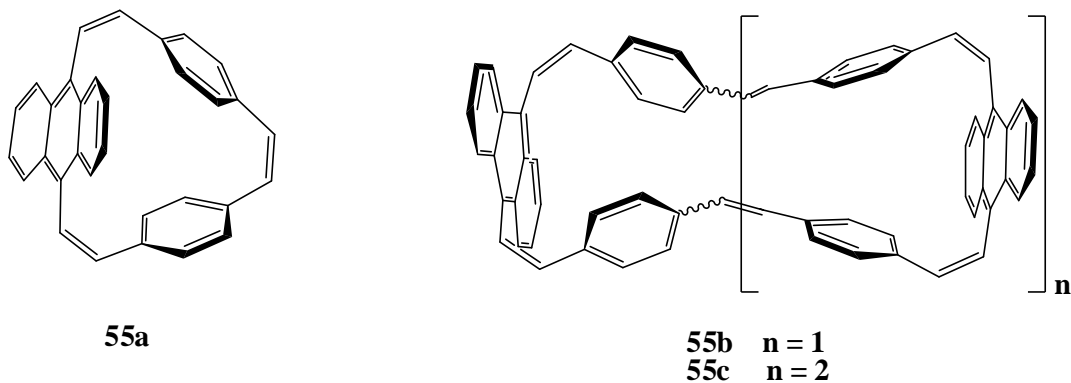
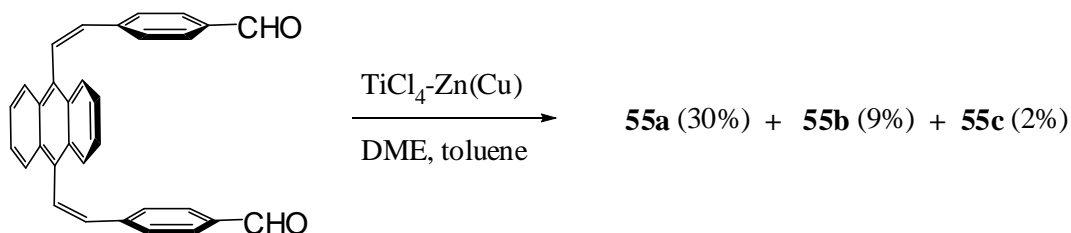


Figure 2-8. Products of the McMurry reaction of **52**.

The products are stable both in solution and solid state at room temperature. The yield of reaction is nearly good.



Scheme 2-16. Synthesis of new [*n*]-*para*-cyclophanes **55a**, **55b** and **55c**.

During the experimental studies, two important factors were found in the carbonyl coupling: 1) the concentration of precursor. 2) the solvent.

2.2.4.2. The effects of concentration

There is a competition between intermolecular and intramolecular coupling in the McMurry reaction of cyclophanes. Intermolecular coupling is favored at higher concentrations of the dialdehyde. On the other hand, slow addition of dialdehyde with low concentration at room temperature directs the reaction toward intramolecular coupling and vice versa.

2.2.4.3. Solvent effects

The solvent has also an the important role in competition between intermolecular and intramolecular coupling in the McMurry reaction. For example, the reaction of dialdehyde **52** in THF solvent gave only monomer **55a** in 20 % yield as the coupling product while in DME solvent monomer **55a** was formed as the main product, besides dimer **55b** in 43 % combined yield. Using the combination of the DME and toluene increased the yield of higher cyclic oligomers namely the

dimer **55b** and trimer **55c**, remarkably. the reactive intermediate are different from those generated in solvents without toluene. Apparently, The reactive intermediates are different from those generated in solvents without toluene. In 2001 Oda *et al.*^[50] reported a similar effect of the solvent in the synthesis of cyclic-*para*-phenylethylenes. They prepared the corresponding higher cyclophanes by a modified McMurry reaction. However, the modified reaction favors the formation of higher cyclic oligomers which are the precursors for the belt-like aromatics. The maximum yields for dimer **55b** and trimer **55c** in the toluene/DME (1:1) solvent mixture are 9 % and 2 %, respectively.

2.2.4.4. Physical properties

The structure of **55a** is clearly supported by ¹H and ¹³C-NMR and X-ray data. The CI and MALDI-TOF mass spectra show the corresponding molecular ion peak ($m/z = 406$). Compound **55a** appears as yellow crystals and is stable under ambient condition for several months without protection from light and air.

Among different stereo-isomers of dimer **55b**, only (*Z,Z,E*)₂ isomer was isolated by crystallization. MALDI-TOF mass spectrum shows the corresponding molecular ion peak ($m/z = 812$). The trimer **55c** appears as red oil and its identification is only based on MALDI-TOF mass spectrometry ($m/z = 1218$). Both compounds, **55b** and **55c** are stable under ambient condition without protection from light and air.

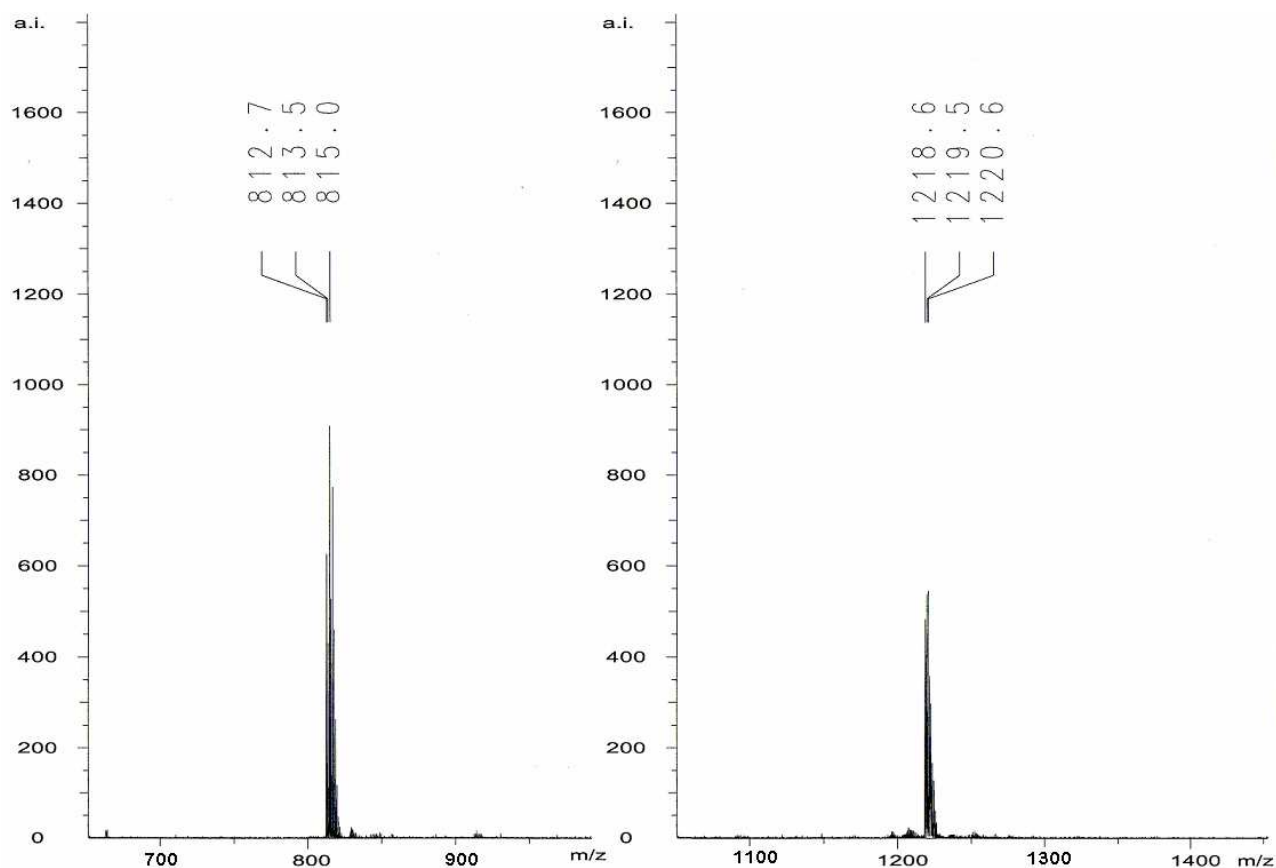


Figure 2-9. MALDI-TOF mass spectrum of **55a** (left) and **55b** (right).

2.2.4.5. NMR spectra

Figure 2-10 shows $^1\text{H-NMR}$ spectrum of **55a** at room temperature. There are a pair of doublets for the benzene protons (AA'XX'), a pair of multiplets for the anthracene protons, a pair of doublets (AA'XX') for the *cis* olefinic protons between benzene and anthracene units and a singlet for the *cis* olefinic protons between two benzene rings. These data indicate C_{2v} symmetry for **55a**.

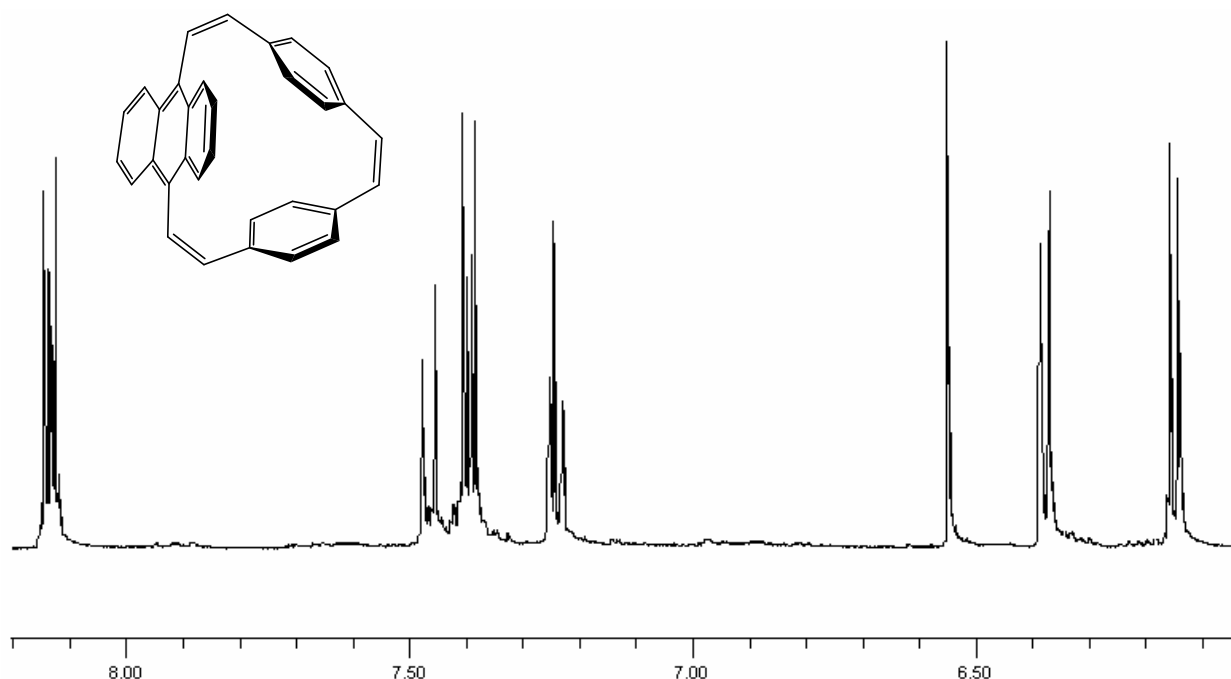


Figure 2-10. $^1\text{H-NMR}$ (500 MHz, CDCl_3/TMS) spectrum of **55a**.

The number of observed signals in the $^{13}\text{C-NMR}$ spectrum of **55a** are in agreement with the number of carbons in the molecule. By using HSQC and COSY NMR techniques, it was possible to assign the olefinic carbons of **55a**. Thus, chemical shifts for the *cis* double bonds between the benzene and anthracene units are 135.6 and 129.4 ppm while, chemical shift for the *cis*-double bond between two benzene rings is 132.7 ppm.

To compare experimental and theoretical data, the theoretical NMR spectrum was calculated by employing GIAO methodology at B3LYP/6-31G(d) level.^[92,93] Geometry of crystal structure was applied in NMR calculation without any optimization. Unlike, the experimental spectrum which shows a simple structure with C_2 symmetry, the calculated spectrum is more complicated. This difference could be interpreted by lack of symmetry in crystal structure (C_s). Thereby, the average theoretical $^1\text{H-NMR}$ chemical shifts listed in table 2-4. The values between theoretical and experimental show an acceptable agreement.

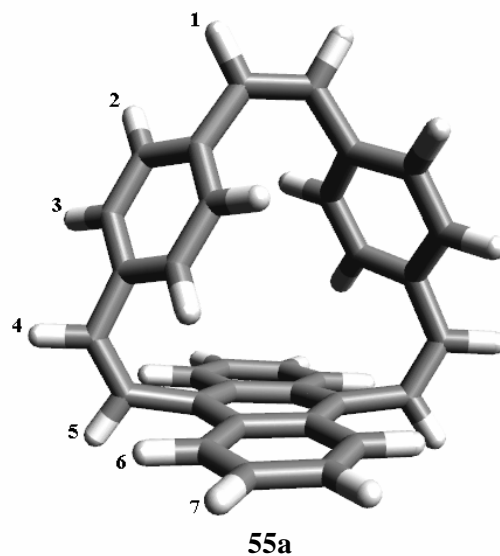


Table 2-4. Computed and experimental $^1\text{H-NMR}$ chemical shifts (ppm) for monomer **55a**.

Atom number	Chemical shifts (ppm)	
	Theoretical ^a	Experimental
H-1	6.48	6.59
H-2	6.13	6.25
H-3	6.36	6.44
H-4	7.23	7.28
H-5	7.50	7.49
H-6	8.11	8.16
H-7	7.37	7.46

^a Average values

Figure 2-11 shows a simple $^1\text{H-NMR}$ spectrum of **55b** at room temperature. There are a pair of doublets for the benzene protons (AA'XX'), a pair of multiplets for the anthracene protons, a pair of doublets (AA'XX') for the *cis* olefinic protons between benzene and anthracene units and a

singlet for the *trans* olefinic protons between two benzene rings. These data indicate to a (*Z,Z,E*)₂ isomer of **55b** with *C*₂ symmetry.

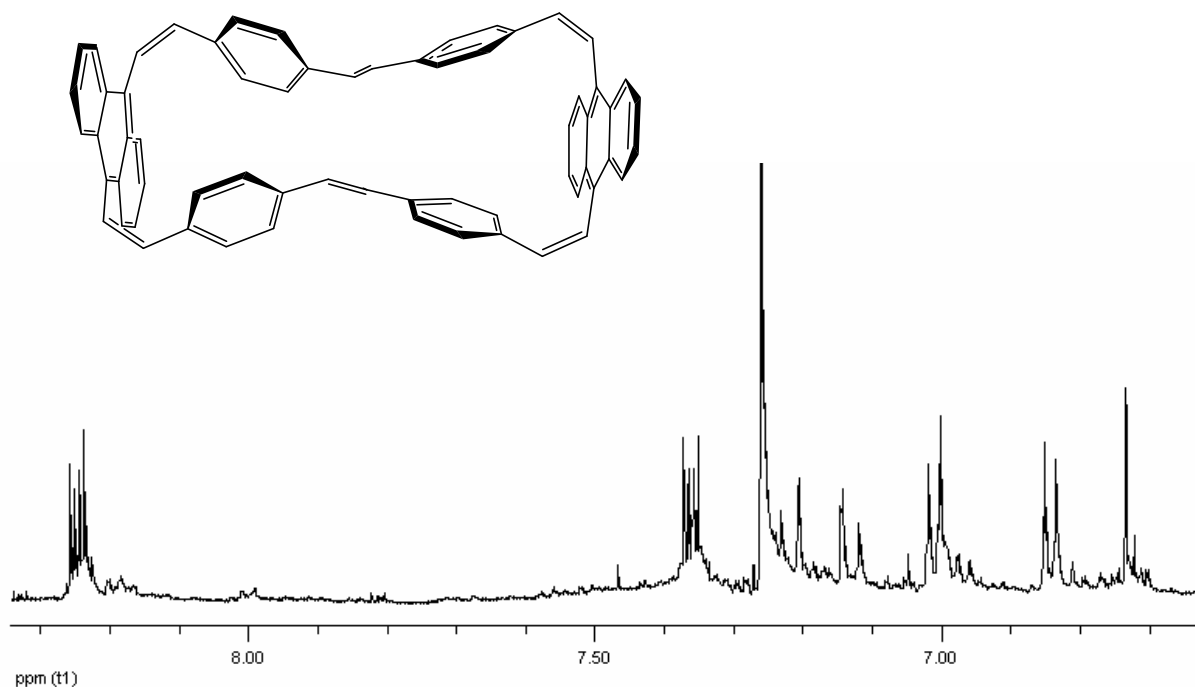


Figure 2-11. ¹H-NMR(500 MHz, CDCl₃/TMS) spectrum of **55b**.

¹H-NMR spectrum of **55c** at room temperature shows a broadened peak in aromatic region.

2.2.4.6. UV-Vis spectra

The absorption spectra of **55a**, **55b** and **55c** are shown in figure 2-12. The compounds show a similar strong absorption around 263 nm. The spectra around 400 nm are concerned to π -bond absorption which shift to longer wavelength region with an increase in size of rings (**55a** < **55b** < **55c**).^[74]

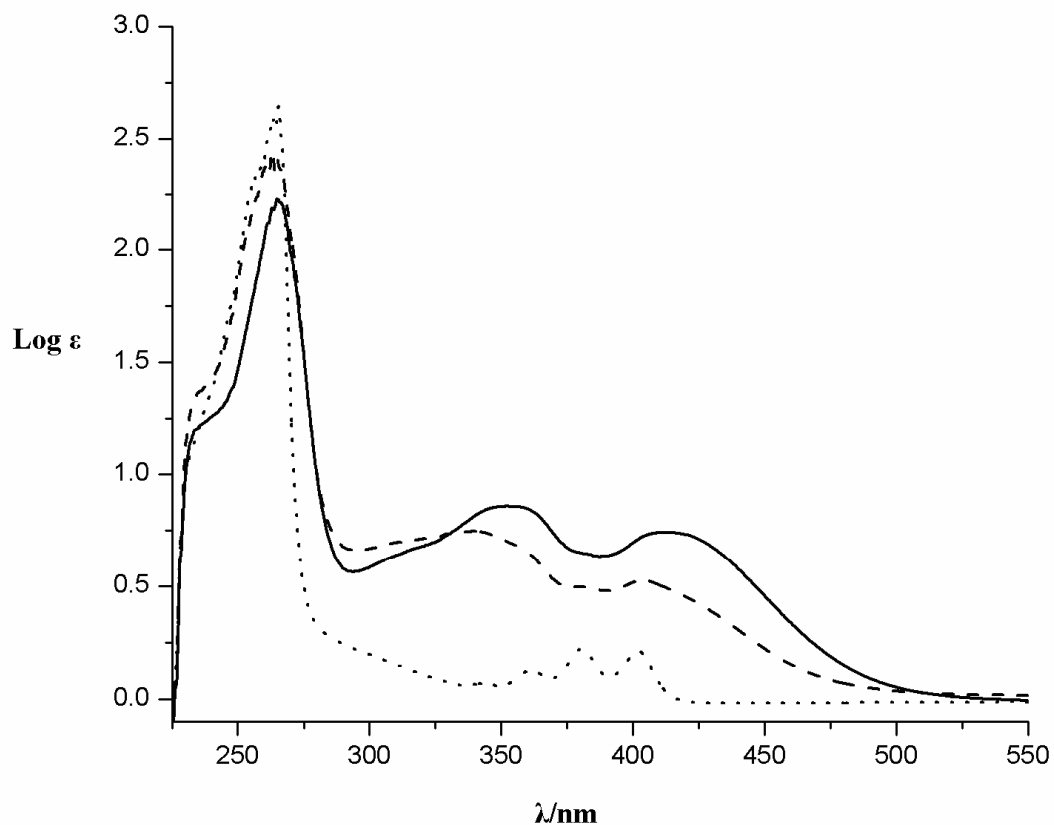


Figure 2-12. UV-Vis spectra of **55a** (dotted line), **55b** (dashed line) and **55c** (solid line) in CH_2Cl_2

2.2.4.7. X-ray analysis of **55a**

Fine needle-like crystals of **55a** were obtained from a CH_2Cl_2 /hexane solution by slow evaporation of the solvent. According to the crystal structure the three double bonds lie approximately in a plane. The phenyl rings are twisted by about 50° and the anthracene unit about 90° with respect to the average plane through the three double bonds (Figure 2-13). A cyclic conjugation of the aryl units and the double bonds, therefore, is not possible. The unit cell contains 8 molecules in which four central molecules overlap same molecules from adjacent unit cells in an edge to edge interaction. Therefore, the crystal possesses open channels that result from the regular arrangement

of the molecules. While, such channels were not observed for four side molecules respect to those of four central molecules .

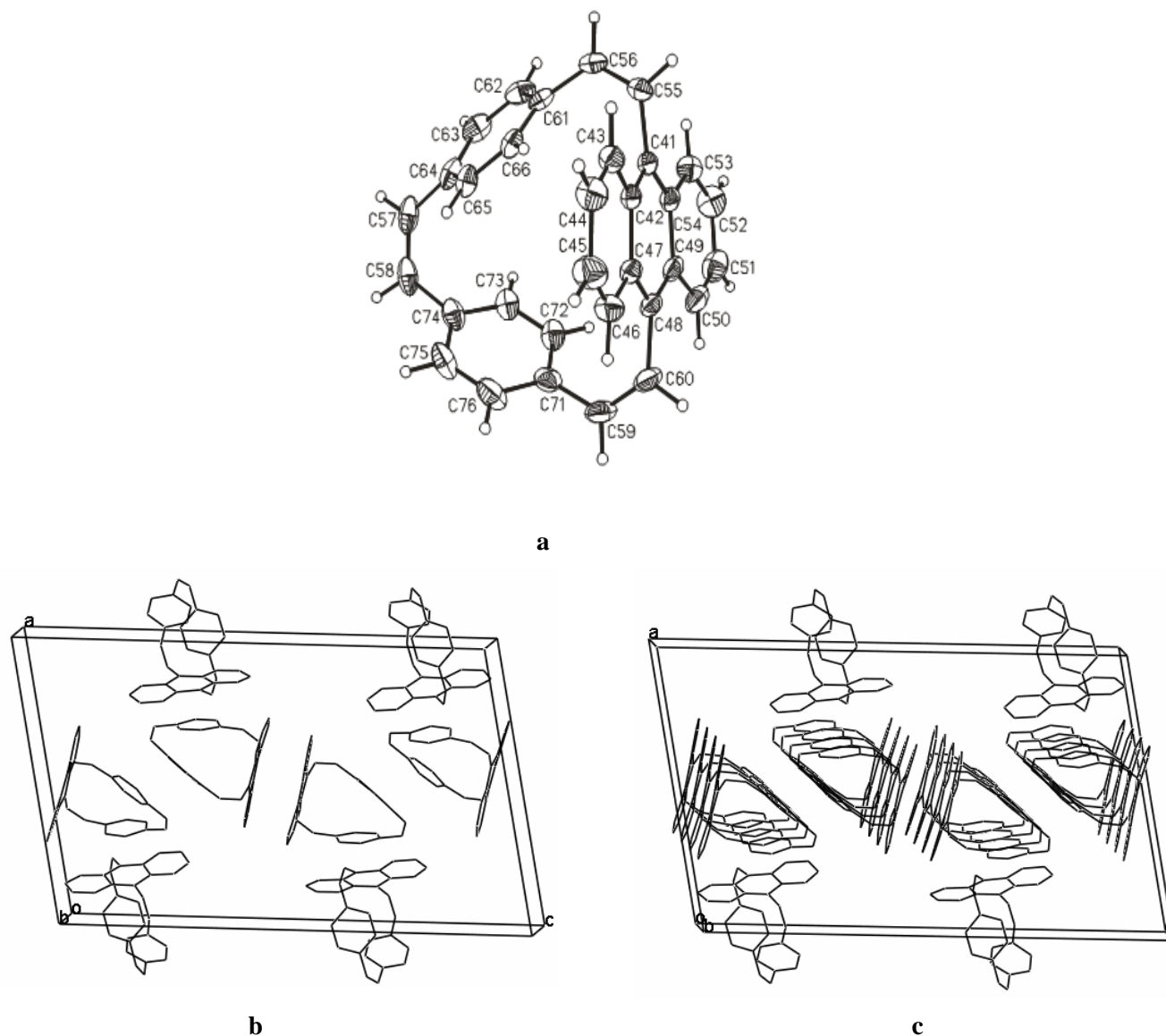


Figure 2-13. ORTEP representation of crystal structure **55a**: a) Molecule of **55a**, b) and c) Views on the molecular packing.

The theoretical studies predict similar structure parameters of monomer **55a**. Full optimization of geometry has been carried out at the B3LYP/6-31G(d) (Figure 2-14). Table 2-5 lists the theoretical structure parameters of **55a** compared to those of X-ray analysis. There is a good agreement between the calculated and the X-ray values.

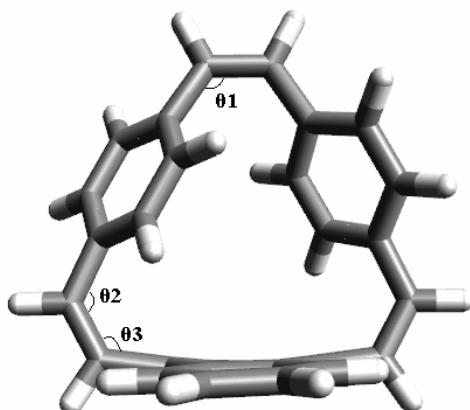


Figure 2-14. Optimized structure of **55a**

Table 2-5. Comparison of calculated and X-ray geometrical data for **55a**

	B3lyp/6-31G(d)	X-ray ^a
Twist angles of benzene rings [°] ^b	48.24	50.65
Twist angle of anthracene unit [°] ^b	89.87	91.30
Olefinic bond length [Å]	1.348	1.330
Olefinic bond angle [Å]	124.66(θ_1), 126.39(θ_2), 125.39(θ_3)	124.32(θ_1), 124.65(θ_2), 123.96(θ_3)

^a Average values. ^b Average plane with respect to the three double bonds.

The structure of **55b** could also be determined by X-ray analysis. X-ray crystallographic analysis shows that **55b** has C_1 (almost D_2) symmetry. The benzene rings are twisted about 6° and the anthracene units are twisted 90° with respect to the average plane through the four *cis* double bonds. The T-type structure of unit cell contains 5 molecules together with 4 molecules of CH_2Cl_2 solvent.

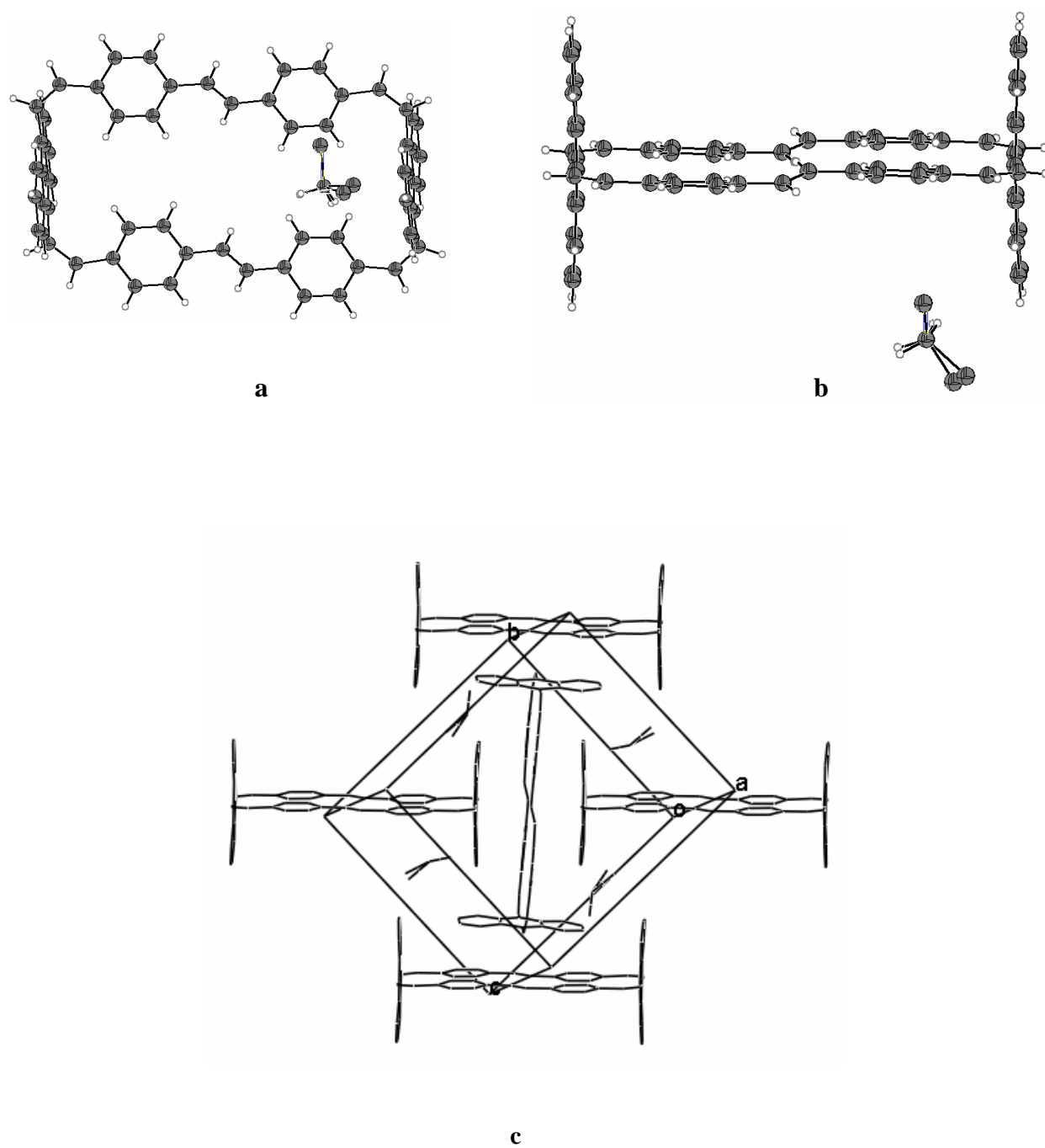


Figure 2-15. ORTEP representation of crystal structure of **55b**: a) Plane view b) Side view and c) View on the molecular packing.

2.2.5. Synthesis and properties of cyclophanes **56b** and **56c**

2.2.5.1. Synthesis

The paracyclophanes **56b** and **56c** and the unexpected ring open compound **56a-b** as unknown cyclophanes were synthesized using the McMurry coupling of *syn*-(*Z,Z*)-1,4-bis[(9-ethenyl-10-formyl)anthracenyl]benzene **43a**.(Figure 2-16)

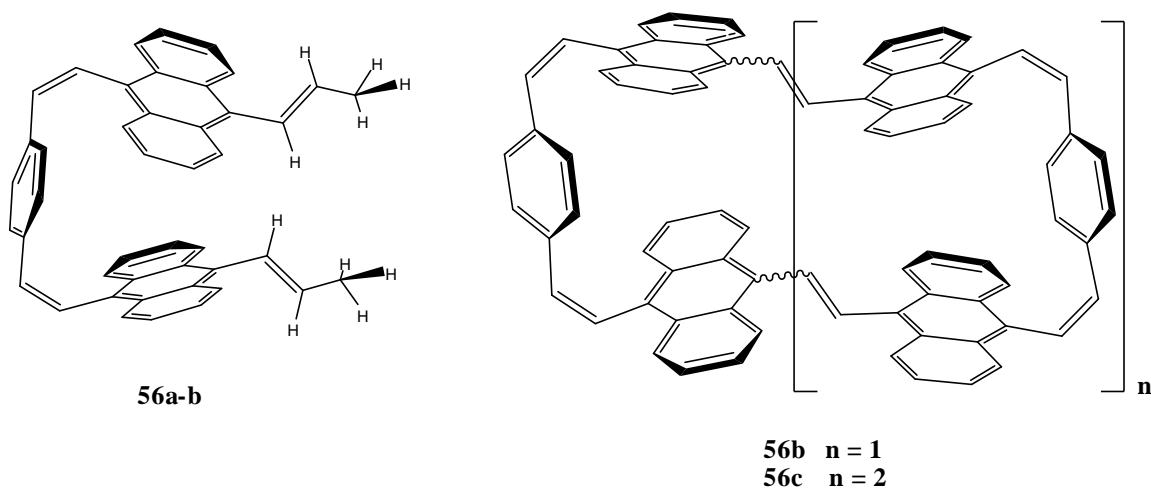
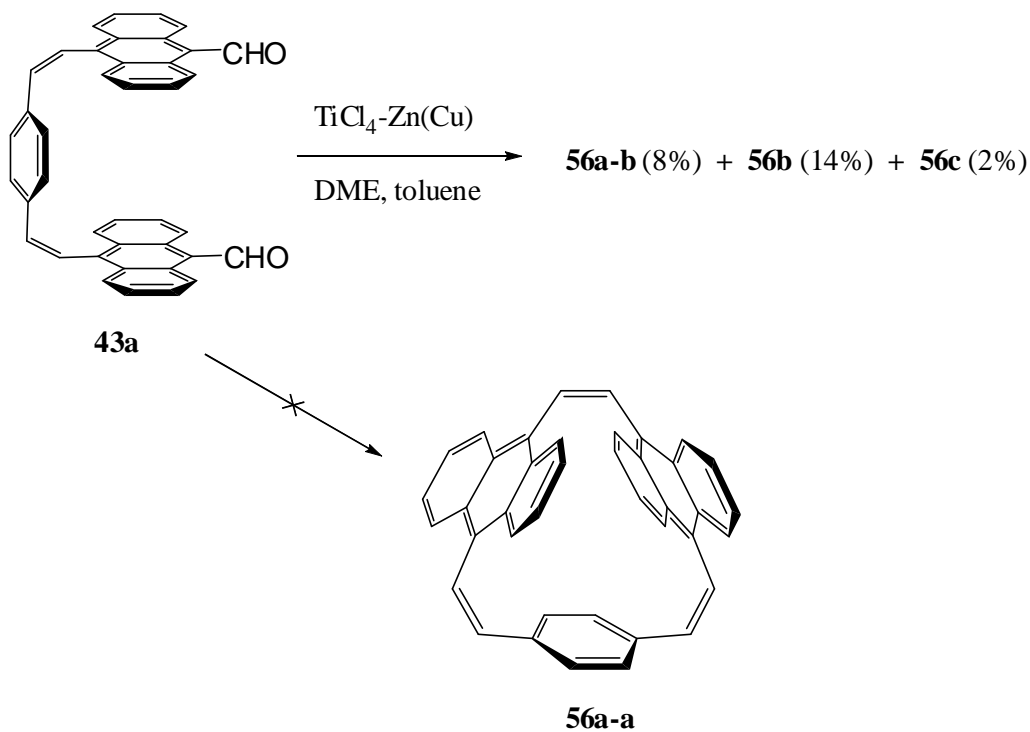


Figure 2-16. Products of the McMurry coupling of **43a**.

Using the same approach and similar conditions, however, the main products were the dimer **56b** and the unexpected open ring compound **56a-b** as well as trimer **56c**, which was formed in lower yields. Probably, the open ring compound **56a-b** is a decomposition product of monomer **56a-a** which was formed because of the sterical hindrance between the two opposed anthracenes as shown in the molecular structure.

The maximum yields for dimer **56b** and trimer **56c** in the toluene/DME (1:1) solvent mixture are 14 % and 2 %, respectively.



Scheme 2-17. Synthesis of new $[n]$ -para-cyclophanes of **56b** and **56c**.

2.2.5.2. Physical properties

Cyclophane **56b**, an orange solid, is fairly stable in air. Purification on silica gel does not lead to decomposition. Its molecular ion peak is observed at $m/z = 1012$ in MALDI-TOF mass spectrum. The trimer **56c** could not be separated by flash column chromatography. Its identification is only based on MALDI-TOF mass spectrometry ($m/z = 1518$). The structure of **56a-b** is clearly supported by the spectral data. Also, CI mass spectrum shows the corresponding molecular ion peak ($m/z = 562$).

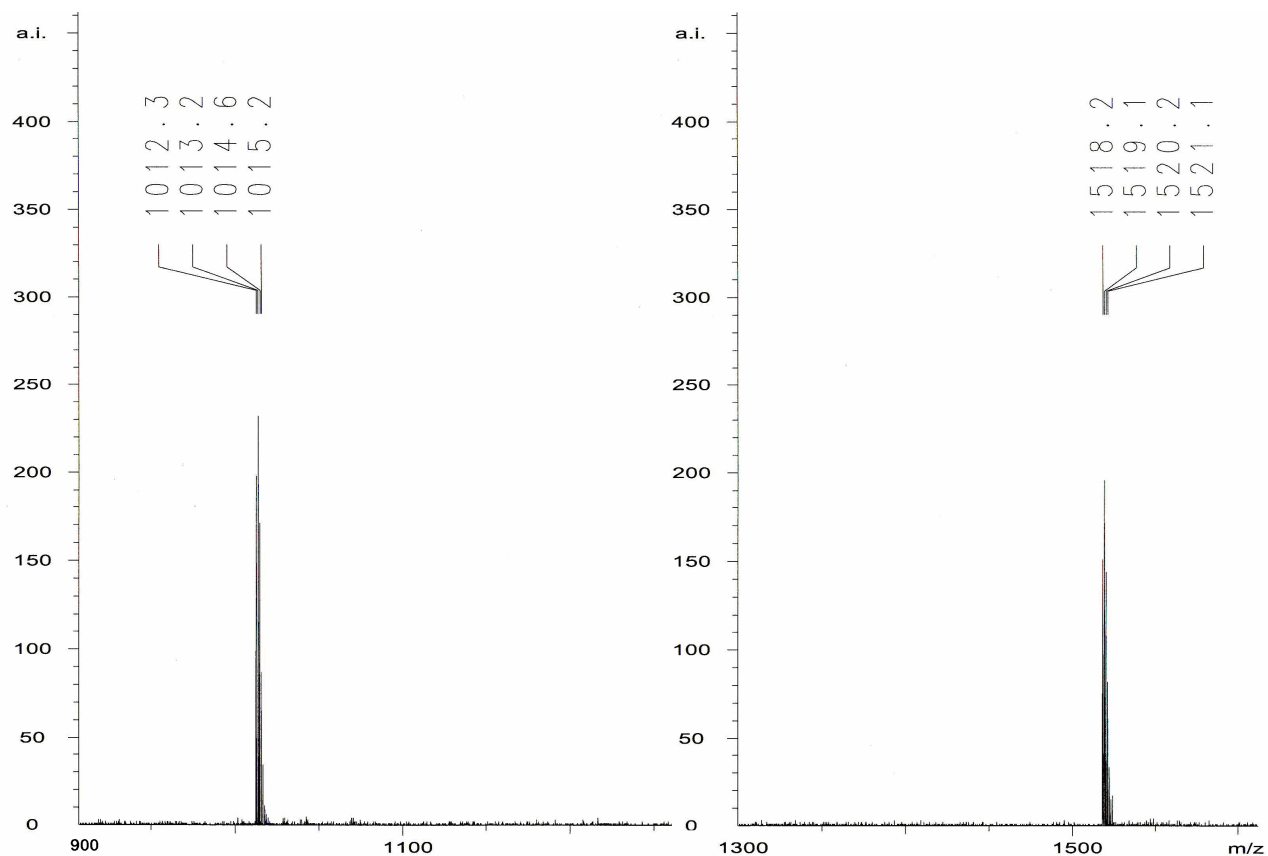


Figure 2-17 . MALDI-TOF mass spectrum of **56b** (left) and **56c** (right).

2.2.5.3. NMR data

The structure of dimer **56b** could be assigned by ^1H and ^{13}C -NMR spectra data. Figure 2-18 presents the ^1H -NMR spectrum of **56b** at room temperature in CD_2Cl_2 . Number of independent hydrogens in the structure are in a good agreement with number of signals in the ^1H -NMR spectrum.

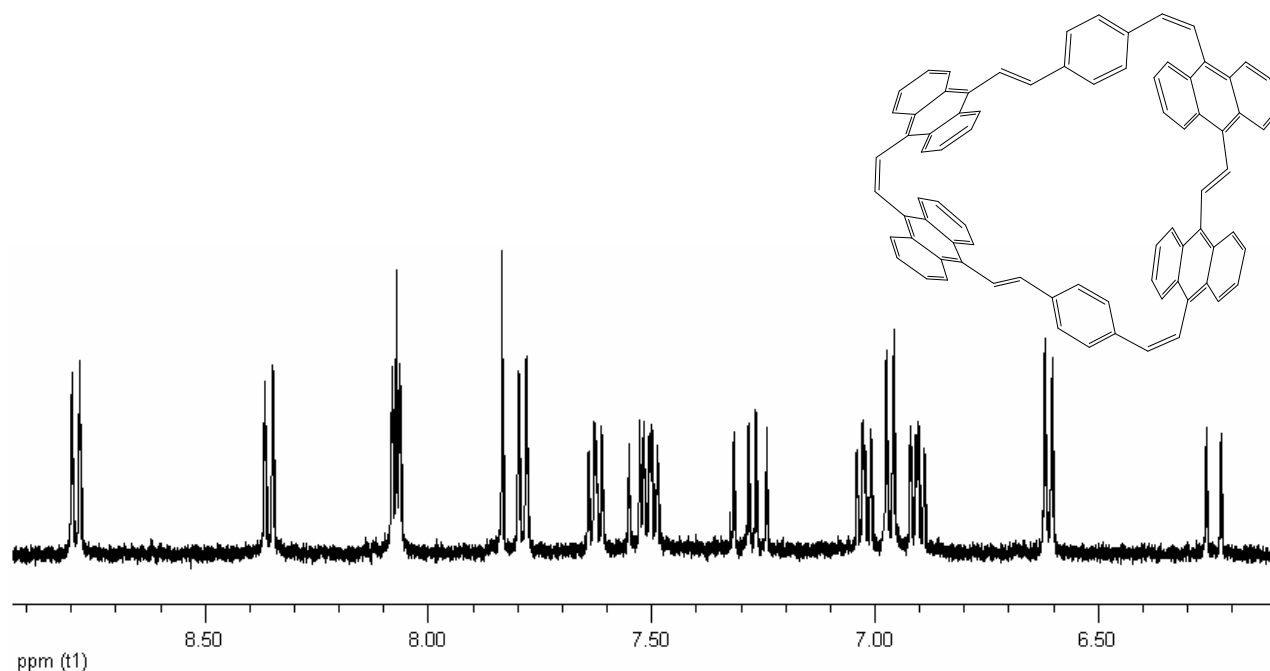


Figure 2-18. ¹H-NMR (500 MHz, CDCl₃/TMS) spectrum of **56b**.

The ¹H and ¹³C-NMR spectra support the structure of **56a-b**, clearly. The ¹H-NMR shows a doublet for the methyl protons in the aliphatic region (2.18 ppm), a quartet for the *cis* olefinic protons connected to the methyl group, a pair of doublets (AA'XX') for the *cis* olefinic protons between anthracene and benzene units, a singlet for the benzene protons, a doublet for the olefinic protons connected to the anthracene unit and two multiplets for the anthracene protons.

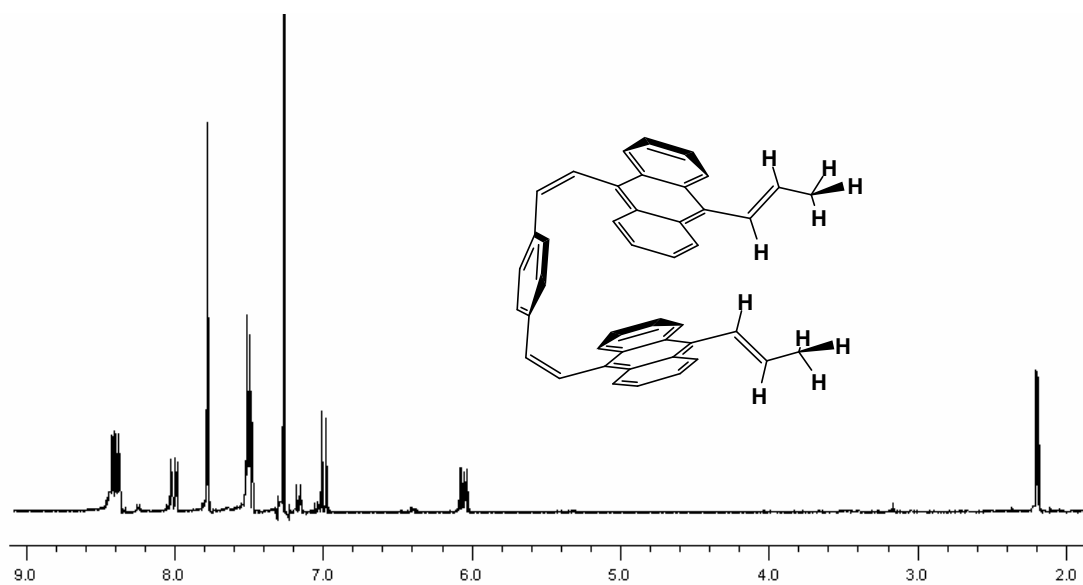


Figure 2-19. ¹H-NMR (500 MHz, CDCl₃/TMS) spectrum of **56a-b**.

¹H-NMR spectrum of **56c** at room temperature shows a broadened peak in aromatic region.

2.2.5.4. X-ray analysis of **56b**

The red cube-like crystals of **56b** were obtained from a benzene solution by slow evaporation of the solvent. The crystal structure are surrounded with several benzene molecules. The unit cell contains 6 independent molecule units together with several benzene molecules. Two of these independent structures have the Möbius topology and others accepted the Hückel topology.

Based on a prediction by Heilbronner,⁹⁴ annulenes with the topology of a Möbius should be stable if they contain $4n$, rather than $4n+2$, π electrons. The first experimental example of a $[4n]$ annulene derivative with a Möbius twist, was synthesized and isolated by Herges *et al.*⁹⁵ Other recent interesting examples are di-*p*-benzihexaphyrin and *meso*-aryl-substituted [28]hexaphyrins(1.1.1.1.1.1) reported by Latos-Grazynski *et al.*⁹⁶ and Atsuhiko Osuka *et al.*⁹⁷ that exhibit Möbius topology.

Herein we reported the synthesis of single (Möbius) and double twisted (Hückel) [36]annulene. All strips with an even number of 180° twists should follow the Hückel rule and all bands with an odd number of twists are Möbius systems.⁹⁸ The structures of the single- and double twisted isomers were confirmed by X-ray analysis (Figure 2-20). The unit cell included three pairs of enantiomers. Two pairs are almost identical and double twisted and hence Hückel. One enantiomeric pair is singly twisted and thus has Möbius topology.

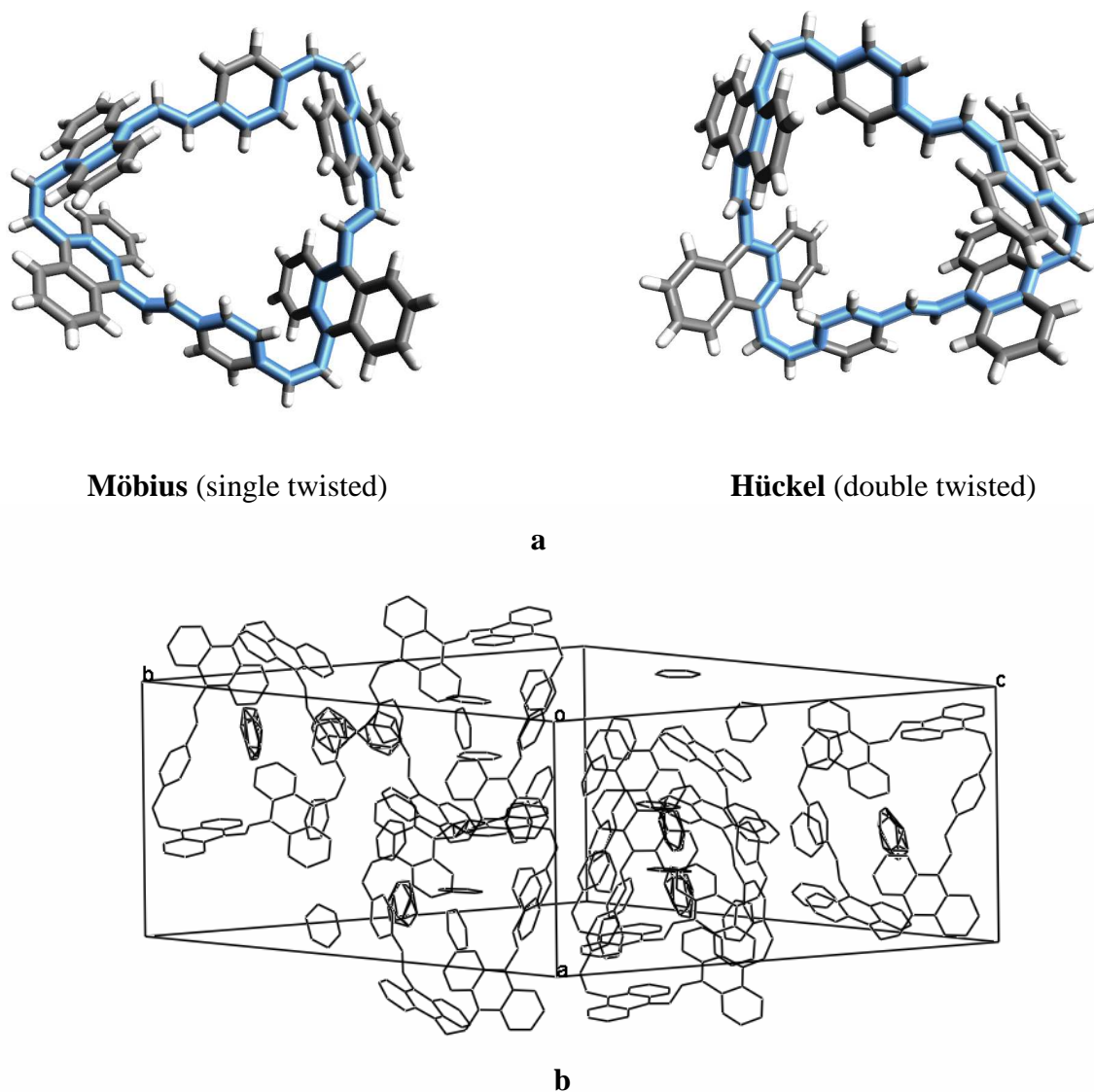


Figure 2-20. a) X-ray structures of the single twisted Möbius and the double twisted Hückel isomer of a [36]annulene. b) view on the unit cell.

2.2.6. Synthesis and properties of cyclophanes **57a-a**, **57b** and **57c**

2.2.6.1. Synthesis

Another new set of cyclophanes containing **57a-a**, **57b**, **57c** and also unexpected ring open compound **57a-b** were synthesized by the McMurry coupling of *syn*-(*Z,Z*)-1,4-bis[(9-ethenyl-10-formyl)anthracenyl]naphthalene **43b** as shown in figure 2-21 and scheme 2-18.

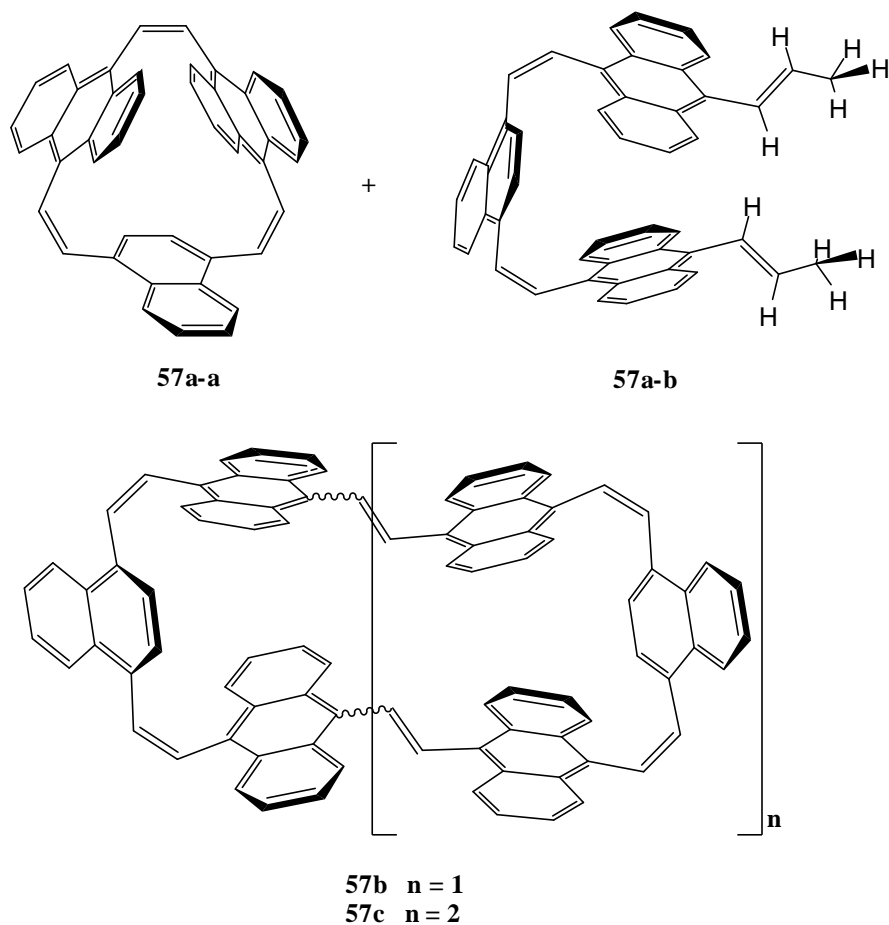
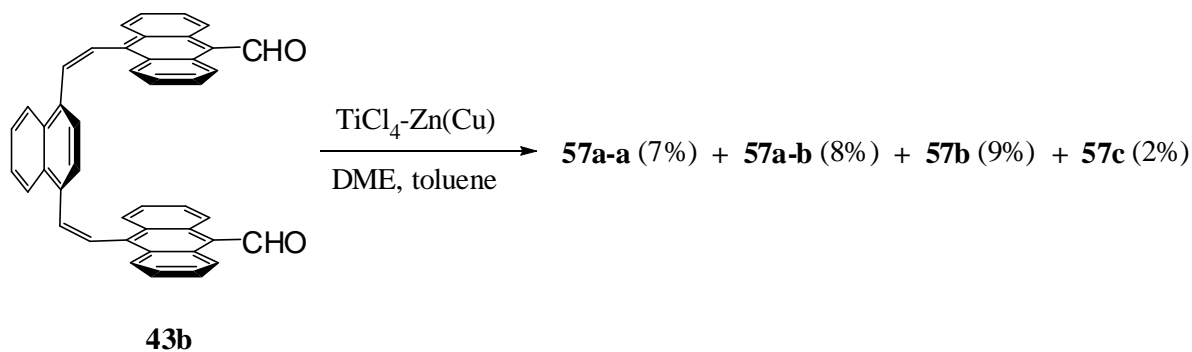
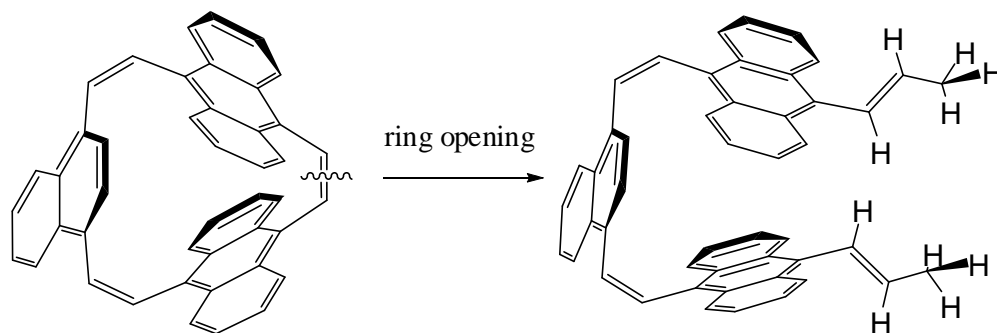


Figure 2-21. Products of McMurry reaction **43b**.

Using the same approach and similar conditions, dimer **57b** was formed in higher yield in comparison with the lower yield of trimer **57c**, monomer **57a-a** and the open ring compound **57a-b**. Compound **57a-b** is a decomposition product of compound **57a-a**, formed as outlined discussing of compound **56a-a**. But, compared to the decomposition of **56a-a**, this was not 100%. Probably, **57a-a** has a more stable molecular structure than **56a-a**.



Scheme 2-18. Synthesis of new $[n]$ -*para*-cyclophanes of **57a-a**, **57b**, **57c**.



Scheme 2-19. The ring opening of **57a-a** under reflux condition.

As already mentioned, intermolecular coupling strategies for the synthesis of higher cyclic oligomers are favored under the high concentrations of the dialdehyde and increased toluene concentration in the solvent mixture (toluene/DME : 1/1). The maximum yields for dimer **57b** and trimer **57c** in the toluene/DME (1:1) solvent mixture are 9 % and 2 %, respectively.

2.2.6.2. Physical properties

The structure of **57a-a** is clearly supported by the NMR spectral and X-ray data. The CI and MALDI-TOF mass spectra show the corresponding molecular ion peak ($m/z = 456$). Compound **57a-a** appears as yellow crystals and is stable under ambient condition for several month without protection from light and air,.

Cyclophane **57b**, an orange solid, is fairly stable in air. Purification on silica gel does not lead to decomposition. Its molecular ion peak is observed at $m/z = 1113$ in MALDI-TOF mass spectrum. The attempts to purify trimer **57c** from dimer **57b** by flash column chromatography and even by analytical HPLC failed. Its identification is only based on MALDI-TOF mass spectrometry ($m/z = 1669$). Both compounds, **57b** and **57c**, are stable under ambient condition, without protection from light and air. The structure of **57a-b** is clearly supported by the NMR spectral data. Moreover, the CI mass spectrum shows the corresponding molecular ion peak ($m/z = 612$).

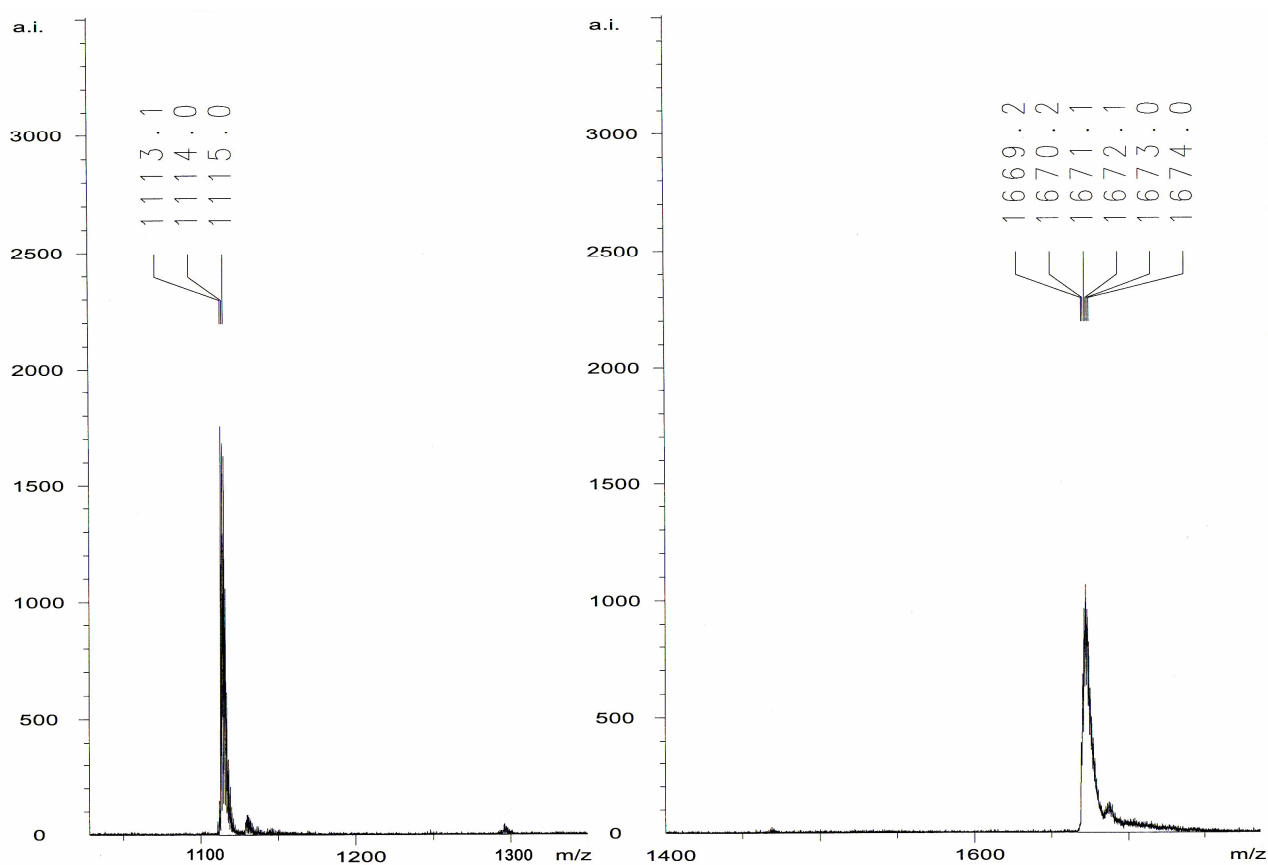


Figure 2-22 . MALDI-TOF mass spectrum of **57b** (left) and **57c** (right).

2.2.6.3. NMR data

Figure 2-23 shows $^1\text{H-NMR}$ spectrum of **57a-a** at room temperature. It shows a pair doublets (AA'XX') for the *cis* olefinic protons between anthracene and naphthalene units and a singlet for the *cis* olefinic protons between two anthracenes units. These data indicate a C_{1v} symmetry for its structure.

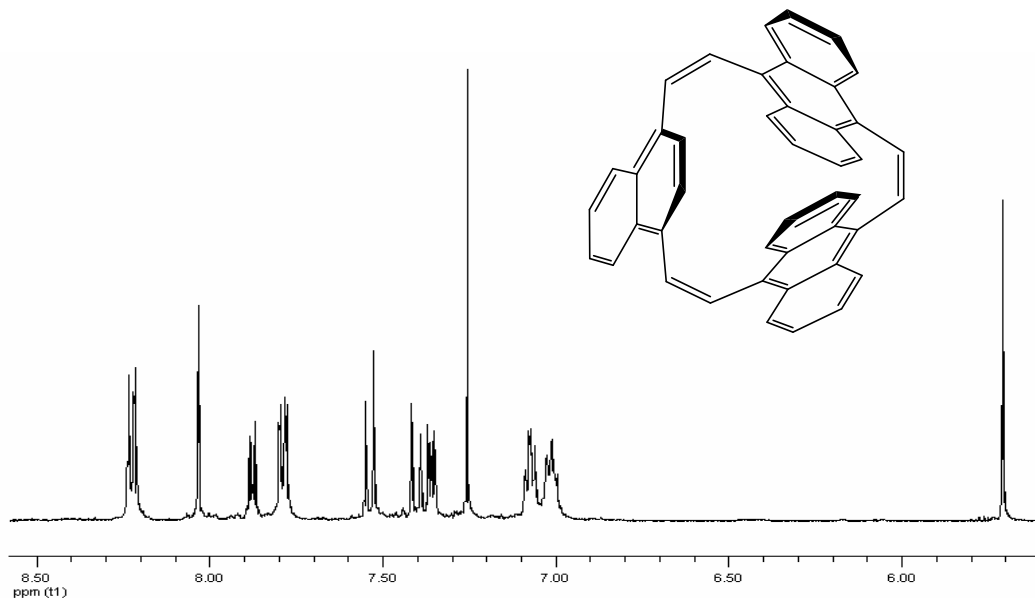
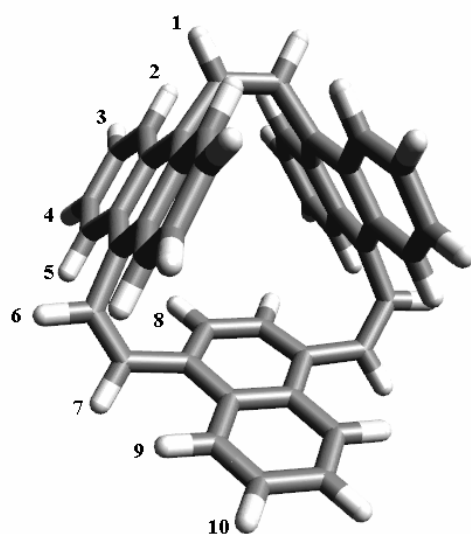


Figure 2-23. $^1\text{H-NMR}$ (500 MHz, CDCl_3/TMS) spectrum of **57a-a**.

The number of observed signals in the $^{13}\text{C-NMR}$ spectrum of **57a-a** are in agreement with the number of carbons in the molecule. Using HSQC and COSY-NMR techniques, it is possible to assign the olefinic carbons of **57a-a**. Thus, chemical shifts for the *cis* double bonds between the anthracene and naphthalene units are 130.4 and 134.2 ppm, while chemical shift for the *cis* double bond between two anthracene units is 134.2 ppm.

The theoretical NMR spectra for compound **57a-a** was constructed by employing GIAO methodology at B3LYP/6-31G(d) level.^[92,93] Geometry of crystal structure was directly applied in NMR calculation without any optimization. The experimental spectrum shows a simple structure with C_2 symmetry in comparison with the complicated calculated spectrum. This difference is due to C_s symmetry of crystal structure. Table 2-6 summarized the experimental and the average theoretical $^1\text{H-NMR}$ chemical shifts. The values show an acceptable agreement.

**57a-a****Table 2-6.** Computed and experimental ¹H-NMR chemical shifts (ppm) for monomer **57a-a**.

Atom number	Chemical shifts (ppm)	
	Theoretical ^a	Experimental
H-1	8.05	8.03
H-2	8.16	8.22
H-3	7.16	7.07
H-4	7.05	7.01
H-5	7.76	7.79
H-6	7.39	7.54
H-7	7.53	7.40
H-8	5.81	5.71
H-9	7.71	7.87
H-10	7.30	7.36

^a Average values.

Figure 2-24 presents the $^1\text{H-NMR}$ spectrum of **57b** at room temperature. The spectrum is more complicated than expected for a single isomer. Probably, it considers three configurations (*ZZ*, *EE* and *EZ*) of the double bonds between two anthracenes in the structure of the ring. Attempts to separate the different stereoisomers failed.

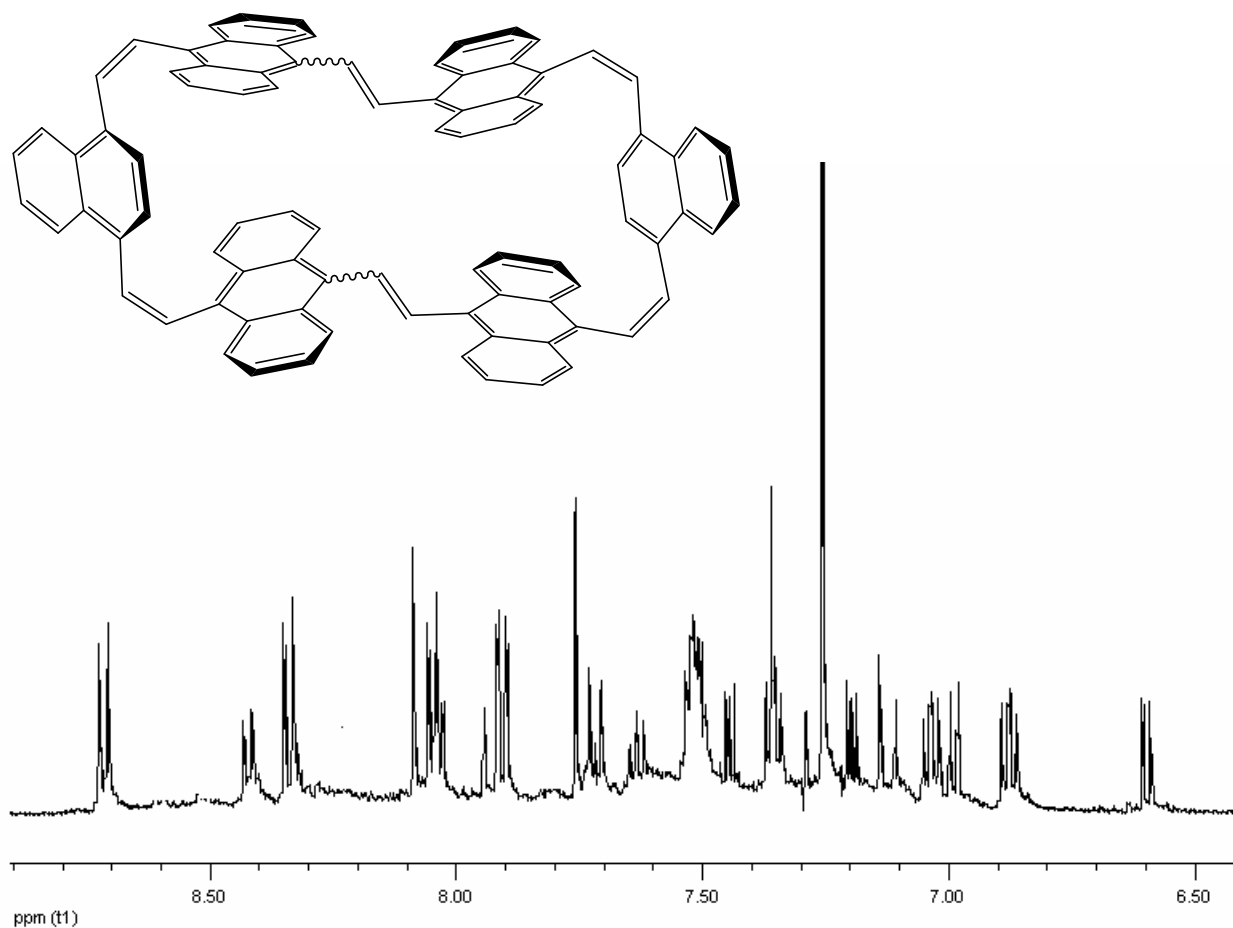


Figure 2-24. $^1\text{H-NMR}$ (500 MHz, CDCl_3/TMS) spectrum of **57b**.

The structure of the opening compound **57a-b** could be assigned by $^1\text{H-}$ and $^{13}\text{C-NMR}$ spectral data. The $^1\text{H-NMR}$ shows a doublet for the methyl protons in the aliphatic region (2.20 ppm), a quartet for the *cis* olefinic protons connected to the methyl group, a pair doublets ($\text{AA}'\text{XX}'$) for the *cis* olefinic protons between anthracene and naphthalene units, a singlet for the naphthalene proton, a

doublet for the olefinic protons connected to the anthracene unit and other signals for the anthracene and naphthalene protons.

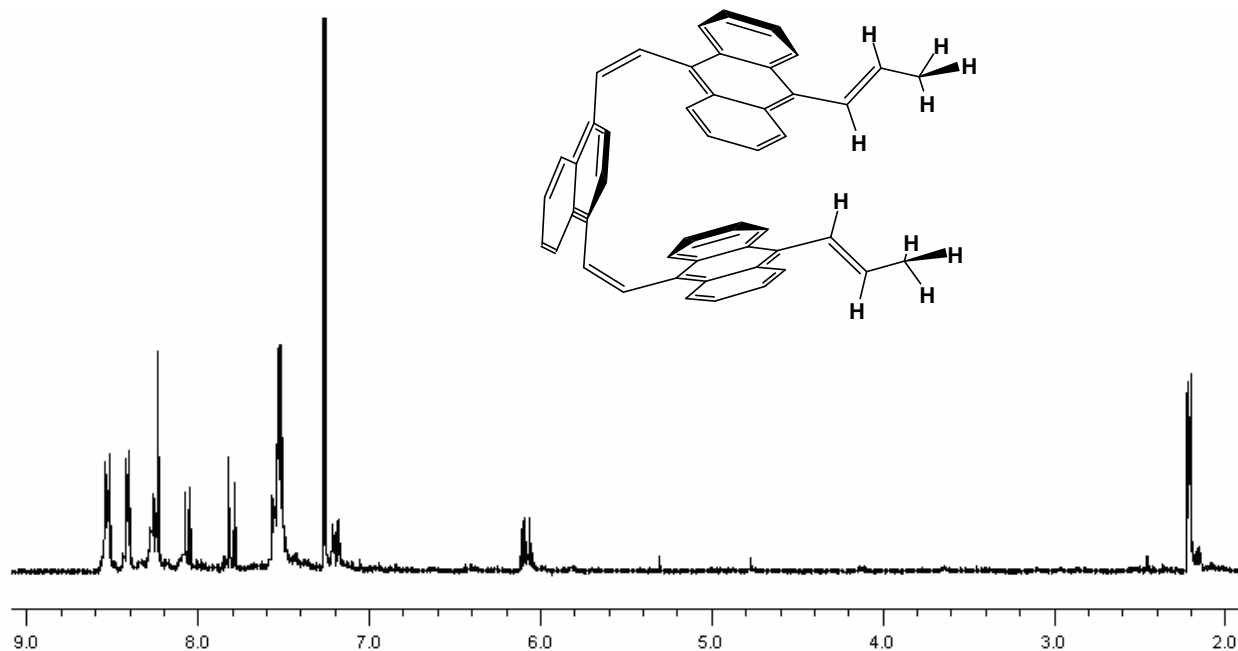


Figure 2-25. $^1\text{H-NMR}$ (500 MHz, CDCl_3/TMS) spectrum of **57a-b**.

2.2.6.4. UV-Vis spectra

Figure 2-26 shows the UV-Vis spectra of **57a-a** and **57b**. The comparison of the spectral data reveals only minor differences with respect to the absorption maxima. Both compounds show a strong absorption around 254 nm. The π -bond absorptions around 400 nm in compound **57b** is shifted and broadened to longer wavelength. This is probably due to an increase in the size and the planarity and consequently, a better conjugation in the ring structure.^[66]

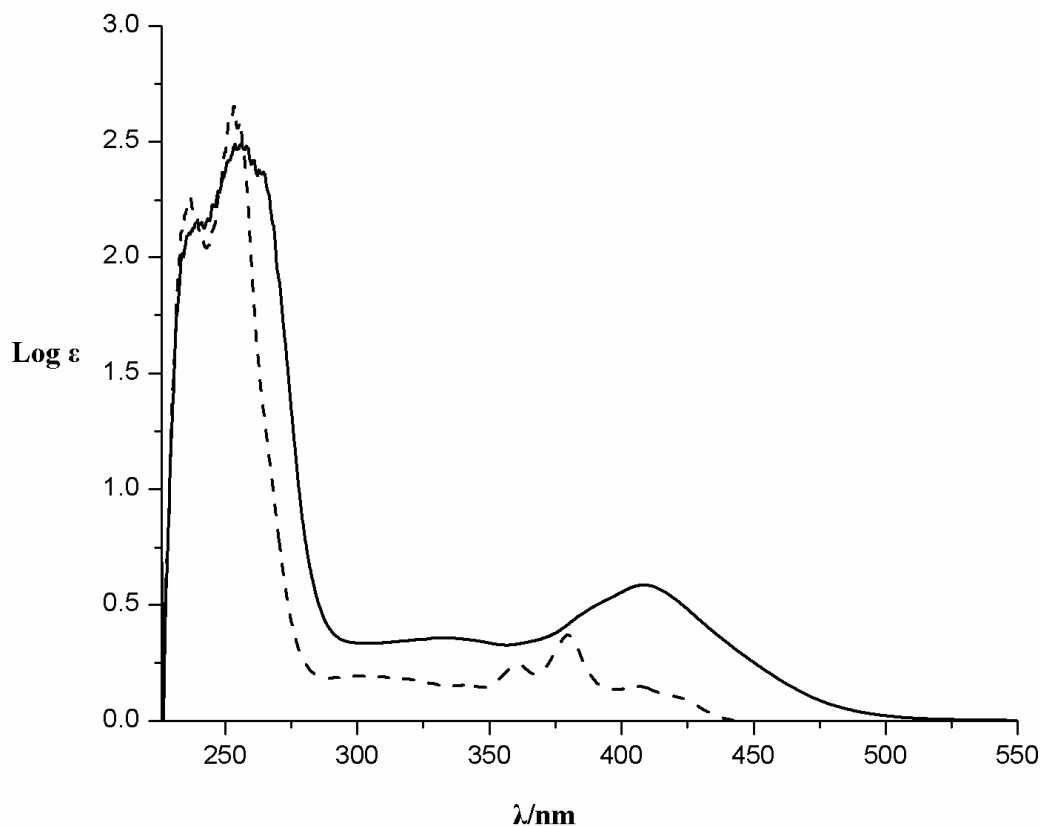


Figure 2-26. UV-Vis spectra of **57a-a** (dashed line) and **57b** (solid line) in CH₂Cl₂.

2.2.6.5. X-ray analysis

The anticipated C_{2v} symmetrical structure of **57a-a** was confirmed by X-ray crystallography analysis (Figure 2-27). The yellow spicular crystals were obtained from a CH₂Cl₂/hexane solution by slow evaporation of the solvent.

In the cone-shaped crystal structure, the naphthalene unit is twisted about 58° and the anthracenes units about 90° with respect to the average plane through the three double bonds. The average cavity size between each aromatic ring and the opposite double bond is amounted to 6.5 Å. The crystal packing includes 4 molecules.

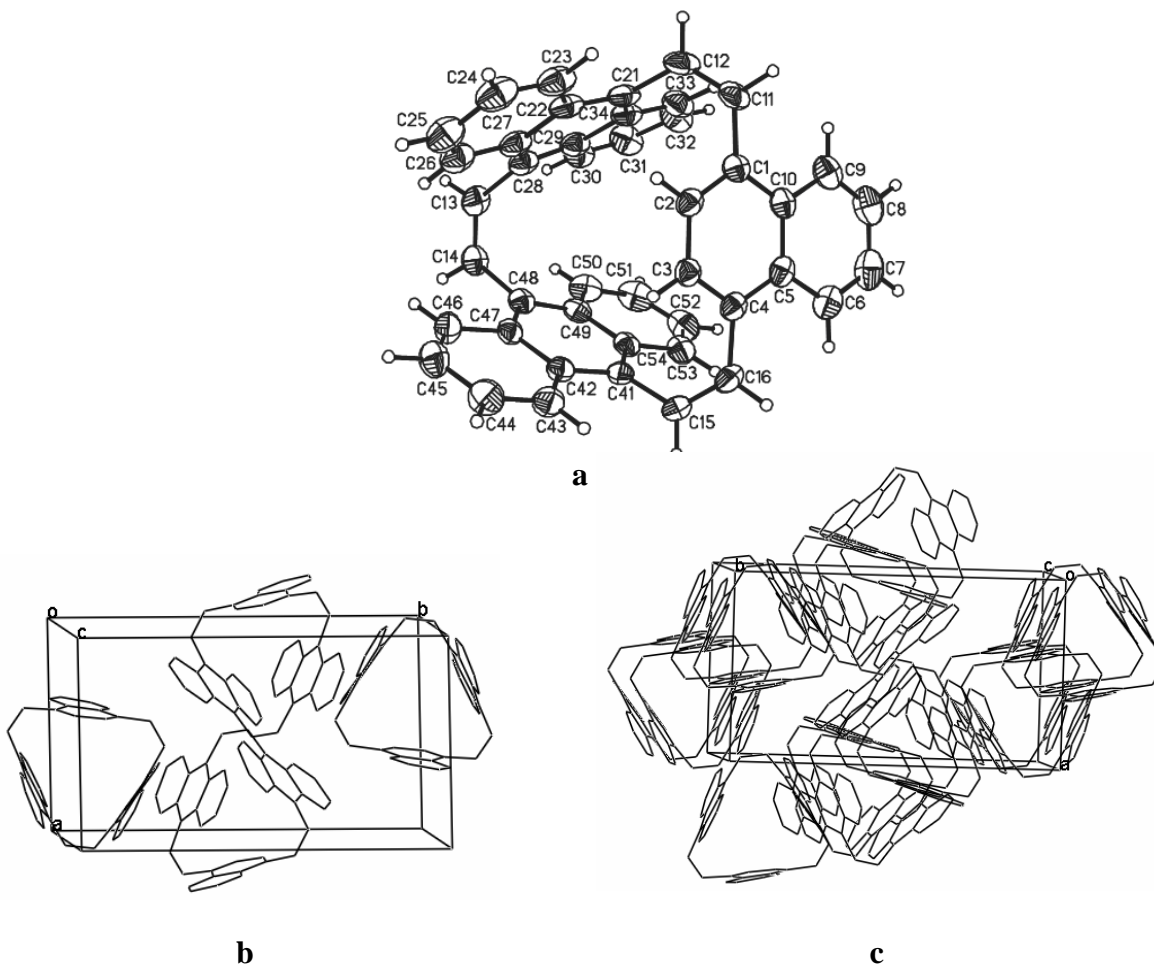


Figure 2-27. ORTEP representation of crystal structure **57a-a**. a) molecule of **57a-a**, b) and c) views on the molecular packing.

A DFT calculation at B3LYP/6-31g(d) level was performed on compound **57a-a** to find the optimum geometry. The calculated structure shows a similar conformation compare to the X-ray structure (Figure 2-28). According to table 2-7, the calculated data are in a good agreement with those of the X-ray analysis. The only remarkable discrepancy between calculated and X-ray values is the twist angle of the naphthalene unit.

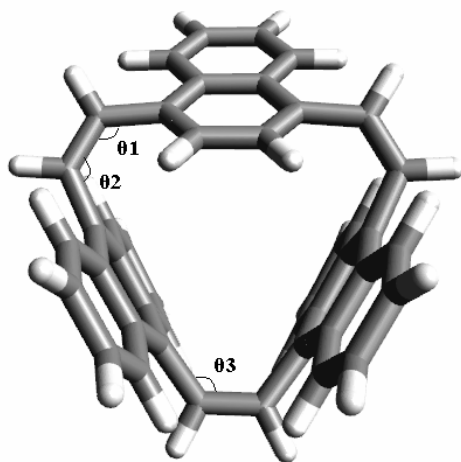


Figure 2-28. The optimized structure of **57a-a**.

Table 2-7. Comparison of calculated and X-ray geometrical data for **57a-a**.

	B3LYP/6-31G(d)	X-ray ^a
Twist angles of naphthalene unit [°] ^b	53.82	58.33
Twist angle of anthracene units [°] ^b	95.72	97.35
Olefinic bond length [Å]	1.344	1.327
Olefinic bond angle [Å]	125.82(θ_1), 124.96(θ_2), 124.87(θ_3)	124.30(θ_1), 123.45(θ_2), 123.06(θ_3)

^a Average values. ^b average plane with respect to the three double bonds.

2.2.7. Synthesis and properties of cyclophanes **58b** and **58c**

2.2.7.1. Synthesis

Unique cyclophanes **58b** and **58c** which contain only anthracene units in their structures, were synthesized by the McMurry coupling of *syn*-(*Z,Z*)-9,10-bis[(9-ethenyl)-10-

formyl)anthracenyl]anthracene **43c**, as shown in figure 2-29 and scheme 2-20. Unfortunately, the ring open compound **58a-b** was only found instead of monomer **58a-a** which has a high symmetry structure.

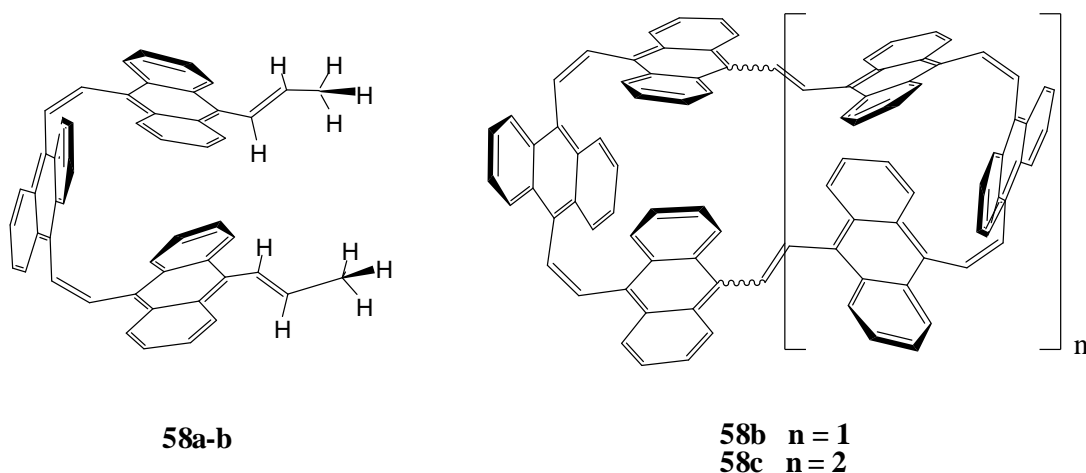
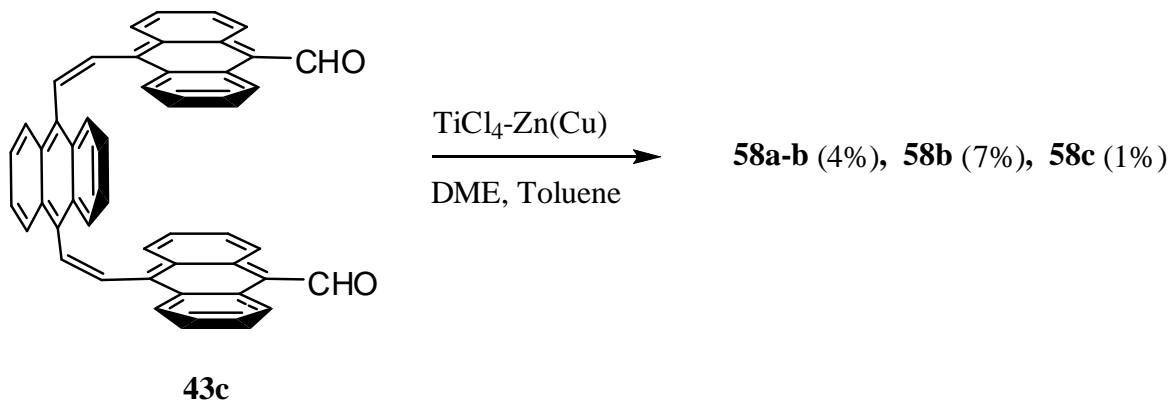
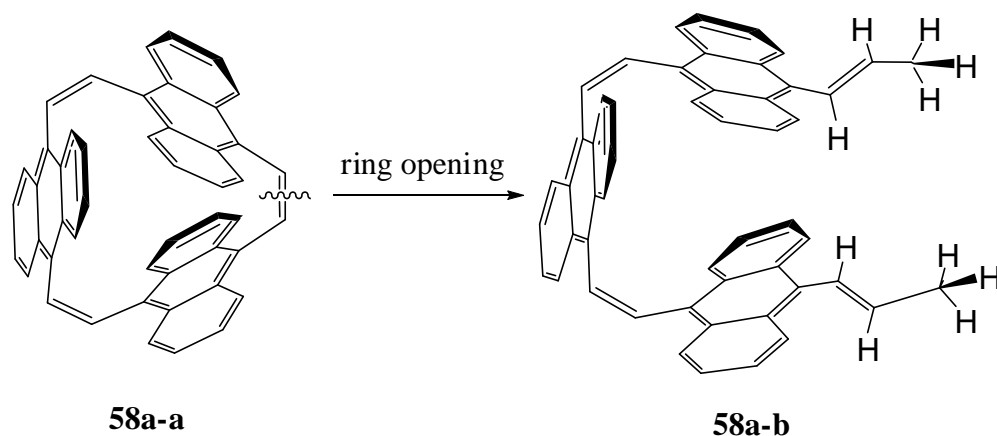


Figure 2-29. Products of McMurry reaction of **43c**.

Using the same approach and similar conditions, however, the main products were the dimer **58b** and the unexpected open ring compound **58a-b**. Trimer **58c** was formed in lower yield. As explained before, the open ring compound **58a-b** is probably, a decomposition compound of monomer **58a-a**.



Scheme 2-20. Synthesis of new $[n]$ -para-cyclophanes of **58b**, **58c**, **58a-b**.



Scheme 2-21. The ring opening of **58a-a** under reflux condition.

The DFT calculation of the monomer **58a-a** at B3LYP/6-31g(d) level predicted a D_{3d} symmetrical structure as the global minimum. According to the structure, the anthracene units are twisted about 90° with respect to the average plane through the three double bonds. The comparison between the yields of the three monomers **55a** (32%), **57a-a** (6%) and **58a-a** (0%) formed under similar conditions using the McMurry reaction, shows clearly that increasing anthracene units in the structure of the monomer lead to increasing instability. As already mentioned before, this instability is the consequence due to sterical hindrance between the two opposed anthracenes in the molecular structure.

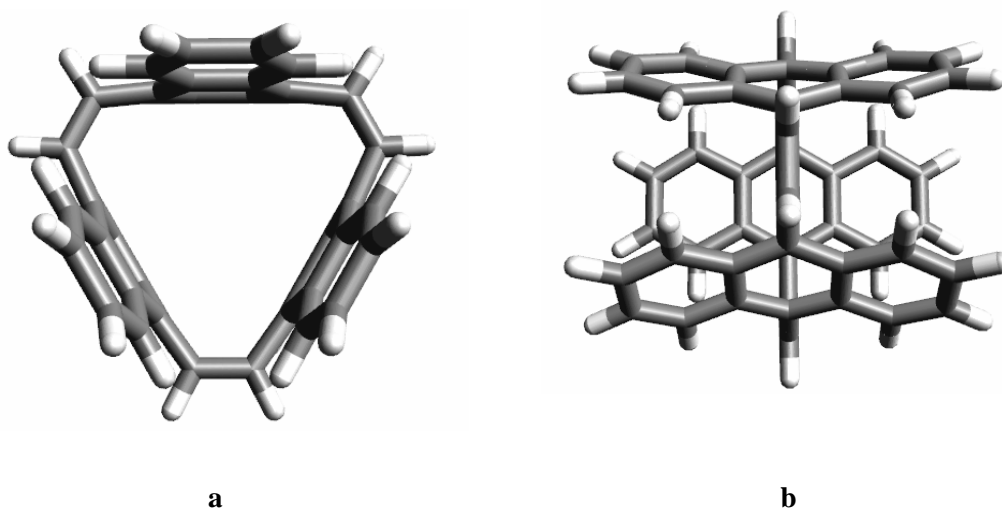


Figure 2-30. The optimized structure of monomer **58a-a** in two views a)top view. b)side view.

By varying the concentration of dialdehyde and toluene, similar effects mentioned in before, were observed in this reaction. Anthracenophanes dimer **58a** and trimer **58c** are both stable in solution and solid state at room temperature under inert gas. The maximum result obtained for dimer **58b**, trimer **58c** and **58a-b** under optimized conditions are 7 %, 1 % and 4%, respectively. However, these novel cyclic-*para*-anthracenophanes could be valuable precursors for the synthesis of the fully conjugated molecular belt **1**, which is the overall target molecule (chapter 1, page 2).

2.2.7.2. Physical properties

Cyclophane **58b**, a red solid, is unstable in the presence of air. Purification on silica gel lead to decomposition. Therefore, purification was performed by flash column chromatography on the neutral silica gel (using 1 ml triethylamine to get rid acid conditions of silica gel) under inert gas. Its molecular ion peak is observed at $m/z = 1212$ in MALDI-TOF mass spectrum. The NMR spectrum of compound **58a-b** clearly supports the structure of an opening compound. CI mass spectrum of the open ring compound **58a-b** shows the corresponding molecular ion peak ($m/z = 662$).

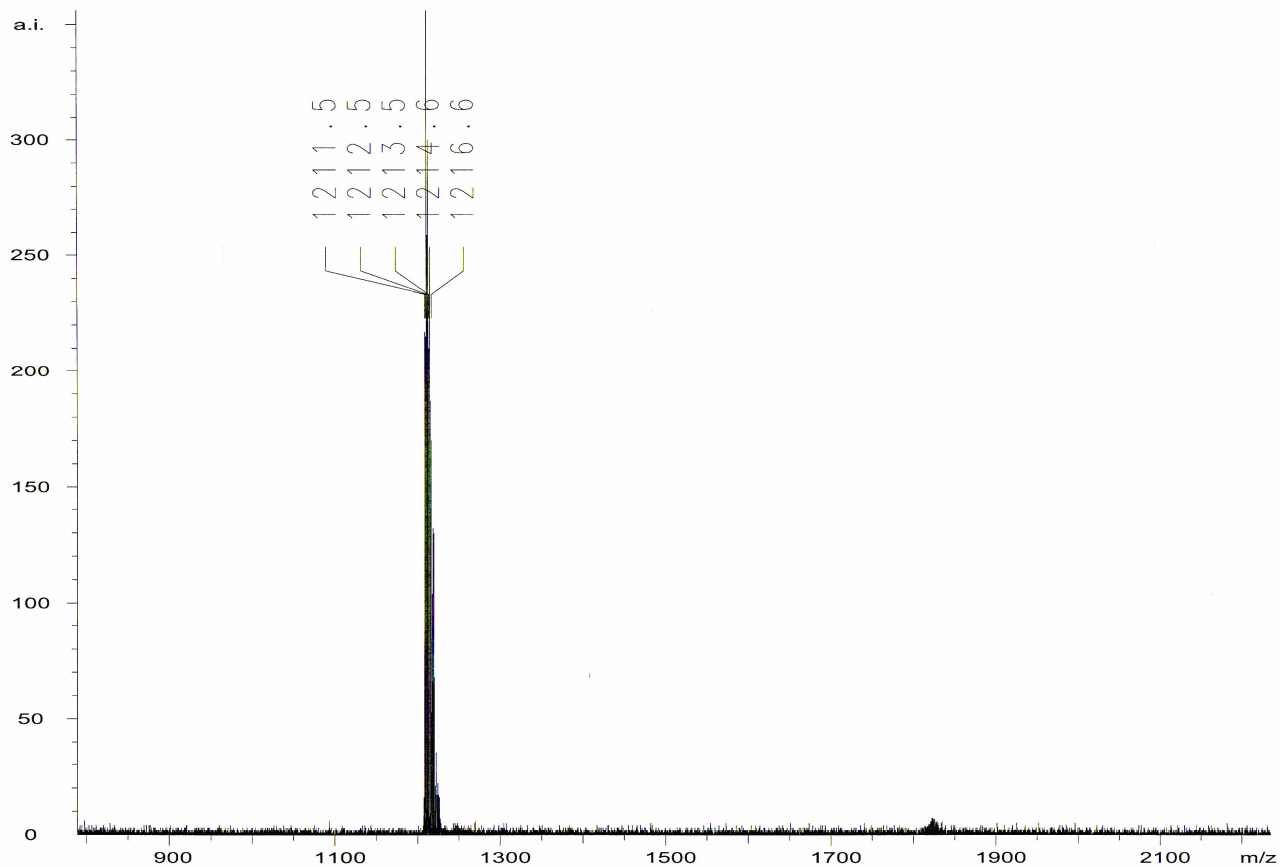


Figure 2-31. MALDI-TOF mass spectrum of mixed **58b**.

2.2.7.3. NMR spectra

The $^1\text{H-NMR}$ of dimer **58b** shows a broadened and complicated spectrum which probably indicates a mixture of stereoisomers. The structure of the open ring compound **58a-b** could be assigned by $^1\text{H-NMR}$ spectrum. It shows a doublet for the methyl protons in the aliphatic region (2.26 ppm), a quartet for the *cis* olefinic protons connected to the methyl group, a singlet for the *cis* olefinic protons between the anthracene units, a doublet for the olefinic protons connected to the anthracene unit and other signals for the anthracene protons.

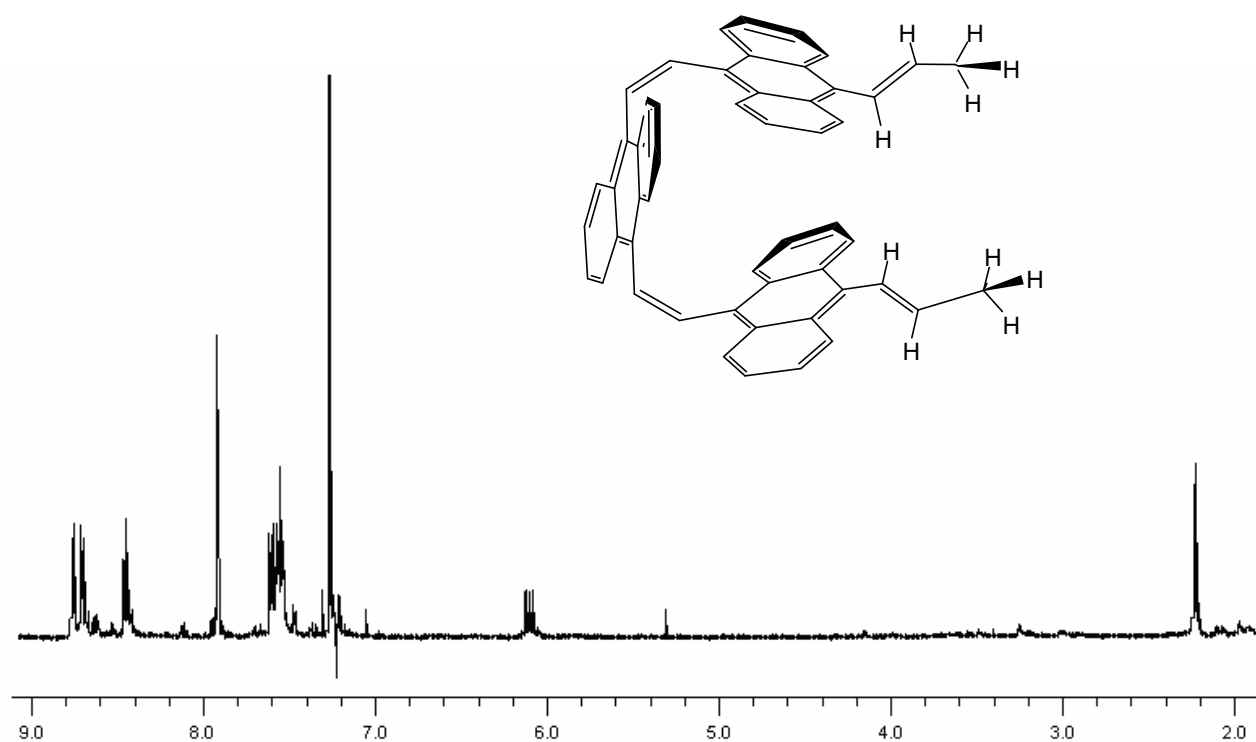


Figure 2-32. ¹H-NMR (500 MHz, CDCl₃/TMS) spectrum of **58a-b**.

2.2.7.4. UV-Vis spectra

Figure 2-33 shows the UV-Vis spectra of **55b**, **56b**, **57b**, **58b**. No significant bathochromic shifts of the longest absorption are observed for them. While, the π -bond absorption around 400 nm are shifted and broadened to longer wavelength region with an increase in the number of anthracene units (**55b** < **56b** < **57b** < **58b**). It is probably, due to the increase of rigidity of the molecules.^[37]

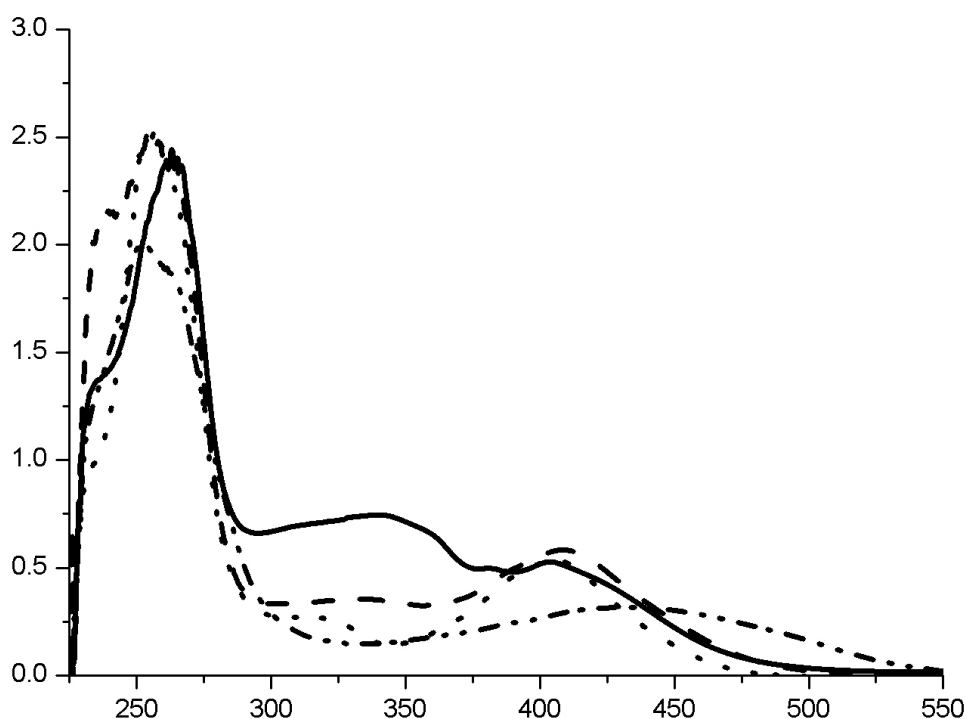


Figure 2-33. UV-Vis spectra of **55b** (solid line), **56b** (dotted line), **57b** (dashed line), **58b** (dashed dotted line) in CH_2Cl_2 .

2.2.8. Anisotropy of current induced density (ACID)

The ACID (Anisotropy of current induced density) is an applicable method to explain the electronic structure of conjugated systems and visualizes the density of delocalized electrons^[99, 100] (both π -electrons and σ -electrons). Figure 2-34 exhibits the ACID plots of **55a** and **57a-a**. At the standard isosurface value of 0.05 the delocalized system includes all bonds. The extent of the conjugated system can be quantified by giving the critical isosurface value (CIV), the lowest ACID value in space between two interacting units. The monomer **55a** has a CIV of 0.06 (between the double bonds and the adjacent anthracene units), which is lower than the value of benzene (CIV = 0.0739). The value for monomer **57a-a** is 0.056 (between the double bonds and the adjacent anthracene and naphthalene units) which is much lower than the value of benzene, but still strong enough to speak of a considerable electronic conjugation in both of them.

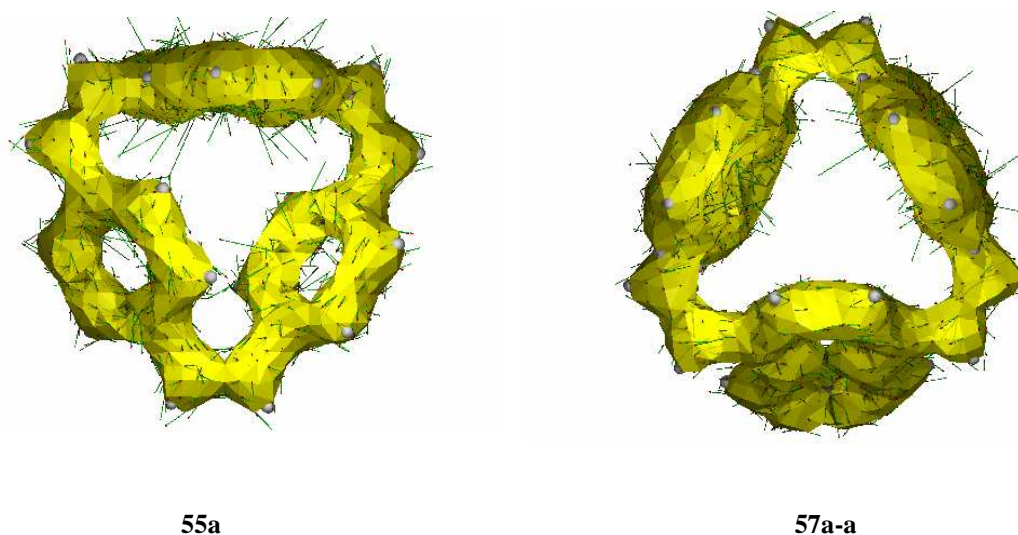


Figure 2-34. ACID plot of monomer **55a** and **57a-a** at an isosurface value of 0.05 at B3LYP/6-31g* level of theory.

2.2.9. Nucleus independent chemical shift (NICS)

In 1996 Schleyer et al.^[101] proposed a new magnetic criterion for aromaticity: a nucleus-independent chemical shift (NICS) which is defined as the negative of the magnetic shielding at some selected point in space, e.g. at a ring center. In general, negative and positive NICS values denote aromaticity and antiaromaticity, respectively. For example, the NICS values at the center of the highly aromatic benzene is ca. -10. For the highly antiaromatic cyclobutadiene (small variations depending on the theoretical level) it is ca. 28. In the case of nonplanar molecules like **55a**, **57a-a** and [2.2.2] paracyclophane, several points can be defined as the center of the ring. Therefore, only approximate NICS values can be given. As expected, these aromatic $4n+2$ π -electron compounds show all negative NICS values ([2.2.2] paracyclophane (-5.6), **55a** (-6.8) and **57a-a** (-9.2)). Introducing anthracene units in the structure of the ring compounds, the NICS values increase, remarkably. The abnormal proton chemical shift of these aromatic compounds, compared to the benzene proton (7.34 ppm), confirms the ring current effects. The upfield chemical shifts of the benzene protons located *inside* the aromatic belts ([2.2.2] paracyclophane, **55a** and **57a-a**) are in good agreement with the NICS values (Figure 2-35).

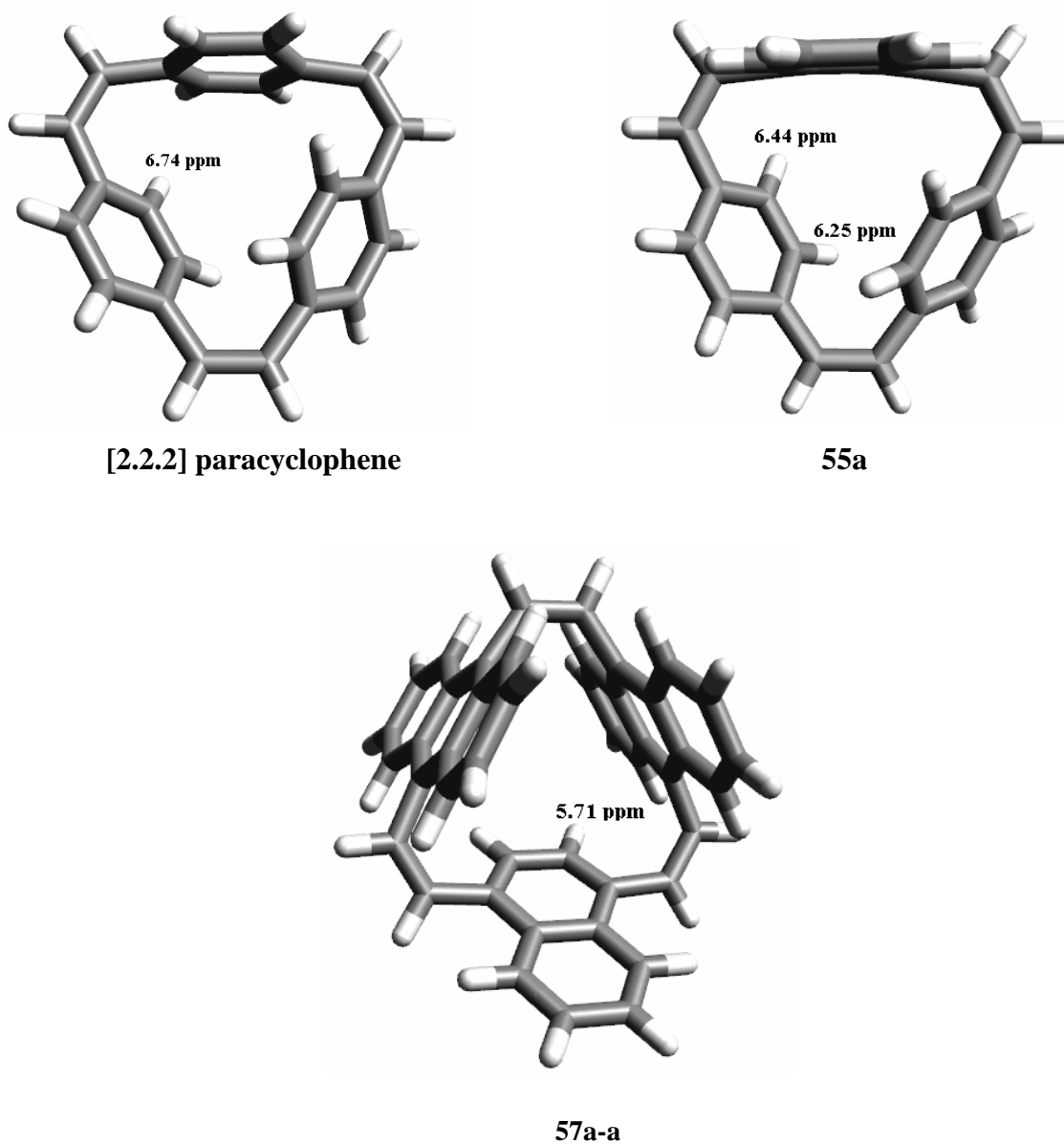


Figure 2-35. The upfield chemical shifts of the benzene protons of [2.2.2] paracyclophane, **55a** and **57a-a** located *inside* aromatic belts.

2.2.10. Conclusion

The width of belt in cyclic-oligoarylacetylene could be extended by introducing anthracene units. The Oda, Kawase, Darabi method to prepare cyclic-*para*-phenyl and naphthyl-acetylenes fails if

anthracene units are used. Therefore, it was essential to develop and optimized a new strategy to synthesize cyclic-*para*-anthrylethylenes, which can be used as precursors for belt-like aromatic compounds.

Finally, a general method was developed to afford a set of new cyclophane using Sonogashira coupling and palladium catalyzed hydrogenation reactions. The ring closure was performed using McMurry reaction. The synthesis was accomplished for the built up of several new compounds the first cyclophanes containing anthracene units. Due to their more suitable ring size, the higher cyclic-oligomers dimer **55b**, **56b**, **57b** and **58b**, as well as trimer **55c**, **56c**, **57c** and **58c**, could be applied as precursor for the synthesis of belt-like aromatic compounds. The accomplished synthesis approach offers a general pathway to build up [*n*]-*para*-arylcyclophane.

Chapter 3: The belt-like conjugated systems

3.1. Synthesis of cyclic[6]-*para*-anthrylacetylene: [6]-CPAA

3.1.1. Introduction

Prior to the discovery of fullerenes, belt-like conjugated systems with p-orbitals aligned perpendicular to the surface of the cyclic moieties were regarded as attractive synthetic targets. Attempts to synthesize several model compounds with belt-like conjugation such as cyclacenes, benzoannulenes, picotubes and cyclic[*n*]-*para*-phenylacetylene have been reported.^[102] These molecules are of great interest. Not only from the synthetic and theoretical point of view, also as host molecules having a well-defined π -electron cavities.^[27, 103]

Another class of molecules similar to cyclic[*n*]-*para*-phenylacetylenes ([*n*]-CPPA) are the cyclic-oligomers of anthrylacetylene namely cyclic[*n*]-*para*-anthrylacetylene ([*n*]CPAA). According to the theoretical calculations (PM3) these compounds have a smooth belt-like structure, similar to a cut piece of a carbon nanotube.

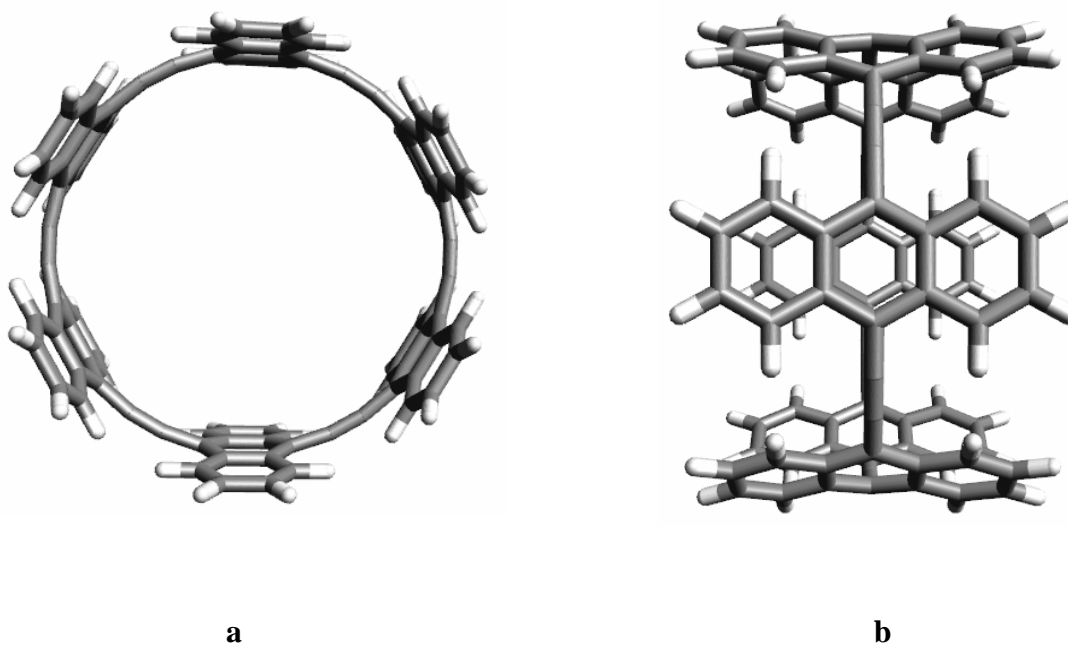


Figure 3-1. Semiempirical (PM3) calculated structure of cyclic [6]-*para*-anthrylacetylene, [6]-CPAA in two views a)top view. b)side view..

The cavity size of [6]-CPAA is identical to that of [6]-CPPA (13.14 Å), but the cavity is deeper than that of [6]-CPPA. It is reasonable to believe that the deeper cavity of [n]-CPAA will allow for more stable complexes with fullerenes. Therefore, these novel substances were attempted to synthesize.

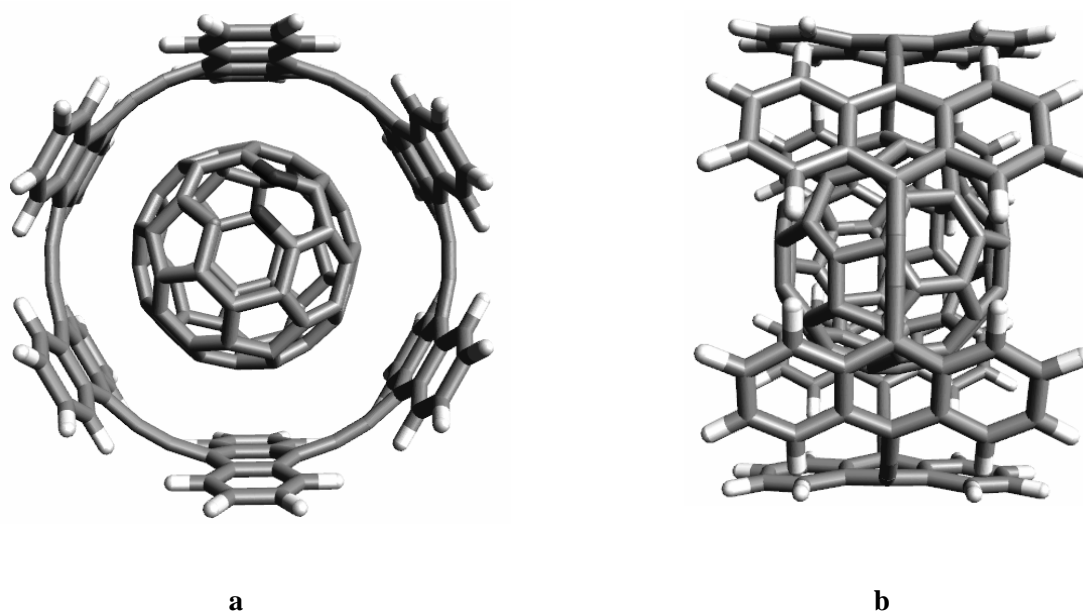


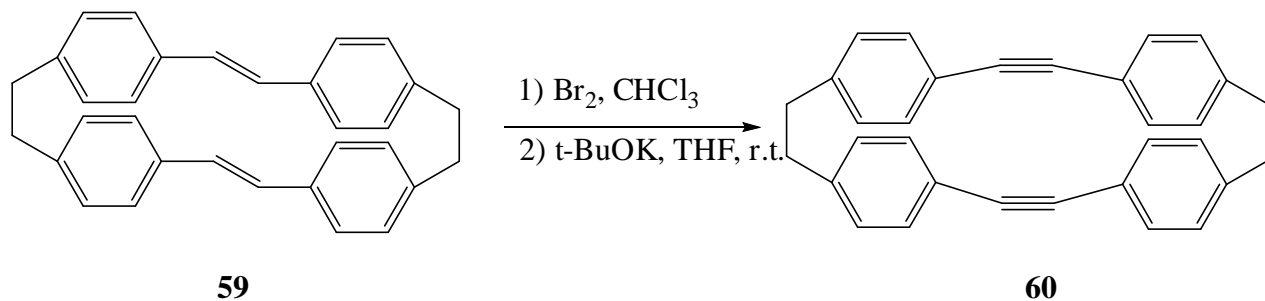
Figure 3-2. Semiempirical (PM3) calculated structure of an anion-type complex of C_{60} with [6]-CPAA in two views a) top view. b) side view.

3.1.2. Recent synthesis challenges toward strained cycloalkynes

The challenges confronting the synthesis of strained cycloalkynes have been discussed in chapter 1. One of the most valuable approaches to these substances involves halogenation-dehalogenation of the corresponding cycloalkenes. Several examples to prepare strained compounds utilizing this method are known in literature.

3.1.2.1. Synthesis of [2.2]-tolanophane **60**

Vögtle *et al.*^[104] in 1992 and Oda *et al.*^[105] in 1993 reported the synthesis of **60** by bromination and dehydrobromination **59** in THF solvent.

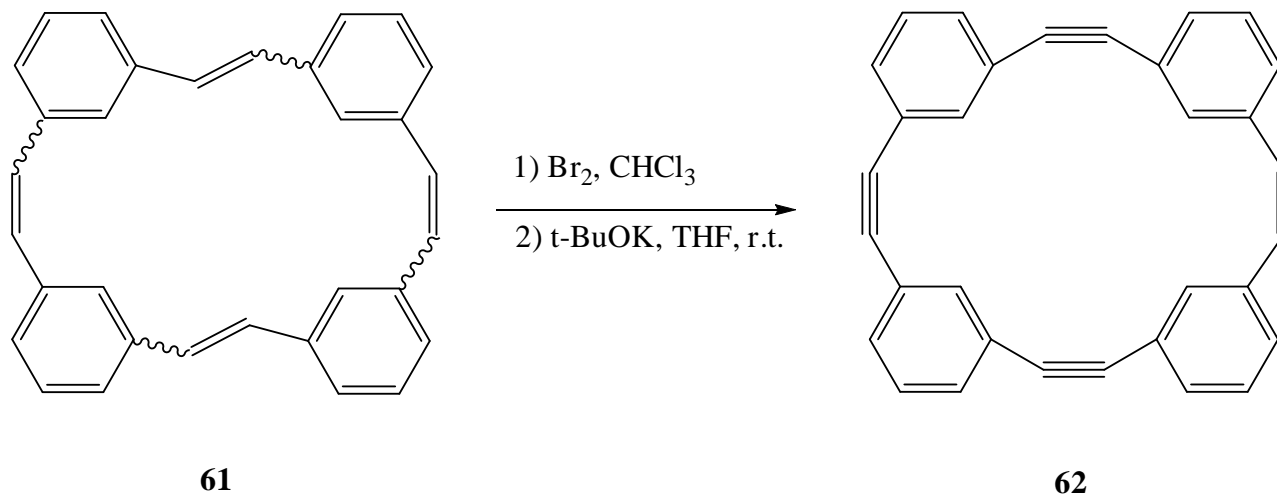


Scheme 3-1. Synthesis of **60** by bromination and dehydrobromination.

The strain of the triple bonds in this molecule is clearly reflected in its ¹³C-NMR spectrum and X-ray crystallographic data.^[104]

3.1.2.2. Synthesis of [2.4]-*meta*-cyclophantetrayne **62**

In another work, Oda *et al.* prepared compound **62** by using the same approach and similar conditions.^[106]

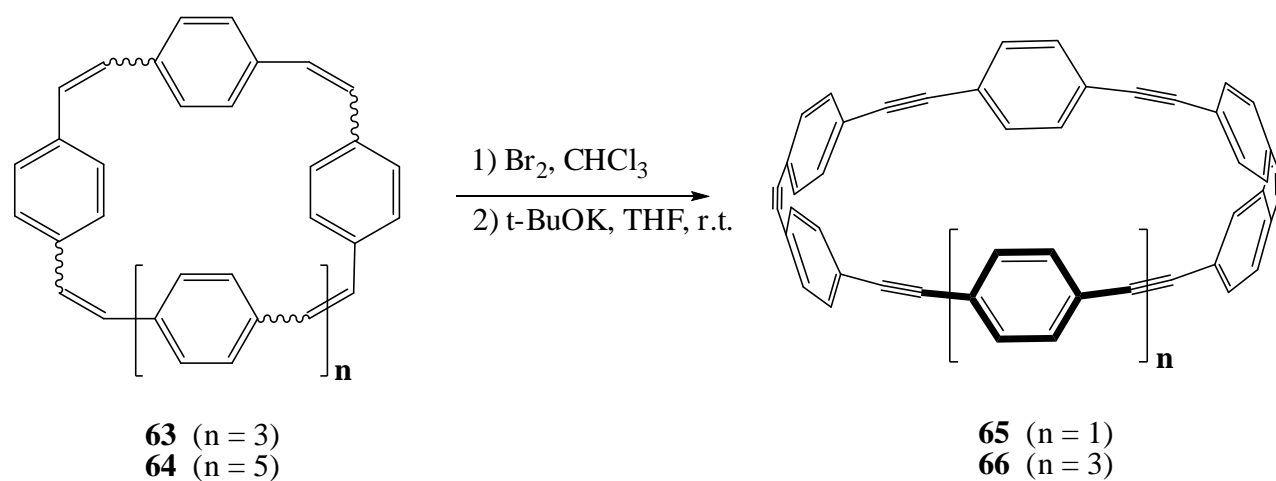


Scheme 3-2. Synthesis of **62** by bromination and dehydrobromination.

The ^{13}C -NMR spectrum and X-ray crystallography data clearly show the existence of strain in the triple bonds of **62**.^[106]

3.1.2.3. Synthesis of [6]-CPPA **65**, [8]-CPPA **66** and [6]-CPNA **68**

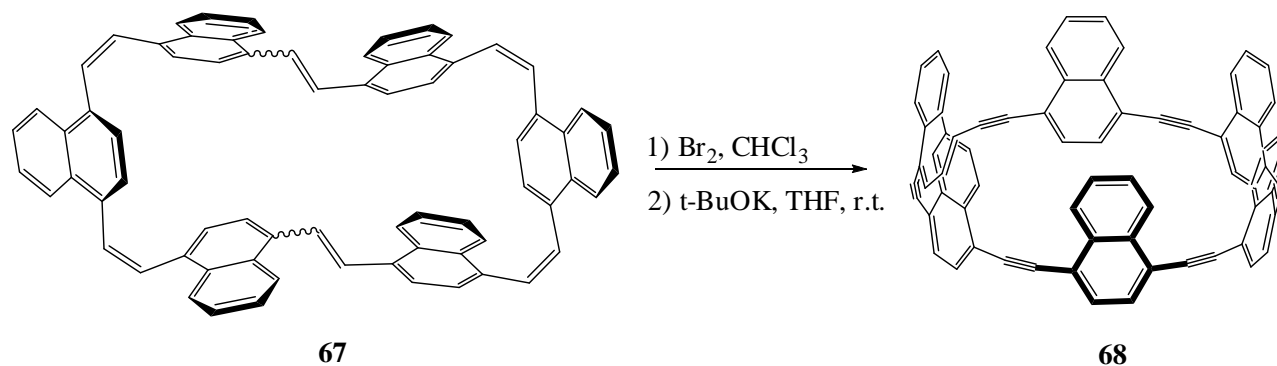
In 1996, Oda *et al.*^[21] synthesized the belt-like conjugated molecules **65** and **66** in excellent yields (85%) by bromination and dehydrobromination cyclophanes **63** and **64**.



Scheme 3-3. Oda, Kawase, Darabi method to synthesize [n]-CPPA.

According to their reports, the obtained compounds are sensitive to oxygen both in solution and in solid state, but fairly stable under inert gas atmosphere.

In 2006, using the same approach and similar conditions, they also prepared cyclic[6]-*para*-naphthylacetylene ([6]-CPNA) **68**.^[39]



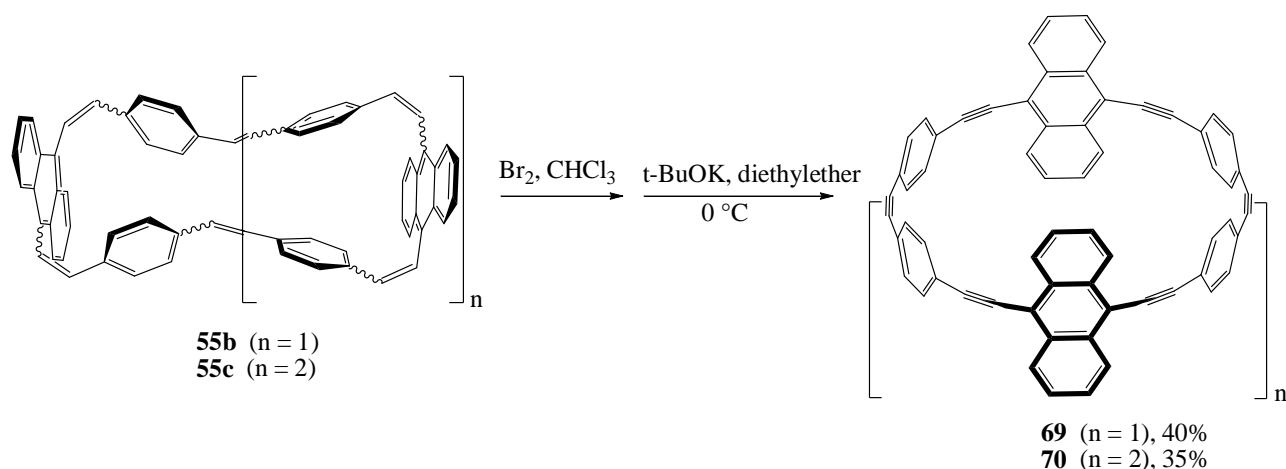
Scheme 3-4. Oda, Kawase, Darabi method to synthesize [6]-CPNA.

Compound **68** is sensitive to acid and oxygen though in solid form it is stable enough to be stored in a refrigerator over a day. The low yield (2.8 %) in comparison with that of CPPA (85 %) indicates an increase of strain relative to compound **65**.

In view of the successful formation and fair stability of these synthesized compounds under basic conditions in spite of sizeable strain, it is expected that the targets of this work, the [n]-CPAA containing anthracene units as well as their derivatives (CPPA and CPNA) could be synthesized in a similar way.

3.1.3. Synthesis of cyclic [6] and [9]-*para*-anthrylacetylene **69** and **70**

In the course of this thesis, bromination of **55b** and **55c** with an excess amount of bromine in chloroform at 0 °C afforded the brominated compounds. Without any purification, the brominated solid were used for the next step. Dehydrobromination of compounds with 24 equivalents *t*-BuOK in diethylether at 0 °C under inert gas atmosphere afforded **69** and **70** in fairly good yields.



Scheme 3-5. Synthesis of [6] and [9]-CPAA **69** and **70** by bromination and dehydrobromination reactions.

Attempts to purify the crude compounds by silica gel chromatography failed led to slow decomposition of **69** and **70**. Since the target molecules have a low solubility in diethyl ether, purification is based on filtration and washing the precipitate with diethyl ether. By dissolving the precipitate in CH_2Cl_2 and separating through short (1cm) silica gel column chromatography, [6] and [9]-CPAA **69** and **70** were isolated as a red solid and a yellow solid, respectively.

3.1.3.1. Physical properties

The structure of CPAA **69** is clearly supported by spectral data. MALDI-TOF mass spectrometry shows the corresponding molecular ion peak ($m/z = 800$) as a major product, besides trace amounts of additional signal ($m/z = 1600$). Since dimer **55b** was only used in the bromination and dehydrobromination, the additional signal proposes a [4+4]-cycloaddition reaction of **69** under laser irradiation in MALDI-TOF measurement.

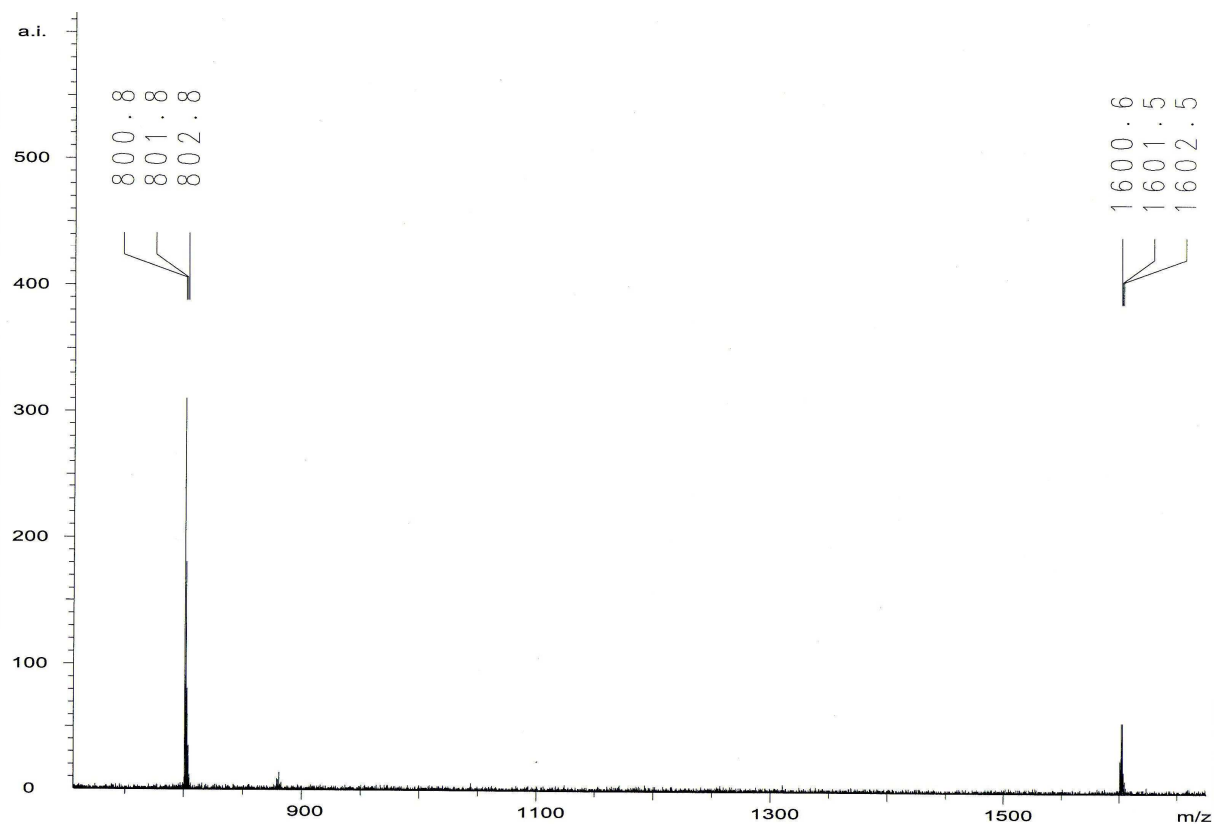
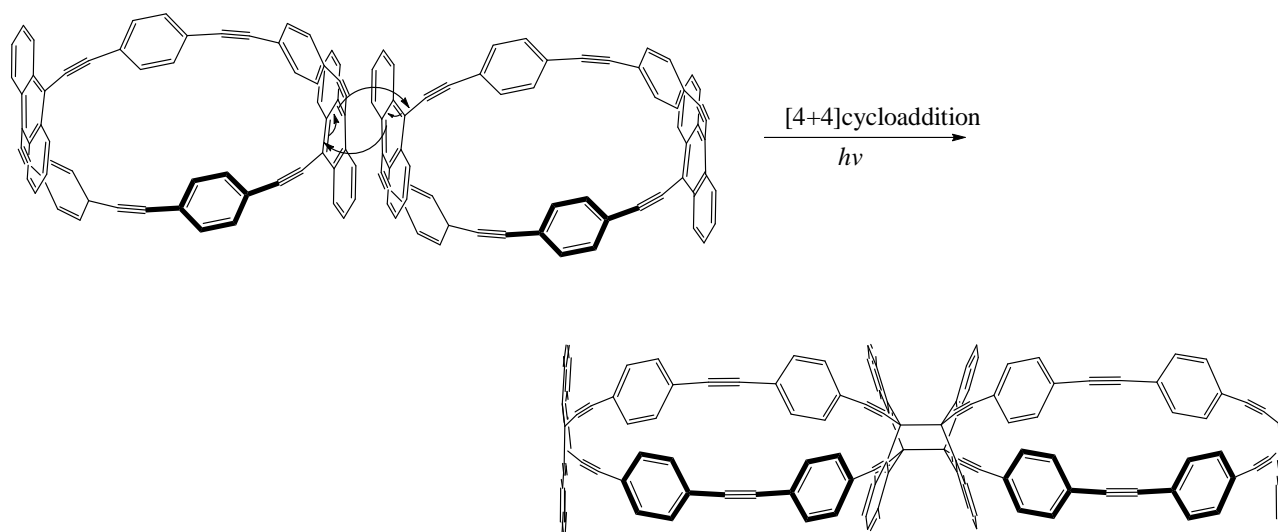


Figure 3-3 . MALDI-TOF mass spectrum of **69**.



Scheme 3-6. The proposed [4+4]-cycloaddition reaction of **69** under laser irradiation in MALDI-TOF measurement.

The structure of CPAA **70** is also supported by spectral data. MALDI-TOF mass spectrometry shows the corresponding molecular ion peak ($m/z = 1200$).

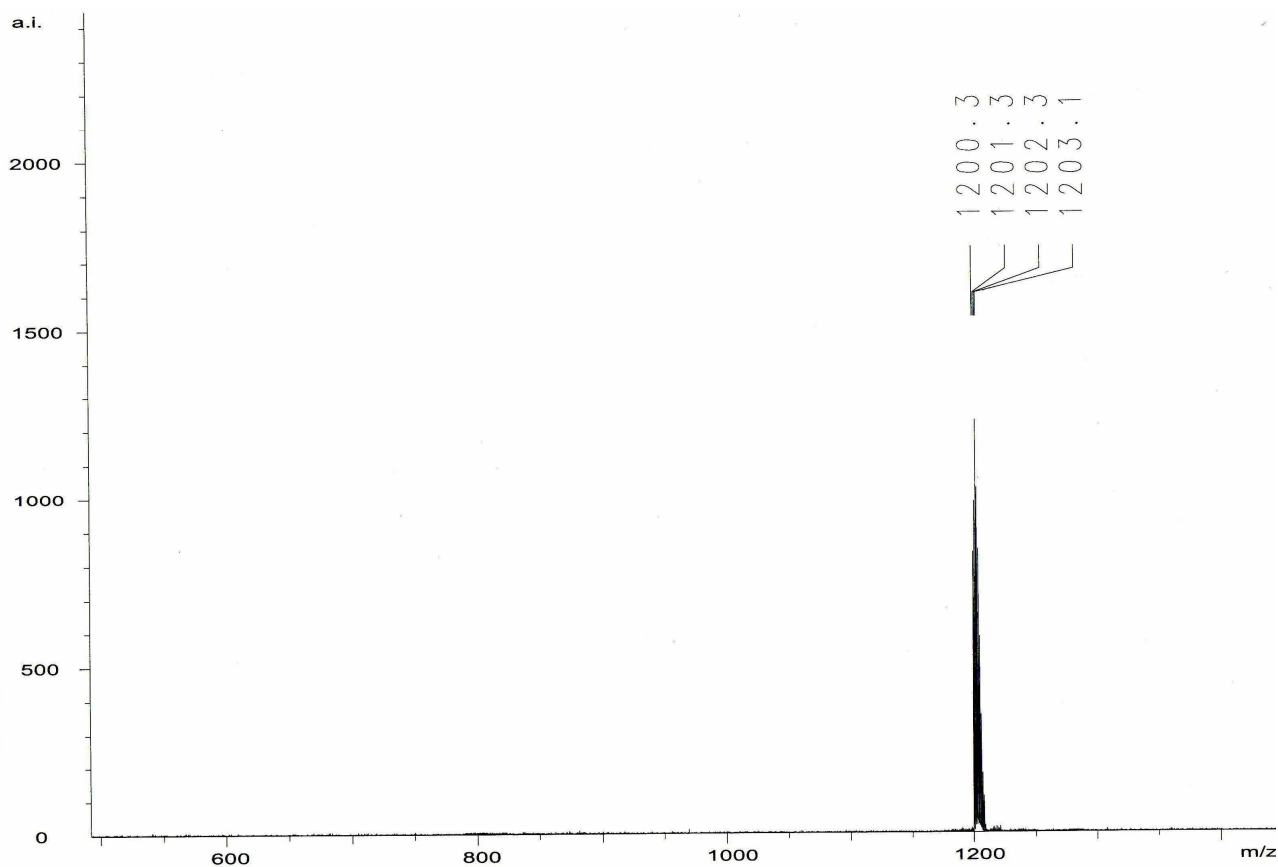


Figure 3-4. MALDI-TOF mass spectrum of **70**.

The [6] and [9]-CPAA **69** and **70** are sensitive to oxygen both in solution and solid states but fairly stable under inert gas atmosphere where it gradually decomposes during a month.

Another physical property of these ringed products is their bright color under UV lamp (365 nm). The fluorescence property of **69** and **70** compare to their olifinic precursors indicate cyclic conjugation over the whole molecule (figure 3-5).

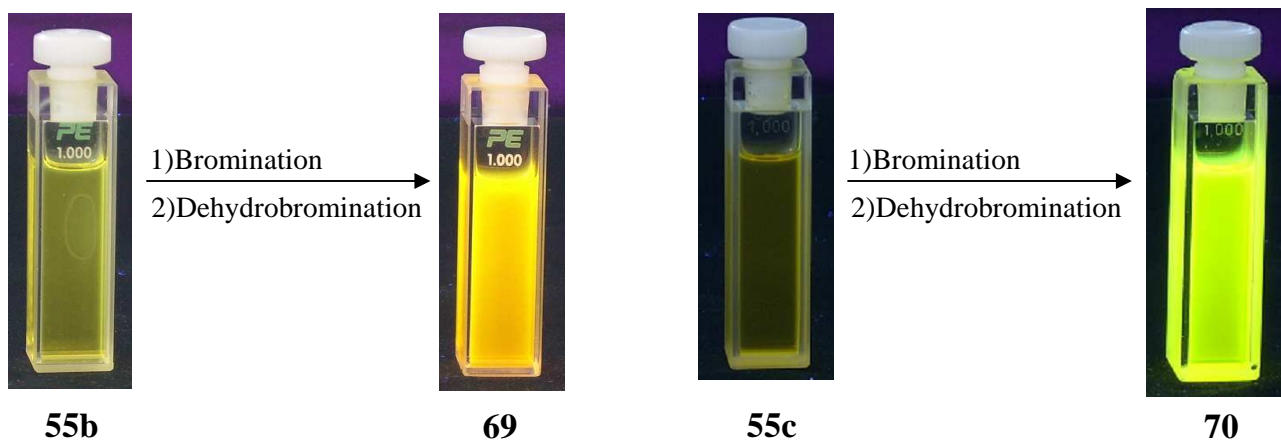


Figure 3-5. Observed optical property of compounds **69** and **70** under UV lamp (366 nm).

3.1.3.2. NMR data

The simple NMR spectra of CPAA **69** strongly support the structure proposed in this work. The ^1H -NMR spectrum of **69** shows a pair of the doublets for the benzene protons (AA'XX') and a pair of the multiplets for the anthracene protons. The ^{13}C -NMR spectrum shows three different signals for sp carbons (111.31, 105.97, 97.31 ppm). These data indicate D_{2h} symmetry for **69**.

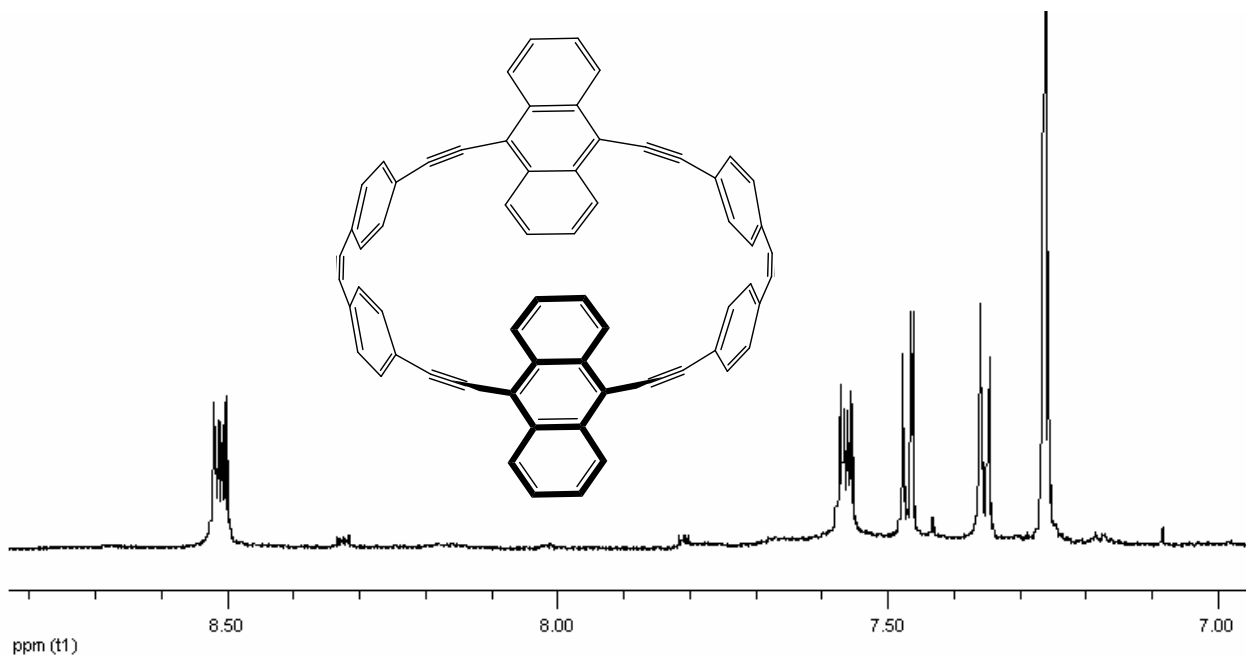


Figure 3-6. ^1H -NMR (600 MHz, CDCl_3/TMS) spectrum of **69**.

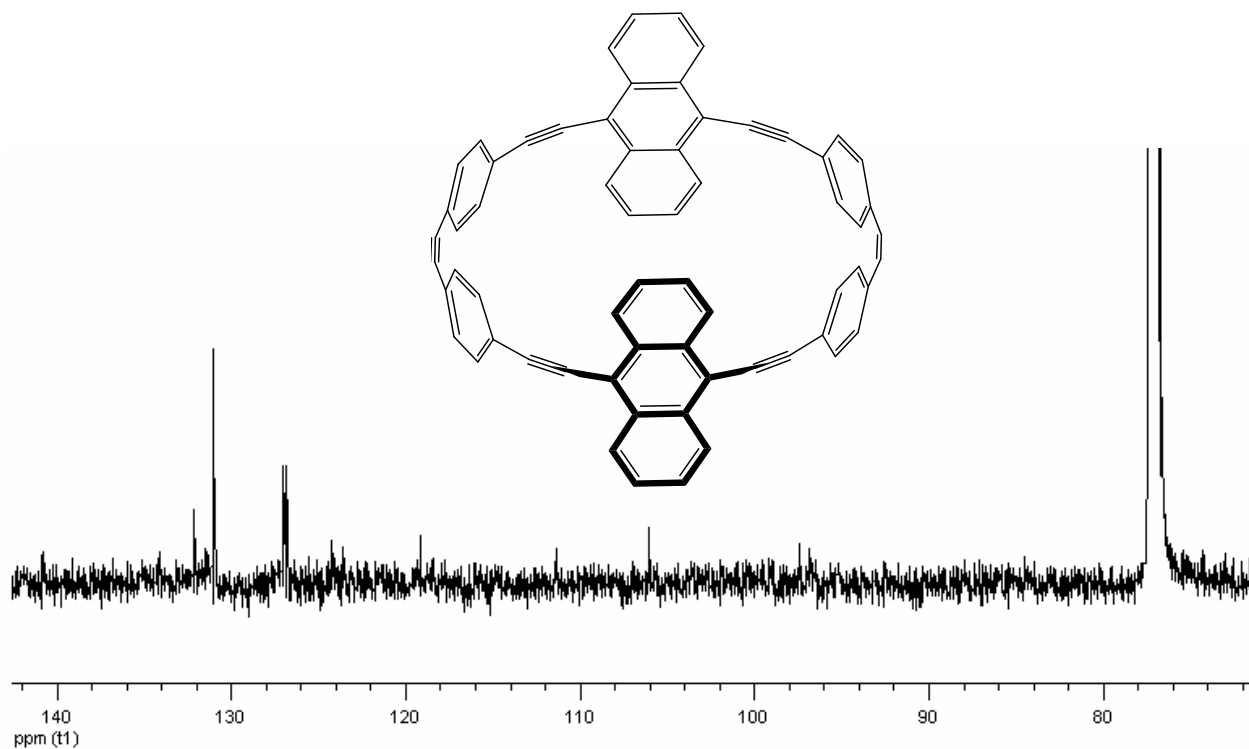


Figure 3-7. $^{13}\text{C-NMR}$ (150.9 MHz, CDCl_3/TMS) spectrum of **69**.

Figure 3-8 shows $^1\text{H-NMR}$ spectrum of **70** at room temperature. Apparently, a pair of doublets for the benzene protons (AA'XX') and a pair of multiplets for the anthracene protons in 7.60 ppm overlap. These data indicate D_{3h} symmetry for **70**.

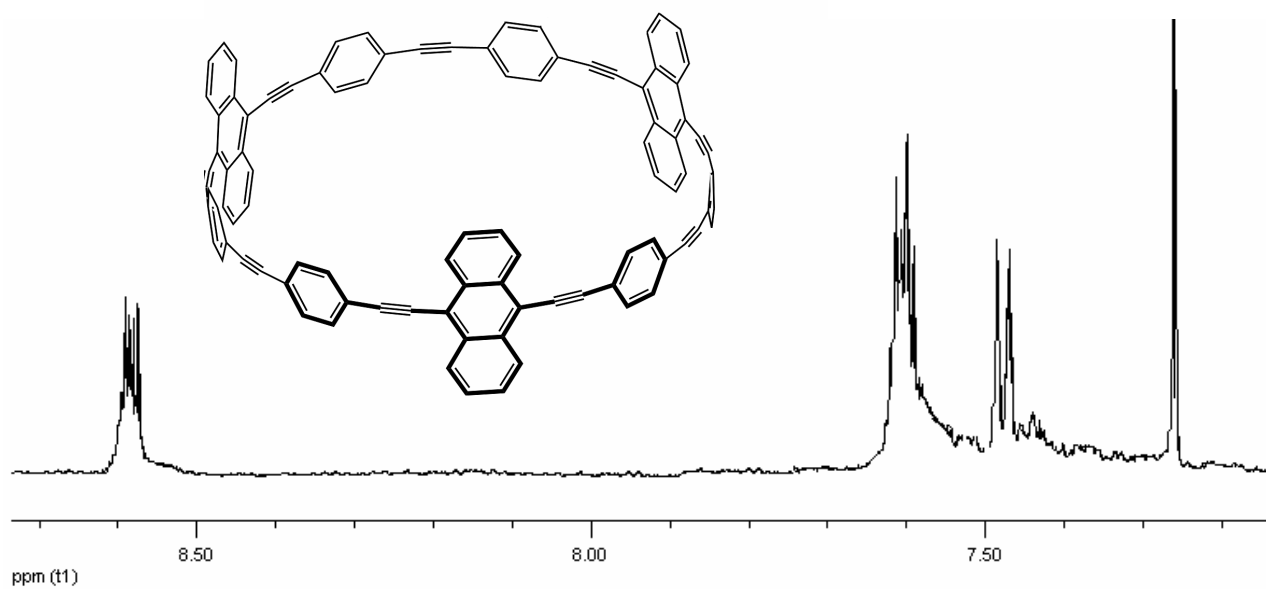
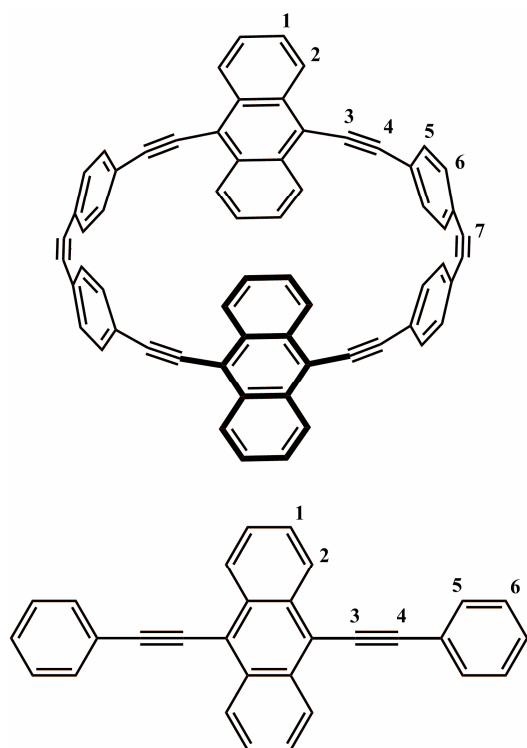


Figure 3-8. $^1\text{H-NMR}$ (600 MHz, CDCl_3/TMS) spectrum of **70**.

Table 3-1 lists the NMR data of [6] and [9]-CPAA **69** and **740** together with that of their acyclic homologue. ^1H -signals of aryl units are shifted to upfield with an increase in the strain of compounds ($\delta_{\text{acyclic}} > \delta_{[9]} > \delta_{[6]}$), it is because of out of plane deformation. ^{13}C -signals of ethynyl carbons are shifted to downfield, with an increase in the strain of compounds ($\delta_{\text{acyclic}} < \delta_{[9]} < \delta_{[6]}$), it is because of rehybridization of sp towards sp^2 .

Table 3-1. Observed ^1H and ^{13}C chemical shift for [6] and [9]-CPAA **69** and **70** and their acyclic homologue.



Number of atom	δ_{acyclic}	$\delta_{[6]}$	$\delta_{[9]}$
H-1	7.70	7.56	7.62
H-2	8.75	8.51	8.59
H-5	7.83	7.47	7.60
H-6	7.49	7.35	7.47
C-3	103.56	111.31	-
C-4	86.97	105.97	103.90
C-7	-	97.31	94.02

3.1.3.3. UV-Vis and fluorescence spectra

Figures 3-9 and 3-10 show absorption spectra of **69** and **70** together with their olefinic precursors **55b** and **55c**, respectively. The UV-Vis spectrum of compounds show similar absorption maxima. The longest wavelength absorptions exhibit a bathochromic shift of about 60 and 40 nm in nanorings **69** and **70** as compare to the olefinic precursors **55b** and **55c**, respectively. It probably indicates better conjugation in nanorings **69** and **70**.

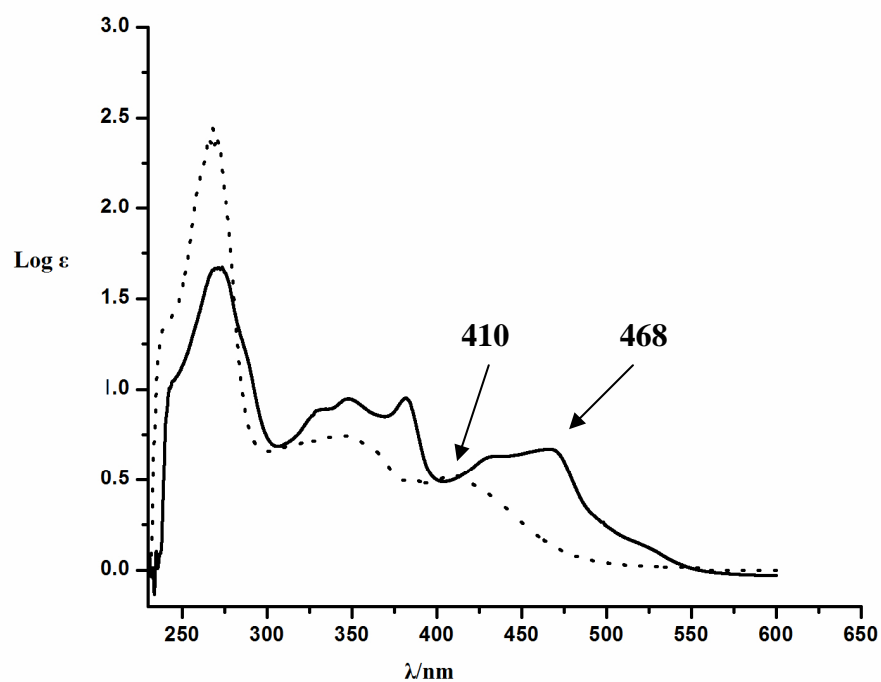


Figure 3-9. UV-Vis spectra of **55b** (doted line), **69** (solid line) in CH_2Cl_2 .

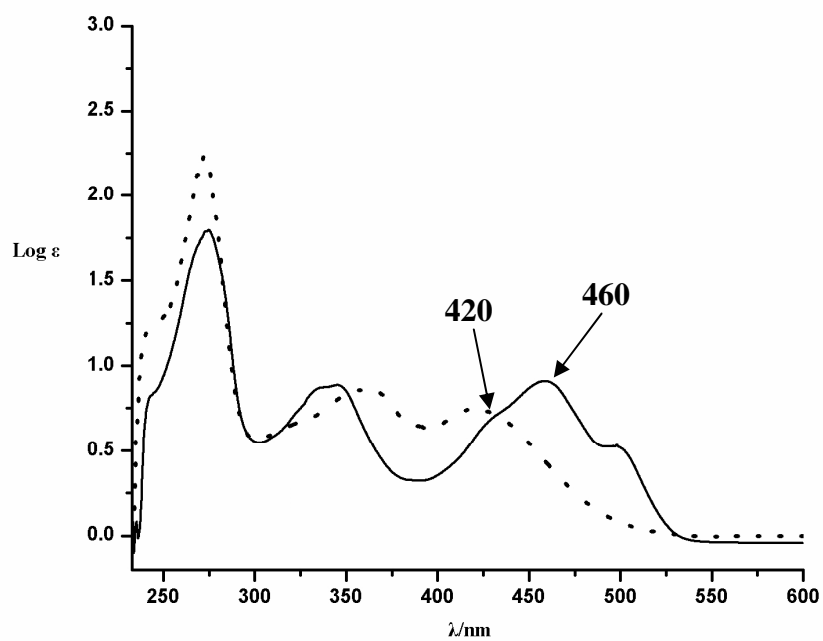


Figure 3-10. UV-Vis spectra of **55c** (doted line), **70** (solid line) in CH_2Cl_2 .

Figure 3-11 shows fluorescence spectra of **69** and **70**. Fluorescence spectra exhibit broadening and bathochromic shift about 100 nm with decrease of the ring size. It could be a consequence of increased strain and rigidity.

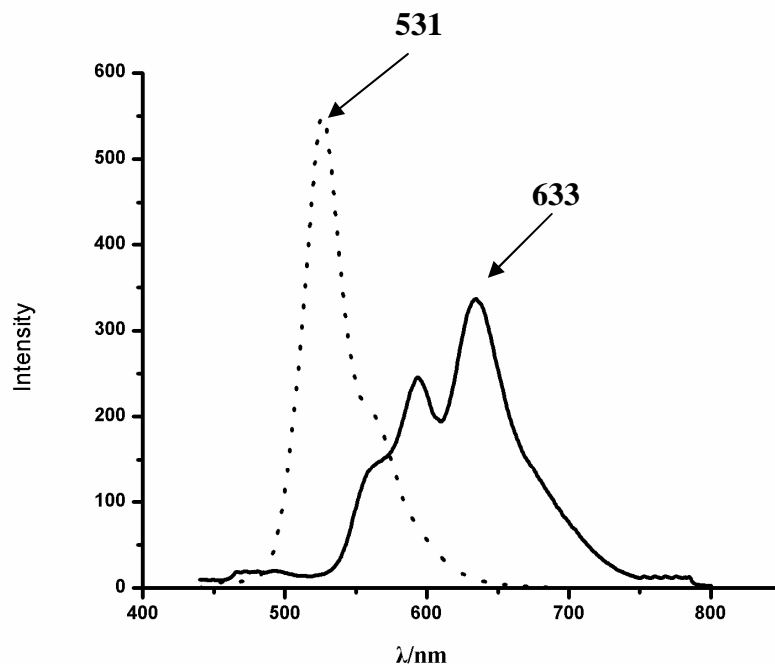


Figure 3-11. Fluorescence spectra of **70** (solid line), **69** (dotted line), in CH_2Cl_2 .

3.1.3.4. Anisotropy of current induced density (ACID)^[100,101]

Figure 3-12 exhibits the ACID plots of **69** at an isosurface value of 0.044. The critical isosurface value (CIV) of the cyclic conjugation over the whole molecule is found between each triple bond and aryl unit at a value of 0.045. It is much lower than the value of benzene (CIV=0.0739) but still strong enough to speak of a considerable electronic conjugation.

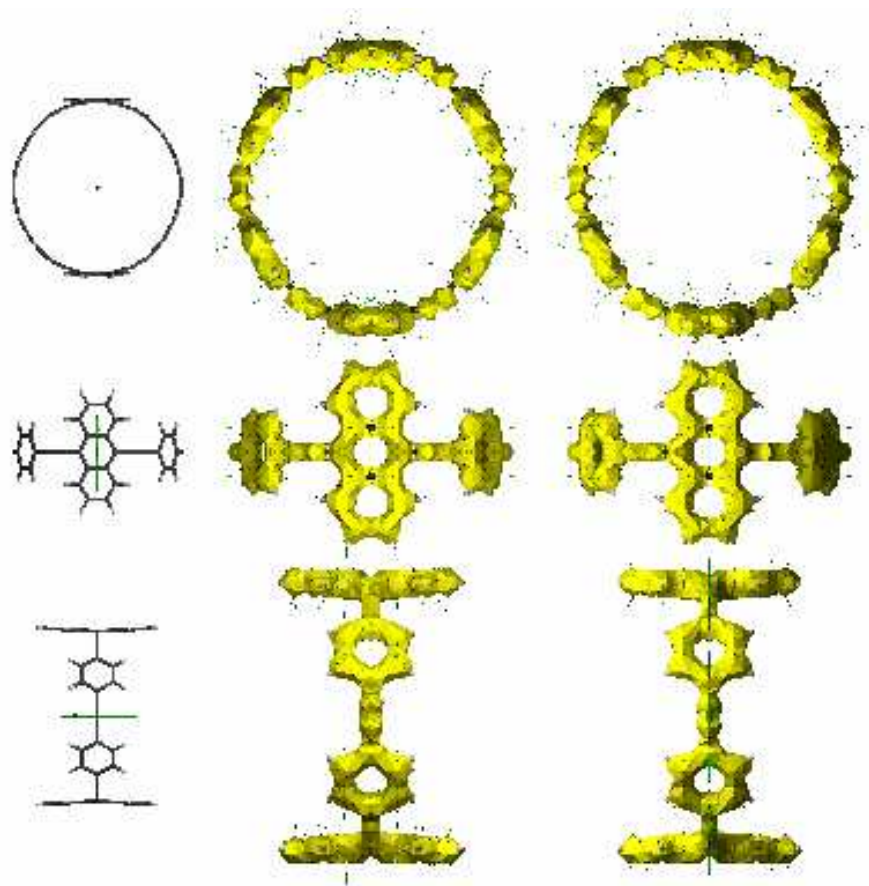
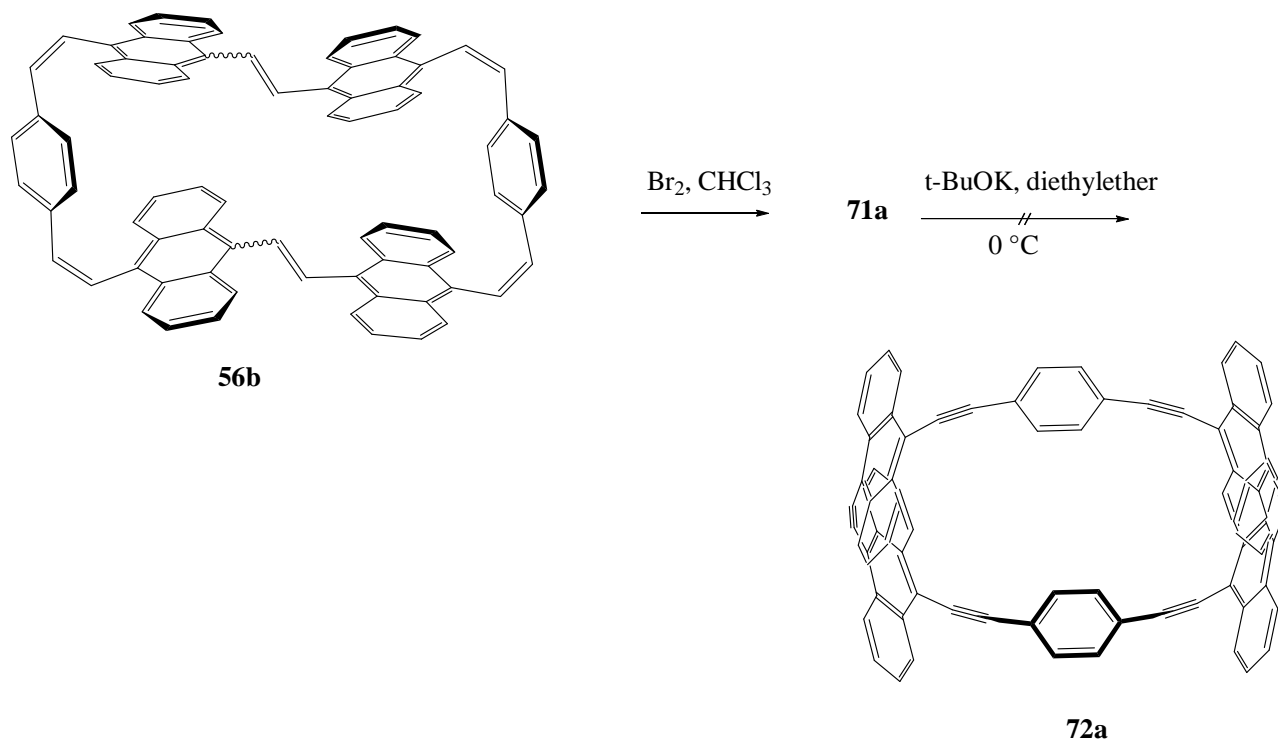


Figure 3-12. ACID plot of **69** at an isosurface value of 0.044 at B3LYP/6-31G(d) level of theory.

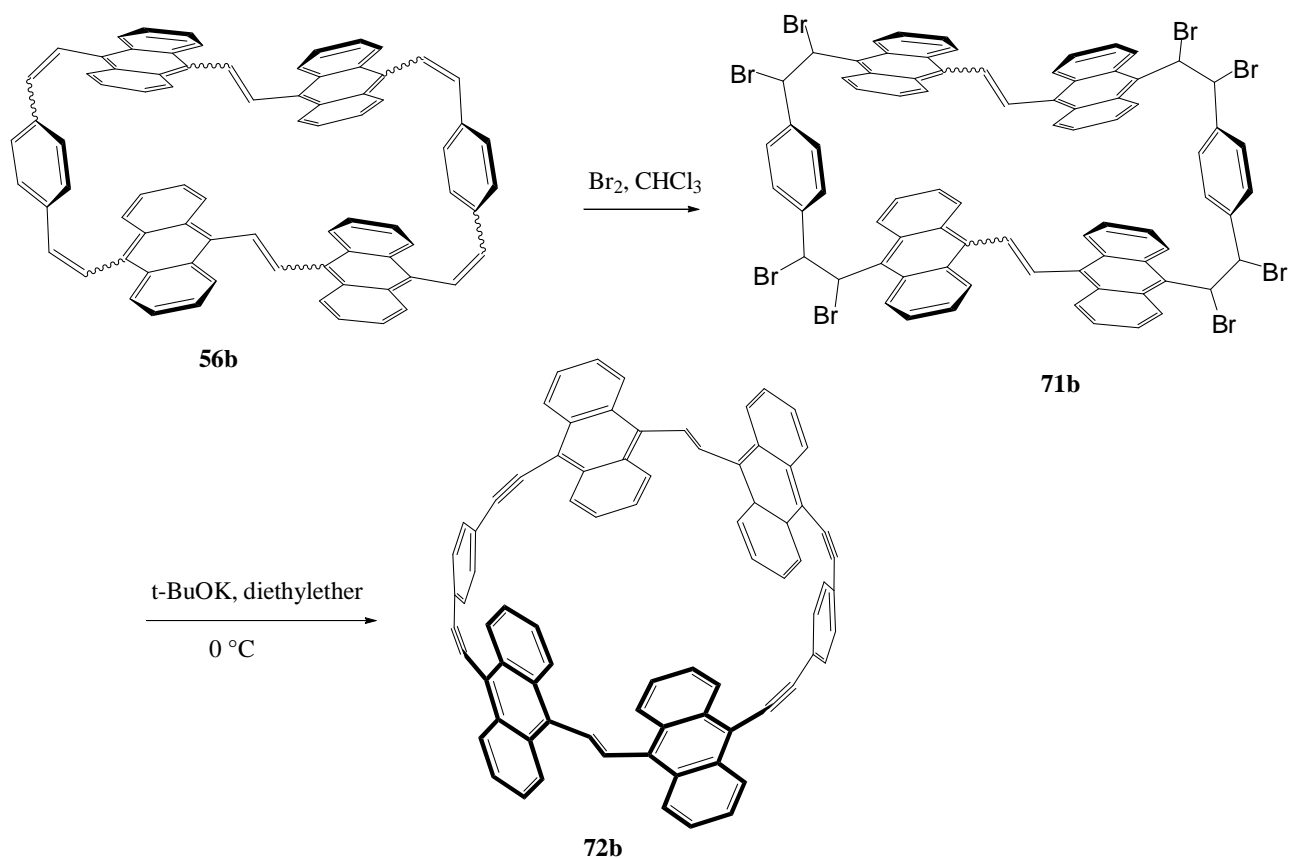
3.1.4. Synthesis of cyclic [6]-*para*-anthrylacetylene **72a**

Using the same approach and similar conditions as in the preparation of **69** and **70**, the nanoring **72a** could not be obtained. Instead, the reaction afforded an instable product which gradually decomposed during the reaction at room temperature under inert gas atmosphere.



Scheme 3-7. Attempted bromination and dehydrobromination reaction of **56b**.

Attempts to purify the crude compound by flash chromatography and analytical HPLC failed, therefore its identification is only based on MALDI-TOF mass spectroscopy. According to the MALDI-TOF mass spectrum, the observed mass for the main product is $m/z = 1004$, corresponding to the molecular formula $\text{C}_{80}\text{H}_{44}$ (expected for **72a**, $\text{C}_{80}\text{H}_{44}$: $m/z = 1000$). The proposed hypothesis for this difference is an incomplete bromination reaction in the first step of scheme 3-7 with regard to the obtained result of the bromination reaction of *cis*-1,2-bis(9-anthryl)ethylene **27** as mentioned in section 2.1.2. (Scheme 2-4). Due to sterical hindrance between the two opposed anthracenes, the bromination might have happened selectively on the other four sites, leaving two double bonds intact. Following dehydrobromination then would yield compound **72b** with the observed $m/z = 1004$, as proposed in scheme 3-8.



Scheme 3-8. Proposed mechanism for bromination and dehydrobromination reaction of **56b**.

The four smaller peaks in figure 3-13 can readily be explained as side products from an incomplete dehydrobromination still containing n HBr equivalents ($n=1-4$). Increasing the basicity of the $t\text{-BuOK}$ by adding crown ether under otherwise identical conditions of scheme 3-7 did not lead to the formation of the desired product. Instead the reaction mixture decomposed and a brown, insoluble polymeric material was obtained. The same happened, when using different solvents (THF, DME and toluene) without crown ether. Attempts to synthesize compound **72a** by a chlorination and dehydrochlorination reaction led to the same result, **72b**.

Future work should focus on improving the bromination conditions of cyclophane **56b** in scheme 3-8.

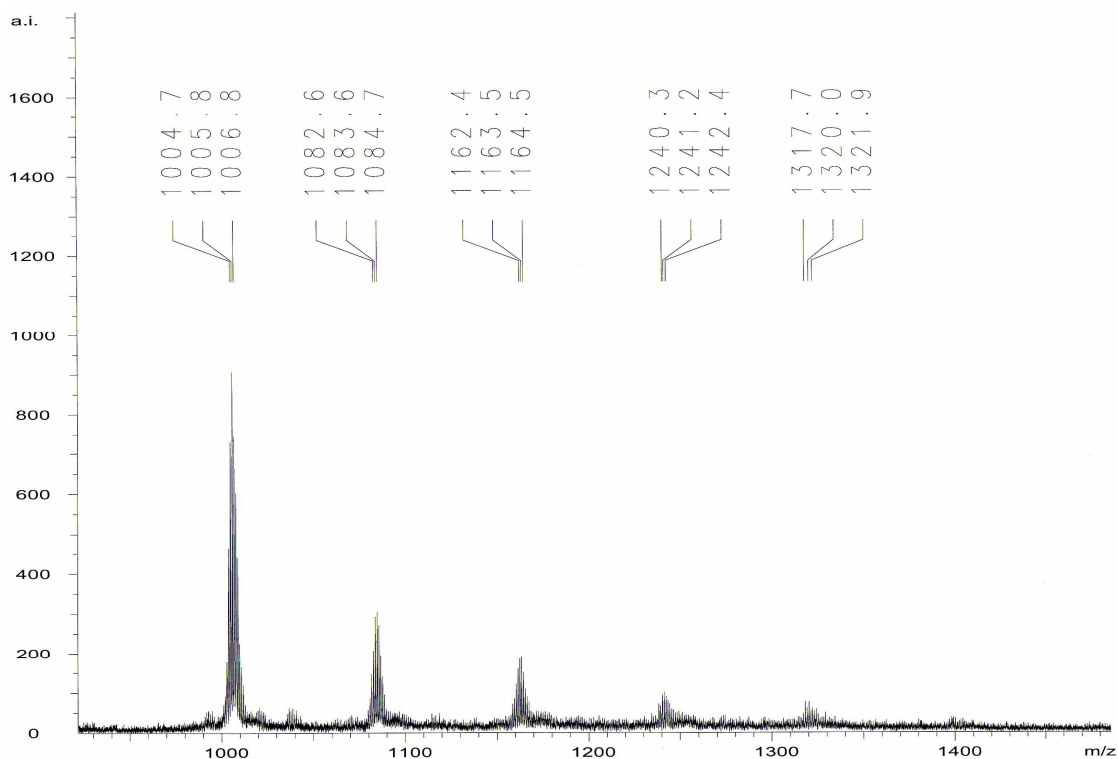


Figure 3-13. MALDI-TOF mass spectrum of resulted product of dehydrobromination of **56b**.

3.1.4.1. Physical properties

The red solid cyclophane **72b** shows a good solubility in dichloromethane and is unstable in the present of air and silica gel. Attempts to purify the crude compound by flash chromatography and even by analytical HPLC failed.

3.1.4.2. UV-Vis spectra

Figure 3-14 shows the UV-Vis spectra of **56b**, **71b** and **72b**. The weak band at 400 nm existing in **56b** has almost vanished in **71b**. This corresponds to the loss of conjugation over the ring. Compound **72b** shows broadening and a bathochromic shift about 25 nm compare to olefinic precursor **56b**. But, the bathochromic shift is significantly less than that of compound **69**. It is

probably due to worse conjugation of the π -electron in the structure of **72b**, induced by the remaining double bonds. 405

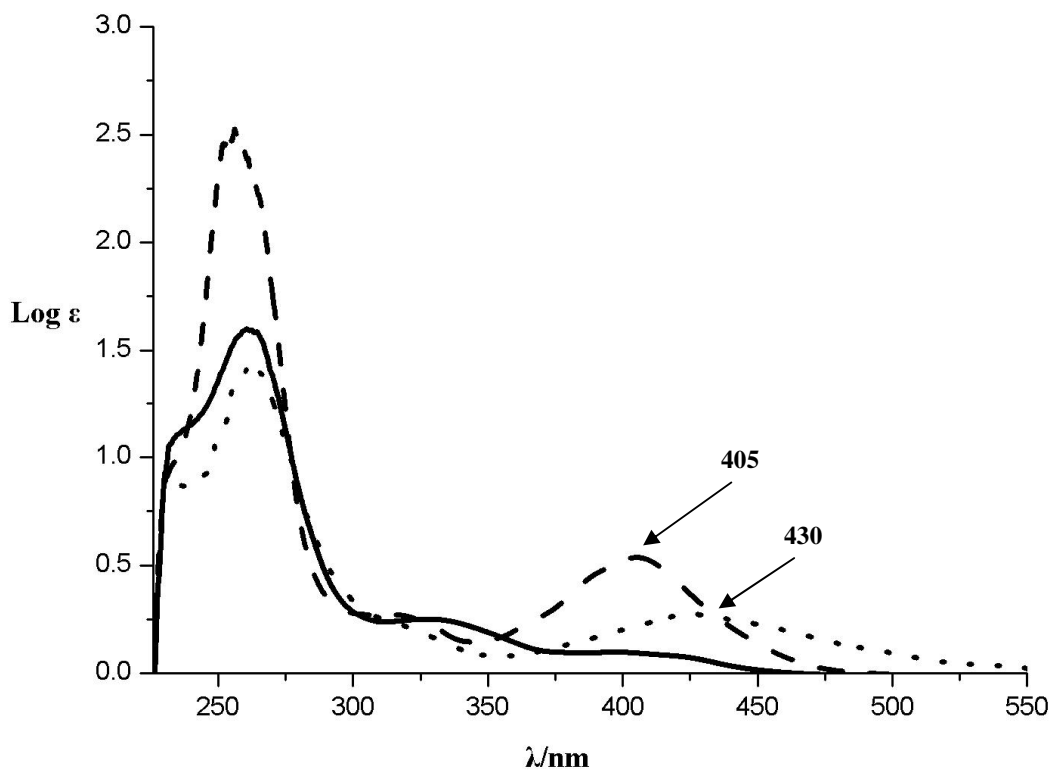


Figure 3-14. UV-Vis spectra of **56b** (dashed line), **71b** (solid line) and **72b** (dotted line) in CH_2Cl_2 .

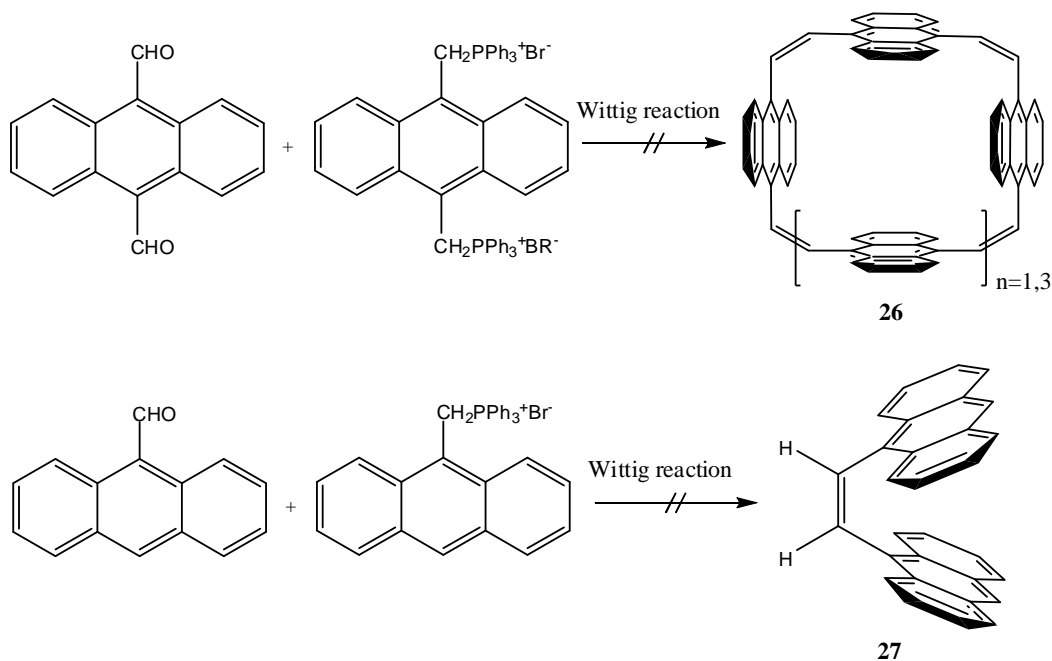
3.1.5. Conclusion

The halogenation and dehydrohalogenation reactions of **55b**, **55c** and **56b** as a simple and efficient access to belt-like aromatics were extensively investigated. The expected products of these reactions are cyclic [6] and [9]-*para*-anthrylacetylenes which could be very important intermediates in the rational synthesis of carbon nanotubes. Based on semiempirical (PM3) calculations, see table 1-1, compound **69**, **70** and **72a** should be accessible to synthesis. In the course of this work the synthesis of the conjugated molecular belt **69** and **70** were done for the first time and unambiguously identified by ^1H , ^{13}C -NMR and MALDI-TOF mass spectroscopy. Despite the

calculated strain energy of **72a** being fairly lower than those of **69**, **67** [6]-CPPA and **70** [6]-CPNA, all attempts to prepare this compound failed. Instead a different compound **72b** could be obtained, which also shows a highly interesting belt-shape. This is probably due to the increased sterical hindrance in the precursor **56b** induced by the additional anthracene units which make the double bonds inaccessible to halogenation under the conditions applied in this work. Experiments to circumvent these problems are in progress.

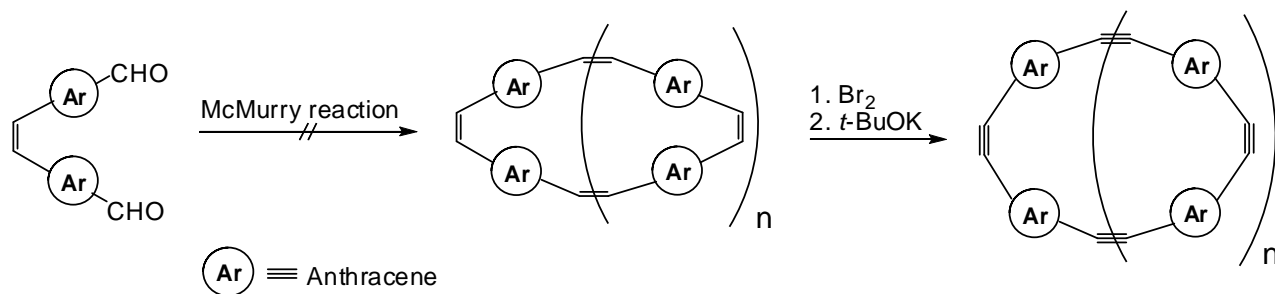
Chapter 4: Summary

Today, nanotechnology has found a great interest in research areas of different scientific fields. Indeed, nanoparticles and nanodevices possess new and promising properties for many applications. Synthesis chemistry provides access to such nanometer sized system because it allows a construction atom by atom. A rational synthesis of carbon nanotubes was therefore proposed using the conjugated molecular belts as precursors. This study was aimed at taking the first steps toward this ambitious goal. Despite the efforts to synthesize all kinds of cyclic-*para*-arylacetylene, cyclic-*para*-anthrylacetylenes have remained unknown to date. The Wittig coupling as a frequently used method for the synthesis of cyclophanes, was not applicable due to sterical hindrance in the 9 and 10 positions of anthracene.



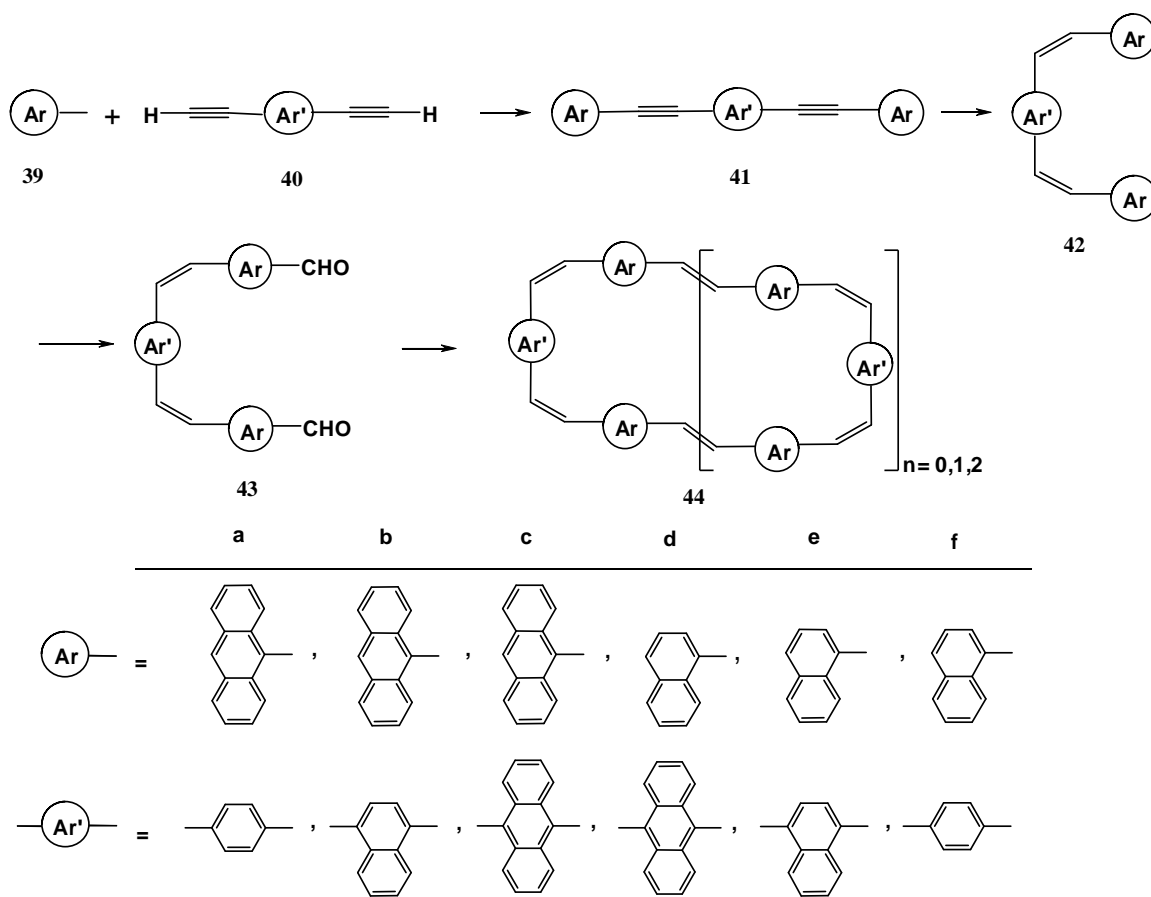
Scheme 4-1. The attempted Wittig reaction for synthesis of anthracenophanes.

The Oda, Kawase, Darabi method to prepare cyclic-*para*-phenyl and *para*-naphthylacetylenes failed if anthracene units were used.



Scheme 4-2. Oda, Kawase, Darabi strategy to synthesize cyclic $[n]$ -*para*-arylacetylene which failed in case of anthracene unit.

The new strategies presented here are based on the synthesis of open ring precursors with a suitable length and bent to provide the necessary preorientation for ring closure.



Scheme 4-3. A new strategy to synthesize cyclic $[n]$ -*para*-arylacetylene.

Using this strategy, however, a new set of the cyclic-*para*-arylethylenes containing anthracene units were synthesized. Among synthesized cyclophanes, crystal structure of **56b** ($n=1$) shows möbius topology.

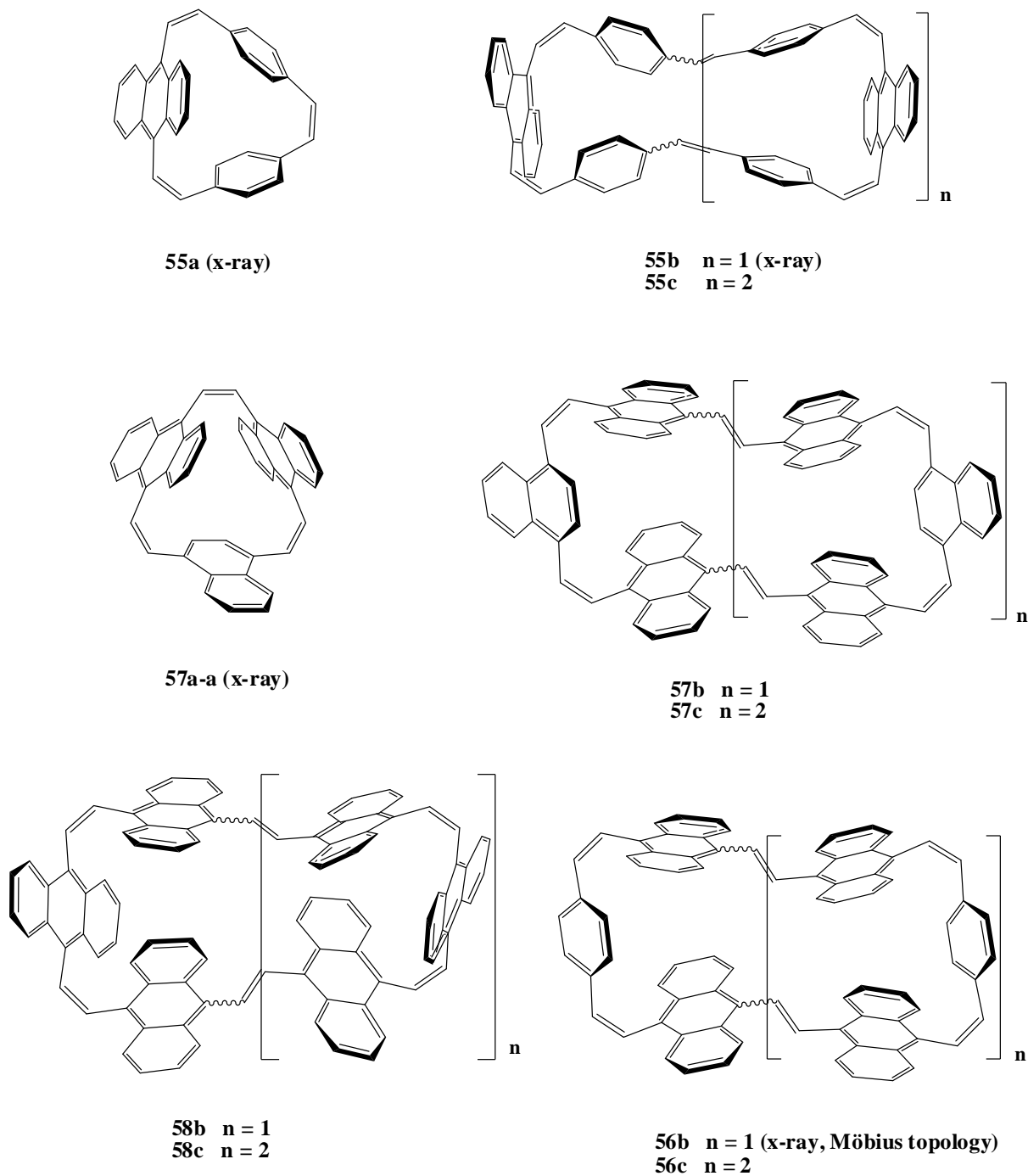
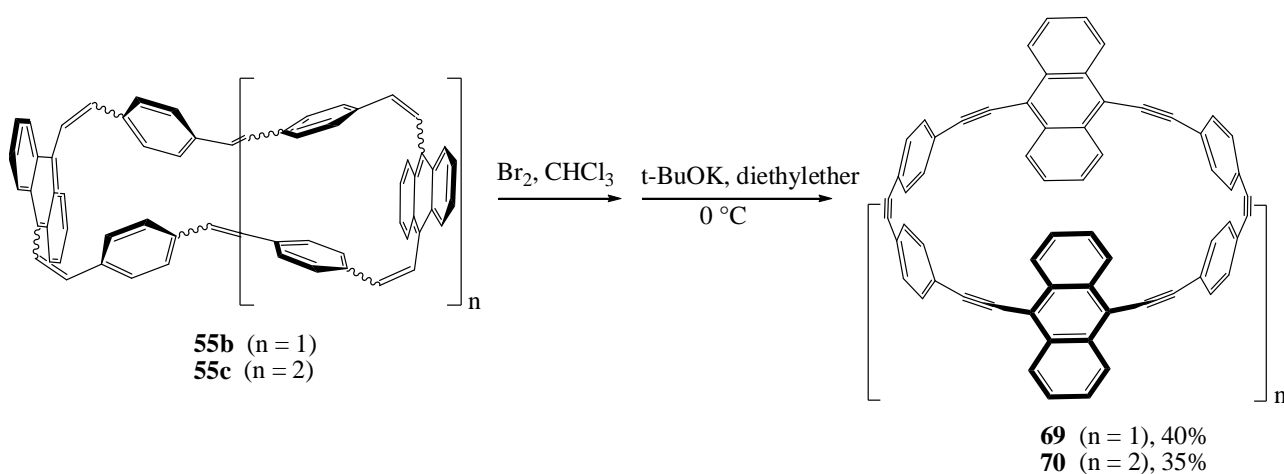


Figure 4-1. The Molecular structures of the new cyclic-*para*-arylethylenes.

The halogenation-dehydrohalogenation reactions as a simple and efficient methodology for the preparation of sterical cyclophanes containing acetylene units was used in the synthesis of cyclic-*para*-anthrylacetylene. Among the presented cyclic-*para*-arylethylenes ($n=1$), only **55b** and **55c** finally allowed the synthesis of the conjugated molecular belt under the bromination and dehydrobromination reactions. Even through different halogen and reaction conditions were applied other cyclic-*para*- anthrylacetylenes could not be prepared. The main reason for this failure is probably sterical hindrance between the two opposed anthracenes, which does not allow to perform the halogenation and dehalogenation procedure to generate the triple bonds. Experiments to circumvent these problems are in progress.



Scheme 4-4. Synthesis of [6] and [9]-CPAA's **69** and **70** by bromination and dehydrobromination reactions.

Chapter 5: Experimental part

5.1. Apparatus

NMR:	BRUKER AC 200	$^1\text{H-NMR}$ (200.1 MHz)	$^{13}\text{C-NMR}$ (50.3 MHz)
	BRUKER ARX 300	$^1\text{H-NMR}$ (300.1 MHz)	$^{13}\text{C-NMR}$ (75.5 MHz)
	BRUKER DRX 500	$^1\text{H-NMR}$ (500.1 MHz)	$^{13}\text{C-NMR}$ (125.8 MHz)
	BRUKER AV 600	$^1\text{H-NMR}$ (600.1 MHz)	$^{13}\text{C-NMR}$ (150.9 MHz)

Samples were solved in deuteriochloroform (CDCl_3). Chemical shifts are reported in units, part per million (ppm), from either tetramethylsilane (0 ppm) or chloroform (7.26 ppm) used as an internal standard. Splitting patterns are designated as s (singlet), d (doublet), t (triplet), q (quartet), sept (septuplet), m (multiplet) and br (broad).

IR: FT-IR Spectrometer Paragon 1000

MS: Finnigan MAT 8200
Bruker BiFlexIIITM MALDI-TOF

UV/Vis: PERKIN ELMER, UV/Vis Spectrometer lambda 14

X-Ray: Siemens P4-Diffractometer and STOE Imaging Plate Diffraction System (IPDS) with $\text{MoK}\alpha$ irradiation. Diffraction information have solved with SHELXS-97.

HPLC: Hewlett-Packard/Agilent Seri 1100/1200

5.2. Common procedure

All reactions were carried out under nitrogen (Schlenk conditions). Solvents were either distilled or dried and distilled (ethylacetate and CH_2Cl_2 : CaH_2 ; DME and toluene: Na, Benzophenone) before use or purchased predried (diisopropylamine: Fluka). Starting materials were ordered from Acros, Merck, Fluka, Aldrich and TCI companies. *Trans*-2-[3-(4-*tert.*-butylphenyl)-2-methyl-2-propenylidene]-malononitrile was used as a matrix in a saturated solution in dichloromethane.

Column chromatography was carried out with the use of Merck Art. 109385 Kieselgel 60 (0.04 – 0.063 mm) SC, neutral alumina Merck Art. 1097 Aluminioxid 90, actively II-III, 70-230 mesh ASTM. Analytical thin layer chromatography (TLC) was performed on Merck Art. POLYGRAM Sil G/UV254 for TLC (0.2 mm thick). Flash chromatography was performed under argon or nitrogen positive pressure for final ringed compounds according to the method reported by still.

The configuration of Analytical HPLC of HEWLETT PACKARD (*hp*) company is: Degasser, Quaternary Pump, Manual Injector bzw, Autosampler, Diode-Array-Detector, Automatic Fraction Sampler and Columns:

Kromasil 100 C18 10 μm , 250 x 10 mm

Kromasil 100 C18 10 μm , 250 x 8 mm

Kromasil 100 C18 10 μm , 250 x 4 mm

Kromasil 100 Sil 10 μm , 250 x 8 mm

Kromasil 100 Sil 10 μm , 250 x 4 mm

MZ Gel SD plus 50 A° 5 μm 300 x 8 mm (GPC)

MZ Gel SD plus 100 A° 5 μm 300 x 8 mm (GPC)

MZ Gel SD plus 500 A° 5 μm 300 x 8 mm (GPC)

5.3. Synthesis

5.3.1. Synthesis of pentachlorocyclopropane^[107]

In a soxhlet apparatus slurry of sodium trichloroacetate (350.0 g, 1.89 mol) in 1300 ml of trichloroethane was placed and refluxed for 3 hours. During this time approximately 0.1 ml of H₂O was absorbed by finger filter containing of calcium hydride. The soxhlet apparatus was removed and 200 ml of dimethoxyethane (DME) was added. The mixture was refluxed for 5 days. A slow stream of CO₂ was observed during this period. The reaction mixture was washed repeatedly with water, dilutes HCl and finally water and then dried over Na₂SO₄. The crude product was purified by fractional distillation to remove excess trichloroethylene. The fractions boiling between 80 and 85 °C (31 mm) gave 205.0 g (51 %) of pentachlorocyclopropane.

5.3.2. Synthesis of tetrachlorocyclopropene^[107]

In a two-necked flask containing a solution of 35.5 g of KOH in 40 ml of water was added 50.0 g (0.223 mmol) of pentachlorocyclopropane. The mixture was stirred and heated to 75 °C till a spontaneous reaction started. The heat was removed and the temperature increase to 88 °C where it was maintained by ice bath. After 25 min the mixture was cooling to 50 °C and 50 ml of ice water and then 25 ml of cold concentrated HCl were added. The organic phase was extracted with CH₂Cl₂, washed with water and dried over Na₂SO₄. The crude product was purified by fractional distillation. The fractions boiling between 71-72 °C (98 mm) gave 33.2 g (80 %) of tetrachlorocyclopropene.

¹³C-NMR (75.5 MHz, CDCl₃/TMS): δ= 122.71, 62.37 ppm.

MS (EI, 70 eV): *m/z* (%): 178 (8), 143 (97), 141 (100), 106 (25).

5.3.3. Synthesis of 2,3-bis-9-anthrylcyclopropenone 29^[65,66]

In a dry two-necked, round-bottom flask equipped with a stirred bar and a nitrogen inlet tube was placed a suspension of aluminum chloride (1.162 g, 6.8 mmol) in dry 1,2-dichloroethane (25 ml).

tetrachlorocyclopropene (1.55 g, 8.4 mmol) was added to mixture and stirred at room temperature for 30 min to give a pale brownish suspension. The mixture was then cooled to -30 °C, and anthracene (3.0 g, 16.8 mmol) was added slowly over a period of 1 h. The deep violet colored reaction mixture was allowed to warm up to 0 °C, and stirred for additional 2 h at that temperature. The reaction mixture was poured into ice-water and stirred for 1 h, then the orange precipitate was filtrated off and washed with acetone to obtain **29** (1.61 g, 70 %).

¹H-NMR (300 MHz, CDCl₃/TMS): δ= 8.76 (2H, s), 8.38 (4H, d), 8.12 (4H, d), 7.50 (4H, m), 7.38 (4H, m) ppm.

MS (EI, 70 eV): *m/z* (%): 378 (100) [M⁺ - 28 (C=O)], 189 (18).

5.3.4. Synthesis of 1,2-di-9-anthrylacetylen **30**^[65,66]

In a dry round-bottom flask equipped with a stirred bar and a nitrogen inlet tube was placed a solution of the 2,3-bis-9-anthrylcyclopropenone (1.5 g, 3.7 mmol) and alumina pellets (0.3 g) in DMSO (20 ml). The mixture was refluxed for 3 h and cooled down to room temperature. Then orange-red crystalline residue was filtered and washed with water and acetone. Recrystallization in a stirred hot dioxane gives an orange red, needle-shaped crystal of **30** (1.30 g, 94 %).

¹H-NMR (300 MHz, CDCl₃/TMS): δ= 8.94 (4H, d), 8.53 (2H, s), 8.14 (4H, d), 7.69 (4H, m), 7.55 (4H, m) ppm.

¹³C-NMR (75.5 MHz, CDCl₃/TMS): δ= 132.81, 131.36, 128.86, 128.02, 126.96, 126.94, 125.79 ppm.

MS (EI, 70 eV): *m/z* (%): 379 (33) [M⁺ + 1], 378 (100) [M⁺], 189 (16).

5.3.5. Synthesis of 1,4-dibromonaphthalene^[108]

In a dry two-necked flask equipped with a stirred bar containing 1-bromonaphthalene (3.10 g, 15 mmol) under nitrogen was charged with 15 ml of dichloromethane. The solution was cooled to -30 °C and initially cooled (-30 °C) bromine (1.65 equiv., 2.64 g, 16.5 mmol) in CH₂Cl₂ (8 ml) was

added dropwise to solution which is protected from light. The reaction mixture was maintained in a freezer at $-30\text{ }^{\circ}\text{C}$ for 2 days in the dark. Recrystallized product was filtered and dissolved in CH_2Cl_2 and then washed with sodiumtiosulfate and dried with sodium sulfate. After evaporating solvent in low pressure, crude product was crystallized in CH_2Cl_2 : PE (1:4) to obtain a white crystal of 1, 4-DBN in a yield of 88% (3.76 g).

$^1\text{H-NMR}$ (300 MHz, CDCl_3/TMS): δ = 8.22 (2H, s), 7.62 (2H, d), 7.60 (2H, m) ppm.

$^{13}\text{C-NMR}$ (75.5 MHz, CDCl_3/TMS): δ = 132.89, 130.03, 127.50, 122.68 ppm.

5.3.6. Synthesis of 9,10-dibromoanthracene^[109]

In a dry two-necked flask equipped with a stirred bar containing anthracene (2.67g, 15 mmol) under nitrogen was charged with 120 ml of dichloromethane. The solution was cooled to $0\text{ }^{\circ}\text{C}$ and initially cooled ($0\text{ }^{\circ}\text{C}$) bromine (5.17 g, 33 mmol) in CH_2Cl_2 (15 ml) was added dropwise to solution which is protected from light. The reaction mixture was stirred for 1 hr. After removing the solvent the precipitated compound was dissolve in CH_2Cl_2 and then washed with sodiumtiosulfate and dried with sodium sulfate. The solvent was evaporated in low pressure. The crude product was crystallized in hot CH_2Cl_2 to obtain 9,10- dibromoanthracene (4.73 g, 94%) as pure yellow needles.

$^1\text{H-NMR}$ (300 MHz, CDCl_3/TMS): δ = 8.55 (4H, m), 7.60 (4H, m) ppm.

$^{13}\text{C-NMR}$ (75.5 MHz, CDCl_3/TMS): δ = 131.38, 128.39, 127.50, 123.68 ppm.

5.3.7. Synthesis of 9-bromoanthracene^[110]

A solution of anthracene (35.0 g, 0.19 mol), *n*-bromosuccinimide (33.5 g, 0.19 mol) and a trace amount of Iodine in carbon tetrachloride (100 ml) was refluxed for 10 h. The brown mixture was filtered and washed with sodiumthiosulfate and sodium hydrogen carbonate. The crude product was crystallized in hot ethanol to obtain 9-bromoanthracene (39.41 g, 78%) as pure yellow needles.

¹H-NMR (300 MHz, CDCl₃/TMS): δ= 8.49 (2H, d), 8.39 (2H, d), 7.96 (1H, s), 7.58 (2H, t), 7.47 (2H, t) ppm.

MS (EI, 70 eV): *m/z* (%): 258 (98) [M⁺], 256 (M⁺+100), 177 (52).

5.3.8. Synthesis of 1,4-Diiodonaphthalene^[111]

In a dry two-necked, round-bottom flask equipped with a stirred bar, a rubber septum and a nitrogen inlet tube was placed 1,4-dibromonaphthalene (3.87, 13.5 mmol) in anhydrous diethyl ether (70 cm³). To the stirred mixture was added *n*-BuLi (14.18 ml, 2.5 M in hexane, 35.45 mmol) via syringe dropwise over the course of 30 min. The resulting mixture was stirred for an additional 10 min after which period iodine crystal (11.52 g, 45.36 mmol) were added in several portions over 5 min. the mixture was stirred for an additional 15 min until the color was a dark brown. The ethereal solution was washed several times with aqueous sodiumthiosulfate (25% w/w), dried over anhydrous magnesium sulfate and the solvent removed under vacuum to obtain a pale yellow solid. The crude product was purified by recrystallization in the CCl₄ (70 cm³) to give white solid of 1,4-diiodonaphthalene (2.62 g, 51% yield).

¹H-NMR (500 MHz, CDCl₃/TMS): δ= 8.22 (2H, d), 7.62 (2H, d), 7.60 (2H, s) ppm.

MS (EI, 70 eV): *m/z* (%): 380 (84) [M⁺], 253 (13) [M⁺-I], 126 (100) [M⁺-2I].

5.3.9. Synthesis of 9,10-Diidoanthracene^[111]

In a dry two-necked, round-bottom flask equipped with a stirred bar, a rubber septum and a nitrogen inlet tube was placed 9,10-dibromoanthracene (4.0, 11.9 mmol) in anhydrous diethyl ether (75 cm³). To the stirred mixture was added *n*-BuLi (12.48 ml, 2.5 M in hexane, 31.2 mmol) via syringe dropwise over the course of 45 min. The resulting mixture was stirred for an additional 15 min after which period iodine crystal (10.15 g, 40 mmol) were added in several portions over 5 min. The mixture was stirred for an additional 15 min until the color was a dark brown. The ethereal solution was washed several times with aqueous sodiumthiosulfate (25% w/w), dried over anhydrous sodium sulfate and the solvent removed under vacuum to obtain a pale yellow solid. The

crude product was purified by recrystallization from CCl_4 (130 cm^3) to give (2.48 g, 48% yield) yellow needles.

$^1\text{H-NMR}$ (500 MHz, CDCl_3/TMS): δ = 8.56 (4H, m), 7.62 (4H, m), 8.14 (4H, d), 7.69 (4H, m), 7.55 (4H, m) ppm.

MS (EI, 70 eV): m/z (%): 430 (100) [M^+], 303 (20), 176 (86).

5.3.10. Synthesis of 1-iodonaphthalene

In a dry two-necked, round-bottom flask equipped with a stirred bar, a rubber septum and a nitrogen inlet tube was placed 1-bromonaphthalene (2.58 g, 12.5 mmol) in anhydrous diethyl ether (30 cm^3). To the stirred mixture was added (6.55 ml, 2.5 M in hexane, 16.38 mmol) via syringe dropwise over the course of 45 min. The resulting mixture was stirred for an additional 15 min after which period iodine crystal (5.33 g, 21.0 mmol) were added in several portions over 5 min. The mixture was stirred for an additional 15 min until the color was a dark brown. The ethereal solution was washed several times with aqueous sodiumthiosulfate (25% w/w), dried over anhydrous sodium sulfate and the solvent removed under vacuum to obtain a pale yellow solid. The crude product was purified by recrystallization from CCl_4 (130 cm^3) to give (2.48 g, 48% yield) yellow needles.

$^1\text{H-NMR}$ (500 MHz, CDCl_3/TMS): δ = 8.06 (2H, m), 7.77 (1H, d), 7.70 (1H, d), 7.52 (1H, m), 7.46 (1H, m), 7.11 (1H, m) ppm.

MS (EI, 70 eV): m/z (%): 254 (85) [M^+], 127 (100), 101 (10).

5.3.11. Synthesis of 9-iodoanthracene

In a dry two-necked, round-bottom flask equipped with a stirred bar, a rubber septum and a nitrogen inlet tube was placed 9-bromoanthracene (4.0, 15.56 mmol) in anhydrous diethyl ether (40 cm^3). To the stirred mixture was added (8.15 ml, 2.5 M in hexane, 20.39 mmol) via syringe dropwise over the course of 45 min. The resulting mixture was stirred for an additional 15 min after

witch period iodine crystal (6.53 g, 26.13 mmol) were added in several portions over 5 min. The mixture was stirred for an additional 15 min until the color was a dark brown. The ethereal solution was washed several times with aqueous sodiumthiosulfate (25% w/w), dried over anhydrous sodium sulfate and the solvent removed under vacuum to obtain a pale yellow solid. The crude product was purified by recrystallization from CCl_4 (50 cm^3) to give (2.13 g, 45% yield) yellow needles.

$^1\text{H-NMR}$ (500 MHz, CDCl_3/TMS): δ = 8.46 (2H, d), 8.44 (1H, s), 7.95 (2H, d), 7.58 (2H, t), 7.49 (2H, t) ppm.

MS (EI, 70 eV): m/z (%): 304 (100) [M^+], 177(57), 152 (12).

5.3.12. Synthesis of 1,4-bis(trimethylsilylethynyl)naphthalene^[111]

In a dry two-necked, round-bottom flask equipped with a stirred bar, a rubber septum and a nitrogen inlet tube was placed 1,4-diiodonaphthalene (3.0, 7.89 mmol) and a catalytic mixture of CuI (20 mg), $\text{Pd}(\text{PPh}_3)_2\text{Cl}_2$ (20 mg) and PPh_3 (60 mg) in $i\text{-Pr}_2\text{NH-THF}$ (100 cm^3 , 1:1 v/v). The solution was stirred for 20 min. at 50 °C and then trimethylsilylethyne (2.52 g, 25.65 mmol) was added. The resulting mixture was refluxed for 8 h at 75 °C. The completion of the reaction was monitored by silica TLC. The solution was allowed to cool to room temperature, filtered and the solvent was removed by evaporation. The crude product was purified by chromatography on silica gel (hexane) to give the desired product as a salmon colored crystalline solid in 95% yield (2.40 g).

5.3.13. Synthesis of 1,4-bis(ethynyl)naphthalene^[111]

In a one-neck round-bottom flask, 1,4-bis-trimethylsilylethynyl naphthalene (2.0 g, 6.24 mmol) was proto-desilylated in THF-methanol (50 cm^3 , 4:1 v/v) using aqueous KOH (0.76 g, 13.36 mmol in 2 cm^3 H_2O). The reaction mixture was stirred for 2 h at room temperature, washed twice with water, dried over MgSO_4 , filtered and concentrated. Chromatography on silica gel (Hexane) gave 0.99 g (90%) result as a brown solid.

¹H-NMR (200 MHz, CDCl₃/TMS): δ= 8.38 (2H, m), 7.67 (2H, s), 7.62 (2H, m), 7.55 (2H, s), ppm.

MS (EI, 70 eV): *m/z* (%): 176 (100) [M⁺], 1741(14), 50(3).

5.3.14. Synthesis of 9,10-bis(trimethylsilylethynyl)anthracene^[111]

In a dry two-necked, round-bottom flask equipped with a stirred bar, a rubber septum and a nitrogen inlet tube was placed 9,10-diiodoanthracene (3.0, 6.9 mmol) and a catalytic mixture of CuI (20 mg), Pd(PPh₃)₂Cl₂ (20 mg) and PPh₃ (60 mg) in *i*-Pr₂NH-THF (100 cm³, 1:1 v/v). The solution was stirred for 20 min. at 50 °C and then trimethylsilylethyne (2.20 g, 22.43 mmol) was added. The resulting mixture was refluxed for 8 h at 75 °C. The completion of the reaction was monitored by silica TLC. The solution was allowed to cool to room temperature, filtered and the solvent was removed by evaporation. The crude product was purified by chromatography on silica gel (hexane) to give the desired product as a deep red crystalline solid in 90% isolated yield (1.91 g).

5.3.15. Synthesis of 9,10-bis(ethynyl)anthracene^[111]

In a one-neck round-bottom flask, 9,10-bis-trimethylsilylethynylanthracene (1.5 g, 4.05 mmol) was proto-desilylated in THF-methanol (50 cm³, 4:1 v/v) using aqueous KOH (0.49 g, 8.68 mmol in 1 cm³ H₂O). The reaction mixture was stirred for 2 h at room temperature, washed twice with water, dried over MgSO₄, filtered and concentrated. Chromatography on silica gel (hexane) gave 0.78 g (85%) result as a dark red solid.

¹H-NMR (500 MHz, CDCl₃/TMS): δ= 8.60 (4H, m), 7.60 (4H, m) ppm.

MS (EI, 70 eV): *m/z* (%): 226 (100) [M⁺], 224 (22).

5.3.16. General procedure for the Sonogashira coupling

A two-necked, round-bottom flask containing (2.0 mmol) of diethynylarene, (4.0 mmol) of iodoarene and a catalytic amount of CuI (25 mg) and Pd(PPh₃)₂ Cl₂ (25 mg) under nitrogen was charged with 40 ml of diisopropylamine. After stirring at room temperature for 2 h, the reaction

mixture was heated to reflux for an additional 30 min to ensure completion. The resulting precipitate was collected by filtration, redissolved in hot toluene, and filtered through a short column (1 cm) of silica gel. The products can be recrystallized by cooling the hot toluene solution.

5.3.17. Synthesis of 1,4-bis(9-ethynylantraceny)benzene 41a

A two-necked, round-bottom flask containing 0.252 g (2 mmol) of 1,4-bis(ethynyl)benzene, 1.216 g (4 mmol) of 1-iodonaphthalene and a catalytic amount of CuI (30 mg) and Pd(PPh₃)₂Cl₂ (30 mg) under nitrogen was charged with 40 ml of diisopropylamine. After stirring at room temperature for 4 h, the reaction mixture was heated to reflux for an additional 30 min to ensure completion. The resulting precipitate was collected by filtration, redissolved in hot toluene, and filtered through a short column (1 cm) of silica gel. An orange solid (0.784 g, 82%) were obtained by cooling the hot toluene solution

¹H-NMR (500 MHz, CDCl₃/TMS): δ = 8.68 (4H, d, J=8.7 Hz, anthracene Hs), 8.48 (2H, s, anthracene Hs), 8.05 (4H, d, J=8.5 Hz, anthracene Hs), 7.85 (4H, s, phenyl Hs), 7.55-7.65 (8H, m, anthracene Hs), ppm.

MS (EI, 70 eV): *m/z* (%): 479 (40) [M⁺ + 1], 478 (100) [M⁺], 239 (20).

5.3.18. Synthesis of 1,4-bis(9-ethynylantraceny)naphthalene 41b

A two-necked, round-bottom flask containing 0.226 g (2 mmol) of 1,4-bis(ethynyl)naphthalene, 1.216 g (4 mmol) of 9-iodoanthracene and a catalytic amount of CuI (30 mg) and Pd(PPh₃)₂Cl₂ (30 mg) under nitrogen was charged with 50 ml of diisopropylamine. After stirring at room temperature for 2 h, the reaction mixture was heated to reflux for an additional 10 min to ensure completion. The resulting precipitate was collected by filtration, redissolved in hot toluene, and filtered through a short column (1 cm) of silica gel. Red solid (0.542 g, 80%) were obtained by cooling the hot toluene solution.

¹H-NMR (500 MHz, CDCl₃/TMS): δ= 8.82 (4H, d, J=8.5 Hz, anthracene Hs), 8.81 (2H, d, J=9.6 Hz, naphthalene Hs), 8.52 (2H, s, anthracene Hs), 8.09 (2H, s, naphthalene Hs), 8.08 (4H, d, J=6.9 Hz, anthracene Hs), 7.79 (2H, m, naphthalene Hs), 7.55-7.68 (8H, m, anthracene Hs) ppm.
MS (EI, 70 eV): *m/z* (%): 529 (48) [M⁺+1], 528 (100) [M⁺], 350 (2), 262 (36), 174 (5).

5.3.19. Synthesis of 9,10-bis(9-ethynylantraceny)anthracene 41c

A two-necked, round-bottom flask containing 0.452 g (2 mmol) of 9,10-bis(ethynyl)anthracene, 1.216 g (4 mmol) of 9-iodoanthracene and a catalytic amount of CuI (30 mg) and Pd(PPh₃)₂Cl₂ (30 mg) under nitrogen was charged with 50 ml of diisopropylamine. After stirring at room temperature for 4 h, the reaction mixture was heated to reflux for an additional 60 min to ensure completion. The resulting precipitate was collected by filtration, redissolved in hot toluene, and filtered through a short column (1 cm) of silica gel. Dark red solid (0.812 g, 70%) were obtained by cooling the hot toluene solution.

¹H-NMR (500 MHz, CDCl₃/TMS): δ= 9.04 (4H, m, middle anthracene Hs), 8.94 (4H, d, J=7.3 Hz, anthracene Hs), 8.56 (2H, s, anthracene Hs), 8.10 (4H, d, J=7.3 Hz, anthracene Hs), 7.76 (4H, m, middle anthracene Hs), 7.59-7.70 (8H, m, anthracene Hs) ppm.
MS (EI, 70 eV): *m/z* (%): 579 (49) [M⁺ + 1], 578 (100) [M⁺], 378 (12), 289 (31), 187 (4).

5.3.20. Synthesis of 9,10-bis(1-ethynynaphthyl)anthracene 41d

A two-necked, round-bottom flask containing 0.452 g (2 mmol) of 9,10-bis(ethynyl)anthracene, 1.016 g (4 mmol) of 1-iodonaphthalene and a catalytic amount of CuI (30 mg) and Pd(PPh₃)₂Cl₂ (30 mg) under nitrogen was charged with 50 ml of diisopropylamine. After stirring at room temperature for 4 h, the reaction mixture was heated to reflux for an additional 45 min to ensure completion. The resulting precipitate was collected by filtration, redissolved in hot toluene, and filtered through a short column (1 cm) of silica gel. Dark green solid (0.717 g, 75%) were obtained by cooling the hot toluene solution.

¹H-NMR (500 MHz, CDCl₃/TMS): δ= 8.87 (4H, m, anthracene Hs), 8.70 (2H, d, J=8.5 Hz), 8.05 (2H, d, J=7.1 Hz), 7.95 (4H, d, J=8.4 Hz), 7.72 (4H, m, anthracene Hs), 7.65 (2H, m), 7.57-7.62 (4H, m) ppm.

¹³C NMR (125.8 MHz, CDCl₃/TMS): δ= 133.43, 133.28, 132.33, 130.94, 129.29, 128.55, 127.44, 127.20, 127.05, 126.65, 126.39, 125.48, 121.17, 118.80, 100.74, 91.31 ppm.

MS (EI, 70 eV): *m/z* (%): 479 (40) [M⁺ + 1], 478 (100) [M⁺], 239 (20).

5.3.21. Synthesis of 1,4-bis(1-ethynynaphthyl)naphthalene 41e

A two-necked, round-bottom flask containing 0.352 g (2.0 mmol) of 1,4-bis(ethynyl)naphthalene, 1.016 g (4.0 mmol) of 1-iodonaphthalene and a catalytic amount of CuI (20 mg) and Pd(PPh₃)₂Cl₂ (20 mg) under nitrogen was charged with 30 ml of diisopropylamine. After stirring at room temperature for 2 h, the reaction mixture was heated to reflux for an additional 10 min to ensure completion. The resulting precipitate was collected by filtration, redissolved in hot toluene, and filtered through a short column (1 cm) of silica gel. Yellow solid (0.727 g, 85%) were obtained by cooling the hot toluene solution.

¹H-NMR (500 MHz, CDCl₃/TMS): δ= 8.64 (2H, m), 8.58 (2H, J=8.4 Hz, d), 7.92 (6H, m), 7.72 (2H, m), 7.67 (2H, t), 7.58 (2H, t), 7.53 (2H, t) ppm.

¹³C-NMR (125.8 MHz, CDCl₃/TMS): δ= 133.38, 133.33, 133.24, 130.78, 129.98, 129.16, 128.47, 127.46, 127.05, 126.84, 126.58, 126.30, 125.39, 121.84, 120.94, 94.28, 92.47 ppm.

MS (EI, 70 eV): *m/z* (%): 429 (35) [M⁺+1], 428 (100) [M⁺], 301 (15), 212 (18).

5.3.22. Synthesis of 1,4-bis(1-ethynynaphthyl)benzene 41f

A two-necked, round-bottom flask containing 0.378 g (3 mmol) of 1,4-bis(ethynyl)benzene, 1.524 g (6 mmol) of 1-iodonaphthalene and a catalytic amount of CuI (20 mg) and Pd(PPh₃)₂Cl₂ (20 mg) under nitrogen was charged with 30 ml of diisopropylamine. After stirring at room temperature For 2 h, the reaction mixture was heated to reflux for an additional 10 min to ensure completion. The

resulting precipitate was collected by filtration, redissolved in hot toluene, and filtered through a short column (1 cm) of silica gel. The products can be recrystallized by cooling the hot toluene solution. Yield 1.01 mg (89 %) cream solid.

¹H-NMR (200 MHz, CDCl₃/TMS): δ = 8.45 (2H, d, J=8.0 Hz.), 8.89 (2H, m), 8.85 (2H, m), 7.78 (2H, d, J=7.9 Hz.), 7.66 (4H, s), 7.63-7.43 (6H, m) ppm. ¹³C

NMR (50.3 MHz, CDCl₃/TMS): δ = 133.25, 131.68, 130.55, 129.03, 128.38, 126.90, 126.52, 126.18, 123.36, 120.69, 94.07, 89.55 ppm. **MS**

(EI, 70 eV): *m/z* (%): 379 (33) [M⁺+1], 378 (100) [M⁺], 189 (18).

3.23. Synthesis of 9,10-bis[(1-ethynyl-4-bromo)phenyl]dihydroanthracene-9,10-diol 48a

To a flask containing 1-bromo-4-ethynyl-benzene (1.0 g, 5.55 mmol) in THF (50 ml) at -70°C, *n*-BuLi (2.22 ml, 2.5 M in hexane, 5.55 mmol) was added slowly while stirring for 2 h. The reaction mixture was then allowed to warm to room temperature and then cooled to -70 °C. A solution of 9,10-anthroquinone (0.577 g, 2.780 mmol) in THF (50 ml) was added dropwise and the solution was then allowed to warm slowly to room temperature and stirred overnight. The deep red resulting mixture was treated with a saturated solution of ammonium chloride and extracted with ethyl acetate. The yellow solvent was concentrated under reduced pressure and subjected to silica gel column chromatography using CH₂Cl₂/ EtOAc gradient to give 1.297 g (85 %) of product as a cream solid.

¹H-NMR (500 MHz, CDCl₃/TMS): δ = 8.22 (4H, m, anthracene Hs), 7.47 (4H, m, anthracene Hs), 7.49 (4H, d, J=8.6 Hz, benzene Hs), 7.44 (4H, d, J=8.6 Hz, benzene Hs), 3.85(2H, s, hydroxyl Hs).

5.3.24. Synthesis of 9,10-bis[(1-ethynyl-4-bromo)phenyl]anthracene 48b

In a two necked, round-bottom flask 9,10-bis[(1-ethynyl-4-bromo)phenyl]dihydroanthracene-9,10-diol **48a** (1.2 g, 2.1 mmol) was dissolved in ethanol (30 ml) and added dropwise to a solution of SnCl₂·2H₂O (0.94 g, 4.2 mmol) in acetic acid glacial (30 ml) while stirring at 60 °C over the course

of 20 min. The precipitate formed was collected by filtration and washed with water to remove acid completely and dried to obtain (0.73 g, 65%) product as an orange powder.

¹H-NMR (500 MHz, CDCl₃/TMS): δ = 8.68 (4H, m, anthracene Hs), 7.67 (4H, m, anthracene Hs), 7.62 (4H, d, J=8.6 Hz, benzene Hs), 7.59 (4H, d, J=8.6 Hz, benzene Hs). **MS** (EI, 70 eV): *m/z* (%): 536 (100) [M⁺], 458 (72) [M⁺-Br], 374 (43) [M⁺-2Br], 268 (15), 187 (44).

5.3.25. General procedure for the Hydrogenation reaction

In a two-necked flask equipped with a gas outlet tube, the unsaturated compound in ethyl acetate (toluene) and palladium catalyst was added. The slurry was vigorously stirred under a hydrogen atmosphere (room temperature). The mixture was filtered through a pad of celite, the solvent evaporated in vacuo to afford a solid product without further purification.

5.3.26. Synthesis of (Z)-1,2-di(9-anthryl)ethenes 27

A two-necked, round-bottom flask and a gas outlet tube, was placed 1,2-di-9-anthrylacetylen (0.400g, 1.05 mmol) in ethyl acetate (450 ml) and Palladium on barium sulfate, 5 % Pd (1 g) as a hydrogenation catalyst. The slurry was vigorously stirred under a hydrogen atmosphere (room temperature, 2h). The mixture was filtered through a pad of celite, the solvent evaporated in vacuo to afford (0.402 g, 98 %) a cream solid product without further purification.

¹H-NMR (300 MHz, CDCl₃/TMS): δ = 8.22 (4H, d, J=8.8 Hz, anthracene Hs), 8.08 (2H, s, anthracene Hs), 8.04 (2H, s, double bond Hs), 7.72 (4H, d, J=8.5 Hz, anthracene Hs), 7.22 (4H, t, anthracene Hs), 7.08 (4H, t, anthracene Hs) ppm.

¹³C-NMR (75.5 MHz, CDCl₃/TMS): δ = 131.54, 131.38, 131.03, 128.37, 127.24, 127.02, 126.56, 126.18, 125.84, 125.72, 124.89, 124.83, 124.78, 124.64, 124.21 ppm.

MS (EI, 70 eV): *m/z* (%): 380 (100) [M⁺], 303 (18), 202 (287), 178 (24).

5.3.27. Synthesis of (Z,Z)-9,10-bis(4-bromo-styryl)anthracene 50

A two-necked, round-bottom flask and a gas outlet tube, was placed 9,10-bis[(1-ethynyl-4-bromo)phenyl]anthracene (0.400g, 0.75 mmol) in ethyl acetate (350 ml) and palladium on barium sulfate, 5 % pd (1 g) as a hydrogenation catalyst. The slurry was vigorously stirred under a hydrogen atmosphere (room temperature, 55 min). The mixture was filtered through a pad of celite, the solvent evaporated in vacuo to afford (0.404 g, 100 %) a yellow solid product without further purification.

¹H-NMR (500 MHz, CDCl₃/TMS): δ = 8.35 (4H, m, anthracene Hs), 7.92 (2H, d, J=16.3 Hz, double bond Hs), 7.54-7.60 (8H, m, benzene Hs), 7.48 (4H, m, anthracene Hs), 6.87 (2H, d, J=16.5 Hz, double bond Hs) ppm.

¹³C-NMR (125.8 MHz, CDCl₃/TMS): δ = 136.34, 133.04, 131.98, 131.25, 131.10, 130.20, 129.52, 128.71, 128.11, 127.72, 126.55, 126.35, 125.93, 125.81, 125.45 ppm.

MS (EI, 70 eV): *m/z* (%): 540(100)[M⁺], 460 (24) [M⁺-Br], 380 (12) [M⁺-2Br], 302 (43), 189 (21).

5.3.28. Synthesis of (Z,Z)-1,4-bis(9-ethenylanthracenyl)benzene 42a

A two-necked, round-bottom flask and a gas outlet tube, was placed 1,4-bis(9-ethenylanthracenyl)benzene (0.400 mg, 0.836 mmol) in ethyl acetate (400 ml) and palladium on barium sulfate, 5 % pd (800 mg) as a hydrogenation catalyst. The slurry was vigorously stirred under a hydrogen atmosphere (room temperature, 40 min). The mixture was filtered through a pad of celite, the solvent evaporated in vacuo to afford (0.404 g, 100 %) a yellow solid product without further purification.

¹H-NMR (500 MHz, CDCl₃/TMS): δ = 8.36 (2H, s, anthracene Hs), 8.03 (4H, d, J=8.8 Hz, anthracene Hs), 7.96 (4H, d, J=8.5 Hz anthracene Hs), 7.27-7.40 (8H, m, anthracene Hs), 7.03 (2H, d, J=12.5 Hz, double bond Hs), δ = 6.87 (2H, d, J=12.45 Hz, double bond Hs), 6.88 (4H, s, phenyl Hs) ppm.

¹³C NMR (125.8 MHz, CDCl₃/TMS): δ = 133.58, 132.37, 131.50, 128.68, 128.62, 128.51, 126.44, 126.32, 126.08, 125.54, 125.26 ppm.

MS (EI, 70 eV): m/z (%): 482 (100) [M^+], 293 (27), 279 (26), 241 (21), 203 (36), 191 (72).

5.3.29. Synthesis of (Z,Z)-1,4-bis(9-ethynylanthracenyl)naphthalene 42b

A two-necked, round-bottom flask and a gas outlet tube, was placed 1,4-bis(9-ethynylanthracenyl)naphthalene (0.400 mg, 0.75 mmol) in toluene (450 ml) and palladium on barium sulfate, 5 % pd (1 g) as a hydrogenation catalyst. The slurry was vigorously stirred under a hydrogen atmosphere at 50 °C (50 min). The mixture was filtered through a pad of celite, the solvent evaporated in vacuo to afford (0.404 g, 100 %) a yellow solid product.

$^1\text{H-NMR}$ (500 MHz, CDCl_3/TMS): δ = 8.30 (2H, m, naphthalene Hs), 8.20 (2H, s, anthracene Hs), 7.97 (4H, d, $J=8.6$ Hz, anthracene Hs), 7.83 (4H, d, $J=8.5$ Hz, anthracene Hs), 7.61 (2H, m, naphthalene Hs), 7.60 (2H, d, $J=12.1$ Hz, double bond Hs), 7.31 (2H, d, $J=12.3$ Hz, double bond Hs), 7.10-7.28 (8H, m, anthracene Hs), 5.99 (2H,s, naphthalene Hs) ppm.

$^{13}\text{C-NMR}$ (125.8 MHz, CDCl_3/TMS): δ = 132.96, 131.80, 131.62, 131.47, 131.18, 128.87, 128.43, 127.76, 126.22, 125.77, 125.62, 125.24, 124.93, 124.41 ppm.

MS (EI, 70 eV): m/z (%): 533 (38) [$M^+ + 1$], 532 (100) [M^+].

5.3.30. Synthesis of (Z,Z)-9,10-bis(9-ethynylanthracenyl)anthracene 42c

A two-necked, round-bottom flask and a gas outlet tube, was placed 9,10-bis(9-ethynylanthracenyl)anthracene (0.400 mg, 0.69 mmol) in toluene (500 ml) and palladium on barium sulfate, 10 % pd (1 g) as a hydrogenation catalyst. The slurry was vigorously stirred under a hydrogen atmosphere at 50 °C (50 min). The mixture was filtered through a pad of celite, the solvent evaporated under reduced pressure to afford (0.404 g, 100 %) an orange solid product.

$^1\text{H-NMR}$ (500 MHz, CDCl_3/TMS): δ = 6.8- 9.15 (30H, m) ppm.

MS (EI, 70 eV): m/z (%): 583 (47) [$M^+ + 1$], 582 (100) [M^+], 379 (24), 291 (11), 179 (8).

5.3.31. Synthesis of (Z,Z)-9,10-bis(1-ethynyl-naphthyl)anthracene 42d

A two-necked, round-bottom flask and a gas outlet tube, was placed 9,10-bis(1-ethynyl-naphthyl)anthracene (0.400 mg, 10 mmol) in ethyl acetate (400 ml) and lindlar catalyst (1 g). The slurry was vigorously stirred under a hydrogen atmosphere (room temperature, 50 min). The mixture was filtered through a pad of celite, the solvent evaporated in vacuo and crystallized in hot toluene to afford (0.303 g, 75 %) a yellow solid product.

¹H-NMR (500 MHz, CDCl₃/TMS): δ= 8.36 (2H, d, J=8.6 Hz), 8.22 (4H, m, anthracene Hs), 7.83 (2H, d, J=12.0 Hz), 7.74 (2H, d, J=8.1 Hz), 7.59 (2H, t), 7.50 (2H, d, J=12.5 Hz), 7.48 (4H, m), 7.18 (4H, m, anthracene Hs), 6.73 (2H, m), 6.66 (2H, b) ppm.

MS (EI, 70 eV): *m/z* (%): 482 (100) [M⁺], 353 (34), 329 (22), 226 (10).

5.3.32. Synthesis of (Z,Z)-1,4-bis(1-ethynyl-naphthyl)naphthalene 42e

A two-necked, round-bottom flask and a gas outlet tube, was placed 1,4-bis(1-ethynyl-naphthyl)naphthalene (0.400 mg, 0.93 mmol) in ethyl acetate (150 ml) and palladium on barium sulfate, 5 % pd, reduced (1.2 g). The slurry was vigorously stirred under a hydrogen atmosphere (room temperature, 60 min). The mixture was filtered through a pad of celite, the solvent evaporated in vacuo and crystallized in hot toluene to afford (0.303 g, 70 %) a yellow solid product.

¹H-NMR (500 MHz, CDCl₃/TMS): δ= 8.19 (2H, m), 8.08 (2H, m), 7.77 (2H, m), 7.60 (2H, d, J=8.0 Hz), 7.56 (2H, m), 7.45 (4H, m), 7.33 (4H, d, J=3.6 Hz), 7.05 (2H, m), 7.00 (2H, d, J=7.1 Hz), 7.68 (2H, s) ppm.

¹³C-NMR (125.8 MHz, CDCl₃/TMS): δ= 134.33, 133.80, 133.54, 132.01, 131.82, 130.19, 130.12, 128.46, 127.34, 126.96, 126.68, 125.92, 125.88, 125.69, 125.23, 125.01, 124.42 ppm. **MS** (EI, 70 eV): *m/z* (%): 433 (35) [M⁺+1], 432 (100) [M⁺], 303 (15), 279 (13).

5.3.33. Synthesis of (Z,Z)-1,4-bis(1-ethynyl-naphthyl)benzene 41f

A two-necked, round-bottom flask and a gas outlet tube, was placed 1,4-bis(1-ethynyl-naphthyl)naphthalene (0.400 mg, 1.06 mmol) in ethyl acetate (120 ml) and palladium on barium sulfate, 5 % pd, reduced (800 g). The slurry was vigorously stirred under a hydrogen atmosphere (room temperature, 50 min). The mixture was filtered through a pad of celite, the solvent evaporated in vacuo and crystallized in hot toluene to afford (0.202 g, 50 %) a yellow solid product.

¹H-NMR (500 MHz, CDCl₃/TMS): δ = 8.00 (2H, d, J=8.1 Hz), 7.82 (2H, d, J=8.1 Hz), 7.73 (2H, m), 7.49 (4H, m), 7.30 (4H, d, J=6.5 Hz), 6.97 (2H, d, J=12.2 Hz), 6.80 (2H, s), 6.70 (2H, d, J=12.2 Hz) ppm.

¹³C-NMR (125.8 MHz, CDCl₃/TMS): (135.63, 135.25, 133.70, 131.65, 131.50, 128.79, 128.43, 127.54, 126.43, 125.99, 125.93, 125.55, 124.91 ppm.

MS (EI, 70 eV): *m/z* (%): 383 (33) [M⁺+1], 382 (100) [M⁺], 252 (3), 191 (10).

5.3.34. Synthesis of (Z,Z)-9,10-bis(4-formyl-styryl)anthracene 52

In a two-necked flask equipped with a nitrogen inlet tube 0.300 g (0.56 mmol) of **50** were dissolved in 30ml dry THF and cooled to -78°C. 1.05 ml (1.68 mmol, 1.6 M) MeLi and 0.99 ml (1.68 mmol, 1.7 M) *t*-BuLi was added in portions during 2 h, separately. After being stirred for 4 h at -78°C, the solution was treated with 1.41 ml (16.8 mmol) DMF and maintained in the same condition for an additional two hour. Then the mixture was quenched by water. The mixture was diluted with diethyl ether, washed several time with water and dried over MgSO₄. The solvent was evaporated and the residue purified by column chromatography on SiO₂ (hexane/ethyl acetate: 2/1) yielding 0.146 g (60 %) as yellow solid

¹H-NMR (500 MHz, CDCl₃/TMS): δ = 10.08 (2H, aldehyde Hs), 8.37 (4H, m, anthracene Hs), 8.12 (2H, d, J=16.3 Hz, double bond Hs), 7.99 (4H, d, J=8.3 Hz, benzene Hs), 7.85 (4H, d, J=8.2 Hz, benzene Hs), 7.52 (4H, m, anthracene Hs), 7.02 (2H, d, J=16.6 Hz, double bond Hs) ppm.

MS (EI, 70 eV): *m/z* (%): 439 (37) [M⁺+1], 438 (100) [M⁺], 303 (10), 226 (6).

5.3.35. General procedure for the formylation reaction

In a two-necked flask with a gas inlet tube, was prepared a suspension of *cis*- hydrogenated compound (1.0 mmol) in CH₂Cl₂ (30 ml) in an ice bath (1°C) under nitrogen atmosphere. To the mixture was slowly added SnCl₄ (3.0 mmol) over 30 min and the reaction was stirred for an additional 30 min in same temperature. Then the reaction was allowed to warm to room temperature and maintained for 10 min and then cooled back to 1°C. Cl₂CHOCH₃ (3.0 mmol) was added and the reaction stirred for one hour, then allowed to warm to room temperature and stirred for 3 h. The reaction mixture was poured on ice and stirred for 1 h, and then the colored solid compound was filtrated off and washed with acetone.

5.3.36. Spectral data for (Z)-1,2-bis[10-formyl-9-anthracenyl]ethene 31: Orange solid (74%).

¹H-NMR (300 MHz, CDCl₃/TMS): δ= 11.59 (2H, s, aldehyde Hs), 9.05 (4H, d, J=8.9 Hz, anthracene Hs), 8.68 (4H, d, J=8.7 Hz, anthracene Hs), 7.79 (2H, s, double bond Hs), 7.75 (4H, t, anthracene Hs), 7.67 (4H, t, anthracene Hs) ppm.

¹³C-NMR (75.5 MHz, CDCl₃/TMS): δ= 193.42, 135.01, 131.74, 129.26, 128.79, 126.57, 126.28, 124.14, 124.05 ppm.

MS (EI, 70 eV): *m/z* (%): 436 (100) [M⁺], 407 (22), 379 (27), 188(26).

IR (KBr): 1668 (C=O) cm⁻¹.

5.3.37. Spectral data for (Z,Z)-1,4-bis[(9-ethenyl-10-formyl)anthracenyl]benzene 43a: Orange solid (72%).

¹H-NMR (500 MHz, CDCl₃/TMS): δ= 11.58 (2H, s, aldehyde Hs), 9.03 (4H, d, J=8.9 Hz, anthracene Hs), 8.49 (4H, d, J=8.8 Hz, anthracene Hs), 8.02 (2H, d, J=16.6 Hz, double bond Hs), 7.80 (4H, s, phenyl Hs), 7.58-7.72 (8H, m, anthracene Hs), 7.02 (2H, d, J=16.6 Hz, double bond Hs) ppm.

MS (EI, 70 eV): *m/z* (%): 538 (91) [M⁺], 510 (37), 481 (10), 322(18), 279 (49), 203 (100).

IR (KBr): 1663 (C=O) cm⁻¹.

5.3.38. Spectral data for (Z,Z)-1,4-bis[(9-ethenyl-10-formyl)anthracenyl]naphthalene 43b:

Brown solid (70 %).

¹H-NMR (500 MHz, CDCl₃/TMS): δ= 11.60 (2H, s, aldehyde Hs), 9.05 (4H, d, J=9.0 Hz, anthracene Hs), 8.60 (4H, d, J=8.7 Hz, anthracene Hs), 8.23 (2H, m, naphthalene Hs), 8.22 (2H, s, naphthalene Hs), 8.08 (2H, d, J=16.3 Hz, double bond Hs), 7.82 (2H, d, J=16.3 Hz, double bond Hs), 7.60-7.72 (8H, m, anthracene Hs) ppm.

MS (EI, 70 eV): *m/z* (%): 588 (37) [M⁺], 560 (13), 371 (33), 250 (14), 203 (100).

IR (KBr): 1667 (C=O) cm⁻¹.

5.3.39. Spectral data for (Z,Z)-9,10-bis[(9-ethenyl-10-formyl)anthracenyl]anthracene 43c:

Brown solid (70 %).

¹H-NMR (500 MHz, CDCl₃/TMS): δ= 11.62 (2H, s, aldehyde Hs), 9.08 (4H, d, J=16.0 Hz, anthracene Hs), 8.77 (4H, d, J=8.7 Hz, anthracene Hs), 8.71 (4H, m, middle anthracene Hs), 7.96 (2H, d, J=1.1 Hz, double bond Hs), 7.66-7.77 (4H, m, anthracene Hs), 7.64 (4H, m, middle anthracene Hs) ppm.

MS (EI, 70 eV): *m/z* (%): 639(40) [M⁺⁺¹], 638 (100) [M⁺], 610 (21), 377(95), 289 (23), 191 (78).

IR (KBr): 1673 (C=O) cm⁻¹.

5.3.40. Spectral data for (Z,Z)-1,4-bis[(1-ethenyl-4-formyl)naphthyl]naphthalene 43e: Green solid (60%).

¹H-NMR (500 MHz, CDCl₃/TMS): δ= 10.45 (2H, s, aldehyde Hs), 9.38 (2H, d, J=8.3 Hz), 8.38 (2H, d, J=8.7 Hz), 8.35 (2H, m), 8.00- 8.15 (8H, m), 7.60-7.80 (8H, m) ppm.

5.3.41. Spectral data for (Z,Z)-1,4-bis[(1-ethenyl-4-formyl)naphthyl]benzene 43f: Green solid (45%).

¹H-NMR (500 MHz, CDCl₃/TMS): δ= 10.41 (2H, s, aldehyde Hs), 9.35 (2H, d, J=8.4 Hz), 8.34 (2H, d, J=8.4 Hz), 7.94-8.02 (6H, m), 7.68-7.76 (8H, m), 7.32 (2H, d, J=16.0 Hz) ppm.

¹³C-NMR (125.8 MHz, CDCl₃, 298 K, TMS): δ= 192.98, 141.88, 137.23, 136.27, 134.15, 131.66, 131.19, 130.75, 128.98, 127.61, 127.13, 125.50, 125.40, 124.16, 122.64 ppm.

MS (EI, 70 eV): *m/z* (%): 439 (36) [M⁺+1], 438 (100) [M⁺], 410 (5), 271(5), 190 (7).

IR (KBr): 1680 (C=O) cm⁻¹.

5.3.42. General procedure for the McMurry coupling

A flame-dried round-bottom flask equipped with a nitrogen inlet tube was charged 650 mg (10 mmol) of Zn-Cu in 50 ml of anhydrous DME. 0.54 ml (5 mmol) of TiCl₄ was added carefully to the mixture at 0°C and the black gray suspension refluxed for 2 hr. After being cooled to room temperature a solution of dialdehyde (0.5 mmol) in 150 ml (DME/toluene: 1:2) was slowly added and the reaction stirred for 2 days in room temperature. After refluxing at 110 °C for 3 h the mixture was filtrated over a pad of neutral alumina, which was washed with dichloromethane. The solvent was evaporated in vacuo and the residue was purified by column chromatography on SiO₂ (hexane/ CH₂Cl₂: 3/1).

5.3.43. Spectral data for compound 38: Yield (%) = 4

¹H-NMR (500 MHz, CDCl₃/TMS): δ= 8.65 (4H, d, anthracene Hs), 8.42 (4H, d, anthracene Hs), 7.83 (2H, s, double bond Hs), 7.52 (8H, m, anthracene Hs), 7.19 (2H, d, double bond Hs), 6.07 (2H, q, double bond Hs), 2.21 (6H, d, methyl Hs) ppm.

¹³C-NMR (125.8 MHz, CDCl₃/ TMS): δ= 134.34, 133.93, 132.03, 129.58, 129.45, 126.93, 126.88, 126.21, 125.48, 124.94, 19.23 ppm.

MS (EI, 70 eV): *m/z* (%): 460 (26) [M⁺], 446 (100), 203 (75).

5.3.44. Spectral data for compound 37: Yield (%) = Only observed by MALDI-TOF MS.

MALDI-TOF MS: *m/z* = 808.67, 809.65, 810.65 (Calcd 809.024 for C₆₄H₄₀).

5.3.45. Spectral data for compound 55a: Yield (%) = 32

¹H-NMR (500 MHz, CDCl₃/TMS): δ= 8.14 (4H, dd, J=3.3, 6.7 Hz, anthracene Hs), 7.47 (2H, d, J=11.4 Hz, double bond Hs), 7.40 (4H, dd, J=3.25, 6.76 Hz, anthracene Hs), 7.25 (2H, d, J=11.5 Hz, double bond Hs), 6.55 (2H, s, double bond Hs), 6.38 (2H, d, J=11.5 Hz, benzene Hs), 6.15 (2H, d, J=8.3 Hz, benzene Hs) ppm.

¹³C-NMR (125.8 MHz, CDCl₃/TMS): δ= 137.15, 135.87, 135.09, 132.87, 132.01, 130.42, 129.42, 128.35, 127.60, 127.03, 125.15 ppm.

MS (EI, 70 eV): *m/z* (%): 407 (34) [M⁺+1], 406 (100) [M⁺], 350 (4), 203 (13).

MALDI-TOF MS: *m/z* 406.26, 407.26, 408.26 (Calcd 406.528 for C₃₂H₂₂).

UV/Vis (CH₂Cl₂): λ_{max} [nm] (log ε) = 264 (2.65), 361 (0.12), 381 (0.22), 402 (0.23).

5.3.46. Spectral data for compound 55b: Yield (%) = 9

¹H-NMR (500 MHz, CDCl₃/TMS): δ= 8.24 (8H, dd, J=3.4, 6.7 Hz, anthracene Hs), 7.36 (8H, dd, J=3.2, 6.84 Hz anthracene Hs), 7.22 (4H, d, J=12.3 Hz, double bond Hs), 7.13 (4H, d, J=12.3 Hz, double bond Hs), 7.01 (8H, d, J=8.5 Hz, benzene Hs), 6.84 (8H, d, J=8.5 Hz, benzene Hs), 6.73 (4H, s, double bond Hs) ppm.

¹³C-NMR (125.8 MHz, CDCl₃/TMS): δ= 136.12, 135.98, 133.62, 132.61, 129.22, 128.62, 127.86, 126.92, 126.40, 126.08, 125.78 ppm.

MALDI-TOF MS: *m/z* 812.1, 813.1, 813.1 (Calcd 813.056 for C₆₄H₄₄).

UV/Vis (CH₂Cl₂): λ_{max} [nm] (log ε) = 263 (2.47), 340 (0.73), 404 (0.51).

5.3.47. Spectral data for compound 55c: Yield (%) = 2

MALDI-TOF MS: *m/z* 1218.1, 1219.1, 1220.1 (Calcd 1219.584 for C₉₆H₆₆).

UV/Vis (CH₂Cl₂): λ_{max} [nm] (log ε) = 265 (2.25), 352 (0.85), 412 (0.75).

5.3.48. Spectral data for compound 56b: Yield (%) = 14

¹H-NMR (500 MHz, CDCl₃/TMS): δ= 8.88 (2H, d, J=8.8 Hz), 8.34 (2H, d, J=8.6 Hz), 8.03 (3H, d, J=8.7 Hz), 7.83 (1H, s), 7.76 (2H, d, J=8.7 Hz), 7.59 (2H, t), 7.46- 7.50 (4H, m), 7.21 (1H, d,

$J=11.8$ Hz), 6.99 (2H, t), 6.97 (2H, d, $J=8.4$ Hz), 6.87 (2H, t), 6.63 (H, d, $J=8.4$ Hz), 6.28 (1H, d, $J=16.5$ Hz) ppm.

$^{13}\text{C-NMR}$ (125.8 MHz, CDCl_3/TMS): $\delta=$ 136.36, 136.02, 134.58, 134.34, 133.15, 132.80, 132.23, 131.99, 131.30, 129.79, 129.26, 128.86, 128.77, 128.70, 127.52, 126.64, 126.49, 126.11, 125.96, 125.74, 125.65, 125.44, 124.35, 124.19 ppm.

MALDI-TOF MS: m/z 1012.24, 1013.21, 1014.21 (Calcd 1013.296 for $\text{C}_{80}\text{H}_{52}$).

UV/Vis (CH_2Cl_2): λ_{max} [nm] ($\log \epsilon$) = 235sh (0.75), 255 (2.55), 320 (0.37), 406 (0.55).

5.3.49. Spectral data for compound 56c: Yield (%) = 2

MALDI-TOF MS: m/z 1518.71, 1519.75, 1520.66, 1672.1 (Calcd 1519.944 for $\text{C}_{120}\text{H}_{78}$).

5.3.50. Spectral data for compound 56a-b: Yield (%) = 8

$^1\text{H-NMR}$ (500 MHz, CDCl_3/TMS): $\delta=$ 8.43 (4H, m, anthracene Hs), 8.38 (4H, m, anthracene Hs), 8.01 (2H, d, double bond Hs), 7.75 (4H, s, benzene Hs), 7.18 (2H, s, double bond Hs), 6.97 (2H, d, double bond Hs), 6.07 (2H, q, double bond Hs), 2.18 (6H, d, methyl Hs) ppm.

MALDI-TOF MS: m/z 562.14, 563.13, 564.14 (Calcd 562.756 for $\text{C}_{44}\text{H}_{34}$).

5.3.51. Spectral data for compound 57a-a: Yield (%) = 7

$^1\text{H-NMR}$ (500 MHz, CDCl_3/TMS): $\delta=$ 8.22 (4H, d, $J=8.6$ Hz, anthracene Hs), 8.03 (2H, s, double bond Hs), 7.88 (2H, dd, $J=3.3, 6.4$ Hz, naphthalene Hs), 7.79 (4H, d, $J=8.6$ Hz, anthracene Hs), 7.53 (2H, d, $J=8.6$ Hz, double bond Hs), 7.40 (2H, d, $J=11.2$ Hz, double bond Hs), 7.35 (2H, dd, $J=3.3, 6.3$ Hz, naphthalene), 7.01-7.07 (8H, m, anthracene Hs), 5.71 (2H, s, naphthalene) ppm.

$^{13}\text{C-NMR}$ (125.8 MHz, CDCl_3/TMS): $\delta=$ 134.15, 132.87, 131.39, 130.87, 130.51, 130.42, 129.42, 128.35, 127.03, 125.85, 125.42, 124.87, 124.52, 124.35, 123.76 ppm.

MS (EI, 70 eV): m/z (%): 557 (48) [M^++1], 556 (100) [M^+], 278 (12).

MALDI-TOF MS: m/z 556.8, 557.8, 558.8 (Calcd 556.708 for $\text{C}_{44}\text{H}_{28}$).

UV/Vis (CH_2Cl_2): λ_{max} [nm] ($\log \epsilon$) = 236 (2.28), 254 (2.68), 361 (0.25), 380 (0.35), 408 (0.12).

5.3.52. Spectral data for compound 57b: Yield (%) = 9**MALDI-TOF MS:** m/z 1112.69, 1113.69, 1114.67, 1115.68 (Calcd 1113.416 for C₈₈H₅₆).**UV/Vis** (CH₂Cl₂): λ_{\max} [nm] (log ϵ) = 235sh (2.15), 256 (2.53), 335 (0.45), 408 (0.58).**5.3.53. Spectral data for compound 57c:** Yield (%) = 2**MALDI-TOF MS:** m/z 1669.2, 1670.2, 1671.1, 1672.1 (Calcd 1670.124 for C₁₃₂H₈₄).**5.3.54. Spectral data for compound 57a-b:** Yield (%) = 8**¹H-NMR** (500 MHz, CDCl₃/TMS): δ = 8.52 (4H, m, anthracene Hs), 8.40 (4H, m, anthracene Hs), 8.25 (2H, m, naphthalene Hs), 8.21 (2H, s, naphthalene Hs), 8.05 (2H, d, double bond Hs), 7.79 (2H, d, double bond Hs), 7.54 (2H, m, naphthalene Hs), 7.51 (8H, m, anthracene Hs), 7.18 (2H, d, double bond Hs), 7.07 (2H, q, double bond Hs), 2.20 (6H, dd, methyl Hs) ppm.**¹³C-NMR** (125.8 MHz, CDCl₃/TMS): δ = 135.40, 134.86, 134.29, 133.89, 132.23, 131.73, 129.79, 129.62, 128.53, 127.01, 126.83, 126.35, 126.32, 125.37, 124.97, 29.72, 19.14 ppm.**MS** (EI, 70 eV): m/z (%): 612 (100) [M⁺].**5.3.55. Spectral data for compound 58a-b:** Yield (%) = 4**¹H-NMR** (500 MHz, CDCl₃/TMS): δ = 8.75 (4H, d, anthracene Hs), 8.69 (4H, d, anthracene Hs), 8.42 (4H, m, anthracene Hs), 7.90 (4H, s, double bond Hs), 7.50- 7.62 (12H, m, anthracene Hs), 7.11 (2H, d, double bond Hs), 6.05 (2H, q, double bond Hs), 2.26 (6H, dd, methyl Hs) ppm.**MS** (EI, 70 eV): m/z (%): 662 (100) [M⁺].**5.3.56. Spectral data for compound 58b:** Yield (%) = 7**MALDI-TOF MS:** m/z 1212.50, 1113.50, 1114.60, 1115.60 (Calcd 1213.536 for C₉₆H₆₀).**UV/Vis** (CH₂Cl₂): λ_{\max} [nm] (log ϵ) = 234sh (1.21), 252 (2.32), 430 (0.32).

5.3.57. Spectral data for compound 58c: Yield (%) = 1**MALDI-TOF MS:** m/z 1820.50, 122.50, 1824.60 (Calcd 1820.304 for C₁₄₄H₉₀).**5.3.58. General procedure for bromination and dehydrobromination of 55b, 55c and 56b**

A 100 ml, two necked round-bottom flask equipped a bar stirrer was charged with 0.02 mmol of desired cyclophanes and 30 ml of CHCl₃. The solution was stirred and a CHCl₃ solution of 0.2 mmol of bromine was added at 0°C. The colorful solution fades gradually to a pale yellow during about 2 hours. The reaction mixture was quenched with saturated solution of NaHSO₃ and then washed with water. The organic layer was separated and dried over anhydrous Na₂SO₄. The solvent was evaporated in vacuum and the residue was directly applied in dehydrobromination reaction without any purification.

To a 0.02 mmol of bromide compounds and freshly distilled diethyl ether (30ml) was added *t*-BuOK (0.2) at 0°C under nitrogen. The pale yellow suspension was immediately changed to deep red. After 30 min, silica gel TLC showed a new spot assignable to products. The mixture was stirred for overnight. The reaction mixture was quenched by water and then the organic layer was separated. Precipitate in organic phase was separated and washed with diethyl ether. Finally, precipitate was dissolved in CH₂Cl₂ and purified by short (1cm) florisil chromatography to obtain CPAA's as a red solid compound.

5.3.59. Spectral data for compound 69: Yield (%) = 40

¹H-NMR (600 MHz, CDCl₃/TMS): δ= 8.51 (8H, m, J=8.6 Hz, anthracene Hs), 7.56 (8H, J=8.6 Hz, m, anthracene Hs), 7.47 (8H, d, J=8.57, 6.4 Hz, benzene Hs), 7.35 (8H, d, J=8.57 Hz, benzene Hs) ppm.

¹³C-NMR (150.9 MHz, CDCl₃/TMS): δ= 137.20, 132.10, 130.99, 126.95, 126.80, 124.01, 123.51, 119.20, 111.31, 105.97, 97.31 ppm.

MALDI-TOF MS: m/z 800.8, 801.8, 802.8 (Calcd 800.96 for C₆₄H₃₂).

UV/Vis (CH₂Cl₂): λ_{max} [nm] (log ε) = 235sh (0.85), 256 (1.70), 262 (1.90), 269 (1.92), 327 (0.55), 382 (0.66), 471 (0.67).

Fluorescence (CH₂Cl₂): λ_{max} [nm] (log ε) = 592 (1.38), 633 (2.53).

5.3.60. Spectral data for compound 70: Yield (%) = 35

¹H-NMR (600 MHz, CDCl₃/TMS): δ= 8.59 (12H, m, J=8.6 Hz, anthracene Hs), 7.62 (12H, J=8.6, m, anthracene Hs), 7.60 (12H, d, J=8.57, 6.4 Hz, benzene Hs), 7.47 (12H, d, J=8.57 Hz, benzene Hs) ppm.

¹³C-NMR (150.9 MHz, CDCl₃/TMS): δ= 136.12, 134.62, 131.55, 131.41, 127.12, 126.92, 124.01, 123.50, 103.90, 94.02 ppm.

MALDI-TOF MS: *m/z* 1200.3, 1201.3, 1202.3 (Calcd 1201.44 for C₉₆H₄₈).

UV/Vis (CH₂Cl₂): λ_{max} [nm] (log ε) = 237sh (0.77), 275 (1.78), 345 (0.87), 460 (0.92), 500 (0.50).

Fluorescence (CH₂Cl₂): λ_{max} [nm] (log ε) = 531 (2.74).

5.3.61. Spectral data for compound 72b

MALDI-TOF MS: *m/z* 1004.7, 1005.8, 1006.8 (Calcd 1005.232 for C₈₀H₄₄).

UV/Vis (CH₂Cl₂): λ_{max} [nm] (log ε) = 229sh (0.95), 261 (1.47), 319 (0.28), 439 (0.32).

5.4. Supplementary data

5.4.1. Appendix A: X-ray crystallography data of 55a

Empirical formula	C ₃₂ H ₂₂	
Formula weight	406.50	
Temperature	170(2) K	
Wavelength	0.71073 Å	
Crystal system	monoclinic	
Space group	P2 ₁ /c	
Unit cell dimensions	a = 17.2168(11) Å	α = 90°.
	b = 9.2565(4) Å	β = 100.571(8)°.
	c = 28.0964(18) Å	γ = 90°.
Volume	4401.7(4) Å ³	
Z	8	
Density (calculated)	1.227 Mg/m ³	
Absorption coefficient	0.069 mm ⁻¹	
F(000)	1712	
Crystal size	0.3 x 0.25 x 0.25 mm ³	
Theta range for data collection	2.32 to 26.98°.	
Index ranges	-19<=h<=21, -11<=k<=11, -35<=l<=35	
Reflections collected	27534	
Independent reflections	9477 [R(int) = 0.0356]	
Completeness to theta = 26.98°	98.9 %	
Refinement method	Full-matrix least-squares on F ²	
Data / restraints / parameters	9477 / 0 / 578	
Goodness-of-fit on F ²	1.026	
Final R indices [I>2σ(I)]	R1 = 0.0402, wR2 = 0.1026	
R indices (all data)	R1 = 0.0549, wR2 = 0.1103	
Extinction coefficient	0.0196(14)	
Largest diff. peak and hole	0.192 and -0.181 e.Å ⁻³	

Comments

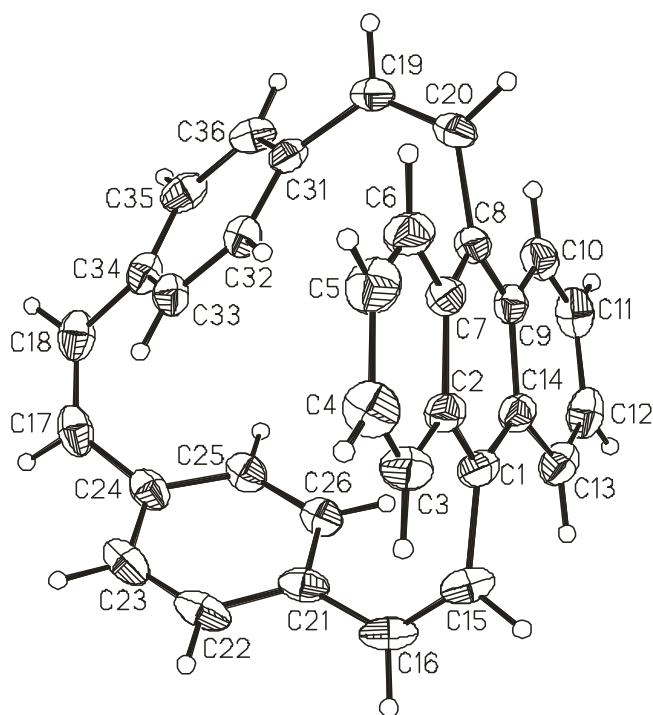
All non-hydrogen atoms were refined anisotropic. All H atoms were located in difference map and were positioned with idealized geometry and refined isotropic using a riding model.

Atomic coordinates ($\times 10^4$) and equivalent isotropic displacement parameters ($\text{\AA}^2 \times 10^3$).

U(eq) is defined as one third of the trace of the orthogonalized U_{ij} tensor.

	x	y	z	U(eq)
C(1)	5664(1)	1109(1)	4540(1)	28(1)
C(2)	4843(1)	1030(1)	4356(1)	27(1)
C(3)	4444(1)	-320(1)	4249(1)	34(1)
C(4)	3649(1)	-383(2)	4080(1)	40(1)
C(5)	3199(1)	902(2)	3995(1)	40(1)
C(6)	3557(1)	2208(2)	4080(1)	35(1)
C(7)	4387(1)	2332(1)	4266(1)	27(1)
C(8)	4762(1)	3688(1)	4329(1)	26(1)
C(9)	5569(1)	3765(1)	4544(1)	26(1)
C(10)	5973(1)	5116(1)	4637(1)	33(1)
C(11)	6746(1)	5177(2)	4857(1)	38(1)
C(12)	7173(1)	3891(2)	5001(1)	38(1)
C(13)	6821(1)	2582(2)	4910(1)	34(1)
C(14)	6011(1)	2457(1)	4668(1)	27(1)
C(15)	6140(1)	-251(1)	4585(1)	35(1)
C(16)	6557(1)	-722(1)	4261(1)	37(1)
C(17)	6695(1)	2272(2)	2477(1)	37(1)
C(18)	6276(1)	3488(2)	2393(1)	36(1)
C(19)	4365(1)	5654(1)	3727(1)	30(1)
C(20)	4327(1)	5038(1)	4151(1)	31(1)
C(21)	6668(1)	13(1)	3809(1)	31(1)
C(22)	6507(1)	-715(1)	3367(1)	39(1)
C(23)	6546(1)	-26(2)	2934(1)	39(1)
C(24)	6757(1)	1430(1)	2929(1)	31(1)
C(25)	6986(1)	2121(1)	3375(1)	30(1)
C(26)	6941(1)	1433(1)	3805(1)	30(1)
C(31)	4807(1)	5100(1)	3363(1)	27(1)
C(32)	4816(1)	3633(1)	3246(1)	27(1)

C(33)	5282(1)	3131(1)	2930(1)	29(1)
C(34)	5754(1)	4069(1)	2713(1)	30(1)
C(35)	5703(1)	5538(2)	2805(1)	34(1)
C(36)	5237(1)	6042(1)	3124(1)	33(1)
C(41)	1787(1)	2166(1)	1263(1)	25(1)
C(42)	1872(1)	2453(1)	1762(1)	25(1)
C(43)	2248(1)	1445(1)	2118(1)	30(1)
C(44)	2316(1)	1713(2)	2599(1)	38(1)
C(45)	1993(1)	2989(2)	2760(1)	44(1)
C(46)	1626(1)	3974(2)	2435(1)	37(1)
C(47)	1563(1)	3767(1)	1926(1)	27(1)
C(48)	1220(1)	4810(1)	1585(1)	29(1)
C(49)	1226(1)	4597(1)	1092(1)	28(1)
C(50)	958(1)	5688(1)	737(1)	37(1)
C(51)	956(1)	5473(2)	260(1)	44(1)
C(52)	1205(1)	4133(2)	95(1)	44(1)
C(53)	1453(1)	3057(2)	418(1)	35(1)
C(54)	1491(1)	3249(1)	927(1)	26(1)
C(55)	2004(1)	731(1)	1083(1)	30(1)
C(56)	1488(1)	-339(1)	959(1)	31(1)
C(57)	-1771(1)	212(2)	1189(1)	41(1)
C(58)	-2027(1)	1412(2)	1371(1)	42(1)
C(59)	116(1)	6236(2)	1819(1)	42(1)
C(60)	862(1)	6138(1)	1758(1)	38(1)
C(61)	655(1)	-309(1)	1023(1)	29(1)
C(62)	33(1)	-705(1)	648(1)	37(1)
C(63)	-748(1)	-582(2)	706(1)	39(1)
C(64)	-942(1)	-53(1)	1132(1)	34(1)
C(65)	-322(1)	252(1)	1516(1)	32(1)
C(66)	456(1)	117(1)	1462(1)	29(1)
C(71)	-483(1)	5073(1)	1700(1)	36(1)
C(72)	-647(1)	4471(2)	1237(1)	36(1)
C(73)	-1166(1)	3325(2)	1133(1)	36(1)
C(74)	-1539(1)	2730(2)	1486(1)	36(1)
C(75)	-1414(1)	3384(2)	1940(1)	49(1)
C(76)	-893(1)	4534(2)	2044(1)	49(1)

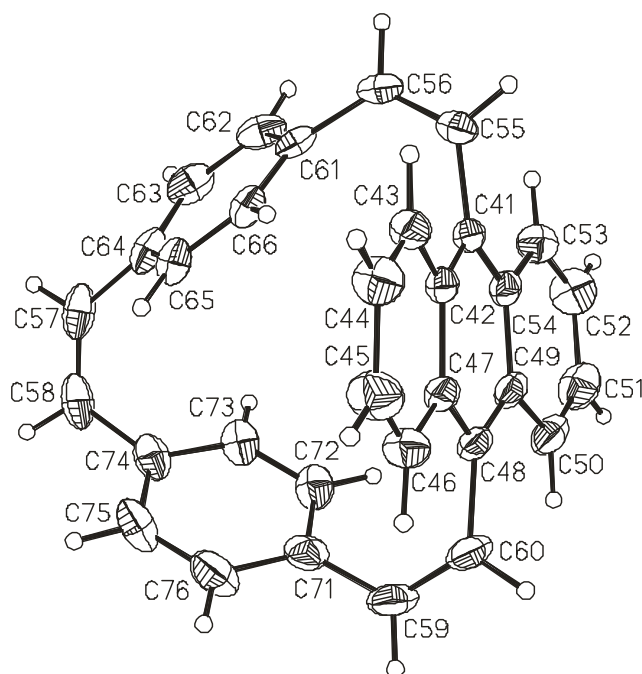

Bond lengths [Å]

C(1)-C(14)	1.4028(17)	C(16)-C(21)	1.4818(19)
C(1)-C(2)	1.4140(17)	C(17)-C(18)	1.334(2)
C(1)-C(15)	1.4952(17)	C(17)-C(24)	1.4782(19)
C(2)-C(3)	1.4309(18)	C(18)-C(34)	1.4850(18)
C(2)-C(7)	1.4358(16)	C(19)-C(20)	1.3329(17)
C(3)-C(4)	1.3658(19)	C(19)-C(31)	1.4744(17)
C(4)-C(5)	1.415(2)	C(21)-C(22)	1.3961(19)
C(5)-C(6)	1.358(2)	C(21)-C(26)	1.3967(17)
C(6)-C(7)	1.4338(17)	C(22)-C(23)	1.386(2)
C(7)-C(8)	1.4075(17)	C(23)-C(24)	1.3961(19)
C(8)-C(9)	1.4118(17)	C(24)-C(25)	1.3971(17)
C(8)-C(20)	1.4949(16)	C(25)-C(26)	1.3814(18)
C(9)-C(10)	1.4312(17)	C(31)-C(36)	1.3947(17)
C(9)-C(14)	1.4382(16)	C(31)-C(32)	1.3974(17)
C(10)-C(11)	1.363(2)	C(32)-C(33)	1.3823(17)
C(11)-C(12)	1.417(2)	C(33)-C(34)	1.4011(17)
C(12)-C(13)	1.358(2)	C(34)-C(35)	1.3897(19)

C(13)-C(14)	1.4398(17)	C(35)-C(36)	1.3886(19)
C(15)-C(16)	1.334(2)		

Bond angles [°]

C(14)-C(1)-C(2)	119.36(11)	C(16)-C(15)-C(1)	124.92(12)
C(14)-C(1)-C(15)	121.72(11)	C(15)-C(16)-C(21)	127.28(12)
C(2)-C(1)-C(15)	118.91(11)	C(18)-C(17)-C(24)	123.27(11)
C(1)-C(2)-C(3)	122.05(11)	C(17)-C(18)-C(34)	124.46(12)
C(1)-C(2)-C(7)	119.89(11)	C(20)-C(19)-C(31)	125.94(11)
C(3)-C(2)-C(7)	118.06(11)	C(19)-C(20)-C(8)	123.57(11)
C(4)-C(3)-C(2)	121.48(12)	C(22)-C(21)-C(26)	117.34(12)
C(3)-C(4)-C(5)	120.40(13)	C(22)-C(21)-C(16)	120.36(12)
C(6)-C(5)-C(4)	120.09(12)	C(26)-C(21)-C(16)	122.29(12)
C(5)-C(6)-C(7)	121.70(12)	C(23)-C(22)-C(21)	121.72(12)
C(8)-C(7)-C(6)	121.40(11)	C(22)-C(23)-C(24)	120.45(12)
C(8)-C(7)-C(2)	120.22(10)	C(23)-C(24)-C(25)	117.69(12)
C(6)-C(7)-C(2)	118.24(11)	C(23)-C(24)-C(17)	122.61(11)
C(7)-C(8)-C(9)	119.44(10)	C(25)-C(24)-C(17)	119.56(12)
C(7)-C(8)-C(20)	120.88(11)	C(26)-C(25)-C(24)	121.46(12)
C(9)-C(8)-C(20)	119.62(11)	C(25)-C(26)-C(21)	120.90(11)
C(8)-C(9)-C(10)	121.94(11)	C(36)-C(31)-C(32)	117.62(11)
C(8)-C(9)-C(14)	119.79(11)	C(36)-C(31)-C(19)	120.26(11)
C(10)-C(9)-C(14)	118.26(11)	C(32)-C(31)-C(19)	122.11(11)
C(11)-C(10)-C(9)	121.37(12)	C(33)-C(32)-C(31)	120.77(11)
C(10)-C(11)-C(12)	120.39(12)	C(32)-C(33)-C(34)	121.44(12)
C(13)-C(12)-C(11)	120.47(12)	C(35)-C(34)-C(33)	117.65(11)
C(12)-C(13)-C(14)	121.29(12)	C(35)-C(34)-C(18)	122.18(12)
C(1)-C(14)-C(9)	120.32(10)	C(33)-C(34)-C(18)	120.17(12)
C(1)-C(14)-C(13)	121.55(11)	C(36)-C(35)-C(34)	120.84(12)
C(9)-C(14)-C(13)	118.09(11)	C(35)-C(36)-C(31)	121.42(12)



Bond lengths [Å]

C(41)-C(54)	1.4069(16)	C(56)-C(61)	1.4789(18)
C(41)-C(42)	1.4079(16)	C(57)-C(58)	1.330(2)
C(41)-C(55)	1.4934(16)	C(57)-C(64)	1.485(2)
C(42)-C(43)	1.4311(17)	C(58)-C(74)	1.483(2)
C(42)-C(47)	1.4363(16)	C(59)-C(60)	1.330(2)
C(43)-C(44)	1.3575(18)	C(59)-C(71)	1.486(2)
C(44)-C(45)	1.415(2)	C(61)-C(66)	1.3950(17)
C(45)-C(46)	1.360(2)	C(61)-C(62)	1.4056(17)
C(46)-C(47)	1.4290(17)	C(62)-C(63)	1.388(2)
C(47)-C(48)	1.4096(17)	C(63)-C(64)	1.389(2)
C(48)-C(49)	1.4025(18)	C(64)-C(65)	1.4016(16)
C(48)-C(60)	1.4947(17)	C(65)-C(66)	1.3810(18)
C(49)-C(50)	1.4339(18)	C(71)-C(76)	1.388(2)
C(49)-C(54)	1.4349(17)	C(71)-C(72)	1.3951(19)
C(50)-C(51)	1.356(2)	C(72)-C(73)	1.3823(19)
C(51)-C(52)	1.418(2)	C(73)-C(74)	1.3917(18)
C(52)-C(53)	1.3621(19)	C(74)-C(75)	1.392(2)
C(53)-C(54)	1.4320(17)	C(75)-C(76)	1.388(2)
C(55)-C(56)	1.3326(18)		

Bond angles [°]

C(54)-C(41)-C(42)	119.54(10)	C(56)-C(55)-C(41)	123.61(11)
C(54)-C(41)-C(55)	119.15(10)	C(55)-C(56)-C(61)	124.71(11)
C(42)-C(41)-C(55)	121.30(10)	C(58)-C(57)-C(64)	124.85(12)
C(41)-C(42)-C(43)	121.53(10)	C(57)-C(58)-C(74)	123.79(12)
C(41)-C(42)-C(47)	120.04(10)	C(60)-C(59)-C(71)	124.66(12)
C(43)-C(42)-C(47)	118.42(11)	C(59)-C(60)-C(48)	124.28(12)
C(44)-C(43)-C(42)	121.36(12)	C(66)-C(61)-C(62)	117.33(12)
C(43)-C(44)-C(45)	120.25(12)	C(66)-C(61)-C(56)	120.88(11)
C(46)-C(45)-C(44)	120.46(12)	C(62)-C(61)-C(56)	121.79(11)
C(45)-C(46)-C(47)	121.47(12)	C(63)-C(62)-C(61)	120.76(12)
C(48)-C(47)-C(46)	122.19(11)	C(62)-C(63)-C(64)	121.43(11)
C(48)-C(47)-C(42)	119.83(11)	C(63)-C(64)-C(65)	117.67(13)
C(46)-C(47)-C(42)	117.98(11)	C(63)-C(64)-C(57)	122.66(11)
C(49)-C(48)-C(47)	119.73(11)	C(65)-C(64)-C(57)	119.66(12)
C(49)-C(48)-C(60)	120.90(11)	C(66)-C(65)-C(64)	120.92(12)
C(47)-C(48)-C(60)	119.36(11)	C(65)-C(66)-C(61)	121.58(11)
C(48)-C(49)-C(50)	121.87(12)	C(76)-C(71)-C(72)	117.55(13)
C(48)-C(49)-C(54)	120.11(11)	C(76)-C(71)-C(59)	121.67(13)
C(50)-C(49)-C(54)	118.01(12)	C(72)-C(71)-C(59)	120.78(12)
C(51)-C(50)-C(49)	121.72(13)	C(73)-C(72)-C(71)	121.14(12)
C(50)-C(51)-C(52)	120.42(12)	C(72)-C(73)-C(74)	121.10(12)
C(53)-C(52)-C(51)	119.93(13)	C(75)-C(74)-C(73)	117.83(13)
C(52)-C(53)-C(54)	121.74(13)	C(75)-C(74)-C(58)	122.96(12)
C(41)-C(54)-C(53)	121.83(11)	C(73)-C(74)-C(58)	119.18(12)
C(41)-C(54)-C(49)	120.03(11)	C(76)-C(75)-C(74)	120.80(13)
C(53)-C(54)-C(49)	118.13(11)	C(75)-C(76)-C(71)	121.35(13)

Anisotropic displacement parameters ($\text{\AA}^2 \times 10^3$) for 55a. The anisotropic displacement factor exponent takes the form: $-2\pi^2 [h^2 a^*2U^{11} + \dots + 2 h k a^* b^* U^{12}]$

	U^{11}	U^{22}	U^{33}	U^{23}	U^{13}	U^{12}
C(1)	26(1)	30(1)	29(1)	7(1)	7(1)	5(1)
C(2)	28(1)	27(1)	27(1)	4(1)	8(1)	3(1)
C(3)	34(1)	29(1)	41(1)	2(1)	9(1)	1(1)

C(4)	35(1)	38(1)	46(1)	-3(1)	7(1)	-7(1)
C(5)	26(1)	51(1)	42(1)	0(1)	2(1)	-2(1)
C(6)	26(1)	41(1)	37(1)	5(1)	6(1)	8(1)
C(7)	27(1)	31(1)	25(1)	3(1)	8(1)	6(1)
C(8)	30(1)	28(1)	23(1)	3(1)	10(1)	7(1)
C(9)	31(1)	28(1)	21(1)	1(1)	9(1)	2(1)
C(10)	42(1)	30(1)	29(1)	-1(1)	12(1)	-1(1)
C(11)	45(1)	39(1)	31(1)	-4(1)	11(1)	-12(1)
C(12)	34(1)	52(1)	27(1)	-1(1)	3(1)	-9(1)
C(13)	29(1)	43(1)	29(1)	6(1)	2(1)	2(1)
C(14)	26(1)	31(1)	25(1)	5(1)	6(1)	2(1)
C(15)	29(1)	29(1)	47(1)	13(1)	6(1)	5(1)
C(16)	26(1)	25(1)	59(1)	9(1)	7(1)	7(1)
C(17)	30(1)	52(1)	31(1)	-13(1)	12(1)	-7(1)
C(18)	32(1)	52(1)	26(1)	-1(1)	9(1)	-8(1)
C(19)	30(1)	24(1)	36(1)	2(1)	5(1)	8(1)
C(20)	33(1)	28(1)	34(1)	-1(1)	11(1)	11(1)
C(21)	20(1)	26(1)	48(1)	0(1)	8(1)	6(1)
C(22)	30(1)	24(1)	64(1)	-11(1)	13(1)	-1(1)
C(23)	30(1)	37(1)	50(1)	-20(1)	9(1)	-1(1)
C(24)	21(1)	37(1)	37(1)	-11(1)	9(1)	0(1)
C(25)	25(1)	27(1)	37(1)	-6(1)	5(1)	-4(1)
C(26)	24(1)	28(1)	36(1)	-4(1)	4(1)	-1(1)
C(31)	24(1)	28(1)	26(1)	5(1)	0(1)	5(1)
C(32)	27(1)	29(1)	25(1)	2(1)	4(1)	-2(1)
C(33)	28(1)	33(1)	25(1)	-3(1)	4(1)	-3(1)
C(34)	25(1)	41(1)	23(1)	3(1)	2(1)	-1(1)
C(35)	27(1)	37(1)	38(1)	14(1)	6(1)	0(1)
C(36)	28(1)	27(1)	41(1)	8(1)	4(1)	3(1)
C(41)	19(1)	22(1)	34(1)	-2(1)	6(1)	-1(1)
C(42)	19(1)	22(1)	34(1)	-2(1)	6(1)	-3(1)
C(43)	27(1)	28(1)	36(1)	0(1)	6(1)	2(1)
C(44)	41(1)	40(1)	34(1)	3(1)	5(1)	4(1)
C(45)	55(1)	46(1)	32(1)	-5(1)	10(1)	3(1)
C(46)	40(1)	33(1)	40(1)	-8(1)	11(1)	1(1)
C(47)	23(1)	22(1)	37(1)	-6(1)	6(1)	-4(1)
C(48)	23(1)	18(1)	44(1)	-6(1)	5(1)	-4(1)

C(49)	22(1)	20(1)	41(1)	-1(1)	2(1)	-5(1)
C(50)	34(1)	23(1)	51(1)	4(1)	3(1)	-3(1)
C(51)	45(1)	36(1)	47(1)	14(1)	0(1)	0(1)
C(52)	46(1)	49(1)	35(1)	6(1)	0(1)	4(1)
C(53)	33(1)	36(1)	34(1)	-1(1)	3(1)	2(1)
C(54)	20(1)	24(1)	34(1)	-1(1)	3(1)	-3(1)
C(55)	30(1)	29(1)	32(1)	-1(1)	9(1)	8(1)
C(56)	42(1)	22(1)	30(1)	-3(1)	6(1)	9(1)
C(57)	30(1)	52(1)	38(1)	11(1)	-4(1)	-20(1)
C(58)	21(1)	65(1)	38(1)	12(1)	3(1)	-10(1)
C(59)	46(1)	26(1)	53(1)	-10(1)	9(1)	9(1)
C(60)	41(1)	20(1)	51(1)	-8(1)	5(1)	-1(1)
C(61)	37(1)	15(1)	32(1)	1(1)	1(1)	1(1)
C(62)	49(1)	26(1)	32(1)	-6(1)	-4(1)	5(1)
C(63)	42(1)	31(1)	38(1)	-5(1)	-11(1)	-3(1)
C(64)	33(1)	28(1)	36(1)	7(1)	-4(1)	-12(1)
C(65)	33(1)	35(1)	27(1)	5(1)	1(1)	-10(1)
C(66)	31(1)	26(1)	28(1)	2(1)	0(1)	-7(1)
C(71)	29(1)	33(1)	45(1)	-2(1)	7(1)	11(1)
C(72)	32(1)	40(1)	35(1)	10(1)	5(1)	1(1)
C(73)	31(1)	46(1)	30(1)	6(1)	3(1)	-2(1)
C(74)	21(1)	49(1)	37(1)	7(1)	5(1)	3(1)
C(75)	37(1)	73(1)	41(1)	-1(1)	19(1)	-3(1)
C(76)	42(1)	66(1)	44(1)	-15(1)	18(1)	0(1)

Hydrogen coordinates ($\times 10^4$) and isotropic displacement parameters ($\text{\AA}^2 \times 10^3$)

	x	y	z	U(eq)
H(3)	4739	-1192	4297	41
H(4)	3396	-1294	4018	48
H(5)	2645	850	3879	48
H(6)	3249	3061	4015	41

H(10)	5696	5988	4542	39
H(11)	7001	6087	4915	45
H(12)	7708	3946	5161	45
H(13)	7116	1731	5009	41
H(15)	6146	-824	4867	42
H(16)	6813	-1629	4326	44
H(17)	6967	1931	2234	44
H(18)	6314	4018	2108	43
H(19)	4081	6530	3653	36
H(20)	4007	5481	4351	38
H(22)	6367	-1708	3362	47
H(23)	6428	-547	2638	46
H(25)	7176	3086	3382	36
H(26)	7098	1932	4103	36
H(32)	4499	2974	3385	32
H(33)	5283	2129	2857	34
H(35)	5990	6205	2648	41
H(36)	5211	7052	3181	39
H(43)	2454	570	2015	36
H(44)	2581	1042	2828	46
H(45)	2032	3160	3097	53
H(46)	1407	4819	2550	45
H(50)	777	6586	840	44
H(51)	787	6225	35	52
H(52)	1198	3985	-240	53
H(53)	1605	2155	302	42
H(55)	2538	573	1054	36
H(56)	1669	-1181	820	38
H(57)	-2146	-531	1089	49
H(58)	-2553	1425	1430	50
H(59)	-46	7112	1947	50
H(60)	1188	6966	1828	45
H(62)	149	-1060	352	45
H(63)	-1158	-866	449	47
H(65)	-438	556	1819	39
H(66)	865	318	1729	35
H(72)	-398	4855	990	43

H(73)	-1269	2938	814	43
H(75)	-1688	3038	2181	59
H(76)	-816	4962	2356	59

5.4.2. Appendix B: X-ray crystallography data of 57a-a

Empirical formula	C ₄₄ H ₂₈	
Formula weight	556.66	
Temperature	170(2) K	
Wavelength	0.71073 Å	
Crystal system	triclinic	
Space group	P-1	
Unit cell dimensions	a = 9.6096(7) Å	α = 77.740(9)°.
	b = 16.8653(12) Å	β = 85.409(9)°.
	c = 19.0003(15) Å	γ = 88.977(9)°.
Volume	2999.5(4) Å ³	
Z	4	
Density (calculated)	1.233 Mg/m ³	
Absorption coefficient	0.070 mm ⁻¹	
F(000)	1168	
Crystal size	0.4 x 0.4 x 0.2 mm ³	
Theta range for data collection	2.46 to 26.02°.	
Index ranges	-11 ≤ h ≤ 11, -20 ≤ k ≤ 20, -23 ≤ l ≤ 23	
Reflections collected	22310	
Independent reflections	11644 [R(int) = 0.0372]	
Completeness to theta = 26.02°	98.6 %	
Refinement method	Full-matrix least-squares on F ²	
Data / restraints / parameters	11644 / 0 / 794	
Goodness-of-fit on F ²	0.987	

Final R indices [$I > 2\sigma(I)$]	R1 = 0.0412, wR2 = 0.1014
R indices (all data)	R1 = 0.0646, wR2 = 0.1116
Extinction coefficient	0.024(2)
Largest diff. peak and hole	0.178 and -0.168 e. \AA^{-3}

Comments

All non-hydrogen atoms were refined anisotropic. All H atoms were located in difference map but were positioned with idealized geometry and refined isotropic using a riding model. There are two crystallographically independent molecules in the asymmetric unit.

Atomic coordinates ($\times 10^4$) and equivalent isotropic displacement parameters ($\text{\AA}^2 \times 10^3$).

U(eq) is defined as one third of the trace of the orthogonalized U_{ij} tensor.

	x	y	z	U(eq)
C(1)	-747(1)	4863(1)	2101(1)	31(1)
C(2)	-615(1)	4871(1)	2816(1)	31(1)
C(3)	-827(1)	5581(1)	3084(1)	30(1)
C(4)	-1216(1)	6295(1)	2646(1)	31(1)
C(5)	-1415(1)	6306(1)	1908(1)	33(1)
C(6)	-1849(2)	7017(1)	1430(1)	42(1)
C(7)	-1993(2)	7026(1)	719(1)	52(1)
C(8)	-1693(2)	6333(1)	441(1)	53(1)
C(9)	-1290(2)	5632(1)	880(1)	43(1)
C(10)	-1157(1)	5590(1)	1628(1)	32(1)
C(11)	-446(2)	4103(1)	1840(1)	39(1)
C(12)	773(2)	3721(1)	1891(1)	44(1)
C(13)	5365(1)	5220(1)	2963(1)	39(1)
C(14)	5150(1)	5890(1)	3216(1)	37(1)
C(15)	-396(2)	7358(1)	3241(1)	36(1)
C(16)	-1403(2)	7039(1)	2948(1)	37(1)
C(21)	2012(2)	4051(1)	2163(1)	38(1)
C(22)	2337(2)	3792(1)	2883(1)	39(1)
C(23)	1572(2)	3156(1)	3374(1)	46(1)

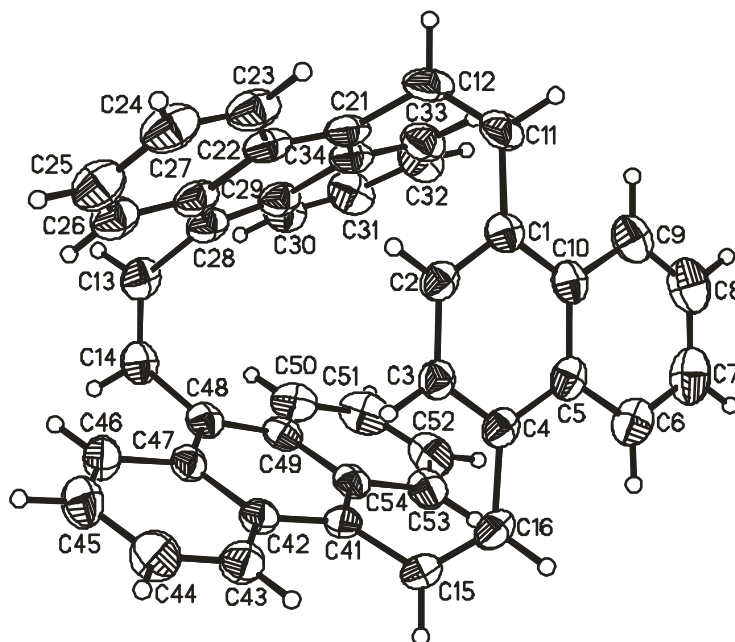
C(24)	1859(2)	2928(1)	4076(1)	52(1)
C(25)	2917(2)	3325(1)	4347(1)	52(1)
C(26)	3672(2)	3936(1)	3902(1)	44(1)
C(27)	3440(1)	4186(1)	3155(1)	38(1)
C(28)	4263(1)	4783(1)	2678(1)	37(1)
C(29)	4052(2)	4961(1)	1938(1)	37(1)
C(30)	4983(2)	5469(1)	1413(1)	44(1)
C(31)	4729(2)	5675(1)	705(1)	52(1)
C(32)	3497(2)	5398(1)	467(1)	54(1)
C(33)	2608(2)	4893(1)	939(1)	46(1)
C(34)	2866(2)	4628(1)	1681(1)	39(1)
C(41)	1067(1)	7039(1)	3253(1)	31(1)
C(42)	1552(1)	6575(1)	3894(1)	31(1)
C(43)	683(2)	6417(1)	4555(1)	40(1)
C(44)	1135(2)	5954(1)	5169(1)	50(1)
C(45)	2492(2)	5619(1)	5169(1)	49(1)
C(46)	3346(2)	5737(1)	4552(1)	40(1)
C(47)	2918(1)	6213(1)	3888(1)	30(1)
C(48)	3788(1)	6327(1)	3242(1)	31(1)
C(49)	3348(2)	6851(1)	2617(1)	32(1)
C(50)	4256(2)	7061(1)	1970(1)	44(1)
C(51)	3806(2)	7547(1)	1364(1)	54(1)
C(52)	2437(2)	7862(1)	1358(1)	51(1)
C(53)	1546(2)	7700(1)	1960(1)	41(1)
C(54)	1969(2)	7197(1)	2617(1)	31(1)
C(61)	-5929(1)	-19(1)	12551(1)	33(1)
C(62)	-5675(1)	453(1)	13036(1)	35(1)
C(63)	-5503(1)	1298(1)	12812(1)	35(1)
C(64)	-5536(1)	1685(1)	12100(1)	32(1)
C(65)	-5799(1)	1218(1)	11581(1)	32(1)
C(66)	-5795(2)	1565(1)	10829(1)	40(1)
C(67)	-6044(2)	1102(1)	10343(1)	46(1)
C(68)	-6330(2)	271(1)	10573(1)	45(1)

Atomic coordinates ($\times 10^4$) and equivalent isotropic displacement parameters ($\text{\AA}^2 \times 10^3$).

U(eq) is defined as one third of the trace of the orthogonalized U_{ij} tensor.

	x	y	z	U(eq)
C(69)	-6312(2)	-91(1)	11286(1)	39(1)
C(70)	-6031(1)	365(1)	11810(1)	32(1)
C(71)	-6041(2)	-913(1)	12792(1)	41(1)
C(72)	-4979(2)	-1377(1)	13053(1)	41(1)
C(73)	377(1)	105(1)	13268(1)	38(1)
C(74)	541(1)	902(1)	13070(1)	38(1)
C(75)	-4130(2)	2934(1)	11995(1)	39(1)
C(76)	-5299(2)	2576(1)	11888(1)	38(1)
C(81)	-3567(2)	-1049(1)	13116(1)	34(1)
C(82)	-2618(2)	-838(1)	12502(1)	35(1)
C(83)	-2921(2)	-953(1)	11805(1)	44(1)
C(84)	-1964(2)	-780(1)	11229(1)	53(1)
C(85)	-619(2)	-489(1)	11303(1)	51(1)
C(86)	-295(2)	-354(1)	11947(1)	43(1)
C(87)	-1277(2)	-499(1)	12565(1)	34(1)
C(88)	-949(1)	-335(1)	13229(1)	34(1)
C(89)	-1871(2)	-580(1)	13848(1)	34(1)
C(90)	-1553(2)	-470(1)	14543(1)	43(1)
C(91)	-2459(2)	-698(1)	15137(1)	54(1)
C(92)	-3762(2)	-1049(1)	15079(1)	54(1)
C(93)	-4108(2)	-1169(1)	14431(1)	45(1)
C(94)	-3188(2)	-948(1)	13791(1)	35(1)
C(101)	-2870(1)	2475(1)	12272(1)	34(1)
C(102)	-1894(1)	2204(1)	11783(1)	34(1)
C(103)	-1999(2)	2418(1)	11020(1)	43(1)
C(104)	-987(2)	2211(1)	10547(1)	53(1)
C(105)	184(2)	1754(1)	10807(1)	53(1)
C(106)	317(2)	1522(1)	11526(1)	43(1)
C(107)	-714(1)	1725(1)	12048(1)	34(1)
C(108)	-589(1)	1482(1)	12792(1)	34(1)
C(109)	-1503(1)	1806(1)	13279(1)	34(1)
C(110)	-1327(2)	1652(1)	14034(1)	43(1)
C(111)	-2176(2)	2002(1)	14494(1)	52(1)
C(112)	-3286(2)	2515(1)	14228(1)	50(1)

C(113)	-3514(2)	2666(1)	13516(1)	43(1)
C(114)	-2638(1)	2324(1)	13010(1)	35(1)



Bond lengths [Å]

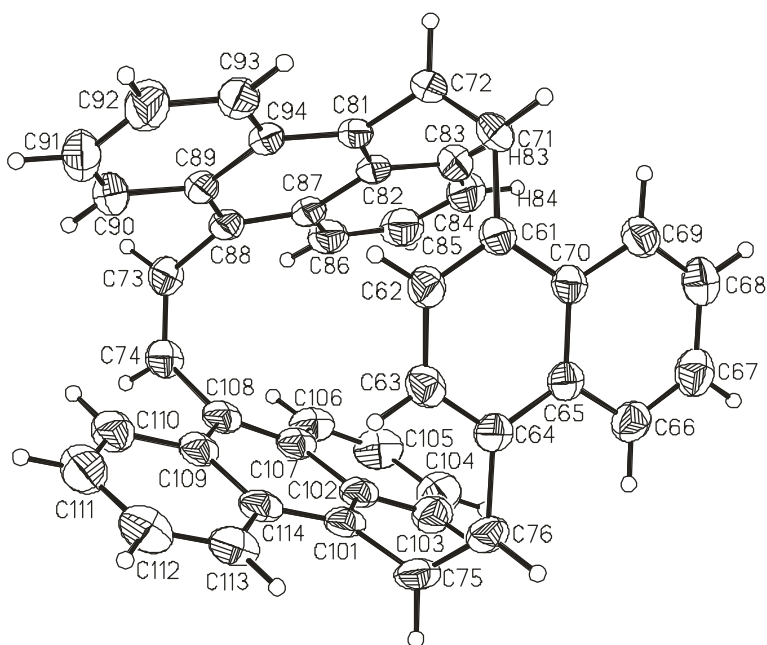
C(1)-C(2)	1.377(2)	C(25)-C(26)	1.364(2)
C(1)-C(10)	1.429(2)	C(26)-C(27)	1.427(2)
C(1)-C(11)	1.486(2)	C(27)-C(28)	1.410(2)
C(2)-C(3)	1.4036(19)	C(28)-C(29)	1.403(2)
C(3)-C(4)	1.375(2)	C(29)-C(30)	1.433(2)
C(4)-C(5)	1.426(2)	C(29)-C(34)	1.443(2)
C(4)-C(16)	1.489(2)	C(30)-C(31)	1.356(2)
C(5)-C(6)	1.420(2)	C(31)-C(32)	1.421(2)
C(5)-C(10)	1.429(2)	C(32)-C(33)	1.355(2)
C(6)-C(7)	1.367(2)	C(33)-C(34)	1.425(2)
C(7)-C(8)	1.398(3)	C(41)-C(42)	1.4082(19)

C(8)-C(9)	1.364(2)	C(41)-C(54)	1.410(2)
C(9)-C(10)	1.424(2)	C(42)-C(43)	1.429(2)
C(11)-C(12)	1.327(2)	C(42)-C(47)	1.4382(19)
C(12)-C(21)	1.495(2)	C(43)-C(44)	1.357(2)
C(13)-C(14)	1.325(2)	C(44)-C(45)	1.412(2)
C(13)-C(28)	1.500(2)	C(45)-C(46)	1.356(2)
C(14)-C(48)	1.493(2)	C(46)-C(47)	1.431(2)
C(15)-C(16)	1.331(2)	C(47)-C(48)	1.4090(19)
C(15)-C(41)	1.496(2)	C(48)-C(49)	1.411(2)
C(21)-C(22)	1.405(2)	C(49)-C(50)	1.433(2)
C(21)-C(34)	1.410(2)	C(49)-C(54)	1.438(2)
C(22)-C(23)	1.432(2)	C(50)-C(51)	1.361(2)
C(22)-C(27)	1.445(2)	C(51)-C(52)	1.410(3)
C(23)-C(24)	1.357(3)	C(52)-C(53)	1.356(2)
C(24)-C(25)	1.415(3)	C(53)-C(54)	1.436(2)

Bond angles [°]

C(2)-C(1)-C(10)	118.95(13)	C(29)-C(28)-C(13)	120.47(13)
C(2)-C(1)-C(11)	119.39(13)	C(27)-C(28)-C(13)	119.75(14)
C(10)-C(1)-C(11)	121.65(13)	C(28)-C(29)-C(30)	122.35(13)
C(1)-C(2)-C(3)	121.69(13)	C(28)-C(29)-C(34)	120.21(14)
C(4)-C(3)-C(2)	121.15(13)	C(30)-C(29)-C(34)	117.43(14)
C(3)-C(4)-C(5)	118.97(13)	C(31)-C(30)-C(29)	121.96(15)
C(3)-C(4)-C(16)	119.46(13)	C(30)-C(31)-C(32)	120.08(16)
C(5)-C(4)-C(16)	121.56(13)	C(33)-C(32)-C(31)	120.14(17)
C(6)-C(5)-C(4)	121.87(14)	C(32)-C(33)-C(34)	121.76(15)
C(6)-C(5)-C(10)	118.13(13)	C(21)-C(34)-C(33)	122.22(14)
C(4)-C(5)-C(10)	120.00(13)	C(21)-C(34)-C(29)	119.50(15)
C(7)-C(6)-C(5)	121.25(16)	C(33)-C(34)-C(29)	118.27(14)
C(6)-C(7)-C(8)	120.45(16)	C(42)-C(41)-C(54)	119.46(13)
C(9)-C(8)-C(7)	120.46(16)	C(42)-C(41)-C(15)	120.67(13)
C(8)-C(9)-C(10)	120.96(16)	C(54)-C(41)-C(15)	119.87(12)
C(9)-C(10)-C(5)	118.69(14)	C(41)-C(42)-C(43)	121.30(13)
C(9)-C(10)-C(1)	122.12(14)	C(41)-C(42)-C(47)	120.37(12)

C(5)-C(10)-C(1)	119.17(12)	C(43)-C(42)-C(47)	118.26(13)
C(12)-C(11)-C(1)	123.30(13)	C(44)-C(43)-C(42)	121.44(15)
C(11)-C(12)-C(21)	123.10(13)	C(43)-C(44)-C(45)	120.34(15)
C(14)-C(13)-C(28)	124.69(13)	C(46)-C(45)-C(44)	120.48(15)
C(13)-C(14)-C(48)	124.89(13)	C(45)-C(46)-C(47)	121.51(14)
C(16)-C(15)-C(41)	123.28(13)	C(48)-C(47)-C(46)	121.90(13)
C(15)-C(16)-C(4)	123.41(13)	C(48)-C(47)-C(42)	120.17(12)
C(22)-C(21)-C(34)	119.92(13)	C(46)-C(47)-C(42)	117.93(12)
C(22)-C(21)-C(12)	121.15(14)	C(47)-C(48)-C(49)	119.18(13)
C(34)-C(21)-C(12)	118.92(15)	C(47)-C(48)-C(14)	120.41(13)
C(21)-C(22)-C(23)	121.74(14)	C(49)-C(48)-C(14)	120.41(12)
C(21)-C(22)-C(27)	120.06(14)	C(48)-C(49)-C(50)	121.43(14)
C(23)-C(22)-C(27)	118.17(15)	C(48)-C(49)-C(54)	120.46(12)
C(24)-C(23)-C(22)	121.47(16)	C(50)-C(49)-C(54)	118.11(13)
C(23)-C(24)-C(25)	120.50(16)	C(51)-C(50)-C(49)	120.88(16)
C(26)-C(25)-C(24)	120.26(18)	C(50)-C(51)-C(52)	120.87(15)
C(25)-C(26)-C(27)	121.62(16)	C(53)-C(52)-C(51)	120.68(16)
C(28)-C(27)-C(26)	122.43(14)	C(52)-C(53)-C(54)	120.85(16)
C(28)-C(27)-C(22)	119.61(14)	C(41)-C(54)-C(53)	121.51(13)
C(26)-C(27)-C(22)	117.95(14)	C(41)-C(54)-C(49)	119.96(12)
C(29)-C(28)-C(27)	119.78(13)	C(53)-C(54)-C(49)	118.53(13)



Bond lengths [Å]

C(61)-C(62)	1.376(2)	C(85)-C(86)	1.353(2)
C(61)-C(70)	1.431(2)	C(86)-C(87)	1.427(2)
C(61)-C(71)	1.483(2)	C(87)-C(88)	1.408(2)
C(62)-C(63)	1.408(2)	C(88)-C(89)	1.407(2)
C(63)-C(64)	1.374(2)	C(89)-C(90)	1.429(2)
C(64)-C(65)	1.426(2)	C(89)-C(94)	1.440(2)
C(64)-C(76)	1.489(2)	C(90)-C(91)	1.361(2)
C(65)-C(66)	1.423(2)	C(91)-C(92)	1.416(3)
C(65)-C(70)	1.429(2)	C(92)-C(93)	1.358(2)
C(66)-C(67)	1.366(2)	C(93)-C(94)	1.430(2)
C(67)-C(68)	1.403(3)	C(101)-C(102)	1.406(2)
C(68)-C(69)	1.364(2)	C(101)-C(114)	1.407(2)
C(69)-C(70)	1.424(2)	C(102)-C(103)	1.430(2)
C(71)-C(72)	1.337(2)	C(102)-C(107)	1.441(2)
C(72)-C(81)	1.497(2)	C(103)-C(104)	1.362(2)
C(73)-C(74)	1.326(2)	C(104)-C(105)	1.414(3)
C(73)-C(88)	1.500(2)	C(105)-C(106)	1.355(2)
C(74)-C(108)	1.500(2)	C(106)-C(107)	1.433(2)
C(75)-C(76)	1.333(2)	C(107)-C(108)	1.400(2)
C(75)-C(101)	1.495(2)	C(108)-C(109)	1.411(2)
C(81)-C(94)	1.405(2)	C(109)-C(110)	1.426(2)
C(81)-C(82)	1.410(2)	C(109)-C(114)	1.442(2)
C(82)-C(83)	1.431(2)	C(110)-C(111)	1.365(2)
C(82)-C(87)	1.443(2)	C(111)-C(112)	1.418(3)
C(83)-C(84)	1.357(3)	C(112)-C(113)	1.357(2)
C(84)-C(85)	1.419(3)	C(113)-C(114)	1.433(2)

Bond angles [°]

C(62)-C(61)-C(70)	118.95(13)	C(89)-C(88)-C(73)	120.62(12)
C(62)-C(61)-C(71)	120.30(13)	C(87)-C(88)-C(73)	119.68(14)
C(70)-C(61)-C(71)	120.71(13)	C(88)-C(89)-C(90)	122.01(13)
C(61)-C(62)-C(63)	121.16(14)	C(88)-C(89)-C(94)	119.99(13)
C(64)-C(63)-C(62)	121.68(13)	C(90)-C(89)-C(94)	117.99(14)

C(63)-C(64)-C(65)	118.90(13)	C(91)-C(90)-C(89)	121.70(15)
C(63)-C(64)-C(76)	119.52(13)	C(90)-C(91)-C(92)	120.29(15)
C(65)-C(64)-C(76)	121.58(13)	C(93)-C(92)-C(91)	120.14(16)
C(66)-C(65)-C(64)	122.50(14)	C(92)-C(93)-C(94)	121.78(15)
C(66)-C(65)-C(70)	117.84(13)	C(81)-C(94)-C(93)	121.63(13)
C(64)-C(65)-C(70)	119.63(13)	C(81)-C(94)-C(89)	120.22(14)
C(67)-C(66)-C(65)	121.25(15)	C(93)-C(94)-C(89)	118.08(13)
C(66)-C(67)-C(68)	120.79(15)	C(102)-C(101)-C(114)	119.65(13)
C(69)-C(68)-C(67)	119.93(15)	C(102)-C(101)-C(75)	119.29(14)
C(68)-C(69)-C(70)	121.16(15)	C(114)-C(101)-C(75)	121.05(13)
C(69)-C(70)-C(65)	118.95(13)	C(101)-C(102)-C(103)	121.88(14)
C(69)-C(70)-C(61)	121.43(14)	C(101)-C(102)-C(107)	119.85(14)
C(65)-C(70)-C(61)	119.58(12)	C(103)-C(102)-C(107)	118.21(13)
C(72)-C(71)-C(61)	122.63(13)	C(104)-C(103)-C(102)	121.53(15)
C(71)-C(72)-C(81)	123.45(13)	C(103)-C(104)-C(105)	120.13(16)
C(74)-C(73)-C(88)	124.48(12)	C(106)-C(105)-C(104)	120.58(16)
C(73)-C(74)-C(108)	124.17(12)	C(105)-C(106)-C(107)	121.66(15)
C(76)-C(75)-C(101)	123.45(13)	C(108)-C(107)-C(106)	122.00(13)
C(75)-C(76)-C(64)	123.45(13)	C(108)-C(107)-C(102)	120.17(13)
C(94)-C(81)-C(82)	119.79(13)	C(106)-C(107)-C(102)	117.82(14)
C(94)-C(81)-C(72)	119.88(14)	C(107)-C(108)-C(109)	119.72(13)
C(82)-C(81)-C(72)	120.33(13)	C(107)-C(108)-C(74)	120.19(13)
C(81)-C(82)-C(83)	122.52(14)	C(109)-C(108)-C(74)	120.05(14)
C(81)-C(82)-C(87)	119.85(13)	C(108)-C(109)-C(110)	122.13(14)
C(83)-C(82)-C(87)	117.63(14)	C(108)-C(109)-C(114)	119.62(13)
C(84)-C(83)-C(82)	121.35(16)	C(110)-C(109)-C(114)	118.23(13)
C(83)-C(84)-C(85)	120.81(15)	C(111)-C(110)-C(109)	121.54(16)
C(86)-C(85)-C(84)	119.94(17)	C(110)-C(111)-C(112)	120.11(17)
C(85)-C(86)-C(87)	121.61(16)	C(113)-C(112)-C(111)	120.55(15)
C(88)-C(87)-C(86)	121.39(14)	C(112)-C(113)-C(114)	121.40(15)
C(88)-C(87)-C(82)	120.09(14)	C(101)-C(114)-C(113)	121.73(14)
C(86)-C(87)-C(82)	118.51(13)	C(101)-C(114)-C(109)	120.12(13)
C(89)-C(88)-C(87)	119.69(13)	C(113)-C(114)-C(109)	118.14(14)

Anisotropic displacement parameters ($\text{\AA}^2 \times 10^3$) for 44b-a. The anisotropic displacement factor exponent takes the form: $-2\pi^2 [h^2 a^{*2} U^{11} + \dots + 2 h k a^* b^* U^{12}]$

	U ¹¹	U ²²	U ³³	U ²³	U ¹³	U ¹²
C(1)	22(1)	31(1)	41(1)	-9(1)	0(1)	-8(1)
C(2)	25(1)	28(1)	39(1)	-4(1)	-2(1)	-1(1)
C(3)	25(1)	32(1)	35(1)	-7(1)	-4(1)	-1(1)
C(4)	21(1)	28(1)	43(1)	-6(1)	-2(1)	-3(1)
C(5)	21(1)	32(1)	41(1)	0(1)	-1(1)	-5(1)
C(6)	36(1)	36(1)	50(1)	4(1)	-3(1)	-4(1)
C(7)	47(1)	55(1)	45(1)	14(1)	-9(1)	-8(1)
C(8)	50(1)	68(1)	36(1)	0(1)	-5(1)	-12(1)
C(9)	36(1)	53(1)	39(1)	-8(1)	0(1)	-12(1)
C(10)	21(1)	38(1)	37(1)	-6(1)	0(1)	-9(1)
C(11)	35(1)	36(1)	49(1)	-16(1)	-4(1)	-13(1)
C(12)	39(1)	32(1)	65(1)	-25(1)	4(1)	-9(1)
C(13)	19(1)	46(1)	52(1)	-11(1)	1(1)	-1(1)
C(14)	22(1)	44(1)	45(1)	-9(1)	-3(1)	-8(1)
C(15)	41(1)	27(1)	42(1)	-10(1)	-6(1)	7(1)
C(16)	32(1)	30(1)	47(1)	-6(1)	-4(1)	7(1)
C(21)	28(1)	30(1)	62(1)	-23(1)	2(1)	1(1)
C(22)	28(1)	27(1)	63(1)	-17(1)	5(1)	0(1)
C(23)	34(1)	31(1)	74(1)	-14(1)	4(1)	-3(1)
C(24)	42(1)	36(1)	73(1)	-5(1)	8(1)	-2(1)
C(25)	43(1)	47(1)	61(1)	-6(1)	4(1)	5(1)
C(26)	32(1)	40(1)	60(1)	-13(1)	1(1)	3(1)
C(27)	24(1)	32(1)	58(1)	-15(1)	2(1)	4(1)
C(28)	21(1)	34(1)	58(1)	-17(1)	1(1)	2(1)
C(29)	26(1)	34(1)	54(1)	-18(1)	2(1)	0(1)
C(30)	29(1)	48(1)	59(1)	-19(1)	3(1)	-7(1)
C(31)	44(1)	58(1)	55(1)	-18(1)	8(1)	-13(1)
C(32)	50(1)	64(1)	52(1)	-22(1)	1(1)	-8(1)
C(33)	36(1)	51(1)	57(1)	-26(1)	-1(1)	-6(1)
C(34)	29(1)	33(1)	58(1)	-22(1)	2(1)	0(1)
C(41)	34(1)	23(1)	37(1)	-9(1)	-6(1)	-1(1)
C(42)	34(1)	27(1)	34(1)	-9(1)	-4(1)	-2(1)

C(43)	42(1)	45(1)	35(1)	-11(1)	0(1)	5(1)
C(44)	57(1)	59(1)	32(1)	-7(1)	4(1)	5(1)
C(45)	58(1)	53(1)	33(1)	-2(1)	-10(1)	5(1)
C(46)	40(1)	42(1)	39(1)	-6(1)	-11(1)	3(1)
C(47)	30(1)	28(1)	34(1)	-8(1)	-6(1)	-4(1)
C(48)	27(1)	29(1)	39(1)	-10(1)	-3(1)	-8(1)
C(49)	36(1)	28(1)	35(1)	-9(1)	-1(1)	-11(1)
C(50)	46(1)	38(1)	45(1)	-9(1)	8(1)	-12(1)
C(51)	75(1)	44(1)	39(1)	-2(1)	12(1)	-18(1)
C(52)	76(1)	37(1)	37(1)	1(1)	-11(1)	-12(1)
C(53)	53(1)	28(1)	41(1)	-2(1)	-12(1)	-8(1)
C(54)	38(1)	23(1)	34(1)	-6(1)	-7(1)	-7(1)
C(61)	22(1)	32(1)	44(1)	-4(1)	-6(1)	-4(1)
C(62)	28(1)	38(1)	37(1)	-4(1)	-5(1)	-5(1)
C(63)	26(1)	37(1)	44(1)	-12(1)	-4(1)	-3(1)
C(64)	18(1)	31(1)	47(1)	-6(1)	-4(1)	3(1)
C(65)	19(1)	34(1)	42(1)	-6(1)	-4(1)	2(1)
C(66)	33(1)	40(1)	46(1)	0(1)	-7(1)	-1(1)
C(67)	44(1)	57(1)	37(1)	-4(1)	-6(1)	-3(1)

Anisotropic displacement parameters ($\text{\AA}^2 \times 10^3$) for 44b-a. The anisotropic displacement factor exponent takes the form: $-2\pi^2 [h^2 a^{*2} U^{11} + \dots + 2 h k a^* b^* U^{12}]$

	U ¹¹	U ²²	U ³³	U ²³	U ¹³	U ¹²
68)	44(1)	55(1)	41(1)	-16(1)	-9(1)	0(1)
C(69)	34(1)	38(1)	49(1)	-12(1)	-8(1)	-2(1)
C(70)	20(1)	34(1)	42(1)	-8(1)	-5(1)	0(1)
C(71)	36(1)	36(1)	50(1)	-4(1)	-13(1)	-14(1)
C(72)	47(1)	27(1)	47(1)	0(1)	-18(1)	-12(1)
C(73)	26(1)	39(1)	50(1)	-10(1)	-14(1)	6(1)
C(74)	21(1)	39(1)	53(1)	-9(1)	-8(1)	-2(1)
C(75)	37(1)	22(1)	58(1)	-6(1)	-5(1)	5(1)
C(76)	32(1)	29(1)	52(1)	-6(1)	-8(1)	9(1)
C(81)	37(1)	21(1)	45(1)	-3(1)	-16(1)	-1(1)

C(82)	44(1)	20(1)	43(1)	-5(1)	-17(1)	5(1)
C(83)	55(1)	34(1)	48(1)	-10(1)	-20(1)	1(1)
C(84)	75(1)	43(1)	43(1)	-12(1)	-18(1)	3(1)
C(85)	66(1)	41(1)	46(1)	-9(1)	-2(1)	2(1)
C(86)	45(1)	31(1)	52(1)	-8(1)	-7(1)	4(1)
C(87)	37(1)	22(1)	43(1)	-4(1)	-12(1)	6(1)
C(88)	31(1)	23(1)	47(1)	-6(1)	-14(1)	5(1)
C(89)	36(1)	25(1)	42(1)	-5(1)	-16(1)	2(1)
C(90)	43(1)	43(1)	46(1)	-8(1)	-18(1)	-4(1)
C(91)	62(1)	61(1)	40(1)	-7(1)	-17(1)	-12(1)
C(92)	59(1)	61(1)	39(1)	1(1)	-8(1)	-15(1)
C(93)	44(1)	42(1)	46(1)	4(1)	-13(1)	-13(1)
C(94)	39(1)	24(1)	41(1)	0(1)	-15(1)	-2(1)
C(101)	28(1)	21(1)	53(1)	-6(1)	-4(1)	-5(1)
C(102)	28(1)	23(1)	50(1)	-5(1)	-4(1)	-6(1)
C(103)	39(1)	37(1)	52(1)	-4(1)	-6(1)	-3(1)
C(104)	57(1)	53(1)	46(1)	-3(1)	3(1)	-7(1)
C(105)	47(1)	49(1)	56(1)	-6(1)	12(1)	-1(1)
C(106)	30(1)	35(1)	61(1)	-5(1)	5(1)	-3(1)
C(107)	23(1)	26(1)	52(1)	-6(1)	-1(1)	-6(1)
C(108)	21(1)	27(1)	55(1)	-8(1)	-5(1)	-6(1)
C(109)	27(1)	28(1)	49(1)	-8(1)	-5(1)	-8(1)
C(110)	38(1)	39(1)	54(1)	-10(1)	-8(1)	-5(1)
C(111)	56(1)	51(1)	49(1)	-14(1)	-5(1)	-8(1)
C(112)	46(1)	46(1)	61(1)	-23(1)	5(1)	-5(1)
C(113)	37(1)	33(1)	61(1)	-16(1)	-1(1)	-2(1)
C(114)	27(1)	24(1)	54(1)	-9(1)	-1(1)	-6(1)

Hydrogen coordinates ($\times 10^4$) and isotropic displacement parameters ($\text{\AA}^2 \times 10^3$)

	x	y	z	U(eq)
H(2)	-374	4383	3136	37
H(3)	-700	5569	3577	36
H(6)	-2042	7496	1609	51

H(7)	-2298	7506	411	63
H(8)	-1770	6350	-57	63
H(9)	-1096	5165	684	51
H(11)	-1162	3879	1624	47
H(12)	863	3214	1749	52
H(13)	6282	5001	2963	47
H(14)	5921	6109	3394	44
H(15)	-616	7811	3453	44
H(16)	-2289	7299	2930	44
H(23)	849	2888	3203	56
H(24)	1345	2500	4388	62
H(25)	3103	3165	4841	62
H(26)	4370	4201	4094	52
H(30)	5802	5668	1565	53
H(31)	5375	6005	369	62
H(32)	3296	5567	-24	64
H(33)	1791	4711	771	55
H(43)	-231	6640	4564	48
H(44)	536	5855	5601	60
H(45)	2809	5308	5604	58
H(46)	4249	5498	4561	48
H(50)	5185	6859	1964	52
H(51)	4422	7676	939	65
H(52)	2135	8192	926	61
H(53)	630	7921	1948	49
H(62)	-5614	203	13530	42
H(63)	-5360	1610	13162	42
H(66)	-5617	2128	10662	48
H(67)	-6022	1347	9843	56
H(68)	-6537	-41	10232	54
H(69)	-6489	-657	11436	47
H(71)	-6901	-1166	12759	49
H(72)	-5128	-1945	13207	49
H(73)	1152	-210	13448	45
H(74)	1431	1120	13106	45
H(75)	-4095	3510	11888	47
H(76)	-6018	2908	11665	45

H(83)	-3811	-1154	11744	53
H(84)	-2198	-854	10771	63
H(85)	54	-389	10900	61
H(86)	609	-159	11990	51
H(90)	-687	-232	14591	52
H(91)	-2217	-621	15593	65
H(92)	-4395	-1201	15495	65
H(93)	-4985	-1406	14401	54
H(103)	-2793	2711	10838	52
H(104)	-1068	2373	10042	64
H(105)	884	1609	10475	63
H(106)	1114	1218	11689	52
H(110)	-602	1299	14221	52
H(111)	-2024	1900	14993	62
H(112)	-3874	2756	14551	60
H(113)	-4271	3006	13349	51

5.4.3. Appendix C: X-ray crystallography data of 55b

Empirical formula	$C_{65.80}H_{47.60}Cl_{3.60}$	
Formula weight	965.86	
Temperature	170(2) K	
Wavelength	0.71073 Å	
Crystal system	monoclinic	
Space group	P2 ₁ /c	
Unit cell dimensions	$a = 11.7662(7)$ Å	$\alpha = 90^\circ$.
	$b = 14.4084(7)$ Å	$\beta = 100.280(8)^\circ$.
	$c = 15.1930(11)$ Å	$\gamma = 90^\circ$.
Volume	$2534.4(3)$ Å ³	
Z	2	
Density (calculated)	1.266 Mg/m ³	

Absorption coefficient	0.255 mm ⁻¹
F(000)	1007
Crystal size	0.2 x 0.1 x 0.1 mm ³
Theta range for data collection	2.47 to 26.02°.
Index ranges	-13<=h<=14, -16<=k<=17, -18<=l<=15
Reflections collected	9527
Independent reflections	4885 [R(int) = 0.0380]
Completeness to theta = 26.02°	97.8 %
Refinement method	Full-matrix least-squares on F ²
Data / restraints / parameters	4885 / 4 / 326
Goodness-of-fit on F ²	1.021
Final R indices [I>2sigma(I)]	R1 = 0.0539, wR2 = 0.1294
R indices (all data)	R1 = 0.0872, wR2 = 0.1454
Extinction coefficient	0.030(5)
Largest diff. peak and hole	0.659 and -0.333 e.Å ⁻³

Comments

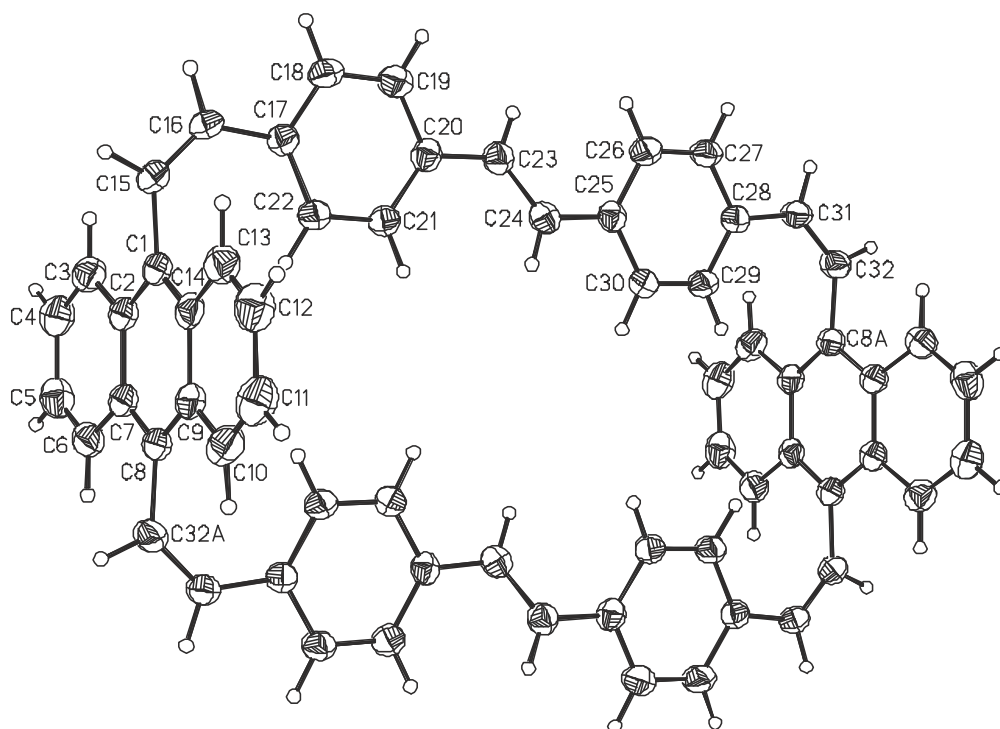
All non-hydrogen atoms were refined anisotropic. All H were positioned with idealized geometry and refined isotropic using a riding model. The structure contains 1.8 molecules of dichloromethane per formula unit, which are disordered and which were refined using a riding model.

Atomic coordinates (x 10⁴) and equivalent isotropic displacement parameters (Å²x 10³).

U(eq) is defined as one third of the trace of the orthogonalized U_{ij} tensor.

	x	y	z	U(eq)
C(1)	4724(2)	8442(1)	1413(1)	30(1)
C(2)	5190(2)	9033(2)	2127(1)	30(1)
C(3)	4496(2)	9718(2)	2462(2)	37(1)

C(4)	4958(2)	10307(2)	3134(2)	43(1)
C(5)	6145(2)	10237(2)	3521(2)	42(1)
C(6)	6832(2)	9596(2)	3230(2)	36(1)
C(7)	6391(2)	8963(2)	2520(1)	31(1)
C(8)	7097(2)	8308(2)	2193(2)	31(1)
C(9)	6635(2)	7733(2)	1467(2)	31(1)
C(10)	7331(2)	7076(2)	1095(2)	40(1)
C(11)	6883(3)	6558(2)	361(2)	47(1)
C(12)	5712(3)	6648(2)	-36(2)	45(1)
C(13)	5009(2)	7242(2)	305(2)	38(1)
C(14)	5437(2)	7808(1)	1068(1)	30(1)
C(15)	3493(2)	8544(2)	975(2)	35(1)
C(16)	2550(2)	8148(2)	1178(2)	34(1)
C(17)	2404(2)	7481(2)	1882(1)	31(1)
C(18)	1299(2)	7128(2)	1872(2)	39(1)
C(19)	1079(2)	6484(2)	2493(2)	41(1)
C(20)	1960(2)	6148(2)	3158(2)	31(1)
C(21)	3071(2)	6516(2)	3183(2)	32(1)
C(22)	3289(2)	7168(2)	2564(2)	33(1)
C(23)	1674(2)	5442(2)	3774(2)	33(1)
C(24)	2400(2)	4883(2)	4307(1)	30(1)
C(25)	2062(2)	4196(1)	4926(1)	29(1)
C(26)	923(2)	3890(2)	4874(2)	36(1)
C(27)	638(2)	3249(2)	5474(2)	35(1)
C(28)	1468(2)	2882(2)	6165(1)	30(1)
C(29)	2607(2)	3190(2)	6218(2)	32(1)
C(30)	2891(2)	3823(2)	5611(2)	32(1)
C(31)	1068(2)	2201(2)	6766(2)	34(1)
C(32)	1643(2)	1711(2)	7443(2)	36(1)
C(33)	7862(4)	4141(3)	1290(3)	76(1)
Cl(1)	8670(1)	4699(1)	2214(1)	74(1)
Cl(2)	8600(3)	4149(3)	385(2)	116(1)
Cl(2')	8379(8)	3864(7)	402(5)	145(5)


Bond lengths [Å]

C(1)-C(14)	1.404(3)	C(17)-C(22)	1.406(3)
C(1)-C(2)	1.411(3)	C(18)-C(19)	1.381(4)
C(1)-C(15)	1.489(3)	C(19)-C(20)	1.397(3)
C(2)-C(3)	1.431(3)	C(20)-C(21)	1.406(3)
C(2)-C(7)	1.436(3)	C(20)-C(23)	1.462(3)
C(3)-C(4)	1.364(3)	C(21)-C(22)	1.385(3)
C(4)-C(5)	1.419(4)	C(23)-C(24)	1.337(3)
C(5)-C(6)	1.354(4)	C(24)-C(25)	1.468(3)
C(6)-C(7)	1.437(3)	C(25)-C(26)	1.400(3)
C(7)-C(8)	1.406(3)	C(25)-C(30)	1.400(3)
C(8)-C(9)	1.409(3)	C(26)-C(27)	1.380(3)
C(8)-C(32A)	1.487(3)	C(27)-C(28)	1.403(3)
C(9)-C(10)	1.432(3)	C(28)-C(29)	1.401(3)
C(9)-C(14)	1.436(3)	C(28)-C(31)	1.473(3)
C(10)-C(11)	1.368(4)	C(29)-C(30)	1.380(3)
C(11)-C(12)	1.408(4)	C(31)-C(32)	1.329(3)

C(12)-C(13)	1.354(4)	C(32)-C(8A)	1.487(3)
C(13)-C(14)	1.434(3)	C(33)-Cl(2')	1.626(9)
C(15)-C(16)	1.331(4)	C(33)-Cl(1)	1.745(4)
C(16)-C(17)	1.472(3)	C(33)-Cl(2)	1.753(5)
C(17)-C(18)	1.393(3)		

Symmetry transformations used to generate equivalent atoms: A -x+1,-y+1,-z+1

Bond angles [°].

C(14)-C(1)-C(2)	120.2(2)	C(15)-C(16)-C(17)	131.1(2)
C(14)-C(1)-C(15)	119.70(19)	C(18)-C(17)-C(22)	117.3(2)
C(2)-C(1)-C(15)	119.9(2)	C(18)-C(17)-C(16)	117.42(19)
C(1)-C(2)-C(3)	121.4(2)	C(22)-C(17)-C(16)	125.3(2)
C(1)-C(2)-C(7)	119.7(2)	C(19)-C(18)-C(17)	121.8(2)
C(3)-C(2)-C(7)	118.8(2)	C(18)-C(19)-C(20)	121.4(2)
C(4)-C(3)-C(2)	121.3(2)	C(19)-C(20)-C(21)	117.1(2)
C(3)-C(4)-C(5)	119.8(2)	C(19)-C(20)-C(23)	118.6(2)
C(6)-C(5)-C(4)	120.9(2)	C(21)-C(20)-C(23)	124.3(2)
C(5)-C(6)-C(7)	121.4(2)	C(22)-C(21)-C(20)	121.4(2)
C(8)-C(7)-C(2)	120.0(2)	C(21)-C(22)-C(17)	121.0(2)
C(8)-C(7)-C(6)	122.3(2)	C(24)-C(23)-C(20)	127.8(2)
C(2)-C(7)-C(6)	117.7(2)	C(23)-C(24)-C(25)	125.3(2)
C(7)-C(8)-C(9)	120.1(2)	C(26)-C(25)-C(30)	117.0(2)
C(7)-C(8)-C(32A)	119.6(2)	C(26)-C(25)-C(24)	122.82(19)
C(9)-C(8)-C(32A)	120.0(2)	C(30)-C(25)-C(24)	120.1(2)
C(8)-C(9)-C(10)	122.0(2)	C(27)-C(26)-C(25)	121.1(2)
C(8)-C(9)-C(14)	119.9(2)	C(26)-C(27)-C(28)	121.9(2)
C(10)-C(9)-C(14)	118.1(2)	C(29)-C(28)-C(27)	117.0(2)
C(11)-C(10)-C(9)	121.2(2)	C(29)-C(28)-C(31)	125.69(19)
C(10)-C(11)-C(12)	120.2(3)	C(27)-C(28)-C(31)	117.3(2)
C(13)-C(12)-C(11)	120.8(2)	C(30)-C(29)-C(28)	121.0(2)
C(12)-C(13)-C(14)	121.2(2)	C(29)-C(30)-C(25)	122.0(2)
C(1)-C(14)-C(13)	121.7(2)	C(32)-C(31)-C(28)	131.2(2)
C(1)-C(14)-C(9)	119.92(19)	C(31)-C(32)-C(8A)	129.3(2)
C(13)-C(14)-C(9)	118.4(2)	Cl(2')-C(33)-Cl(1)	123.4(4)

C(16)-C(15)-C(1)	129.7(2)	Cl(2')-C(33)-Cl(2)	16.1(5)
		Cl(1)-C(33)-Cl(2)	110.7(3)

Symmetry transformations used to generate equivalent atoms: A -x+1,-y+1,-z+1

Anisotropic displacement parameters ($\text{\AA}^2 \times 10^3$). The anisotropic displacement factor exponent takes the form: $-2\pi^2 [h^2 a^{*2} U_{11} + \dots + 2 h k a^* b^* U_{12}]$

	U_{11}	U_{22}	U_{33}	U_{23}	U_{13}	U_{12}
C(1)	31(1)	30(1)	27(1)	9(1)	2(1)	-2(1)
C(2)	33(1)	30(1)	27(1)	7(1)	5(1)	-1(1)
C(3)	36(1)	37(1)	38(1)	7(1)	8(1)	3(1)
C(4)	51(2)	36(1)	44(1)	0(1)	12(1)	4(1)
C(5)	54(2)	37(1)	34(1)	-2(1)	5(1)	-7(1)
C(6)	38(1)	38(1)	32(1)	5(1)	2(1)	-6(1)
C(7)	33(1)	31(1)	28(1)	10(1)	2(1)	-2(1)
C(8)	29(1)	33(1)	30(1)	11(1)	3(1)	-2(1)
C(9)	34(1)	29(1)	31(1)	9(1)	6(1)	0(1)
C(10)	41(1)	39(1)	41(1)	9(1)	11(1)	7(1)
C(11)	58(2)	40(1)	45(2)	1(1)	16(1)	8(1)
C(12)	59(2)	36(1)	39(1)	-5(1)	8(1)	-1(1)
C(13)	43(1)	35(1)	33(1)	4(1)	-1(1)	-3(1)
C(14)	38(1)	26(1)	26(1)	7(1)	3(1)	-2(1)
C(15)	35(1)	35(1)	31(1)	10(1)	-4(1)	1(1)
C(16)	31(1)	35(1)	31(1)	6(1)	-5(1)	2(1)
C(17)	31(1)	29(1)	30(1)	1(1)	2(1)	0(1)
C(18)	30(1)	45(1)	40(1)	11(1)	-4(1)	1(1)
C(19)	31(1)	45(1)	46(1)	10(1)	2(1)	-4(1)
C(20)	35(1)	30(1)	29(1)	1(1)	5(1)	1(1)
C(21)	33(1)	32(1)	28(1)	2(1)	-2(1)	-1(1)
C(22)	30(1)	35(1)	31(1)	4(1)	-2(1)	-3(1)
C(23)	34(1)	32(1)	34(1)	2(1)	8(1)	-2(1)
C(24)	34(1)	30(1)	25(1)	-6(1)	5(1)	-4(1)
C(25)	34(1)	26(1)	25(1)	-3(1)	3(1)	-2(1)
C(26)	35(1)	38(1)	31(1)	6(1)	-3(1)	-1(1)
C(27)	28(1)	40(1)	34(1)	5(1)	-2(1)	-3(1)

C(28)	28(1)	30(1)	29(1)	0(1)	2(1)	-1(1)
C(29)	29(1)	35(1)	30(1)	4(1)	-1(1)	0(1)
C(30)	30(1)	30(1)	34(1)	0(1)	1(1)	-2(1)
C(31)	26(1)	40(1)	36(1)	7(1)	2(1)	-2(1)
C(32)	29(1)	41(1)	38(1)	11(1)	5(1)	-6(1)
C(33)	69(3)	76(3)	80(3)	15(2)	4(2)	-9(2)
Cl(1)	59(1)	69(1)	91(1)	1(1)	3(1)	-16(1)
Cl(2)	119(2)	162(3)	74(2)	52(2)	36(2)	88(2)
Cl(2')	121(6)	171(8)	106(6)	-88(6)	-82(5)	105(5)

Hydrogen coordinates ($\times 10^4$) and isotropic displacement parameters ($\text{\AA}^2 \times 10^3$)

	x	y	z	U(eq)
H(3)	3698	9763	2212	44
H(4)	4486	10763	3342	52
H(5)	6461	10646	3992	50
H(6)	7624	9563	3502	43
H(10)	8119	7000	1363	48
H(11)	7364	6135	117	56
H(12)	5411	6288	-548	54
H(13)	4219	7283	33	46
H(15)	3361	8952	476	42
H(16)	1850	8328	802	41
H(18)	681	7336	1426	47
H(19)	313	6264	2468	49
H(21)	3687	6314	3635	38
H(22)	4048	7407	2600	40
H(23)	878	5372	3799	40
H(24)	3199	4935	4284	36
H(26)	336	4128	4418	43
H(27)	-142	3051	5418	42
H(29)	3193	2960	6678	38
H(30)	3674	4012	5659	38
H(31)	258	2093	6649	41

H(32)	1183	1316	7737	43
H(33A)	7109	4459	1117	91
H(33B)	7711	3492	1450	91
H(33C)	7570	3560	1516	91
H(33D)	7178	4537	1085	91

5.4.4. Appendix D: X-ray crystallography data of 56b

Empirical formula	$C_{116}H_{88}$	
Formula weight	1481.86	
Temperature	170(2) K	
Wavelength	0.71073 Å	
Crystal system	triclinic	
Space group	P-1	
Unit cell dimensions	$a = 15.3793(11)$ Å	$\alpha = 116.046(7)^\circ$.
	$b = 29.488(2)$ Å	$\beta = 91.063(9)^\circ$.
	$c = 31.100(2)$ Å	$\gamma = 93.008(8)^\circ$.
Volume	$12640.5(15)$ Å ³	
Z	6	
Density (calculated)	1.168 Mg/m ³	
Absorption coefficient	0.066 mm ⁻¹	
F(000)	4704	
Crystal size	? x ? x ? mm ³	
Theta range for data collection	1.78 to 22.40°.	
Index ranges	$-16 \leq h \leq 16$, $-31 \leq k \leq 31$, $-33 \leq l \leq 33$	
Reflections collected	72374	
Independent reflections	32247 [R(int) = 0.0328]	
Completeness to theta = 22.40°	98.6 %	
Refinement method	Full-matrix least-squares on F ²	
Data / restraints / parameters	32247 / 2602 / 3274	
Goodness-of-fit on F ²	1.022	
Final R indices [I > 2σ(I)]	R1 = 0.0564, wR2 = 0.1467	

R indices (all data)	R1 = 0.0846, wR2 = 0.1650
Extinction coefficient	0.0046(4)
Largest diff. peak and hole	0.359 and -0.224 e.Å ⁻³

Comments

All non-hydrogen atoms were refined anisotropic. All H were positioned with idealized geometry and refined isotropic using a riding model. Some of the benzene molecules and two carbon atoms in one of the three crystallographically independent molecules are disordered and were refined using a riding model.

Atomic coordinates (x 10⁴) and equivalent isotropic displacement parameters (Å² x 10³).
U(eq) is defined as one third of the trace of the orthogonalized U_{ij} tensor.

	x	y	z	U(eq)
C(1)	7102(2)	9446(1)	288(1)	42(1)
C(2)	7043(2)	9442(1)	740(1)	46(1)
C(3)	6985(2)	9897(1)	1170(1)	53(1)
C(4)	6927(2)	9892(1)	1601(1)	68(1)
C(5)	6923(2)	9427(2)	1630(1)	84(1)
C(6)	6975(2)	8986(2)	1232(2)	82(1)
C(7)	7042(2)	8968(1)	767(1)	59(1)
C(8)	7126(2)	8512(1)	348(1)	70(1)
C(9)	7280(2)	8524(1)	-93(1)	57(1)
C(10)	7448(2)	8083(1)	-526(2)	78(1)
C(11)	7552(2)	8102(1)	-947(1)	81(1)
C(12)	7502(2)	8558(1)	-970(1)	70(1)
C(13)	7351(2)	8987(1)	-579(1)	52(1)
C(14)	7249(2)	8997(1)	-120(1)	48(1)
C(15)	7093(3)	7998(2)	310(2)	54(1)
C(16)	6370(3)	7811(2)	423(2)	64(2)
C(15')	6729(9)	8097(4)	532(4)	47(2)
C(16')	6789(17)	7743(8)	391(8)	117(7)
C(17)	6197(2)	7315(1)	439(1)	63(1)
C(18)	5384(2)	7072(1)	239(1)	56(1)
C(19)	4837(2)	7228(1)	-49(1)	71(1)
C(20)	4060(3)	6983(2)	-248(1)	83(1)
C(21)	3771(2)	6559(2)	-194(1)	79(1)
C(22)	4245(2)	6398(1)	75(1)	63(1)
C(23)	5059(2)	6648(1)	308(1)	50(1)
C(24)	5536(2)	6490(1)	605(1)	46(1)
C(25)	6374(2)	6716(1)	786(1)	46(1)
C(26)	6887(2)	6556(1)	1077(1)	56(1)
C(27)	7704(2)	6767(1)	1242(1)	70(1)
C(28)	8054(2)	7160(2)	1139(1)	84(1)
C(29)	7581(2)	7334(2)	884(1)	83(1)
C(30)	6726(2)	7124(1)	695(1)	58(1)
C(31)	5162(2)	6084(1)	721(1)	57(1)
C(32)	4421(2)	6092(1)	937(1)	62(1)

C(33)	3826(2)	6507(1)	1113(1)	60(1)
C(34)	4123(2)	7012(1)	1330(1)	51(1)
C(35)	3545(2)	7388(1)	1471(1)	52(1)
C(36)	2653(2)	7283(1)	1406(1)	54(1)
C(37)	2355(2)	6774(1)	1187(2)	93(1)
C(38)	2929(2)	6400(1)	1052(2)	98(1)
C(39)	2072(2)	7700(1)	1563(1)	54(1)
C(40)	1211(2)	7675(1)	1520(1)	52(1)
C(41)	678(2)	8119(1)	1704(1)	46(1)
C(42)	158(2)	8219(1)	1381(1)	48(1)
C(43)	128(2)	7895(1)	877(1)	60(1)
C(44)	-328(2)	8005(1)	562(1)	71(1)
C(45)	-796(2)	8443(1)	724(1)	68(1)
C(46)	-796(2)	8760(1)	1200(1)	56(1)
C(47)	-316(2)	8667(1)	1548(1)	46(1)
C(48)	-312(2)	8996(1)	2041(1)	42(1)
C(49)	157(2)	8877(1)	2367(1)	42(1)
C(50)	140(2)	9181(1)	2875(1)	50(1)

Atomic coordinates ($\times 10^4$) and equivalent isotropic displacement parameters ($\text{\AA}^2 \times 10^3$).
 $U(\text{eq})$ is defined as one third of the trace of the orthogonalized U_{ij} tensor.

	x	y	z	$U(\text{eq})$
C(51)	652(2)	9097(1)	3187(1)	58(1)
C(52)	1203(2)	8693(1)	3020(1)	59(1)
C(53)	1209(2)	8378(1)	2547(1)	52(1)
C(54)	688(2)	8449(1)	2198(1)	43(1)
C(55)	-818(2)	9457(1)	2215(1)	46(1)
C(56)	-612(2)	9882(1)	2179(1)	43(1)
C(57)	194(2)	10007(1)	1984(1)	39(1)
C(58)	1004(2)	10097(1)	2239(1)	39(1)
C(59)	1070(2)	10111(1)	2702(1)	48(1)
C(60)	1852(2)	10198(1)	2946(1)	57(1)
C(61)	2623(2)	10282(1)	2745(1)	57(1)
C(62)	2591(2)	10290(1)	2312(1)	50(1)
C(63)	1788(2)	10206(1)	2043(1)	41(1)
C(64)	1741(2)	10240(1)	1606(1)	41(1)
C(65)	924(2)	10194(1)	1374(1)	40(1)
C(66)	833(2)	10275(1)	954(1)	49(1)
C(67)	40(2)	10249(1)	743(1)	56(1)
C(68)	-718(2)	10122(1)	922(1)	56(1)
C(69)	-669(2)	10033(1)	1316(1)	48(1)
C(70)	146(2)	10073(1)	1562(1)	41(1)
C(71)	2550(2)	10335(1)	1396(1)	50(1)
C(72)	3120(2)	10008(1)	1189(1)	49(1)
C(73)	3945(2)	10073(1)	981(1)	43(1)
C(74)	4323(2)	10543(1)	1055(1)	46(1)
C(75)	5095(2)	10581(1)	846(1)	44(1)
C(76)	5523(2)	10155(1)	561(1)	39(1)
C(77)	5135(2)	9683(1)	480(1)	43(1)
C(78)	4368(2)	9645(1)	689(1)	46(1)
C(79)	6352(2)	10218(1)	359(1)	42(1)

C(80)	7019(2)	9920(1)	238(1)	43(1)
C(1A)	10522(1)	2850(1)	3598(1)	33(1)
C(2A)	10453(1)	2833(1)	4045(1)	34(1)
C(3A)	10343(1)	3272(1)	4479(1)	39(1)
C(4A)	10280(2)	3252(1)	4906(1)	45(1)
C(5A)	10326(2)	2785(1)	4926(1)	48(1)
C(6A)	10436(2)	2357(1)	4525(1)	45(1)
C(7A)	10499(1)	2355(1)	4064(1)	37(1)
C(8A)	10627(1)	1911(1)	3646(1)	39(1)
C(9A)	10790(1)	1939(1)	3212(1)	37(1)
C(10A)	10975(2)	1507(1)	2789(1)	46(1)
C(11A)	11100(2)	1536(1)	2369(1)	51(1)
C(12A)	11029(2)	1997(1)	2345(1)	49(1)
C(13A)	10840(2)	2419(1)	2738(1)	41(1)
C(14A)	10726(1)	2416(1)	3191(1)	35(1)
C(15A)	10547(2)	1408(1)	3643(1)	44(1)
C(16A)	9832(2)	1251(1)	3781(1)	47(1)
C(17A)	9599(2)	762(1)	3792(1)	41(1)
C(18A)	8802(2)	502(1)	3562(1)	40(1)
C(19A)	8302(2)	660(1)	3261(1)	48(1)
C(20A)	7552(2)	403(1)	3027(1)	56(1)
C(21A)	7251(2)	-38(1)	3062(1)	55(1)
C(22A)	7692(2)	-198(1)	3346(1)	47(1)
C(23A)	8472(2)	66(1)	3612(1)	39(1)

Atomic coordinates ($\times 10^4$) and equivalent isotropic displacement parameters ($\text{\AA}^2 \times 10^3$).
 $U(\text{eq})$ is defined as one third of the trace of the orthogonalized U_{ij} tensor.

	x	y	z	U(eq)
C(24A)	8928(2)	-89(1)	3918(1)	38(1)
C(25A)	9747(2)	153(1)	4130(1)	39(1)
C(26A)	10241(2)	-3(1)	4428(1)	46(1)
C(27A)	11036(2)	221(1)	4625(1)	54(1)
C(28A)	11391(2)	630(1)	4549(1)	56(1)
C(29A)	10934(2)	803(1)	4278(1)	49(1)
C(30A)	10102(2)	577(1)	4059(1)	41(1)
C(31A)	8555(2)	-511(1)	4010(1)	46(1)
C(32A)	7776(2)	-540(1)	4184(1)	46(1)
C(33A)	7131(2)	-153(1)	4336(1)	43(1)
C(34A)	7382(2)	361(1)	4582(1)	48(1)
C(35A)	6768(2)	718(1)	4713(1)	52(1)
C(36A)	5883(2)	586(1)	4604(1)	48(1)
C(37A)	5628(2)	73(1)	4358(1)	56(1)
C(38A)	6242(2)	-286(1)	4230(1)	54(1)
C(39A)	5267(2)	989(1)	4761(1)	54(1)
C(40A)	4428(2)	957(1)	4678(1)	51(1)
C(41A)	3886(2)	1398(1)	4870(1)	44(1)
C(42A)	3481(2)	1565(1)	4562(1)	43(1)
C(43A)	3529(2)	1297(1)	4050(1)	53(1)
C(44A)	3168(2)	1469(1)	3758(1)	58(1)
C(45A)	2717(2)	1913(1)	3944(1)	55(1)
C(46A)	2643(2)	2177(1)	4424(1)	45(1)

C(47A)	3026(1)	2019(1)	4753(1)	40(1)
C(48A)	2958(1)	2296(1)	5254(1)	37(1)
C(49A)	3307(2)	2107(1)	5560(1)	39(1)
C(50A)	3206(2)	2355(1)	6065(1)	44(1)
C(51A)	3553(2)	2179(1)	6362(1)	53(1)
C(52A)	4030(2)	1743(1)	6175(1)	59(1)
C(53A)	4144(2)	1496(1)	5698(1)	53(1)
C(54A)	3788(2)	1661(1)	5369(1)	42(1)
C(55A)	2488(2)	2769(1)	5452(1)	39(1)
C(56A)	2714(1)	3204(1)	5441(1)	37(1)
C(57A)	3528(1)	3333(1)	5253(1)	34(1)
C(58A)	4344(1)	3374(1)	5486(1)	33(1)
C(59A)	4415(2)	3314(1)	5918(1)	40(1)
C(60A)	5199(2)	3369(1)	6150(1)	45(1)
C(61A)	5968(2)	3489(1)	5970(1)	45(1)
C(62A)	5931(2)	3554(1)	5564(1)	41(1)
C(63A)	5126(1)	3498(1)	5305(1)	35(1)
C(64A)	5081(1)	3582(1)	4889(1)	34(1)
C(65A)	4260(1)	3576(1)	4677(1)	35(1)
C(66A)	4173(2)	3691(1)	4276(1)	44(1)
C(67A)	3380(2)	3693(1)	4079(1)	51(1)
C(68A)	2618(2)	3571(1)	4258(1)	49(1)
C(69A)	2663(2)	3451(1)	4632(1)	42(1)
C(70A)	3481(1)	3453(1)	4860(1)	36(1)
C(71A)	5886(2)	3683(1)	4681(1)	39(1)
C(72A)	6504(2)	3363(1)	4510(1)	40(1)
C(73A)	7318(1)	3436(1)	4299(1)	36(1)
C(74A)	7668(2)	3908(1)	4363(1)	39(1)
C(75A)	8433(1)	3953(1)	4153(1)	37(1)
C(76A)	8887(1)	3533(1)	3877(1)	33(1)

Atomic coordinates ($\times 10^4$) and equivalent isotropic displacement parameters ($\text{\AA}^2 \times 10^3$).
U(eq) is defined as one third of the trace of the orthogonalized U_{ij} tensor.

	x	y	z	U(eq)
C(77A)	8526(1)	3057(1)	3805(1)	38(1)
C(78A)	7763(1)	3014(1)	4019(1)	38(1)
C(79A)	9710(1)	3609(1)	3677(1)	36(1)
C(80A)	10395(1)	3324(1)	3557(1)	36(1)
C(1B)	6364(1)	3889(1)	2965(1)	35(1)
C(2B)	6427(1)	3877(1)	2505(1)	36(1)
C(3B)	6498(2)	3415(1)	2084(1)	41(1)
C(4B)	6568(2)	3406(1)	1646(1)	48(1)
C(5B)	6593(2)	3860(1)	1602(1)	51(1)
C(6B)	6532(2)	4307(1)	1988(1)	46(1)
C(7B)	6426(1)	4341(1)	2458(1)	37(1)
C(8B)	6325(1)	4804(1)	2863(1)	37(1)
C(9B)	6125(1)	4802(1)	3308(1)	35(1)
C(10B)	5859(2)	5236(1)	3707(1)	38(1)
C(11B)	5708(2)	5232(1)	4134(1)	43(1)
C(12B)	5820(2)	4789(1)	4194(1)	45(1)
C(13B)	6045(2)	4362(1)	3821(1)	41(1)

C(14B)	6178(1)	4341(1)	3357(1)	34(1)
C(15B)	6462(2)	5277(1)	2815(1)	41(1)
C(16B)	6871(2)	5705(1)	3132(1)	42(1)
C(17B)	7135(2)	6147(1)	3048(1)	38(1)
C(18B)	7976(2)	6388(1)	3218(1)	39(1)
C(19B)	8554(2)	6239(1)	3498(1)	43(1)
C(20B)	9337(2)	6497(1)	3684(1)	50(1)
C(21B)	9602(2)	6916(1)	3606(1)	54(1)
C(22B)	9107(2)	7052(1)	3323(1)	48(1)
C(23B)	8291(2)	6790(1)	3110(1)	40(1)
C(24B)	7794(2)	6914(1)	2792(1)	41(1)
C(25B)	6950(2)	6687(1)	2634(1)	40(1)
C(26B)	6422(2)	6810(1)	2321(1)	47(1)
C(27B)	5590(2)	6612(1)	2190(1)	56(1)
C(28B)	5217(2)	6281(1)	2367(1)	53(1)
C(29B)	5702(2)	6141(1)	2654(1)	46(1)
C(30B)	6597(2)	6318(1)	2782(1)	39(1)
C(31B)	8152(2)	7294(1)	2636(1)	47(1)
C(32B)	8878(2)	7277(1)	2409(1)	48(1)
C(33B)	9492(2)	6874(1)	2241(1)	44(1)
C(34B)	9232(2)	6365(1)	2095(1)	53(1)
C(35B)	9820(2)	5996(1)	1951(1)	57(1)
C(36B)	10696(2)	6111(1)	1952(1)	53(1)
C(37B)	10968(2)	6607(1)	2087(1)	70(1)
C(38B)	10369(2)	6986(1)	2224(1)	66(1)
C(39B)	11302(2)	5697(1)	1799(1)	58(1)
C(40B)	12149(2)	5734(1)	1841(1)	54(1)
C(41B)	12707(2)	5304(1)	1663(1)	44(1)
C(42B)	13206(2)	5203(1)	1992(1)	43(1)
C(43B)	13184(2)	5510(1)	2497(1)	55(1)
C(44B)	13641(2)	5402(1)	2815(1)	61(1)
C(45B)	14165(2)	4989(1)	2654(1)	58(1)
C(46B)	14214(2)	4685(1)	2176(1)	49(1)
C(47B)	13735(2)	4778(1)	1827(1)	41(1)
C(48B)	13789(2)	4468(1)	1332(1)	40(1)
C(49B)	13343(2)	4593(1)	1004(1)	45(1)

Atomic coordinates ($\times 10^4$) and equivalent isotropic displacement parameters ($\text{\AA}^2 \times 10^3$).

$U(\text{eq})$ is defined as one third of the trace of the orthogonalized U_{ij} tensor.

	x	y	z	$U(\text{eq})$
C(50B)	13435(2)	4319(1)	499(1)	59(1)
C(51B)	12974(3)	4421(1)	184(1)	81(1)
C(52B)	12375(3)	4800(1)	347(1)	89(1)
C(53B)	12278(2)	5077(1)	817(1)	63(1)
C(54B)	12768(2)	4999(1)	1169(1)	46(1)
C(55B)	14329(2)	4022(1)	1158(1)	44(1)
C(56B)	14138(2)	3586(1)	1176(1)	42(1)
C(57B)	13320(1)	3444(1)	1353(1)	37(1)
C(58B)	12520(2)	3357(1)	1093(1)	40(1)
C(59B)	12461(2)	3363(1)	636(1)	52(1)
C(60B)	11690(2)	3274(1)	387(1)	64(1)

C(61B)	10911(2)	3172(1)	576(1)	66(1)
C(62B)	10932(2)	3151(1)	1000(1)	55(1)
C(63B)	11730(2)	3237(1)	1276(1)	42(1)
C(64B)	11765(2)	3191(1)	1708(1)	41(1)
C(65B)	12569(2)	3236(1)	1947(1)	39(1)
C(66B)	12649(2)	3148(1)	2361(1)	51(1)
C(67B)	13434(2)	3176(1)	2582(1)	61(1)
C(68B)	14199(2)	3306(1)	2407(1)	62(1)
C(69B)	14162(2)	3406(1)	2023(1)	49(1)
C(70B)	13359(2)	3366(1)	1769(1)	38(1)
C(71B)	10946(2)	3077(1)	1901(1)	52(1)
C(72B)	10389(2)	3399(1)	2132(1)	46(1)
C(73B)	9560(2)	3321(1)	2326(1)	40(1)
C(74B)	9190(2)	2844(1)	2238(1)	41(1)
C(75B)	8417(2)	2793(1)	2438(1)	41(1)
C(76B)	7972(1)	3213(1)	2726(1)	35(1)
C(77B)	8344(2)	3691(1)	2816(1)	40(1)
C(78B)	9119(2)	3739(1)	2617(1)	42(1)
C(79B)	7146(2)	3138(1)	2925(1)	39(1)
C(80B)	6463(2)	3425(1)	3032(1)	38(1)
C(1D)	1721(3)	4638(1)	5434(1)	76(1)
C(2D)	1824(2)	4777(1)	5908(1)	73(1)
C(3D)	1120(2)	4884(1)	6187(1)	72(1)
C(4D)	304(2)	4844(1)	5981(2)	83(1)
C(5D)	211(3)	4704(1)	5501(2)	91(1)
C(6D)	918(3)	4605(1)	5229(1)	87(1)
C(1E)	1676(2)	6687(1)	4507(1)	77(1)
C(2E)	1707(2)	6174(2)	4348(2)	83(1)
C(3E)	1723(2)	5868(1)	3863(2)	88(1)
C(4E)	1708(2)	6071(2)	3547(1)	82(1)
C(5E)	1680(2)	6585(1)	3707(1)	76(1)
C(6E)	1663(2)	6889(1)	4183(1)	75(1)
C(1F)	8406(2)	3156(2)	300(1)	85(1)
C(2F)	8457(2)	2643(2)	145(2)	95(1)
C(3F)	8540(3)	2449(2)	468(2)	99(1)
C(4F)	8571(2)	2760(2)	946(2)	89(1)
C(5F)	8525(2)	3270(2)	1101(1)	82(1)
C(6F)	8444(2)	3468(2)	779(2)	86(1)
C(1G)	8549(2)	1150(1)	593(1)	79(1)
C(2G)	9143(3)	1462(1)	944(1)	85(1)
C(3G)	9951(3)	1574(2)	823(1)	91(1)
C(4G)	10162(2)	1377(2)	353(1)	86(1)

**Atomic coordinates ($\times 10^4$) and equivalent isotropic displacement parameters ($\text{\AA}^2 \times 10^3$).
 $U(\text{eq})$ is defined as one third of the trace of the orthogonalized U_{ij} tensor.**

	x	y	z	$U(\text{eq})$
C(5G)	9565(2)	1071(1)	1(1)	80(1)
C(6G)	8753(2)	955(1)	124(1)	78(1)
C(1H)	2851(3)	7493(2)	2770(2)	99(1)
C(2H)	3675(3)	7362(2)	2756(2)	91(1)
C(3H)	4100(3)	7396(1)	3163(1)	88(1)

C(4H)	3696(3)	7556(2)	3585(2)	94(1)
C(5H)	2831(3)	7679(2)	3596(2)	111(2)
C(6H)	2414(3)	7634(2)	3177(2)	105(1)
C(1I)	6177(2)	1177(1)	6445(2)	86(1)
C(2I)	6438(2)	920(1)	5991(1)	82(1)
C(3I)	6838(2)	478(1)	5863(1)	81(1)
C(4I)	6981(2)	301(1)	6196(1)	81(1)
C(5I)	6722(3)	564(2)	6653(2)	89(1)
C(6I)	6322(3)	1000(2)	6776(2)	95(1)
C(1J)	-701(4)	4658(2)	1928(2)	122(2)
C(2J)	-657(4)	4990(2)	2398(2)	118(2)
C(3J)	128(4)	5094(2)	2643(2)	124(2)
C(4J)	864(4)	4879(2)	2436(2)	120(2)
C(5J)	814(4)	4544(2)	1943(2)	130(2)
C(6J)	9(4)	4441(2)	1697(2)	115(2)
C(1K)	4203(3)	1820(2)	7826(2)	118(2)
C(2K)	3552(4)	1823(2)	8115(2)	135(2)
C(3K)	2721(4)	1678(2)	7942(2)	118(2)
C(4K)	2533(3)	1528(1)	7466(1)	85(1)
C(5K)	3170(3)	1527(1)	7175(1)	83(1)
C(6K)	4001(3)	1672(2)	7352(1)	106(1)
C(1L)	6439(3)	1757(2)	636(2)	91(1)
C(2L)	5633(3)	1725(1)	434(1)	85(1)
C(3L)	4948(2)	1879(2)	713(2)	94(1)
C(4L)	5062(3)	2059(2)	1198(2)	100(1)
C(5L)	5866(4)	2077(1)	1396(2)	101(1)
C(6L)	6550(3)	1928(2)	1115(2)	100(1)
C(1M)	8983(3)	1496(2)	5425(1)	94(1)
C(2M)	9142(3)	1459(2)	5842(2)	95(1)
C(3M)	9959(3)	1564(2)	6051(1)	89(1)
C(4M)	10627(3)	1693(1)	5834(1)	84(1)
C(5M)	10461(3)	1735(1)	5415(1)	88(1)
C(6M)	9647(3)	1642(2)	5218(1)	98(1)
C(1N)	4944(2)	7(2)	2190(2)	108(2)
C(2N)	4963(2)	520(2)	2341(2)	107(1)
C(3N)	5030(3)	841(2)	2824(2)	114(2)
C(4N)	5093(2)	649(2)	3144(2)	108(2)
C(5N)	5075(2)	141(2)	3001(2)	106(1)
C(6N)	5001(3)	-183(2)	2521(2)	111(2)
C(1O)	3125(5)	8945(2)	1693(2)	112(2)
C(2O)	2295(4)	8922(2)	1470(3)	135(2)
C(3O)	2254(4)	8622(2)	952(3)	131(2)
C(4O)	2984(5)	8394(2)	748(2)	131(2)
C(5O)	3703(4)	8433(2)	986(2)	140(2)
C(6O)	3778(4)	8707(2)	1442(2)	120(2)
C(1P)	8547(3)	1323(1)	2123(2)	88(1)
C(2P)	8587(2)	1537(1)	2607(2)	81(1)
C(3P)	7848(3)	1662(1)	2851(1)	77(1)

Atomic coordinates ($\times 10^4$) and equivalent isotropic displacement parameters ($\text{\AA}^2 \times 10^3$).

U(eq) is defined as one third of the trace of the orthogonalized U_{ij} tensor.

	x	y	z	U(eq)
C(4P)	7065(2)	1569(2)	2610(2)	93(1)
C(5P)	7032(3)	1358(2)	2121(2)	109(2)
C(6P)	7772(4)	1236(2)	1883(1)	105(2)
C(1Q)	3371(2)	2044(2)	2897(1)	87(1)
C(2Q)	3953(2)	2357(1)	3256(1)	81(1)
C(3Q)	4793(2)	2436(1)	3147(2)	86(1)
C(4Q)	5031(2)	2204(2)	2679(2)	91(1)
C(5Q)	4452(3)	1889(2)	2325(2)	101(1)
C(6Q)	3627(3)	1809(2)	2439(1)	100(1)
C(1R)	2015(2)	4365(1)	3454(1)	71(1)
C(2R)	1803(2)	4548(1)	3923(1)	70(1)
C(3R)	2383(2)	4867(1)	4279(1)	75(1)
C(4R)	3184(2)	5002(1)	4164(1)	83(1)
C(5R)	3402(2)	4817(2)	3697(1)	84(1)
C(6R)	2818(2)	4498(1)	3338(1)	76(1)
C(1S)	6730(5)	4897(3)	564(2)	87(2)
C(2S)	5961(4)	4929(2)	802(3)	75(1)
C(3S)	6027(5)	5185(2)	1309(3)	79(2)
C(4S)	6834(6)	5370(3)	1539(2)	76(2)
C(5S)	7552(4)	5317(2)	1283(2)	85(2)
C(6S)	7495(4)	5087(3)	794(2)	90(2)
C(1S1)	6395(15)	4920(8)	644(6)	79(6)
C(2S1)	5997(10)	5117(8)	1063(8)	73(5)
C(3S1)	6480(13)	5307(10)	1488(7)	78(7)
C(4S1)	7357(11)	5240(6)	1501(6)	91(5)
C(5S1)	7731(10)	4983(8)	1078(7)	116(6)
C(6S1)	7245(14)	4808(9)	664(7)	134(9)
C(1T)	4187(10)	-2209(8)	5310(4)	86(4)
C(2T)	4233(8)	-1915(6)	5793(4)	92(4)
C(3T)	3526(7)	-1667(5)	6022(4)	83(4)
C(4T)	2764(8)	-1732(5)	5747(3)	91(3)
C(5T)	2714(8)	-2047(4)	5255(3)	78(3)
C(6T)	3436(10)	-2277(7)	5045(5)	80(5)
C(1T1)	3408(11)	-2144(8)	5092(5)	89(5)
C(2T1)	2933(8)	-1906(5)	5481(6)	103(4)
C(3T1)	3296(11)	-1797(6)	5924(5)	105(5)
C(4T1)	4126(11)	-1912(6)	5970(4)	95(4)
C(5T1)	4586(6)	-2168(4)	5574(4)	80(3)
C(6T1)	4236(10)	-2271(8)	5131(4)	72(3)
C(1U)	166(6)	5667(4)	619(3)	82(2)
C(2U)	-131(15)	6137(7)	748(6)	98(7)
C(5U)	236(7)	5560(4)	-183(3)	86(3)
C(3U)	-251(7)	6312(3)	412(4)	96(3)
C(4U)	-136(11)	6010(6)	-63(5)	83(5)
C(6U)	359(5)	5385(3)	155(3)	84(2)
C(1U1)	536(6)	5931(4)	653(3)	85(2)
C(2U1)	-309(11)	6061(6)	681(5)	77(5)
C(3U1)	-736(6)	6036(4)	281(3)	84(2)
C(4U1)	-356(12)	5873(8)	-149(6)	118(9)
C(5U1)	514(9)	5788(5)	-158(5)	109(5)

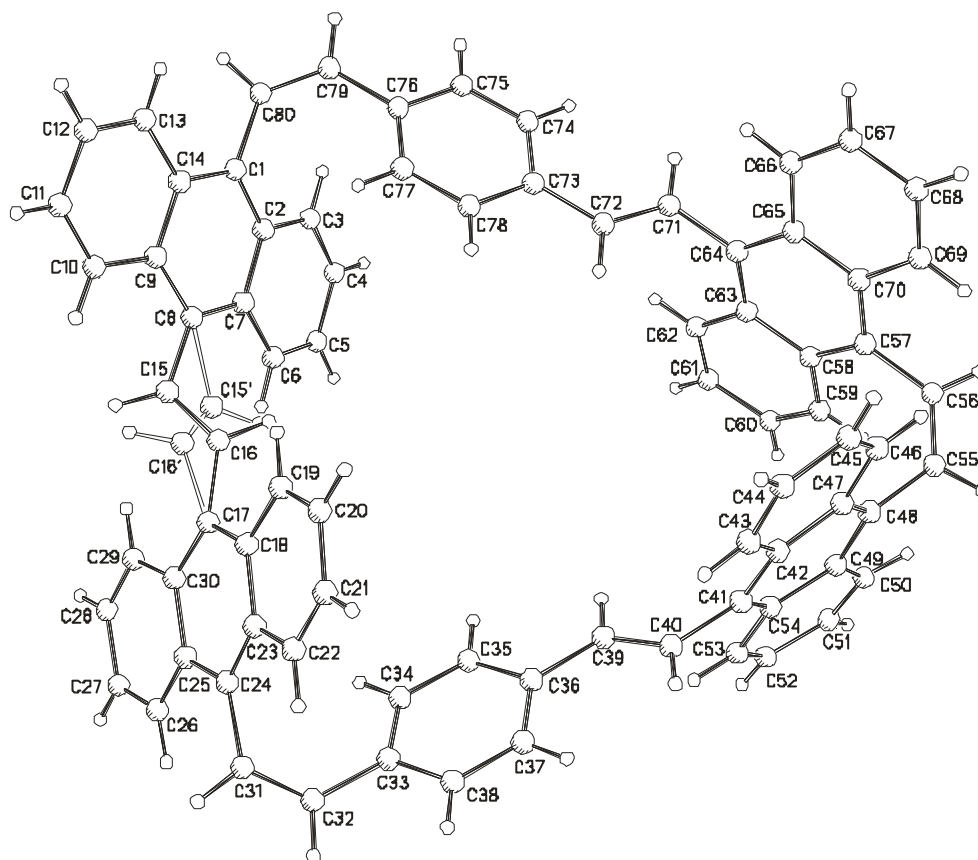
C(6U1)

960(5)

5801(3)

238(3)

90(2)


Bond lengths [Å] and angles [°].

C(1)-C(14)	1.408(4)	C(18)-C(19)	1.448(4)
C(1)-C(2)	1.415(4)	C(19)-C(20)	1.351(5)
C(1)-C(80)	1.483(3)	C(20)-C(21)	1.383(5)
C(2)-C(3)	1.428(4)	C(21)-C(22)	1.349(4)
C(2)-C(7)	1.438(4)	C(22)-C(23)	1.427(4)
C(3)-C(4)	1.351(4)	C(23)-C(24)	1.415(4)
C(4)-C(5)	1.413(5)	C(24)-C(25)	1.406(4)
C(5)-C(6)	1.354(6)	C(24)-C(31)	1.484(4)
C(6)-C(7)	1.430(5)	C(25)-C(26)	1.431(4)
C(7)-C(8)	1.418(5)	C(25)-C(30)	1.436(4)
C(8)-C(9)	1.410(5)	C(26)-C(27)	1.358(4)
C(8)-C(15)	1.465(5)	C(27)-C(28)	1.413(5)
C(8)-C(15')	1.657(14)	C(28)-C(29)	1.341(5)
C(9)-C(14)	1.437(4)	C(29)-C(30)	1.422(4)
C(9)-C(10)	1.442(5)	C(31)-C(32)	1.329(4)
C(10)-C(11)	1.349(5)	C(32)-C(33)	1.477(4)
C(11)-C(12)	1.383(5)	C(33)-C(34)	1.384(4)
C(12)-C(13)	1.351(4)	C(33)-C(38)	1.389(5)
C(13)-C(14)	1.427(4)	C(34)-C(35)	1.380(4)
C(15)-C(16)	1.336(7)	C(35)-C(36)	1.381(4)
C(16)-C(17)	1.496(6)	C(36)-C(37)	1.396(4)

C(15')-C(16')	0.95(2)	C(36)-C(39)	1.467(4)
C(16')-C(17)	1.58(3)	C(37)-C(38)	1.371(5)
C(17)-C(18)	1.397(4)	C(39)-C(40)	1.325(4)
C(17)-C(30)	1.423(4)	C(40)-C(41)	1.480(4)
C(18)-C(23)	1.425(4)	C(41)-C(42)	1.411(4)

Bond lengths [\AA] and angles [$^\circ$].

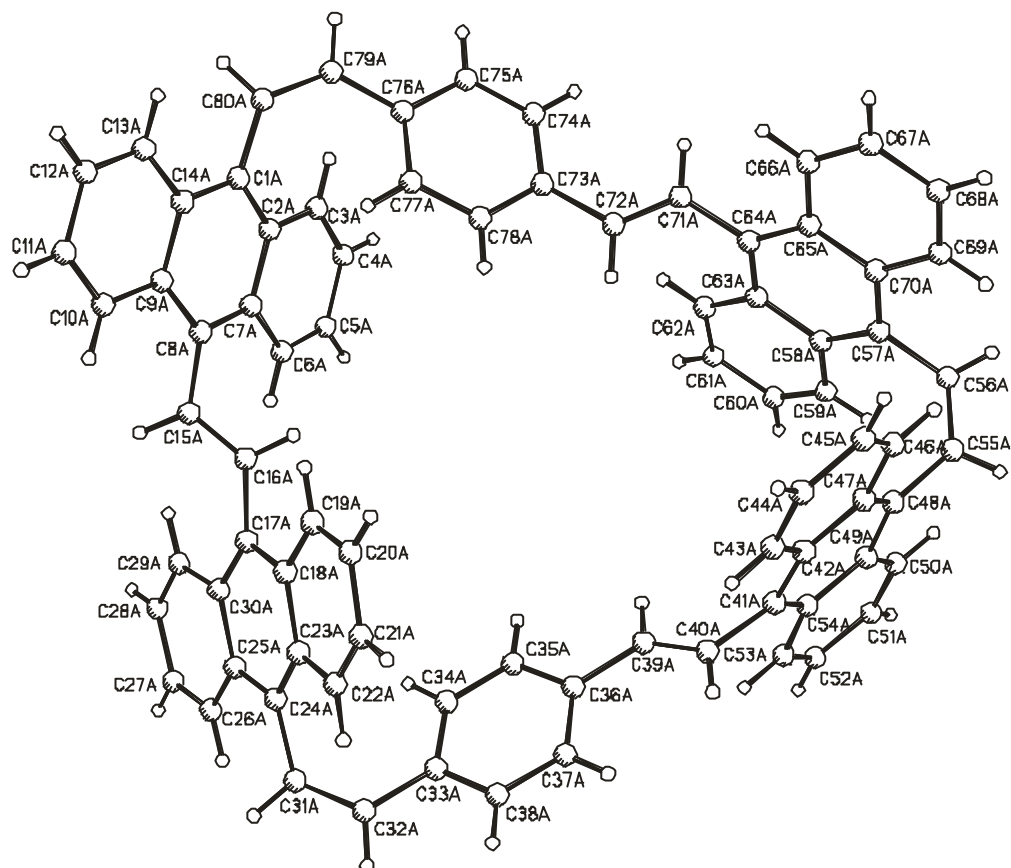
C(41)-C(54)	1.413(4)	C(60)-C(61)	1.412(4)
C(42)-C(43)	1.430(4)	C(61)-C(62)	1.356(4)
C(42)-C(47)	1.433(4)	C(62)-C(63)	1.426(3)
C(43)-C(44)	1.354(4)	C(63)-C(64)	1.408(3)
C(44)-C(45)	1.408(5)	C(64)-C(65)	1.406(3)
C(45)-C(46)	1.358(4)	C(64)-C(71)	1.487(4)
C(46)-C(47)	1.431(4)	C(65)-C(66)	1.433(3)
C(47)-C(48)	1.408(4)	C(65)-C(70)	1.438(3)
C(48)-C(49)	1.410(3)	C(66)-C(67)	1.357(4)
C(48)-C(55)	1.493(4)	C(67)-C(68)	1.404(4)
C(49)-C(50)	1.435(4)	C(68)-C(69)	1.363(4)
C(49)-C(54)	1.442(3)	C(69)-C(70)	1.428(3)
C(50)-C(51)	1.354(4)	C(71)-C(72)	1.294(4)
C(51)-C(52)	1.409(4)	C(72)-C(73)	1.475(3)
C(52)-C(53)	1.352(4)	C(73)-C(78)	1.393(4)
C(53)-C(54)	1.429(4)	C(73)-C(74)	1.394(3)
C(55)-C(56)	1.330(4)	C(74)-C(75)	1.388(4)
C(56)-C(57)	1.488(3)	C(75)-C(76)	1.387(3)
C(57)-C(70)	1.410(3)	C(76)-C(77)	1.399(3)
C(57)-C(58)	1.412(3)	C(76)-C(79)	1.471(3)
C(58)-C(59)	1.425(3)	C(77)-C(78)	1.381(3)
C(58)-C(63)	1.443(3)	C(79)-C(80)	1.337(3)
C(59)-C(60)	1.360(4)		
C(14)-C(1)-C(2)	119.9(2)	C(15)-C(16)-C(17)	129.3(5)
C(14)-C(1)-C(80)	119.3(2)	C(16')-C(15')-C(8)	128(2)
C(2)-C(1)-C(80)	120.9(2)	C(15')-C(16')-C(17)	129(3)
C(1)-C(2)-C(3)	121.8(2)	C(18)-C(17)-C(30)	119.9(2)
C(1)-C(2)-C(7)	119.1(3)	C(18)-C(17)-C(16)	114.2(3)
C(3)-C(2)-C(7)	119.1(2)	C(30)-C(17)-C(16)	125.2(3)
C(4)-C(3)-C(2)	121.7(3)	C(18)-C(17)-C(16')	133.7(8)
C(3)-C(4)-C(5)	119.6(3)	C(30)-C(17)-C(16')	105.6(8)
C(6)-C(5)-C(4)	120.9(3)	C(16)-C(17)-C(16')	25.4(8)
C(5)-C(6)-C(7)	122.0(3)	C(17)-C(18)-C(23)	120.5(2)
C(8)-C(7)-C(6)	122.8(3)	C(17)-C(18)-C(19)	122.7(3)
C(8)-C(7)-C(2)	120.4(3)	C(23)-C(18)-C(19)	116.8(3)
C(6)-C(7)-C(2)	116.8(3)	C(20)-C(19)-C(18)	122.0(3)
C(9)-C(8)-C(7)	120.1(3)	C(19)-C(20)-C(21)	120.4(3)
C(9)-C(8)-C(15)	112.8(3)	C(22)-C(21)-C(20)	120.5(4)
C(7)-C(8)-C(15)	127.1(3)	C(21)-C(22)-C(23)	122.1(3)
C(9)-C(8)-C(15')	137.5(5)	C(24)-C(23)-C(18)	120.0(3)
C(7)-C(8)-C(15')	99.9(5)	C(24)-C(23)-C(22)	121.8(3)
C(15)-C(8)-C(15')	31.0(4)	C(18)-C(23)-C(22)	118.2(3)
C(8)-C(9)-C(14)	118.9(3)	C(25)-C(24)-C(23)	119.4(2)
C(8)-C(9)-C(10)	123.5(3)	C(25)-C(24)-C(31)	120.1(2)

C(14)-C(9)-C(10)	117.6(3)	C(23)-C(24)-C(31)	120.5(3)
C(11)-C(10)-C(9)	122.3(3)	C(24)-C(25)-C(26)	121.0(2)
C(10)-C(11)-C(12)	119.4(3)	C(24)-C(25)-C(30)	120.5(2)
C(13)-C(12)-C(11)	121.7(3)	C(26)-C(25)-C(30)	118.4(3)
C(12)-C(13)-C(14)	121.9(3)	C(27)-C(26)-C(25)	120.8(3)
C(1)-C(14)-C(13)	121.8(2)	C(26)-C(27)-C(28)	120.4(3)
C(1)-C(14)-C(9)	121.1(3)	C(29)-C(28)-C(27)	120.6(3)
C(13)-C(14)-C(9)	117.1(3)	C(28)-C(29)-C(30)	121.8(3)
C(16)-C(15)-C(8)	119.5(5)	C(29)-C(30)-C(17)	123.0(3)

Bond lengths [Å] and angles [°].

C(29)-C(30)-C(25)	117.9(3)	C(56)-C(55)-C(48)	126.8(2)
C(17)-C(30)-C(25)	119.0(3)	C(55)-C(56)-C(57)	127.1(2)
C(32)-C(31)-C(24)	126.1(2)	C(70)-C(57)-C(58)	119.3(2)
C(31)-C(32)-C(33)	126.5(2)	C(70)-C(57)-C(56)	120.3(2)
C(34)-C(33)-C(38)	117.1(3)	C(58)-C(57)-C(56)	120.3(2)
C(34)-C(33)-C(32)	122.6(3)	C(57)-C(58)-C(59)	121.6(2)
C(38)-C(33)-C(32)	120.3(3)	C(57)-C(58)-C(63)	120.2(2)
C(35)-C(34)-C(33)	120.7(3)	C(59)-C(58)-C(63)	118.1(2)
C(34)-C(35)-C(36)	122.3(3)	C(60)-C(59)-C(58)	121.5(3)
C(35)-C(36)-C(37)	116.8(3)	C(59)-C(60)-C(61)	120.3(3)
C(35)-C(36)-C(39)	119.7(2)	C(62)-C(61)-C(60)	120.4(2)
C(37)-C(36)-C(39)	123.4(3)	C(61)-C(62)-C(63)	121.6(3)
C(38)-C(37)-C(36)	120.8(3)	C(64)-C(63)-C(62)	122.0(2)
C(37)-C(38)-C(33)	122.2(3)	C(64)-C(63)-C(58)	119.9(2)
C(40)-C(39)-C(36)	128.4(3)	C(62)-C(63)-C(58)	118.0(2)
C(39)-C(40)-C(41)	124.4(2)	C(65)-C(64)-C(63)	119.8(2)
C(42)-C(41)-C(54)	119.5(2)	C(65)-C(64)-C(71)	120.2(2)
C(42)-C(41)-C(40)	119.7(2)	C(63)-C(64)-C(71)	120.0(2)
C(54)-C(41)-C(40)	120.8(2)	C(64)-C(65)-C(66)	121.9(2)
C(41)-C(42)-C(43)	121.2(2)	C(64)-C(65)-C(70)	120.2(2)
C(41)-C(42)-C(47)	120.4(2)	C(66)-C(65)-C(70)	117.8(2)
C(43)-C(42)-C(47)	118.3(2)	C(67)-C(66)-C(65)	121.6(2)
C(44)-C(43)-C(42)	121.5(3)	C(66)-C(67)-C(68)	120.4(2)
C(43)-C(44)-C(45)	120.5(3)	C(69)-C(68)-C(67)	120.5(3)
C(46)-C(45)-C(44)	120.2(3)	C(68)-C(69)-C(70)	121.3(2)
C(45)-C(46)-C(47)	121.7(3)	C(57)-C(70)-C(69)	121.5(2)
C(48)-C(47)-C(46)	121.9(2)	C(57)-C(70)-C(65)	120.2(2)
C(48)-C(47)-C(42)	120.4(2)	C(69)-C(70)-C(65)	118.3(2)
C(46)-C(47)-C(42)	117.8(2)	C(72)-C(71)-C(64)	125.5(2)
C(47)-C(48)-C(49)	119.2(2)	C(71)-C(72)-C(73)	129.1(2)
C(47)-C(48)-C(55)	120.3(2)	C(78)-C(73)-C(74)	117.6(2)
C(49)-C(48)-C(55)	120.5(2)	C(78)-C(73)-C(72)	119.0(2)
C(48)-C(49)-C(50)	121.5(2)	C(74)-C(73)-C(72)	123.4(2)
C(48)-C(49)-C(54)	120.6(2)	C(75)-C(74)-C(73)	120.9(2)
C(50)-C(49)-C(54)	117.9(2)	C(76)-C(75)-C(74)	121.4(2)
C(51)-C(50)-C(49)	121.6(2)	C(75)-C(76)-C(77)	117.6(2)
C(50)-C(51)-C(52)	120.3(3)	C(75)-C(76)-C(79)	119.2(2)
C(53)-C(52)-C(51)	120.3(3)	C(77)-C(76)-C(79)	123.2(2)
C(52)-C(53)-C(54)	122.1(2)	C(78)-C(77)-C(76)	120.9(2)
C(41)-C(54)-C(53)	122.8(2)	C(77)-C(78)-C(73)	121.5(2)

C(41)-C(54)-C(49)	119.6(2)	C(80)-C(79)-C(76)	129.0(2)
C(53)-C(54)-C(49)	117.5(2)	C(79)-C(80)-C(1)	127.6(2)


Bond lengths [Å] and angles [°].

C(1A)-C(14A)	1.404(3)	C(21A)-C(22A)	1.358(4)
C(1A)-C(2A)	1.418(3)	C(22A)-C(23A)	1.425(4)
C(1A)-C(80A)	1.481(3)	C(23A)-C(24A)	1.415(3)
C(2A)-C(3A)	1.423(3)	C(24A)-C(25A)	1.411(3)
C(2A)-C(7A)	1.442(3)	C(24A)-C(31A)	1.483(3)
C(3A)-C(4A)	1.359(3)	C(25A)-C(26A)	1.428(3)
C(4A)-C(5A)	1.414(4)	C(25A)-C(30A)	1.442(3)
C(5A)-C(6A)	1.350(4)	C(26A)-C(27A)	1.356(4)
C(6A)-C(7A)	1.437(3)	C(27A)-C(28A)	1.413(4)
C(7A)-C(8A)	1.408(3)	C(28A)-C(29A)	1.360(4)
C(8A)-C(9A)	1.414(3)	C(29A)-C(30A)	1.423(4)
C(8A)-C(15A)	1.479(3)	C(31A)-C(32A)	1.338(4)
C(9A)-C(10A)	1.420(4)	C(32A)-C(33A)	1.474(3)
C(9A)-C(14A)	1.444(3)	C(33A)-C(34A)	1.392(4)
C(10A)-C(11A)	1.363(4)	C(33A)-C(38A)	1.395(4)
C(11A)-C(12A)	1.405(4)	C(34A)-C(35A)	1.381(4)
C(12A)-C(13A)	1.356(4)	C(35A)-C(36A)	1.389(4)
C(13A)-C(14A)	1.428(3)	C(36A)-C(37A)	1.392(4)
C(15A)-C(16A)	1.320(3)	C(36A)-C(39A)	1.475(4)
C(16A)-C(17A)	1.483(3)	C(37A)-C(38A)	1.387(4)
C(17A)-C(18A)	1.410(3)	C(39A)-C(40A)	1.300(4)
C(17A)-C(30A)	1.416(3)	C(40A)-C(41A)	1.482(4)

C(18A)-C(23A)	1.431(3)	C(41A)-C(42A)	1.405(4)
C(18A)-C(19A)	1.441(3)	C(41A)-C(54A)	1.411(3)
C(19A)-C(20A)	1.352(4)	C(42A)-C(47A)	1.432(3)
C(20A)-C(21A)	1.405(4)	C(42A)-C(43A)	1.439(4)

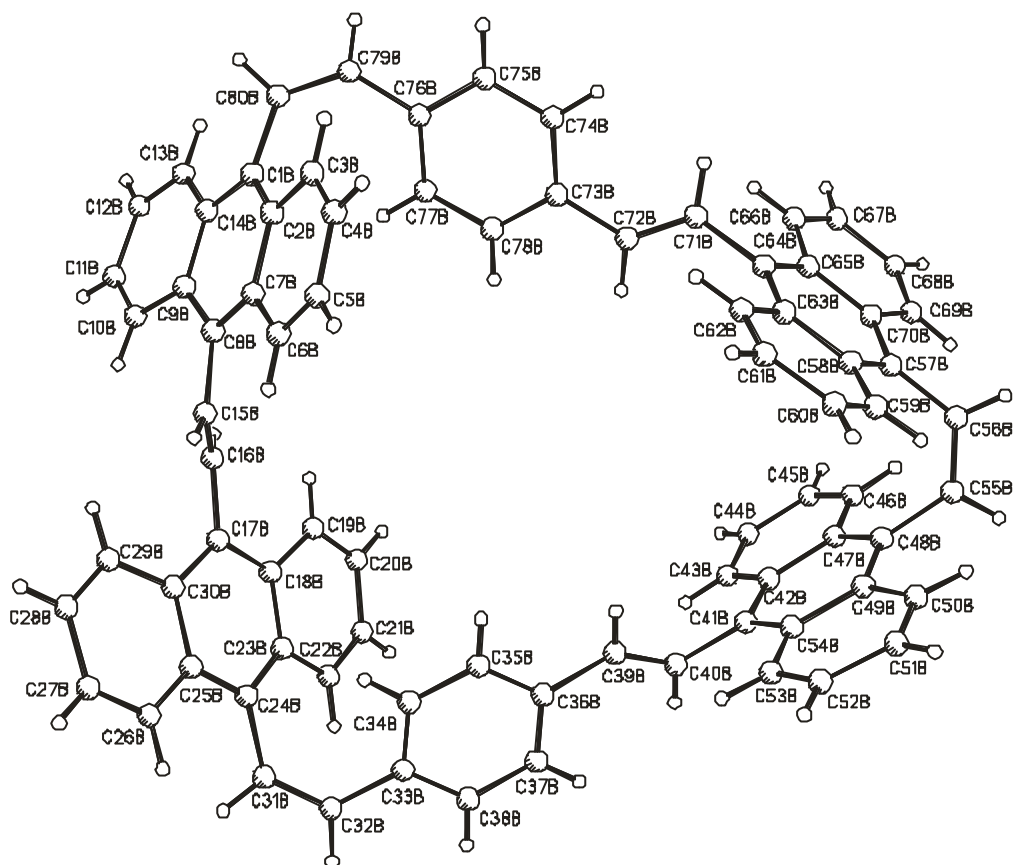
Bond lengths [Å] and angles [°].

C(43A)-C(44A)	1.345(4)	C(61A)-C(62A)	1.356(3)
C(44A)-C(45A)	1.405(4)	C(62A)-C(63A)	1.427(3)
C(45A)-C(46A)	1.356(4)	C(63A)-C(64A)	1.418(3)
C(46A)-C(47A)	1.427(3)	C(64A)-C(65A)	1.410(3)
C(47A)-C(48A)	1.415(3)	C(64A)-C(71A)	1.484(3)
C(48A)-C(49A)	1.410(3)	C(65A)-C(70A)	1.432(3)
C(48A)-C(55A)	1.488(3)	C(65A)-C(66A)	1.434(3)
C(49A)-C(50A)	1.428(3)	C(66A)-C(67A)	1.357(4)
C(49A)-C(54A)	1.436(3)	C(67A)-C(68A)	1.404(4)
C(50A)-C(51A)	1.356(4)	C(68A)-C(69A)	1.358(3)
C(51A)-C(52A)	1.410(4)	C(69A)-C(70A)	1.432(3)
C(52A)-C(53A)	1.355(4)	C(71A)-C(72A)	1.322(3)
C(53A)-C(54A)	1.424(4)	C(72A)-C(73A)	1.472(3)
C(55A)-C(56A)	1.326(3)	C(73A)-C(78A)	1.391(3)
C(56A)-C(57A)	1.493(3)	C(73A)-C(74A)	1.393(3)
C(57A)-C(58A)	1.410(3)	C(74A)-C(75A)	1.384(3)
C(57A)-C(70A)	1.416(3)	C(75A)-C(76A)	1.392(3)
C(58A)-C(59A)	1.433(3)	C(76A)-C(77A)	1.401(3)
C(58A)-C(63A)	1.436(3)	C(76A)-C(79A)	1.470(3)
C(59A)-C(60A)	1.358(3)	C(77A)-C(78A)	1.386(3)
C(60A)-C(61A)	1.413(4)	C(79A)-C(80A)	1.336(3)
		C(17A)-C(18A)-C(23A)	121.0(2)
C(14A)-C(1A)-C(2A)	119.88(19)	C(17A)-C(18A)-C(19A)	121.3(2)
C(14A)-C(1A)-C(80A)	119.54(19)	C(23A)-C(18A)-C(19A)	117.7(2)
C(2A)-C(1A)-C(80A)	120.6(2)	C(20A)-C(19A)-C(18A)	121.6(2)
C(1A)-C(2A)-C(3A)	122.6(2)	C(19A)-C(20A)-C(21A)	120.3(2)
C(1A)-C(2A)-C(7A)	119.1(2)	C(22A)-C(21A)-C(20A)	120.4(3)
C(3A)-C(2A)-C(7A)	118.3(2)	C(21A)-C(22A)-C(23A)	121.7(2)
C(4A)-C(3A)-C(2A)	122.1(2)	C(24A)-C(23A)-C(22A)	122.4(2)
C(3A)-C(4A)-C(5A)	119.7(2)	C(24A)-C(23A)-C(18A)	119.3(2)
C(6A)-C(5A)-C(4A)	120.6(2)	C(22A)-C(23A)-C(18A)	118.2(2)
C(5A)-C(6A)-C(7A)	122.0(2)	C(25A)-C(24A)-C(23A)	119.7(2)
C(8A)-C(7A)-C(6A)	122.1(2)	C(25A)-C(24A)-C(31A)	120.1(2)
C(8A)-C(7A)-C(2A)	120.6(2)	C(23A)-C(24A)-C(31A)	120.2(2)
C(6A)-C(7A)-C(2A)	117.2(2)	C(24A)-C(25A)-C(26A)	121.5(2)
C(7A)-C(8A)-C(9A)	119.9(2)	C(24A)-C(25A)-C(30A)	120.7(2)
C(7A)-C(8A)-C(15A)	121.3(2)	C(26A)-C(25A)-C(30A)	117.8(2)
C(9A)-C(8A)-C(15A)	118.7(2)	C(27A)-C(26A)-C(25A)	121.8(2)
C(8A)-C(9A)-C(10A)	122.0(2)	C(26A)-C(27A)-C(28A)	120.3(2)
C(8A)-C(9A)-C(14A)	119.2(2)	C(29A)-C(28A)-C(27A)	120.1(3)
C(10A)-C(9A)-C(14A)	118.8(2)	C(28A)-C(29A)-C(30A)	121.8(2)
C(11A)-C(10A)-C(9A)	121.4(2)	C(17A)-C(30A)-C(29A)	122.8(2)
C(10A)-C(11A)-C(12A)	120.1(2)	C(17A)-C(30A)-C(25A)	119.0(2)
C(13A)-C(12A)-C(11A)	120.7(2)	C(29A)-C(30A)-C(25A)	118.1(2)
C(12A)-C(13A)-C(14A)	121.8(2)	C(32A)-C(31A)-C(24A)	126.7(2)

C(1A)-C(14A)-C(13A)	122.0(2)	C(31A)-C(32A)-C(33A)	126.8(2)
C(1A)-C(14A)-C(9A)	120.7(2)	C(34A)-C(33A)-C(38A)	117.2(2)
C(13A)-C(14A)-C(9A)	117.3(2)	C(34A)-C(33A)-C(32A)	121.6(2)
C(16A)-C(15A)-C(8A)	121.1(2)	C(38A)-C(33A)-C(32A)	121.2(2)
C(15A)-C(16A)-C(17A)	130.3(2)	C(35A)-C(34A)-C(33A)	120.6(2)
C(18A)-C(17A)-C(30A)	119.8(2)	C(34A)-C(35A)-C(36A)	122.3(2)
C(18A)-C(17A)-C(16A)	117.5(2)	C(35A)-C(36A)-C(37A)	117.3(2)
C(30A)-C(17A)-C(16A)	122.4(2)	C(35A)-C(36A)-C(39A)	119.1(2)

Bond lengths [Å] and angles [°].

C(37A)-C(36A)-C(39A)	123.6(2)	C(57A)-C(58A)-C(63A)	120.35(19)
C(38A)-C(37A)-C(36A)	120.5(3)	C(59A)-C(58A)-C(63A)	118.2(2)
C(37A)-C(38A)-C(33A)	122.1(2)	C(60A)-C(59A)-C(58A)	121.3(2)
C(40A)-C(39A)-C(36A)	129.6(3)	C(59A)-C(60A)-C(61A)	120.4(2)
C(39A)-C(40A)-C(41A)	123.6(3)	C(62A)-C(61A)-C(60A)	120.4(2)
C(42A)-C(41A)-C(54A)	119.5(2)	C(61A)-C(62A)-C(63A)	121.7(2)
C(42A)-C(41A)-C(40A)	120.6(2)	C(64A)-C(63A)-C(62A)	121.9(2)
C(54A)-C(41A)-C(40A)	119.9(2)	C(64A)-C(63A)-C(58A)	120.0(2)
C(41A)-C(42A)-C(47A)	120.3(2)	C(62A)-C(63A)-C(58A)	118.1(2)
C(41A)-C(42A)-C(43A)	121.6(2)	C(65A)-C(64A)-C(63A)	119.52(19)
C(47A)-C(42A)-C(43A)	118.1(2)	C(65A)-C(64A)-C(71A)	119.74(19)
C(44A)-C(43A)-C(42A)	121.2(3)	C(63A)-C(64A)-C(71A)	120.7(2)
C(43A)-C(44A)-C(45A)	120.9(3)	C(64A)-C(65A)-C(70A)	120.12(19)
C(46A)-C(45A)-C(44A)	120.3(3)	C(64A)-C(65A)-C(66A)	121.8(2)
C(45A)-C(46A)-C(47A)	121.6(2)	C(70A)-C(65A)-C(66A)	118.0(2)
C(48A)-C(47A)-C(46A)	121.7(2)	C(67A)-C(66A)-C(65A)	121.5(2)
C(48A)-C(47A)-C(42A)	120.4(2)	C(66A)-C(67A)-C(68A)	120.4(2)
C(46A)-C(47A)-C(42A)	117.9(2)	C(69A)-C(68A)-C(67A)	120.6(2)
C(49A)-C(48A)-C(47A)	119.1(2)	C(68A)-C(69A)-C(70A)	121.4(2)
C(49A)-C(48A)-C(55A)	120.6(2)	C(57A)-C(70A)-C(65A)	120.4(2)
C(47A)-C(48A)-C(55A)	120.3(2)	C(57A)-C(70A)-C(69A)	121.4(2)
C(48A)-C(49A)-C(50A)	121.3(2)	C(65A)-C(70A)-C(69A)	118.1(2)
C(48A)-C(49A)-C(54A)	120.3(2)	C(72A)-C(71A)-C(64A)	124.5(2)
C(50A)-C(49A)-C(54A)	118.4(2)	C(71A)-C(72A)-C(73A)	127.6(2)
C(51A)-C(50A)-C(49A)	121.5(2)	C(78A)-C(73A)-C(74A)	117.7(2)
C(50A)-C(51A)-C(52A)	120.1(2)	C(78A)-C(73A)-C(72A)	118.8(2)
C(53A)-C(52A)-C(51A)	120.5(2)	C(74A)-C(73A)-C(72A)	123.4(2)
C(52A)-C(53A)-C(54A)	121.9(2)	C(75A)-C(74A)-C(73A)	120.9(2)
C(41A)-C(54A)-C(53A)	122.2(2)	C(74A)-C(75A)-C(76A)	121.7(2)
C(41A)-C(54A)-C(49A)	120.2(2)	C(75A)-C(76A)-C(77A)	117.5(2)
C(53A)-C(54A)-C(49A)	117.7(2)	C(75A)-C(76A)-C(79A)	118.90(19)
C(56A)-C(55A)-C(48A)	127.8(2)	C(77A)-C(76A)-C(79A)	123.6(2)
C(55A)-C(56A)-C(57A)	127.0(2)	C(78A)-C(77A)-C(76A)	120.7(2)
C(58A)-C(57A)-C(70A)	119.2(2)	C(77A)-C(78A)-C(73A)	121.6(2)
C(58A)-C(57A)-C(56A)	120.51(19)	C(80A)-C(79A)-C(76A)	129.6(2)
C(70A)-C(57A)-C(56A)	120.06(19)	C(79A)-C(80A)-C(1A)	128.5(2)
C(57A)-C(58A)-C(59A)	121.4(2)		


Bond lengths [Å] and angles [°].

C(1B)-C(14B)	1.403(3)	C(21B)-C(22B)	1.353(4)
C(1B)-C(2B)	1.422(3)	C(22B)-C(23B)	1.424(4)
C(1B)-C(80B)	1.486(3)	C(23B)-C(24B)	1.419(3)
C(2B)-C(3B)	1.425(3)	C(24B)-C(25B)	1.405(4)
C(2B)-C(7B)	1.439(3)	C(24B)-C(31B)	1.487(3)
C(3B)-C(4B)	1.358(3)	C(25B)-C(26B)	1.430(3)
C(4B)-C(5B)	1.405(4)	C(25B)-C(30B)	1.442(3)
C(5B)-C(6B)	1.346(4)	C(26B)-C(27B)	1.356(4)
C(6B)-C(7B)	1.433(3)	C(27B)-C(28B)	1.419(4)
C(7B)-C(8B)	1.411(3)	C(28B)-C(29B)	1.360(4)
C(8B)-C(9B)	1.426(3)	C(29B)-C(30B)	1.430(4)
C(8B)-C(15B)	1.470(3)	C(31B)-C(32B)	1.325(4)
C(9B)-C(10B)	1.423(3)	C(32B)-C(33B)	1.471(4)
C(9B)-C(14B)	1.440(3)	C(33B)-C(38B)	1.380(4)
C(10B)-C(11B)	1.357(3)	C(33B)-C(34B)	1.397(4)
C(11B)-C(12B)	1.417(3)	C(34B)-C(35B)	1.375(4)
C(12B)-C(13B)	1.353(4)	C(35B)-C(36B)	1.371(4)
C(13B)-C(14B)	1.435(3)	C(36B)-C(37B)	1.370(4)
C(15B)-C(16B)	1.329(4)	C(36B)-C(39B)	1.487(4)

C(16B)-C(17B)	1.474(3)	C(37B)-C(38B)	1.409(4)
C(17B)-C(18B)	1.415(3)	C(39B)-C(40B)	1.301(4)
C(17B)-C(30B)	1.418(3)	C(40B)-C(41B)	1.472(4)
C(18B)-C(23B)	1.432(3)	C(41B)-C(54B)	1.405(4)
C(18B)-C(19B)	1.446(3)	C(41B)-C(42B)	1.410(4)
C(19B)-C(20B)	1.362(4)	C(42B)-C(43B)	1.431(4)
C(20B)-C(21B)	1.402(4)	C(42B)-C(47B)	1.433(3)

Bond lengths [Å] and angles [°].

C(43B)-C(44B)	1.358(4)	C(63B)-C(64B)	1.410(3)
C(44B)-C(45B)	1.403(4)	C(64B)-C(65B)	1.399(3)
C(45B)-C(46B)	1.364(4)	C(64B)-C(71B)	1.488(3)
C(46B)-C(47B)	1.431(3)	C(65B)-C(66B)	1.426(3)
C(47B)-C(48B)	1.410(3)	C(65B)-C(70B)	1.446(3)
C(48B)-C(49B)	1.406(3)	C(66B)-C(67B)	1.358(4)
C(48B)-C(55B)	1.490(3)	C(67B)-C(68B)	1.409(4)
C(49B)-C(50B)	1.431(4)	C(68B)-C(69B)	1.352(4)
C(49B)-C(54B)	1.439(4)	C(69B)-C(70B)	1.425(3)
C(50B)-C(51B)	1.345(4)	C(71B)-C(72B)	1.288(4)
C(51B)-C(52B)	1.409(5)	C(72B)-C(73B)	1.470(3)
C(52B)-C(53B)	1.341(4)	C(73B)-C(78B)	1.388(3)
C(53B)-C(54B)	1.425(4)	C(73B)-C(74B)	1.398(3)
C(55B)-C(56B)	1.328(3)	C(74B)-C(75B)	1.383(3)
C(56B)-C(57B)	1.494(3)	C(75B)-C(76B)	1.394(3)
C(57B)-C(58B)	1.407(3)	C(76B)-C(77B)	1.398(3)
C(57B)-C(70B)	1.410(3)	C(76B)-C(79B)	1.472(3)
C(58B)-C(59B)	1.430(3)	C(77B)-C(78B)	1.383(3)
C(58B)-C(63B)	1.443(3)	C(79B)-C(80B)	1.336(3)
C(59B)-C(60B)	1.352(4)	C(18B)-C(17B)-C(30B)	119.2(2)
C(60B)-C(61B)	1.420(4)	C(18B)-C(17B)-C(16B)	118.4(2)
C(14B)-C(1B)-C(2B)	119.5(2)	C(30B)-C(17B)-C(16B)	122.3(2)
C(14B)-C(1B)-C(80B)	119.9(2)	C(17B)-C(18B)-C(23B)	120.5(2)
C(2B)-C(1B)-C(80B)	120.6(2)	C(17B)-C(18B)-C(19B)	122.3(2)
C(1B)-C(2B)-C(3B)	121.8(2)	C(23B)-C(18B)-C(19B)	117.2(2)
C(1B)-C(2B)-C(7B)	119.5(2)	C(20B)-C(19B)-C(18B)	121.4(2)
C(3B)-C(2B)-C(7B)	118.6(2)	C(19B)-C(20B)-C(21B)	120.3(2)
C(4B)-C(3B)-C(2B)	121.6(2)	C(22B)-C(21B)-C(20B)	120.5(3)
C(3B)-C(4B)-C(5B)	119.8(2)	C(21B)-C(22B)-C(23B)	121.7(2)
C(6B)-C(5B)-C(4B)	120.9(2)	C(24B)-C(23B)-C(22B)	121.8(2)
C(5B)-C(6B)-C(7B)	122.1(2)	C(24B)-C(23B)-C(18B)	119.7(2)
C(8B)-C(7B)-C(6B)	122.7(2)	C(22B)-C(23B)-C(18B)	118.6(2)
C(8B)-C(7B)-C(2B)	120.5(2)	C(25B)-C(24B)-C(23B)	119.7(2)
C(6B)-C(7B)-C(2B)	116.9(2)	C(25B)-C(24B)-C(31B)	119.8(2)
C(7B)-C(8B)-C(9B)	119.4(2)	C(23B)-C(24B)-C(31B)	120.5(2)
C(7B)-C(8B)-C(15B)	118.6(2)	C(24B)-C(25B)-C(26B)	121.4(2)
C(9B)-C(8B)-C(15B)	122.0(2)	C(24B)-C(25B)-C(30B)	120.2(2)
C(10B)-C(9B)-C(8B)	122.8(2)	C(26B)-C(25B)-C(30B)	118.4(2)
C(10B)-C(9B)-C(14B)	118.1(2)	C(27B)-C(26B)-C(25B)	121.5(2)
C(8B)-C(9B)-C(14B)	119.1(2)	C(26B)-C(27B)-C(28B)	120.2(2)
C(11B)-C(10B)-C(9B)	121.8(2)	C(29B)-C(28B)-C(27B)	120.4(3)
C(10B)-C(11B)-C(12B)	120.2(2)	C(28B)-C(29B)-C(30B)	121.6(2)

C(13B)-C(12B)-C(11B)	120.2(2)	C(17B)-C(30B)-C(29B)	122.6(2)
C(12B)-C(13B)-C(14B)	121.7(2)	C(17B)-C(30B)-C(25B)	119.8(2)
C(1B)-C(14B)-C(13B)	121.3(2)	C(29B)-C(30B)-C(25B)	117.6(2)
C(1B)-C(14B)-C(9B)	120.9(2)	C(32B)-C(31B)-C(24B)	127.1(2)
C(13B)-C(14B)-C(9B)	117.8(2)	C(31B)-C(32B)-C(33B)	128.0(2)
C(16B)-C(15B)-C(8B)	126.6(2)	C(38B)-C(33B)-C(34B)	116.4(2)
C(15B)-C(16B)-C(17B)	125.9(2)	C(38B)-C(33B)-C(32B)	120.8(2)
C(61B)-C(62B)	1.344(4)	C(34B)-C(33B)-C(32B)	122.8(2)
C(62B)-C(63B)	1.431(4)	C(35B)-C(34B)-C(33B)	121.9(3)

Bond lengths [Å] and angles [°].

C(36B)-C(35B)-C(34B)	121.6(3)	C(70B)-C(57B)-C(56B)	119.7(2)
C(37B)-C(36B)-C(35B)	117.7(3)	C(57B)-C(58B)-C(59B)	122.0(2)
C(37B)-C(36B)-C(39B)	123.0(3)	C(57B)-C(58B)-C(63B)	120.2(2)
C(35B)-C(36B)-C(39B)	119.2(2)	C(59B)-C(58B)-C(63B)	117.7(2)
C(36B)-C(37B)-C(38B)	121.2(3)	C(60B)-C(59B)-C(58B)	121.7(3)
C(33B)-C(38B)-C(37B)	121.1(3)	C(59B)-C(60B)-C(61B)	120.3(3)
C(40B)-C(39B)-C(36B)	128.3(3)	C(62B)-C(61B)-C(60B)	120.5(3)
C(39B)-C(40B)-C(41B)	125.0(3)	C(61B)-C(62B)-C(63B)	121.6(3)
C(54B)-C(41B)-C(42B)	119.3(2)	C(64B)-C(63B)-C(62B)	121.9(2)
C(54B)-C(41B)-C(40B)	121.1(2)	C(64B)-C(63B)-C(58B)	119.9(2)
C(42B)-C(41B)-C(40B)	119.6(2)	C(62B)-C(63B)-C(58B)	118.2(2)
C(41B)-C(42B)-C(43B)	121.4(2)	C(65B)-C(64B)-C(63B)	120.0(2)
C(41B)-C(42B)-C(47B)	120.5(2)	C(65B)-C(64B)-C(71B)	120.3(2)
C(43B)-C(42B)-C(47B)	118.1(2)	C(63B)-C(64B)-C(71B)	119.7(2)
C(44B)-C(43B)-C(42B)	121.5(3)	C(64B)-C(65B)-C(66B)	122.3(2)
C(43B)-C(44B)-C(45B)	120.6(3)	C(64B)-C(65B)-C(70B)	120.1(2)
C(46B)-C(45B)-C(44B)	120.4(3)	C(66B)-C(65B)-C(70B)	117.7(2)
C(45B)-C(46B)-C(47B)	121.3(2)	C(67B)-C(66B)-C(65B)	122.1(2)
C(48B)-C(47B)-C(46B)	121.5(2)	C(66B)-C(67B)-C(68B)	119.9(2)
C(48B)-C(47B)-C(42B)	120.2(2)	C(69B)-C(68B)-C(67B)	120.7(3)
C(46B)-C(47B)-C(42B)	118.3(2)	C(68B)-C(69B)-C(70B)	121.7(2)
C(49B)-C(48B)-C(47B)	119.2(2)	C(57B)-C(70B)-C(69B)	122.0(2)
C(49B)-C(48B)-C(55B)	120.3(2)	C(57B)-C(70B)-C(65B)	120.0(2)
C(47B)-C(48B)-C(55B)	120.5(2)	C(69B)-C(70B)-C(65B)	117.9(2)
C(48B)-C(49B)-C(50B)	121.5(2)	C(72B)-C(71B)-C(64B)	125.8(2)
C(48B)-C(49B)-C(54B)	120.5(2)	C(71B)-C(72B)-C(73B)	129.8(2)
C(50B)-C(49B)-C(54B)	118.0(2)	C(78B)-C(73B)-C(74B)	117.4(2)
C(51B)-C(50B)-C(49B)	121.5(3)	C(78B)-C(73B)-C(72B)	119.3(2)
C(50B)-C(51B)-C(52B)	120.2(3)	C(74B)-C(73B)-C(72B)	123.3(2)
C(53B)-C(52B)-C(51B)	120.7(3)	C(75B)-C(74B)-C(73B)	121.0(2)
C(52B)-C(53B)-C(54B)	121.8(3)	C(74B)-C(75B)-C(76B)	121.3(2)
C(41B)-C(54B)-C(53B)	122.4(2)	C(75B)-C(76B)-C(77B)	117.7(2)
C(41B)-C(54B)-C(49B)	120.0(2)	C(75B)-C(76B)-C(79B)	119.3(2)
C(53B)-C(54B)-C(49B)	117.6(2)	C(77B)-C(76B)-C(79B)	122.9(2)
C(56B)-C(55B)-C(48B)	126.5(2)	C(78B)-C(77B)-C(76B)	120.6(2)
C(55B)-C(56B)-C(57B)	126.2(2)	C(77B)-C(78B)-C(73B)	121.9(2)
C(58B)-C(57B)-C(70B)	119.5(2)	C(80B)-C(79B)-C(76B)	128.3(2)
C(58B)-C(57B)-C(56B)	120.7(2)	C(79B)-C(80B)-C(1B)	127.4(2)

Bond lengths [Å] and angles [°].

C(1D)-C(2D)	1.350(5)	C(1E)-C(2E)	1.372(5)
C(1D)-C(6D)	1.359(5)	C(1E)-C(6E)	1.379(5)
C(2D)-C(3D)	1.362(5)	C(2E)-C(3E)	1.376(5)
C(3D)-C(4D)	1.372(5)	C(3E)-C(4E)	1.358(5)
C(4D)-C(5D)	1.366(5)	C(4E)-C(5E)	1.373(5)
C(5D)-C(6D)	1.355(6)	C(5E)-C(6E)	1.354(5)
C(2D)-C(1D)-C(6D)	120.7(3)	C(2E)-C(1E)-C(6E)	120.0(3)
C(1D)-C(2D)-C(3D)	120.1(3)	C(1E)-C(2E)-C(3E)	119.2(4)
C(2D)-C(3D)-C(4D)	119.6(3)	C(4E)-C(3E)-C(2E)	120.4(3)
C(5D)-C(4D)-C(3D)	119.6(3)	C(3E)-C(4E)-C(5E)	120.3(4)
C(6D)-C(5D)-C(4D)	120.3(3)	C(6E)-C(5E)-C(4E)	119.9(4)
C(5D)-C(6D)-C(1D)	119.7(3)	C(5E)-C(6E)-C(1E)	120.3(3)
C(1F)-C(6F)	1.363(5)	C(1G)-C(6G)	1.362(5)
C(1F)-C(2F)	1.382(5)	C(1G)-C(2G)	1.367(5)
C(2F)-C(3F)	1.362(6)	C(2G)-C(3G)	1.371(5)
C(3F)-C(4F)	1.361(5)	C(3G)-C(4G)	1.367(5)
C(4F)-C(5F)	1.370(5)	C(4G)-C(5G)	1.365(5)
C(5F)-C(6F)	1.367(5)	C(5G)-C(6G)	1.381(5)
C(6F)-C(1F)-C(2F)	119.2(4)	C(6G)-C(1G)-C(2G)	120.4(3)
C(3F)-C(2F)-C(1F)	120.5(4)	C(1G)-C(2G)-C(3G)	119.6(4)
C(4F)-C(3F)-C(2F)	120.2(4)	C(4G)-C(3G)-C(2G)	120.4(4)
C(3F)-C(4F)-C(5F)	119.6(4)	C(5G)-C(4G)-C(3G)	120.0(3)
C(6F)-C(5F)-C(4F)	120.6(4)	C(4G)-C(5G)-C(6G)	119.6(3)
C(1F)-C(6F)-C(5F)	120.0(4)	C(1G)-C(6G)-C(5G)	120.0(3)
C(1H)-C(2H)	1.340(5)	C(1I)-C(2I)	1.358(5)
C(1H)-C(6H)	1.351(6)	C(1I)-C(6I)	1.363(5)
C(2H)-C(3H)	1.377(5)	C(2I)-C(3I)	1.368(5)
C(3H)-C(4H)	1.359(5)	C(3I)-C(4I)	1.368(5)
C(4H)-C(5H)	1.394(6)	C(4I)-C(5I)	1.367(5)
C(5H)-C(6H)	1.390(6)	C(5I)-C(6I)	1.356(5)
C(2H)-C(1H)-C(6H)	120.5(4)	C(2I)-C(1I)-C(6I)	120.3(3)
C(1H)-C(2H)-C(3H)	120.2(4)	C(1I)-C(2I)-C(3I)	119.8(3)
C(4H)-C(3H)-C(2H)	121.2(4)	C(2I)-C(3I)-C(4I)	119.8(3)
C(3H)-C(4H)-C(5H)	118.5(4)	C(5I)-C(4I)-C(3I)	119.9(3)
C(6H)-C(5H)-C(4H)	119.0(4)	C(6I)-C(5I)-C(4I)	120.0(3)
C(1H)-C(6H)-C(5H)	120.5(4)	C(5I)-C(6I)-C(1I)	120.1(4)
C(1J)-C(6J)	1.347(7)	C(1K)-C(2K)	1.357(6)
C(1J)-C(2J)	1.354(6)	C(1K)-C(6K)	1.364(5)
C(2J)-C(3J)	1.362(6)	C(2K)-C(3K)	1.350(6)
C(3J)-C(4J)	1.357(7)	C(3K)-C(4K)	1.363(5)
C(4J)-C(5J)	1.411(6)	C(4K)-C(5K)	1.347(5)
C(5J)-C(6J)	1.391(6)	C(5K)-C(6K)	1.352(5)
C(6J)-C(1J)-C(2J)	122.0(6)	C(2K)-C(1K)-C(6K)	118.6(4)
C(1J)-C(2J)-C(3J)	118.4(6)	C(3K)-C(2K)-C(1K)	121.2(4)
C(4J)-C(3J)-C(2J)	122.7(5)	C(2K)-C(3K)-C(4K)	119.4(4)
C(3J)-C(4J)-C(5J)	118.4(5)	C(5K)-C(4K)-C(3K)	120.2(4)
C(6J)-C(5J)-C(4J)	118.2(6)	C(4K)-C(5K)-C(6K)	120.1(4)
C(1J)-C(6J)-C(5J)	120.3(5)	C(5K)-C(6K)-C(1K)	120.6(4)

Bond lengths [Å] and angles [°].

C(1L)-C(6L)	1.350(6)	C(1M)-C(6M)	1.366(5)
C(1L)-C(2L)	1.360(5)	C(1M)-C(2M)	1.368(5)
C(2L)-C(3L)	1.345(5)	C(2M)-C(3M)	1.359(5)
C(3L)-C(4L)	1.363(6)	C(3M)-C(4M)	1.365(5)
C(4L)-C(5L)	1.359(6)	C(4M)-C(5M)	1.381(5)
C(5L)-C(6L)	1.346(6)	C(5M)-C(6M)	1.344(5)
C(6L)-C(1L)-C(2L)	120.2(4)	C(6M)-C(1M)-C(2M)	119.9(4)
C(3L)-C(2L)-C(1L)	119.8(4)	C(3M)-C(2M)-C(1M)	120.3(4)
C(2L)-C(3L)-C(4L)	119.9(4)	C(2M)-C(3M)-C(4M)	119.7(4)
C(5L)-C(4L)-C(3L)	119.9(4)	C(3M)-C(4M)-C(5M)	119.7(4)
C(6L)-C(5L)-C(4L)	119.9(4)	C(6M)-C(5M)-C(4M)	120.2(3)
C(5L)-C(6L)-C(1L)	120.2(4)	C(5M)-C(6M)-C(1M)	120.1(4)
C(1N)-C(2N)	1.373(6)	C(1O)-C(6O)	1.318(7)
C(1N)-C(6N)	1.376(6)	C(1O)-C(2O)	1.425(7)
C(2N)-C(3N)	1.378(6)	C(2O)-C(3O)	1.455(7)
C(3N)-C(4N)	1.349(6)	C(3O)-C(4O)	1.360(7)
C(4N)-C(5N)	1.360(6)	C(4O)-C(5O)	1.290(7)
C(5N)-C(6N)	1.372(6)	C(5O)-C(6O)	1.284(6)
C(2N)-C(1N)-C(6N)	119.9(4)	C(6O)-C(1O)-C(2O)	121.4(5)
C(1N)-C(2N)-C(3N)	119.6(5)	C(1O)-C(2O)-C(3O)	113.9(5)
C(4N)-C(3N)-C(2N)	119.8(5)	C(4O)-C(3O)-C(2O)	117.3(5)
C(3N)-C(4N)-C(5N)	121.3(4)	C(5O)-C(4O)-C(3O)	123.7(5)
C(4N)-C(5N)-C(6N)	119.6(5)	C(6O)-C(5O)-C(4O)	121.2(6)
C(5N)-C(6N)-C(1N)	119.8(5)	C(5O)-C(6O)-C(1O)	122.4(6)
C(1P)-C(6P)	1.346(6)	C(1Q)-C(6Q)	1.358(5)
C(1P)-C(2P)	1.351(5)	C(1Q)-C(2Q)	1.368(5)
C(2P)-C(3P)	1.352(5)	C(2Q)-C(3Q)	1.374(5)
C(3P)-C(4P)	1.356(5)	C(3Q)-C(4Q)	1.374(5)
C(4P)-C(5P)	1.364(6)	C(4Q)-C(5Q)	1.359(5)
C(5P)-C(6P)	1.346(6)	C(5Q)-C(6Q)	1.360(5)
C(6P)-C(1P)-C(2P)	120.0(4)	C(6Q)-C(1Q)-C(2Q)	120.1(3)
C(1P)-C(2P)-C(3P)	120.1(3)	C(1Q)-C(2Q)-C(3Q)	119.3(4)
C(2P)-C(3P)-C(4P)	120.1(3)	C(4Q)-C(3Q)-C(2Q)	119.6(3)
C(3P)-C(4P)-C(5P)	119.4(4)	C(5Q)-C(4Q)-C(3Q)	120.8(3)
C(6P)-C(5P)-C(4P)	120.0(4)	C(4Q)-C(5Q)-C(6Q)	119.0(4)
C(5P)-C(6P)-C(1P)	120.5(4)	C(1Q)-C(6Q)-C(5Q)	121.2(4)
C(1R)-C(2R)	1.368(5)	C(3R)-C(4R)	1.375(5)
C(1R)-C(6R)	1.378(4)	C(4R)-C(5R)	1.366(5)
C(2R)-C(3R)	1.366(5)	C(5R)-C(6R)	1.374(5)
C(2R)-C(1R)-C(6R)	120.1(3)	C(5R)-C(4R)-C(3R)	120.2(3)
C(3R)-C(2R)-C(1R)	120.2(3)	C(4R)-C(5R)-C(6R)	120.0(3)
C(2R)-C(3R)-C(4R)	119.8(3)	C(5R)-C(6R)-C(1R)	119.6(3)

Bond lengths [Å] and angles [°].

C(1S)-C(6S)	1.326(8)	C(1S1)-C(2S1)	1.347(13)
C(1S)-C(2S)	1.392(9)	C(1S1)-C(6S1)	1.373(13)
C(2S)-C(3S)	1.416(8)	C(2S1)-C(3S1)	1.370(13)
C(3S)-C(4S)	1.380(10)	C(3S1)-C(4S1)	1.376(13)
C(4S)-C(5S)	1.350(8)	C(4S1)-C(5S1)	1.355(13)
C(5S)-C(6S)	1.365(7)	C(5S1)-C(6S1)	1.351(13)
C(6S)-C(1S)-C(2S)	122.5(5)	C(2S1)-C(1S1)-C(6S1)	116.3(13)
C(1S)-C(2S)-C(3S)	116.8(5)	C(1S1)-C(2S1)-C(3S1)	120.2(13)
C(4S)-C(3S)-C(2S)	119.5(5)	C(2S1)-C(3S1)-C(4S1)	121.5(14)
C(5S)-C(4S)-C(3S)	120.2(5)	C(5S1)-C(4S1)-C(3S1)	117.6(13)
C(4S)-C(5S)-C(6S)	120.9(5)	C(6S1)-C(5S1)-C(4S1)	119.8(13)
C(1S)-C(6S)-C(5S)	120.0(5)	C(5S1)-C(6S1)-C(1S1)	122.9(15)
C(1T)-C(6T)	1.360(12)	C(1T1)-C(2T1)	1.353(12)
C(1T)-C(2T)	1.363(12)	C(1T1)-C(6T1)	1.364(12)
C(2T)-C(3T)	1.370(12)	C(2T1)-C(3T1)	1.371(12)
C(3T)-C(4T)	1.391(11)	C(3T1)-C(4T1)	1.358(12)
C(4T)-C(5T)	1.397(10)	C(4T1)-C(5T1)	1.364(11)
C(5T)-C(6T)	1.355(12)	C(5T1)-C(6T1)	1.366(11)
C(6T)-C(1T)-C(2T)	121.2(12)	C(2T1)-C(1T1)-C(6T1)	121.9(12)
C(1T)-C(2T)-C(3T)	120.6(11)	C(1T1)-C(2T1)-C(3T1)	118.6(11)
C(2T)-C(3T)-C(4T)	117.9(11)	C(4T1)-C(3T1)-C(2T1)	120.2(11)
C(3T)-C(4T)-C(5T)	121.2(11)	C(3T1)-C(4T1)-C(5T1)	120.5(11)
C(6T)-C(5T)-C(4T)	118.5(11)	C(4T1)-C(5T1)-C(6T1)	119.6(10)
C(5T)-C(6T)-C(1T)	120.6(12)	C(1T1)-C(6T1)-C(5T1)	119.0(11)
C(1U)-C(6U)	1.360(9)	C(1U1)-C(6U1)	1.363(12)
C(1U)-C(2U)	1.370(13)	C(1U1)-C(2U1)	1.367(13)
C(2U)-C(3U)	1.366(12)	C(2U1)-C(3U1)	1.365(11)
C(5U)-C(4U)	1.371(11)	C(3U1)-C(4U1)	1.363(12)
C(5U)-C(6U)	1.373(9)	C(4U1)-C(5U1)	1.371(13)
C(3U)-C(4U)	1.371(11)	C(5U1)-C(6U1)	1.385(15)
C(6U)-C(1U)-C(2U)	118.9(9)	C(6U1)-C(1U1)-C(2U1)	120.5(9)
C(3U)-C(2U)-C(1U)	120.2(12)	C(3U1)-C(2U1)-C(1U1)	119.1(11)
C(4U)-C(5U)-C(6U)	120.3(8)	C(4U1)-C(3U1)-C(2U1)	122.2(11)
C(2U)-C(3U)-C(4U)	121.0(10)	C(3U1)-C(4U1)-C(5U1)	117.4(14)
C(3U)-C(4U)-C(5U)	118.0(9)	C(4U1)-C(5U1)-C(6U1)	121.2(12)
C(1U)-C(6U)-C(5U)	120.8(7)	C(1U1)-C(6U1)-C(5U1)	118.9(9)

Anisotropic displacement parameters ($\text{\AA}^2 \times 10^3$). The anisotropic displacement factor exponent takes the form: $-2\pi^2 [h^2 a^{*2} U_{11} + \dots + 2 h k a^* b^* U_{12}]$

	U_{11}	U_{22}	U_{33}	U_{23}	U_{13}	U_{12}
C(1)	32(1)	41(1)	50(2)	18(1)	2(1)	3(1)
C(2)	34(1)	56(2)	53(2)	28(1)	-3(1)	3(1)
C(3)	40(1)	68(2)	53(2)	27(2)	3(1)	6(1)
C(4)	49(2)	99(3)	56(2)	36(2)	1(1)	7(2)
C(5)	60(2)	143(4)	73(2)	72(3)	-8(2)	-3(2)
C(6)	72(2)	108(3)	96(3)	74(3)	-24(2)	-13(2)
C(7)	47(2)	70(2)	75(2)	48(2)	-14(1)	-2(1)
C(8)	60(2)	56(2)	105(3)	47(2)	-27(2)	-3(2)
C(9)	49(2)	45(2)	76(2)	25(2)	-15(1)	6(1)
C(10)	61(2)	33(2)	120(3)	17(2)	-11(2)	11(1)
C(11)	78(2)	59(2)	77(2)	4(2)	1(2)	16(2)
C(12)	69(2)	58(2)	64(2)	7(2)	7(2)	19(2)
C(13)	49(2)	51(2)	52(2)	16(2)	4(1)	13(1)
C(14)	36(1)	41(2)	62(2)	19(1)	-2(1)	7(1)
C(15)	46(2)	56(3)	74(3)	40(2)	13(2)	15(2)
C(16)	26(2)	92(4)	115(4)	82(4)	2(2)	6(3)
C(17)	66(2)	75(2)	73(2)	54(2)	15(2)	6(2)
C(18)	69(2)	61(2)	48(2)	33(2)	16(1)	20(2)
C(19)	94(3)	79(2)	55(2)	39(2)	20(2)	36(2)
C(20)	93(3)	104(3)	45(2)	24(2)	2(2)	50(2)
C(21)	76(2)	92(3)	57(2)	19(2)	-1(2)	26(2)
C(22)	63(2)	65(2)	52(2)	14(2)	10(1)	18(2)
C(23)	58(2)	50(2)	41(1)	17(1)	18(1)	20(1)
C(24)	56(2)	43(2)	43(1)	20(1)	18(1)	18(1)
C(25)	52(2)	53(2)	41(1)	25(1)	17(1)	16(1)
C(26)	63(2)	65(2)	48(2)	30(2)	19(1)	22(2)
C(27)	64(2)	95(3)	56(2)	37(2)	9(2)	28(2)
C(28)	56(2)	109(3)	97(3)	54(2)	8(2)	3(2)
C(29)	66(2)	110(3)	101(3)	75(3)	2(2)	-6(2)
C(30)	54(2)	70(2)	62(2)	39(2)	14(1)	5(1)
C(31)	63(2)	41(2)	72(2)	29(2)	21(2)	19(1)
C(32)	65(2)	43(2)	90(2)	37(2)	31(2)	17(1)
C(33)	64(2)	46(2)	81(2)	36(2)	32(2)	16(1)
C(34)	56(2)	46(2)	54(2)	25(1)	16(1)	12(1)
C(35)	59(2)	38(1)	55(2)	18(1)	14(1)	8(1)
C(36)	54(2)	41(2)	70(2)	25(1)	25(1)	11(1)
C(37)	56(2)	44(2)	172(4)	39(2)	41(2)	10(2)
C(38)	63(2)	41(2)	184(4)	40(2)	49(2)	9(2)
C(39)	53(2)	38(2)	70(2)	21(1)	21(1)	6(1)
C(40)	56(2)	37(1)	62(2)	18(1)	17(1)	7(1)
C(41)	45(1)	39(1)	53(2)	18(1)	14(1)	1(1)
C(42)	43(1)	47(2)	48(2)	16(1)	11(1)	2(1)
C(43)	57(2)	56(2)	51(2)	8(2)	8(1)	6(1)
C(44)	61(2)	82(2)	46(2)	7(2)	3(1)	10(2)
C(45)	55(2)	89(2)	50(2)	21(2)	0(1)	12(2)
C(46)	45(2)	69(2)	50(2)	22(2)	4(1)	12(1)
C(47)	36(1)	50(2)	49(2)	19(1)	11(1)	6(1)
C(48)	35(1)	46(1)	46(1)	21(1)	12(1)	6(1)
C(49)	41(1)	43(1)	47(1)	23(1)	14(1)	7(1)
C(50)	59(2)	50(2)	48(2)	25(1)	22(1)	18(1)

C(51)	78(2)	60(2)	46(2)	28(2)	18(1)	23(2)
-------	-------	-------	-------	-------	-------	-------

Anisotropic displacement parameters ($\text{\AA}^2 \times 10^3$). The anisotropic

displacement factor exponent takes the form: $-2\pi^2 [h^2 a^{*2} U_{11} + \dots + 2 h k a^* b^*$

$U_{12}]$

	U_{11}	U_{22}	U_{33}	U_{23}	U_{13}	U_{12}
C(52)	73(2)	64(2)	52(2)	35(2)	14(1)	22(2)
C(53)	59(2)	47(2)	57(2)	28(1)	16(1)	19(1)
C(54)	43(1)	40(1)	49(2)	21(1)	14(1)	5(1)
C(55)	39(1)	57(2)	45(1)	25(1)	13(1)	13(1)
C(56)	40(1)	50(2)	41(1)	19(1)	11(1)	17(1)
C(57)	39(1)	34(1)	38(1)	11(1)	7(1)	12(1)
C(58)	43(1)	30(1)	41(1)	11(1)	2(1)	9(1)
C(59)	53(2)	42(1)	48(2)	19(1)	1(1)	7(1)
C(60)	70(2)	50(2)	52(2)	23(1)	-12(1)	6(1)
C(61)	53(2)	46(2)	68(2)	21(2)	-19(1)	2(1)
C(62)	41(1)	41(2)	61(2)	16(1)	-5(1)	4(1)
C(63)	39(1)	30(1)	49(1)	12(1)	1(1)	9(1)
C(64)	39(1)	31(1)	47(1)	11(1)	6(1)	8(1)
C(65)	41(1)	36(1)	38(1)	10(1)	7(1)	6(1)
C(66)	50(2)	51(2)	44(1)	18(1)	9(1)	3(1)
C(67)	60(2)	65(2)	46(2)	28(1)	1(1)	2(1)
C(68)	49(2)	71(2)	51(2)	29(2)	-5(1)	5(1)
C(69)	38(1)	57(2)	50(2)	25(1)	3(1)	5(1)
C(70)	40(1)	39(1)	38(1)	13(1)	6(1)	9(1)
C(71)	44(2)	40(2)	62(2)	18(1)	10(1)	3(1)
C(72)	47(2)	37(1)	61(2)	20(1)	13(1)	7(1)
C(73)	39(1)	40(1)	49(1)	19(1)	5(1)	3(1)
C(74)	45(1)	38(1)	50(2)	14(1)	7(1)	10(1)
C(75)	42(1)	35(1)	53(2)	17(1)	5(1)	4(1)
C(76)	38(1)	38(1)	43(1)	18(1)	2(1)	6(1)
C(77)	39(1)	37(1)	50(1)	16(1)	5(1)	8(1)
C(78)	43(1)	36(1)	57(2)	17(1)	9(1)	4(1)
C(79)	43(1)	40(1)	47(1)	21(1)	5(1)	5(1)
C(80)	40(1)	42(1)	46(1)	18(1)	7(1)	2(1)
C(1A)	26(1)	35(1)	41(1)	19(1)	5(1)	3(1)
C(2A)	25(1)	39(1)	42(1)	20(1)	3(1)	4(1)
C(3A)	33(1)	39(1)	46(1)	19(1)	3(1)	5(1)
C(4A)	42(1)	50(2)	39(1)	17(1)	6(1)	7(1)
C(5A)	44(1)	63(2)	43(2)	29(2)	8(1)	10(1)
C(6A)	43(1)	52(2)	50(2)	32(2)	7(1)	8(1)
C(7A)	29(1)	43(1)	44(1)	24(1)	6(1)	6(1)
C(8A)	34(1)	39(1)	50(2)	24(1)	5(1)	6(1)
C(9A)	30(1)	37(1)	44(1)	18(1)	3(1)	5(1)
C(10A)	48(1)	32(1)	54(2)	16(1)	7(1)	8(1)
C(11A)	59(2)	44(2)	44(2)	14(1)	10(1)	10(1)
C(12A)	59(2)	48(2)	42(1)	19(1)	11(1)	11(1)

C(13A)	40(1)	42(1)	45(1)	23(1)	6(1)	6(1)
C(14A)	27(1)	34(1)	43(1)	17(1)	3(1)	3(1)
C(15A)	45(1)	40(1)	55(2)	27(1)	10(1)	10(1)
C(16A)	47(2)	48(2)	57(2)	31(1)	10(1)	12(1)
C(17A)	43(1)	41(1)	46(1)	25(1)	11(1)	8(1)
C(18A)	44(1)	42(1)	39(1)	20(1)	14(1)	12(1)
C(19A)	52(2)	56(2)	46(1)	29(1)	10(1)	15(1)
C(20A)	59(2)	68(2)	44(2)	27(2)	6(1)	20(2)
C(21A)	47(2)	68(2)	46(2)	21(2)	2(1)	8(1)
C(22A)	49(2)	45(2)	41(1)	13(1)	11(1)	6(1)

Anisotropic displacement parameters ($\text{\AA}^2 \times 10^3$). The anisotropic

displacement factor exponent takes the form: $-2\pi^2 [h^2 a^{*2} U_{11} + \dots + 2 h k a^* b^*$

$U_{12}]$

	U_{11}	U_{22}	U_{33}	U_{23}	U_{13}	U_{12}
C(23A)	40(1)	39(1)	38(1)	16(1)	13(1)	11(1)
C(24A)	42(1)	32(1)	40(1)	15(1)	15(1)	11(1)
C(25A)	45(1)	39(1)	37(1)	19(1)	15(1)	13(1)
C(26A)	56(2)	50(2)	43(1)	28(1)	15(1)	16(1)
C(27A)	54(2)	66(2)	51(2)	33(2)	5(1)	15(1)
C(28A)	49(2)	64(2)	57(2)	28(2)	-1(1)	5(1)
C(29A)	47(2)	51(2)	55(2)	27(1)	7(1)	5(1)
C(30A)	43(1)	43(1)	40(1)	21(1)	10(1)	8(1)
C(31A)	52(2)	36(1)	54(2)	23(1)	14(1)	12(1)
C(32A)	55(2)	35(1)	56(2)	25(1)	16(1)	8(1)
C(33A)	49(2)	38(1)	47(1)	22(1)	16(1)	6(1)
C(34A)	47(1)	40(2)	53(2)	16(1)	12(1)	6(1)
C(35A)	53(2)	34(1)	59(2)	11(1)	14(1)	6(1)
C(36A)	50(2)	37(1)	56(2)	19(1)	17(1)	9(1)
C(37A)	46(2)	43(2)	76(2)	24(2)	14(1)	4(1)
C(38A)	55(2)	34(1)	70(2)	20(1)	16(1)	2(1)
C(39A)	55(2)	34(1)	69(2)	17(1)	16(1)	5(1)
C(40A)	56(2)	34(1)	55(2)	13(1)	15(1)	9(1)
C(41A)	47(1)	31(1)	48(2)	13(1)	15(1)	3(1)
C(42A)	42(1)	37(1)	44(1)	15(1)	9(1)	0(1)
C(43A)	56(2)	43(2)	46(2)	7(1)	9(1)	3(1)
C(44A)	58(2)	65(2)	40(2)	13(1)	0(1)	1(1)
C(45A)	48(2)	66(2)	47(2)	22(2)	1(1)	4(1)
C(46A)	35(1)	54(2)	45(2)	20(1)	4(1)	5(1)
C(47A)	31(1)	40(1)	46(1)	17(1)	8(1)	0(1)
C(48A)	31(1)	36(1)	43(1)	17(1)	12(1)	3(1)
C(49A)	40(1)	36(1)	43(1)	18(1)	13(1)	6(1)
C(50A)	53(2)	38(1)	45(1)	18(1)	19(1)	15(1)
C(51A)	73(2)	47(2)	44(2)	22(1)	19(1)	20(1)
C(52A)	84(2)	55(2)	53(2)	33(2)	19(2)	26(2)
C(53A)	70(2)	42(2)	56(2)	28(1)	23(1)	22(1)
C(54A)	47(1)	35(1)	47(1)	19(1)	14(1)	7(1)
C(55A)	32(1)	47(2)	42(1)	22(1)	10(1)	9(1)
C(56A)	33(1)	41(1)	39(1)	18(1)	9(1)	11(1)

C(57A)	34(1)	32(1)	34(1)	13(1)	7(1)	9(1)
C(58A)	36(1)	29(1)	34(1)	12(1)	6(1)	8(1)
C(59A)	46(1)	39(1)	37(1)	16(1)	7(1)	9(1)
C(60A)	53(2)	48(2)	37(1)	19(1)	1(1)	12(1)
C(61A)	40(1)	51(2)	41(1)	16(1)	-4(1)	8(1)
C(62A)	33(1)	43(1)	43(1)	15(1)	2(1)	6(1)
C(63A)	35(1)	29(1)	37(1)	10(1)	6(1)	8(1)
C(64A)	33(1)	31(1)	35(1)	11(1)	7(1)	6(1)
C(65A)	36(1)	35(1)	34(1)	13(1)	6(1)	4(1)
C(66A)	44(1)	51(2)	41(1)	25(1)	6(1)	3(1)
C(67A)	52(2)	63(2)	46(1)	32(1)	-1(1)	4(1)
C(68A)	40(1)	62(2)	52(2)	31(1)	-4(1)	5(1)
C(69A)	33(1)	51(2)	48(1)	26(1)	2(1)	5(1)
C(70A)	36(1)	34(1)	35(1)	12(1)	7(1)	8(1)
C(71A)	37(1)	38(1)	42(1)	18(1)	5(1)	2(1)
C(72A)	36(1)	37(1)	46(1)	19(1)	7(1)	4(1)
C(73A)	32(1)	38(1)	37(1)	16(1)	4(1)	3(1)

Anisotropic displacement parameters ($\text{\AA}^2 \times 10^3$). The anisotropic

displacement factor exponent takes the form: $-2\pi^2 [h^2 a^{*2} U_{11} + \dots + 2 h k a^* b^*$

$U_{12}]$

	U_{11}	U_{22}	U_{33}	U_{23}	U_{13}	U_{12}
C(74A)	36(1)	33(1)	44(1)	13(1)	6(1)	8(1)
C(75A)	34(1)	30(1)	46(1)	17(1)	4(1)	1(1)
C(76A)	30(1)	33(1)	37(1)	18(1)	2(1)	3(1)
C(77A)	34(1)	32(1)	45(1)	14(1)	6(1)	7(1)
C(78A)	34(1)	32(1)	50(1)	19(1)	6(1)	2(1)
C(79A)	36(1)	32(1)	42(1)	19(1)	5(1)	2(1)
C(80A)	33(1)	35(1)	43(1)	20(1)	7(1)	1(1)
C(1B)	27(1)	34(1)	43(1)	17(1)	2(1)	2(1)
C(2B)	27(1)	41(1)	40(1)	18(1)	3(1)	5(1)
C(3B)	38(1)	38(1)	44(1)	15(1)	1(1)	5(1)
C(4B)	46(1)	48(2)	41(1)	11(1)	3(1)	7(1)
C(5B)	57(2)	57(2)	38(1)	20(1)	8(1)	12(1)
C(6B)	50(2)	50(2)	45(2)	25(1)	8(1)	10(1)
C(7B)	32(1)	39(1)	39(1)	18(1)	2(1)	6(1)
C(8B)	35(1)	40(1)	39(1)	19(1)	2(1)	6(1)
C(9B)	30(1)	36(1)	40(1)	17(1)	2(1)	5(1)
C(10B)	38(1)	36(1)	43(1)	18(1)	5(1)	7(1)
C(11B)	47(1)	39(1)	42(1)	15(1)	10(1)	8(1)
C(12B)	52(2)	48(2)	38(1)	20(1)	11(1)	9(1)
C(13B)	40(1)	43(2)	45(1)	24(1)	3(1)	5(1)
C(14B)	27(1)	37(1)	40(1)	19(1)	4(1)	4(1)
C(15B)	43(1)	43(2)	41(1)	21(1)	4(1)	10(1)
C(16B)	47(1)	45(2)	42(1)	24(1)	9(1)	9(1)
C(17B)	46(1)	35(1)	35(1)	17(1)	11(1)	12(1)
C(18B)	46(1)	37(1)	36(1)	16(1)	12(1)	11(1)
C(19B)	52(2)	41(1)	41(1)	21(1)	9(1)	14(1)
C(20B)	50(2)	54(2)	47(2)	21(1)	3(1)	11(1)

C(21B)	49(2)	53(2)	55(2)	21(1)	-2(1)	0(1)
C(22B)	51(2)	40(1)	51(2)	19(1)	10(1)	4(1)
C(23B)	48(1)	33(1)	40(1)	15(1)	16(1)	14(1)
C(24B)	49(2)	35(1)	42(1)	19(1)	17(1)	15(1)
C(25B)	47(1)	38(1)	39(1)	19(1)	15(1)	18(1)
C(26B)	55(2)	49(2)	46(1)	27(1)	16(1)	19(1)
C(27B)	58(2)	68(2)	51(2)	33(2)	7(1)	23(1)
C(28B)	48(2)	57(2)	57(2)	26(2)	5(1)	13(1)
C(29B)	46(2)	46(2)	51(2)	24(1)	11(1)	12(1)
C(30B)	45(1)	38(1)	36(1)	17(1)	14(1)	13(1)
C(31B)	55(2)	38(1)	56(2)	26(1)	18(1)	16(1)
C(32B)	57(2)	37(1)	58(2)	27(1)	15(1)	8(1)
C(33B)	51(2)	42(2)	46(1)	23(1)	16(1)	10(1)
C(34B)	54(2)	43(2)	64(2)	24(1)	23(1)	10(1)
C(35B)	63(2)	44(2)	66(2)	25(1)	27(1)	13(1)
C(36B)	60(2)	45(2)	55(2)	21(1)	11(1)	12(1)
C(37B)	42(2)	66(2)	101(2)	34(2)	16(2)	7(1)
C(38B)	55(2)	45(2)	92(2)	24(2)	23(2)	3(1)
C(39B)	66(2)	43(2)	65(2)	23(1)	17(2)	7(1)
C(40B)	57(2)	46(2)	52(2)	15(1)	9(1)	13(1)
C(41B)	45(1)	40(1)	48(2)	19(1)	8(1)	6(1)
C(42B)	41(1)	42(1)	45(1)	16(1)	9(1)	2(1)
C(43B)	56(2)	51(2)	47(2)	12(1)	7(1)	9(1)
C(44B)	60(2)	68(2)	41(2)	12(2)	1(1)	6(2)

Anisotropic displacement parameters ($\text{\AA}^2 \times 10^3$). The anisotropic

displacement factor exponent takes the form: $-2\pi^2 [h^2 a^{*2} U_{11} + \dots + 2 h k a^* b^*$

$U_{12}]$

	U_{11}	U_{22}	U_{33}	U_{23}	U_{13}	U_{12}
C(45B)	45(2)	75(2)	50(2)	25(2)	-5(1)	4(1)
C(46B)	37(1)	58(2)	53(2)	26(1)	3(1)	5(1)
C(47B)	33(1)	42(1)	46(1)	19(1)	8(1)	1(1)
C(48B)	35(1)	43(1)	47(2)	24(1)	12(1)	5(1)
C(49B)	52(2)	44(2)	45(1)	23(1)	15(1)	12(1)
C(50B)	79(2)	59(2)	48(2)	28(2)	25(1)	30(2)
C(51B)	130(3)	82(2)	41(2)	29(2)	25(2)	59(2)
C(52B)	140(3)	90(3)	50(2)	36(2)	16(2)	64(2)
C(53B)	89(2)	57(2)	50(2)	26(2)	15(2)	35(2)
C(54B)	53(2)	42(1)	45(2)	21(1)	12(1)	11(1)
C(55B)	34(1)	55(2)	51(2)	28(1)	15(1)	12(1)
C(56B)	38(1)	48(2)	44(1)	23(1)	13(1)	15(1)
C(57B)	34(1)	38(1)	41(1)	16(1)	8(1)	10(1)
C(58B)	40(1)	37(1)	44(1)	17(1)	5(1)	9(1)
C(59B)	54(2)	57(2)	48(2)	26(1)	3(1)	8(1)
C(60B)	65(2)	76(2)	59(2)	36(2)	-9(2)	7(2)
C(61B)	53(2)	71(2)	71(2)	30(2)	-16(2)	4(2)
C(62B)	40(2)	59(2)	65(2)	28(2)	-4(1)	5(1)
C(63B)	35(1)	37(1)	54(2)	19(1)	3(1)	7(1)
C(64B)	38(1)	35(1)	46(1)	14(1)	9(1)	5(1)

C(65B)	39(1)	36(1)	40(1)	14(1)	6(1)	2(1)
C(66B)	53(2)	56(2)	49(2)	27(1)	9(1)	-3(1)
C(67B)	63(2)	74(2)	56(2)	40(2)	-5(1)	-9(2)
C(68B)	48(2)	85(2)	66(2)	47(2)	-10(1)	-9(2)
C(69B)	38(1)	63(2)	54(2)	33(1)	0(1)	0(1)
C(70B)	36(1)	37(1)	40(1)	15(1)	7(1)	6(1)
C(71B)	44(2)	38(1)	68(2)	19(1)	13(1)	2(1)
C(72B)	44(1)	38(1)	57(2)	22(1)	13(1)	4(1)
C(73B)	36(1)	40(1)	45(1)	21(1)	5(1)	4(1)
C(74B)	41(1)	37(1)	45(1)	16(1)	8(1)	10(1)
C(75B)	38(1)	35(1)	51(1)	22(1)	5(1)	3(1)
C(76B)	33(1)	36(1)	41(1)	20(1)	0(1)	4(1)
C(77B)	35(1)	35(1)	48(1)	16(1)	5(1)	5(1)
C(78B)	40(1)	36(1)	54(2)	22(1)	5(1)	2(1)
C(79B)	38(1)	36(1)	47(1)	22(1)	5(1)	2(1)
C(80B)	37(1)	35(1)	45(1)	20(1)	8(1)	3(1)
C(1D)	87(3)	47(2)	94(3)	28(2)	33(2)	18(2)
C(2D)	53(2)	66(2)	111(3)	51(2)	-11(2)	1(2)
C(3D)	99(3)	57(2)	68(2)	35(2)	4(2)	3(2)
C(4D)	61(2)	76(2)	134(4)	66(3)	34(2)	18(2)
C(5D)	70(2)	80(3)	139(4)	67(3)	-37(3)	-22(2)
C(6D)	135(4)	48(2)	68(2)	19(2)	-14(2)	-21(2)
C(1E)	44(2)	85(3)	83(2)	20(2)	0(2)	-2(2)
C(2E)	47(2)	95(3)	118(3)	60(3)	1(2)	-4(2)
C(3E)	56(2)	59(2)	138(4)	33(3)	12(2)	-3(2)
C(4E)	48(2)	82(3)	89(2)	14(2)	9(2)	-6(2)
C(5E)	51(2)	79(3)	92(3)	35(2)	0(2)	-2(2)
C(6E)	53(2)	60(2)	102(3)	27(2)	-8(2)	5(2)
C(1F)	57(2)	94(3)	94(3)	33(3)	8(2)	-1(2)
C(2F)	68(2)	86(3)	88(3)	-1(2)	27(2)	-11(2)
C(3F)	83(3)	67(3)	129(4)	27(3)	22(3)	-7(2)
C(4F)	60(2)	89(3)	107(3)	36(3)	7(2)	-8(2)

Anisotropic displacement parameters ($\text{\AA}^2 \times 10^3$). The anisotropic

displacement factor exponent takes the form: $-2\pi^2 [h^2 a^{*2} U_{11} + \dots + 2 h k a^* b^*$

$U_{12}]$

	U_{11}	U_{22}	U_{33}	U_{23}	U_{13}	U_{12}
C(5F)	50(2)	87(3)	79(2)	10(2)	0(2)	3(2)
C(6F)	63(2)	71(2)	95(3)	12(2)	-2(2)	8(2)
C(1G)	68(2)	62(2)	106(3)	35(2)	20(2)	7(2)
C(2G)	91(3)	78(2)	82(2)	32(2)	17(2)	3(2)
C(3G)	83(3)	105(3)	82(3)	41(2)	-6(2)	-13(2)
C(4G)	66(2)	105(3)	88(3)	45(2)	5(2)	-3(2)
C(5G)	86(3)	77(2)	79(2)	35(2)	15(2)	9(2)
C(6G)	79(2)	61(2)	89(3)	31(2)	-6(2)	1(2)
C(1H)	102(3)	82(3)	111(3)	41(3)	-14(3)	17(2)
C(2H)	101(3)	82(3)	89(3)	34(2)	1(2)	31(2)
C(3H)	93(3)	78(2)	96(3)	39(2)	4(2)	34(2)
C(4H)	129(4)	81(3)	93(3)	54(2)	11(3)	32(2)

C(5H)	134(4)	87(3)	141(4)	71(3)	62(3)	35(3)
C(6H)	76(3)	96(3)	161(5)	74(3)	1(3)	11(2)
C(1I)	86(3)	75(2)	112(3)	51(2)	18(2)	28(2)
C(2I)	84(2)	86(3)	94(3)	57(2)	3(2)	7(2)
C(3I)	77(2)	84(3)	75(2)	28(2)	8(2)	4(2)
C(4I)	75(2)	69(2)	105(3)	41(2)	5(2)	18(2)
C(5I)	95(3)	97(3)	100(3)	63(3)	19(2)	33(2)
C(6I)	106(3)	101(3)	89(3)	49(3)	31(2)	42(2)
C(1J)	187(6)	71(3)	94(4)	26(3)	-23(4)	1(3)
C(2J)	167(5)	79(3)	100(3)	38(3)	-14(3)	-36(3)
C(3J)	157(5)	123(4)	86(3)	50(3)	-19(4)	-62(4)
C(4J)	156(5)	84(3)	103(4)	33(3)	-18(3)	-54(3)
C(5J)	197(6)	53(2)	139(5)	47(3)	7(4)	-31(3)
C(6J)	180(5)	61(3)	86(3)	21(2)	-34(4)	-22(3)
C(1K)	122(4)	152(4)	86(3)	62(3)	-16(3)	-34(3)
C(2K)	178(5)	169(5)	55(2)	51(3)	-1(3)	-44(4)
C(3K)	142(4)	126(4)	79(3)	39(3)	34(3)	-4(3)
C(4K)	109(3)	59(2)	93(3)	39(2)	10(2)	9(2)
C(5K)	107(3)	81(2)	61(2)	33(2)	3(2)	-16(2)
C(6K)	113(3)	140(4)	62(2)	46(3)	5(2)	-26(3)
C(1L)	84(3)	87(3)	125(4)	63(3)	38(3)	30(2)
C(2L)	108(3)	73(2)	81(2)	38(2)	7(2)	10(2)
C(3L)	64(2)	92(3)	143(4)	69(3)	-4(3)	4(2)
C(4L)	104(3)	70(3)	131(4)	43(3)	55(3)	32(2)
C(5L)	140(4)	61(2)	84(3)	19(2)	-1(3)	-25(3)
C(6L)	77(3)	101(3)	135(4)	69(3)	-21(3)	-25(2)
C(1M)	106(3)	86(3)	78(2)	29(2)	13(2)	-12(2)
C(2M)	116(3)	92(3)	96(3)	58(2)	38(3)	8(2)
C(3M)	123(3)	80(3)	87(3)	55(2)	32(3)	32(2)
C(4M)	97(3)	52(2)	100(3)	28(2)	19(2)	20(2)
C(5M)	116(3)	71(2)	74(2)	30(2)	33(2)	-4(2)
C(6M)	124(4)	103(3)	58(2)	31(2)	15(2)	-21(3)
C(1N)	53(2)	124(4)	93(3)	0(3)	-8(2)	1(2)
C(2N)	55(2)	131(4)	120(4)	44(4)	3(2)	-16(2)
C(3N)	70(3)	92(3)	140(5)	17(4)	15(3)	-16(2)
C(4N)	59(2)	110(4)	98(3)	-5(3)	21(2)	-12(2)
C(5N)	51(2)	136(4)	106(3)	33(3)	-2(2)	-7(2)
C(6N)	62(2)	100(3)	133(4)	17(3)	-17(3)	9(2)
C(1O)	175(5)	59(3)	82(3)	16(2)	0(4)	-25(3)
C(2O)	149(5)	37(2)	215(7)	51(3)	73(5)	-1(3)

Anisotropic displacement parameters ($\text{\AA}^2 \times 10^3$). The anisotropic

displacement factor exponent takes the form: $-2\pi^2 [h^2 a^{*2} U_{11} + \dots + 2 h k a^* b^*$

$U_{12}]$

	U_{11}	U_{22}	U_{33}	U_{23}	U_{13}	U_{12}
C(3O)	115(4)	105(4)	173(6)	68(4)	-39(4)	-50(3)
C(4O)	145(5)	145(5)	84(3)	43(3)	-12(4)	-65(5)
C(5O)	161(6)	98(4)	126(5)	24(4)	12(4)	-51(4)
C(6O)	158(5)	71(3)	123(4)	37(3)	-1(4)	2(3)

C(1P)	86(3)	62(2)	110(3)	30(2)	37(3)	11(2)
C(2P)	59(2)	79(2)	118(3)	58(3)	-13(2)	-3(2)
C(3P)	106(3)	62(2)	67(2)	33(2)	9(2)	5(2)
C(4P)	65(2)	108(3)	133(4)	77(3)	33(2)	24(2)
C(5P)	75(3)	148(4)	130(4)	92(4)	-39(3)	-40(3)
C(6P)	139(4)	84(3)	70(2)	18(2)	4(3)	-40(3)
C(1Q)	64(2)	124(3)	75(2)	49(2)	1(2)	-12(2)
C(2Q)	90(3)	84(2)	74(2)	41(2)	5(2)	-13(2)
C(3Q)	88(3)	68(2)	108(3)	48(2)	-24(2)	-24(2)
C(4Q)	67(2)	74(3)	127(4)	38(3)	22(2)	3(2)
C(5Q)	101(3)	86(3)	92(3)	19(2)	29(2)	-20(2)
C(6Q)	96(3)	125(4)	69(2)	37(2)	-3(2)	-34(3)
C(1R)	70(2)	57(2)	88(2)	36(2)	-14(2)	-11(2)
C(2R)	57(2)	59(2)	99(3)	39(2)	12(2)	3(2)
C(3R)	81(2)	64(2)	80(2)	32(2)	9(2)	-2(2)
C(4R)	77(2)	89(3)	84(2)	43(2)	-14(2)	-20(2)
C(5R)	64(2)	112(3)	84(3)	54(2)	-3(2)	-16(2)
C(6R)	79(2)	81(2)	72(2)	38(2)	3(2)	-2(2)
C(1S)	85(5)	111(5)	51(3)	22(3)	25(4)	0(5)
C(2S)	92(4)	53(3)	79(4)	30(3)	7(4)	-8(3)
C(3S)	114(6)	48(3)	74(4)	23(3)	46(4)	14(3)
C(4S)	107(7)	64(4)	44(3)	14(2)	12(3)	-5(5)
C(5S)	102(4)	86(4)	59(3)	26(3)	4(3)	-8(3)
C(6S)	83(4)	119(5)	52(3)	23(3)	14(3)	-11(4)
C(1T)	121(9)	50(7)	86(10)	29(9)	29(8)	-10(6)
C(2T)	92(7)	82(7)	74(9)	11(8)	22(6)	-24(5)
C(3T)	56(5)	87(9)	69(6)	5(5)	-1(4)	-34(6)
C(4T)	112(8)	77(7)	45(5)	-4(5)	-7(5)	-24(6)
C(5T)	115(8)	37(5)	50(5)	-8(4)	-1(5)	-3(5)
C(6T)	120(9)	26(7)	77(7)	7(4)	5(6)	8(5)
C(1T1)	136(11)	62(12)	78(9)	43(7)	-18(8)	-11(7)
C(2T1)	109(8)	63(10)	126(13)	34(11)	0(10)	-21(7)
C(3T1)	135(13)	75(8)	88(10)	25(7)	38(9)	-40(9)
C(4T1)	139(11)	78(6)	50(6)	16(6)	-3(7)	-47(7)
C(5T1)	85(6)	65(6)	94(7)	42(6)	-7(5)	-27(5)
C(6T1)	109(8)	43(6)	65(6)	25(6)	18(6)	-6(5)
C(1U)	78(6)	96(7)	88(6)	55(6)	-7(5)	8(5)
C(2U)	78(9)	121(15)	90(9)	42(9)	-14(7)	15(9)
C(5U)	88(6)	101(8)	81(5)	46(6)	24(5)	40(6)
C(3U)	89(6)	67(5)	131(10)	43(6)	-20(6)	0(5)
C(4U)	99(8)	98(11)	95(9)	75(9)	29(8)	52(9)
C(6U)	71(5)	75(5)	115(7)	49(5)	8(4)	18(4)
C(1U1)	82(6)	80(6)	94(6)	40(5)	-14(5)	3(5)
C(2U1)	79(10)	71(7)	80(8)	30(6)	11(7)	25(7)
C(3U1)	85(6)	92(6)	85(6)	47(5)	-3(5)	28(5)
C(4U1)	152(17)	91(10)	117(12)	53(8)	-39(11)	1(10)
C(5U1)	150(13)	89(8)	119(8)	72(7)	19(8)	6(8)
C(6U1)	70(5)	103(6)	119(7)	67(6)	4(5)	13(4)

Hydrogen coordinates ($\times 10^4$) and isotropic displacement parameters ($\text{\AA}^2 \times 10^3$).

	x	y	z	U(eq)
H(3)	6987	10211	1153	64
H(4)	6889	10199	1883	81
H(5)	6882	9424	1934	100
H(6)	6968	8679	1262	99
H(10)	7486	7769	-513	93
H(11)	7659	7804	-1226	97
H(12)	7576	8569	-1268	85
H(13)	7311	9292	-611	63
H(15)	7582	7799	206	65
H(16)	5897	8024	505	77
H(15')	6403	8230	813	57
H(16')	7271	7631	192	140
H(19)	5030	7512	-98	85
H(20)	3710	7101	-428	99
H(21)	3235	6381	-347	95
H(22)	4029	6109	111	76
H(26)	6653	6299	1156	67
H(27)	8043	6650	1427	84
H(28)	8630	7301	1252	101
H(29)	7823	7606	829	99
H(31)	5482	5792	632	68
H(32)	4258	5802	983	75
H(34)	4732	7100	1381	61
H(35)	3768	7731	1618	62
H(37)	1747	6685	1131	112
H(38)	2707	6057	912	118
H(39)	2350	8031	1715	65
H(40)	914	7349	1361	63
H(43)	434	7595	761	72
H(44)	-331	7785	229	85
H(45)	-1114	8517	501	82
H(46)	-1123	9051	1304	67
H(50)	-241	9449	2995	60
H(51)	640	9310	3521	70
H(52)	1573	8642	3241	70
H(53)	1569	8101	2443	62
H(55)	-1343	9445	2367	55
H(56)	-1023	10134	2290	52
H(59)	556	10058	2843	57
H(60)	1879	10201	3253	68
H(61)	3168	10334	2914	69
H(62)	3116	10353	2185	60
H(66)	1341	10349	821	59
H(67)	-2	10317	472	67
H(68)	-1269	10099	768	68
H(69)	-1187	9941	1428	58
H(71)	2659	10664	1415	60
H(72)	2987	9680	1167	58
H(74)	4048	10841	1251	55
H(75)	5337	10905	899	53
H(77)	5403	9384	278	52

H(78)	4122	9321	633	55
-------	------	------	-----	----

Hydrogen coordinates ($\times 10^4$) and isotropic displacement parameters ($\text{\AA}^2 \times 10^3$).

	x	y	z	U(eq)
H(79)	6423	10512	306	51
H(80)	7495	10023	104	51
H(3A)	10312	3589	4471	47
H(4A)	10205	3552	5190	54
H(5A)	10280	2771	5224	57
H(6A)	10473	2048	4548	54
H(10A)	11012	1191	2799	55
H(11A)	11235	1243	2091	61
H(12A)	11115	2014	2050	59
H(13A)	10782	2724	2711	49
H(15A)	11018	1194	3541	53
H(16A)	9398	1489	3890	56
H(19A)	8505	951	3226	58
H(20A)	7226	521	2838	67
H(21A)	6736	-224	2886	66
H(22A)	7475	-495	3367	57
H(26A)	10007	-272	4490	56
H(27A)	11356	103	4815	64
H(28A)	11949	785	4686	67
H(29A)	11177	1081	4234	59
H(31A)	8906	-789	3937	55
H(32A)	7622	-842	4212	56
H(34A)	7982	467	4661	57
H(35A)	6957	1065	4883	62
H(37A)	5028	-32	4277	67
H(38A)	6052	-634	4066	65
H(39A)	5519	1321	4951	65
H(40A)	4149	633	4483	61
H(43A)	3822	992	3916	63
H(44A)	3218	1289	3421	69
H(45A)	2464	2029	3733	65
H(46A)	2328	2473	4543	54
H(50A)	2889	2650	6196	53
H(51A)	3473	2349	6697	64
H(52A)	4274	1622	6384	71
H(53A)	4470	1203	5579	63
H(55A)	1963	2759	5605	47
H(56A)	2314	3461	5566	44
H(59A)	3904	3235	6045	48
H(60A)	5230	3326	6435	55
H(61A)	6514	3525	6133	55
H(62A)	6454	3639	5451	49
H(66A)	4683	3768	4146	52
H(67A)	3340	3777	3817	61
H(68A)	2065	3573	4117	59

H(69A)	2140	3363	4744	51
H(71A)	5963	3999	4669	47
H(72A)	6413	3049	4526	48
H(74A)	7378	4203	4553	46
H(75A)	8653	4278	4198	44
H(77A)	8807	2761	3608	45
H(78A)	7540	2689	3974	46

Hydrogen coordinates ($\times 10^4$) and isotropic displacement parameters ($\text{\AA}^2 \times 10^3$).

	x	y	z	U(eq)
H(79A)	9764	3904	3627	43
H(80A)	10862	3441	3428	43
H(3B)	6495	3107	2112	50
H(4B)	6601	3092	1370	58
H(5B)	6654	3853	1295	61
H(6B)	6561	4608	1948	55
H(10B)	5784	5537	3673	46
H(11B)	5528	5527	4393	52
H(12B)	5736	4792	4497	54
H(13B)	6116	4068	3867	49
H(15B)	6236	5275	2528	49
H(16B)	7006	5730	3441	51
H(19B)	8384	5956	3554	52
H(20B)	9705	6392	3867	60
H(21B)	10133	7106	3753	65
H(22B)	9309	7329	3265	57
H(26B)	6660	7035	2203	56
H(27B)	5255	6696	1978	67
H(28B)	4625	6157	2286	63
H(29B)	5441	5921	2771	55
H(31B)	7823	7580	2708	56
H(32B)	9020	7559	2346	58
H(34B)	8632	6271	2096	63
H(35B)	9614	5654	1848	68
H(37B)	11571	6696	2087	84
H(38B)	10573	7325	2306	79
H(39B)	11037	5363	1652	69
H(40B)	12429	6064	1999	64
H(43B)	12841	5795	2613	65
H(44B)	13606	5609	3149	73
H(45B)	14488	4920	2880	69
H(46B)	14573	4408	2073	59
H(50B)	13830	4058	383	71
H(51B)	13053	4237	-150	98
H(52B)	12036	4861	121	107
H(53B)	11871	5331	917	76
H(55B)	14863	4052	1021	53
H(56B)	14561	3342	1065	50
H(59B)	12975	3430	504	62

H(60B)	11670	3279	84	77
H(61B)	10370	3119	403	79
H(62B)	10405	3078	1118	66
H(66B)	12137	3066	2486	61
H(67B)	13467	3109	2853	73
H(68B)	14748	3323	2561	75
H(69B)	14685	3505	1919	59
H(71B)	10824	2737	1848	62
H(72B)	10536	3737	2185	55
H(74B)	9473	2550	2038	50
H(75B)	8185	2464	2378	49
H(77B)	8063	3985	3017	48
H(78B)	9356	4068	2681	51

Hydrogen coordinates ($\times 10^4$) and isotropic displacement parameters ($\text{\AA}^2 \times 10^3$).

	x	y	z	U(eq)
H(79B)	7090	2850	2986	46
H(80B)	5988	3320	3165	46
H(1D)	2215	4563	5241	91
H(2D)	2389	4800	6048	87
H(3D)	1192	4987	6521	87
H(4D)	-192	4913	6172	99
H(5D)	-352	4676	5358	109
H(6D)	852	4512	4895	105
H(1E)	1663	6902	4840	92
H(2E)	1717	6032	4569	99
H(3E)	1746	5513	3750	106
H(4E)	1716	5857	3213	99
H(5E)	1673	6725	3485	91
H(6E)	1641	7244	4294	90
H(1F)	8344	3291	75	102
H(2F)	8434	2423	-188	114
H(3F)	8575	2095	359	119
H(4F)	8626	2625	1171	107
H(5F)	8548	3489	1434	98
H(6F)	8415	3822	890	103
H(1G)	7990	1069	676	95
H(2G)	8997	1600	1271	102
H(3G)	10366	1789	1066	109
H(4G)	10726	1452	272	103
H(5G)	9707	939	-326	96
H(6G)	8337	739	-119	93
H(1H)	2572	7486	2492	119
H(2H)	3967	7246	2463	110
H(3H)	4687	7305	3149	105
H(4H)	3996	7583	3866	113
H(5H)	2531	7793	3885	134
H(6H)	1817	7702	3177	125

H(1I)	5892	1481	6533	104
H(2I)	6344	1047	5762	99
H(3I)	7015	295	5545	98
H(4I)	7261	-5	6109	98
H(5I)	6823	441	6884	107
H(6I)	6141	1182	7094	113
H(1J)	-1248	4576	1756	146
H(2J)	-1161	5145	2553	141
H(3J)	163	5328	2973	149
H(4J)	1399	4951	2618	144
H(5J)	1318	4393	1783	155
H(6J)	-42	4218	1364	138
H(1K)	4787	1918	7950	142
H(2K)	3684	1929	8447	163
H(3K)	2272	1682	8148	142
H(4K)	1951	1422	7340	102
H(5K)	3036	1424	6844	100
H(6K)	4447	1672	7145	127
H(1L)	6926	1658	439	109
H(2L)	5554	1595	96	102

Hydrogen coordinates ($\times 10^4$) and isotropic displacement parameters ($\text{\AA}^2 \times 10^3$).

	x	y	z	U(eq)
H(3L)	4385	1862	574	112
H(4L)	4581	2171	1396	120
H(5L)	5945	2195	1733	121
H(6L)	7113	1942	1253	120
H(1M)	8411	1420	5280	112
H(2M)	8679	1359	5987	113
H(3M)	10064	1548	6346	107
H(4M)	11204	1754	5971	101
H(5M)	10923	1829	5266	106
H(6M)	9533	1678	4934	117
H(1N)	4892	-217	1858	129
H(2N)	4931	654	2113	129
H(3N)	5032	1197	2931	137
H(4N)	5151	873	3476	129
H(5N)	5113	13	3232	127
H(6N)	4989	-538	2418	133
H(1O)	3208	9136	2030	134
H(2O)	1812	9088	1644	162
H(3O)	1737	8587	765	158
H(4O)	2964	8194	411	157
H(5O)	4185	8257	822	168
H(6O)	4325	8738	1603	144
H(1P)	9066	1233	1953	106
H(2P)	9134	1600	2777	97
H(3P)	7878	1814	3191	92

H(4P)	6545	1652	2779	111
H(5P)	6488	1296	1949	130
H(6P)	7746	1088	1543	126
H(1Q)	2788	1990	2968	104
H(2Q)	3779	2519	3577	97
H(3Q)	5206	2649	3393	103
H(4Q)	5607	2264	2602	110
H(5Q)	4621	1727	2003	121
H(6Q)	3223	1584	2194	121
H(1R)	1608	4146	3207	85
H(2R)	1250	4453	4001	84
H(3R)	2234	4994	4604	90
H(4R)	3587	5225	4412	99
H(5R)	3958	4908	3619	100
H(6R)	2967	4370	3012	91
H(1S)	6705	4733	223	105
H(2S)	5419	4785	632	89
H(3S)	5519	5228	1488	95
H(4S)	6884	5535	1879	91
H(5S)	8106	5442	1445	102
H(6S)	8004	5064	618	108
H(1S1)	6103	4862	351	95
H(2S1)	5381	5125	1065	87
H(3S1)	6202	5489	1779	94
H(4S1)	7687	5368	1797	109
H(5S1)	8334	4926	1073	140
H(6S1)	7503	4599	374	161

Hydrogen coordinates ($\times 10^4$) and isotropic displacement parameters ($\text{\AA}^2 \times 10^3$).

	x	y	z	U(eq)
H(1T)	4689	-2371	5156	104
H(2T)	4759	-1880	5972	110
H(3T)	3556	-1457	6357	100
H(4T)	2268	-1560	5897	109
H(5T)	2185	-2099	5071	93
H(6T)	3418	-2486	4710	95
H(1T1)	3158	-2224	4784	107
H(2T1)	2360	-1816	5448	124
H(3T1)	2965	-1641	6201	126
H(4T1)	4388	-1813	6280	114
H(5T1)	5147	-2273	5605	96
H(6T1)	4565	-2429	4854	86
H(1U)	235	5540	849	99
H(2U)	-253	6343	1072	117
H(5U)	410	5369	-501	103
H(3U)	-416	6648	509	116
H(4U)	-309	6109	-303	100
H(6U)	582	5062	63	101
H(1U1)	830	5932	925	102

H(2U1)	-595	6168	974	93
H(3U1)	-1317	6135	304	101
H(4U1)	-681	5821	-432	142
H(5U1)	815	5720	-442	131
H(6U1)	1552	5719	221	109

6. References

- [1] A. Javey, H. Kin, M. Brink, Q. Wang, P. Mceuen, H. Dai, *Nature Materials*. **2002**, *1*, 241.
- [2] J. Kong, N. R. Franklin, C. Zhou, M. G. Chapline, S. P. Peng, K. Cho, H. Dail, *Science*. **2000**, *286*, 622.
- [3] I. S. Nandhakumar, T. J. Gordon-smith, G. S. Attard, D. C. Smith, *Small*. **2005**, *1*, 405.
- [4] S. Lagorsse, F. D. Magalhães, A. Mendes, *Journal of Membrane Science*. **2007**, *301*, 29.
- [5] W. B. Choi, D. S. Chung, Y. W. Jin, J. M. Kim, *Appl. Phys. Lett.* **1999**, *75*, 3129.
- [6] G. Che, B. B. Lakshmi, C. R. Martin, E. R. Fisher, *Chem. Mater.* **1998**, *10*, 260.
- [7] J. I. Sohn, C. Nam, S. Lee, *Applied Surface Science*. **2002**, *197-198*, 568.
- [8] A. Roch, O. Jost, B. Schultrich, E. Beer, *Phys. Stat. Sol.* **2007**, *(b) 244*, 3907.
- [9] R. Faust, *Angew. Chem. Int. Ed. Engl.* **1998**, *37*, 2825.
- [10] S. A. M. Ludwig, *Toward [O_n] Paracyclophanes as Templates for the Synthesis of Nanotubes*, Fribourg University. **2007**.
- [11] H. W. Kroto, J. R. Heath, S. C. O'Brien, F. R. Curl, R. E. Smalley, *Nature*. **1985**, *318*, 162.
- [12] S. Iijima, *Nature*. **1991**, *354*, 56.
- [13] L.T. Scott, *Angew. Chem. Int. Ed.Engl.* **2003**, *42*, 4133.
- [14] F. Diederich, *J. Am. Chem. Soc.* **1990**, *112*, 4966.
- [15] Y. Tobe, *Angew. Chem. Int. Ed.Engl.* **1996**, *35*, 1800.
- [16] J. F. Stoddart, *J. Am. Chem. Soc.* **1992**, *114*, 6330.
- [17] F. Vögtle, *Chem. Ber.* **1993**, *126*, 1723.
- [18] M. M. Haley, *Chem. Commun.* **1997**, 1121.
- [19] M. Iyoda, *Tetrahedron Lett.* **2004**, *45*, 359.
- [20] H. D. Becker, K. Sandros, L. Hansen, *J. Org. Chem.* **1981**, *46*, 821.
- [21] T. Kawase, H. R. Darabi, M. Oda, *Angew. Chem. Int. Ed. Engl.* **1996**, *35*, 2664.
- [22] S. Kammermeier, P. G. Jones, R. Herges, *Angew. Chem. Int. Ed. Engl.* **1996**, *35*, 2669.
- [23] B. Esser, F. Rominger, R. Gleiter, *J. Am. Chem. Soc.* **2008**, *130*, 6716.
- [24] R. H. Friend, R. W. Gmer, A. B. Holmes, J. H. Burroughes, R. H. Marks, C. Taliani, D. D. C. Bradley, D. A. D. Santos, J. L. Bredas, M. Lögdlund, W. R. Salaneck, *Nature*. **1999**, *397*, 121.
- [25] H. Sirringhaus, P. L. Brown, R. H. Friend, M. M. Nielsen, K. Bechgaard, D. M. De leeuw, *Nature*. **1999**, *401*, 685.

- [26] L. Schmidt-mende, A. Fechtenkötter, K. Müllen, E. Moons, R. H. Friend, J. D. Mackenzie, *Science*. **2001**, *293*, 1119.
- [27] T. Kawase, H. Kurata, *Chem. Rev.* **2006**, *106*, 5250.
- [28] R. Herges, *Modern Cyclophane Chemistry*, R. Gleiter, H. Hopf. **2005**, 337.
- [29] F. Vögtle, *Top. Curr. Chem.* **1983**, *115*, 157.
- [30] A. Schröder, H. B. Meikelburger, F. Vögtle, *Top. Curr. Chem.* **1994**, *172*, 179.
- [31] X. Lu, Z. Chen, *Chem. Rev.* **2005**, *105*, 3643.
- [32] P. R. Ashton, G. R. Brown, N. S. Isaacs, J. P. Mathias, D. J. Williams, *J. Am. Chem. Soc.* **1992**, *114*, 6330.
- [33] P. R. Ashton, U. Girreser, F. H. Kohnke, F. M. Raymo, J. F. Stoddart, D. J. Williams, *J. Am. Chem. Soc.* **1993**, *115*, 5422.
- [34] M. Iyoda, Y. Kuwatani, T. Yamauchi, M. Oda, *Chem. Commun.* **1988**, 65.
- [35] D. L. Mohler, K. P. C. Vollhardt, S. Wolff, *Angew. Chem.* **1990**, *102*, 1200.
- [36] Y. Kuwatani, T. Yoshida, A. Kusaka, M. Iyoda, *Tetrahedron Lett.* **2000**, *41*, 359.
- [37] T. Yoshida, Y. Kuwatani, K. Hara, M. Yosida, M. Iyoda, S. Nagase, *Tetrahedron Lett.* **2001**, *42*, 53.
- [38] S. Kammermeier, P. G. Jones, R. Herges, *Angew. Chem. Int. Ed. Engl.* **1997**, *36*, 2200.
- [39] T. Kawase, M. Oda, *Pure Appl. Chem.* **2006**, *78*, 831.
- [40] T. Kawase, *SYNLETT*. **2007**, *17*, 2609.
- [41] H. Heier, *Angew. Chem. Int. Ed. Engl.* **1992**, *31*, 1399.
- [42] B. Thulin, O. Wennerström, I. Somfai, B. Chmielarz, *Acta. Chem. Scand.* **1977**, *B 31*, 135.
- [43] D. Tanner, B. Thulin, O. Wennerström, *Acta. Chem. Scand. B.* **1979**, *33*, 443.
- [44] B. Thulin, O. Wennerström, I. Somfai, *Acta. Chem. Scand. B.* **1978**, *32*, 109.
- [45] T. Mukaiyama, T. Sato, *Chem. Lett.* **1973**, 1041.
- [46] S. Tyrlic, I. Wolochwicz, *Bull. Soc. Chim. Fr.* **1973**, 2147.
- [47] J. E. McMurry, M. P. Fleming, *J. Am. Chem. Soc.* **1989**, *89*, 1513.
- [48] J. E. McMurry, *Chem. Rev.* **1989**, *89*, 1513.
- [49] D. Tanner, O. Wennerström, U. Norinder, *Tetrahedron.* **1986**, *42*, 4499.
- [50] T. Kawase, N. Ueda, K. Tanaka, Y. Seirai, M. Oda, *Tetrahedron Letters.* **2001**, *42*, 5509.
- [51] H. R. Darabi, T. Kawase, M. Oda, *Tetrahedron Letters.* **1995**, *36*, 9525.

- [52] H. Meier, E. Voigt, *Tetrahedron*. **1972**, 28, 187; H. Meier, N. Hanold, T. Molz, H. J. Bissinger, H. Kolshorn, J. Zountsas, *Tetrahedron*. **1986**, 42, 1711.
- [53] P. J. Stang, *Chem. Rev.*, **1978**, 78, 383-405; P. J. Stang, *Acc. Chem. Res.* **1982**, 15, 348; A. P. Marchand, K. C. V. Ramanaiah, S. G. Bott, J. C. Gilbert, S. Kirschner, *Tetrahedron Letters*. **1996**, 45, 8101.
- [54] D. Y. Curtin, W. H. Richardson, *J. Am. Chem. Soc.* **1959**, 81, 4719.
- [55] A. Krebs, W. Cholcha, M. Müller, T. Eicher, H. Pielartzik, H. Schnöckel, *Tetrahedron Lett.* **1984**, 25, 5027.
- [56] H. Meier, E. Voigt, *Tetrahedron*. **1972**, 28, 187; H. Meier, N. Hanold, T. Molz, H. J. Bissinger, H. Kolshorn, J. Zountsas, *Tetrahedron*. **1986**, 42, 1711.
- [57] O. M. Behr, G. Hglinton, I. A. Lardy, R. A. Raphael, *J. Chem. Soc.* **1964**, 1151.
- [58] J. Zhang, D. J. Pesak, J. L. Ludwick, J. S. Moore, *J. Am. Chem. Soc.* **1994**, 116, 4227.
- [59] H. N. C. Henry, P. J. Garratt, F. Sondheimer, *J. Am. Chem. Soc.* **1974**, 96, 5604.
- [60] R. Destro, T. Pilati, M. Simonetta, *J. Am. Chem. Soc.* **1975**, 97, 658.
- [61] D. Tanner, O. Wennerström, *Acta. Chem. Scand. B.* **1983**, 37, 693.
- [62] U. Norinder, D. Tanner, O. Wennerström, *Tetrahedron Letters*. **1983**, 24, 5411.
- [63] S. Nakatsuli, K. Matsuda, Y. Uesugi, K. Nakashima, S. Akiyama, G. Katzer, G. Fabian, *Chem. Soc. PERKIN TRANS.* **1991**, 2, 861.
- [64] M. J. Cravey, D. J. Doss, *J. Org. Chem.* **1988**, 53, 5963.
- [65] D. H. Wadsworth, B. A. Donatelli, *Synthesis Communications*. **1981**, 285.
- [66] H. D. Becker, K. Sandros, L. Hansen, *J. Org. Chem.* **1981**, 46, 821.
- [67] H. D. Becker, K. Sandros. *J. Org. Chem.* **1987**, 52, 5205.
- [68] G. A. O. Ohannesian, M. Arranaghi, *Chem. Rev.* **1987**, 87, 671.
- [69] I. Raston, O. Wennerström, *Acta., Chem. Scand. B.* **1983**, 36, 655.
- [70] W. Hai-zeng, *Huaxue Shiji*. **2003**, 25, 309.
- [71] H. Kashida, T. Takatsu, H. Asanuma, *Tetrahedron Letters*. **2007**, 48, 6759.
- [72] J. McMurry, *Chem. Rev.* **1989**, 89, 1513.
- [73] M. S. Khan, M. R. A. Al-Mandhary, S. Al-Saadi, P. R. Raithby, A. Köhler, S. J. Teat, *J. Mater. Chem.* **1994**, 4, 299.
- [74] S. Toyota, M. Goichi, M. Kotani, *Angew. Chem. Int. Ed. Engl.* **2004**, 116, 2298.
- [75] S. Toyota, S. Suzuki, M. Goichi, *J. Chem. Eur.* **2006**, 12, 2482.

- [76] D. Zhao, J. S. Moore, *Chem. Commun.* **2003**, 807.
- [77] M. M. Haley, J. J. Pak, S. C. Brand, *Top. Curr. Chem.* **1999**, 201, 81.
- [78] J. K. Young, J. S. Moore, *Modern Acetylen Chemistry* (EDS. P. J. Stang, F. Diederich), VCH, Weinheim. **1995**, chap. 12.
- [79] J. M. Kehoe, J. H. Kiely, J. J. English, C. A. Johnson, R. C. Petersen, M. M. Haley, *Org. Lett.* **2000**, 2, 969.
- [80] J. G. Rodriguez, J. L. Tejedor, *J. Org. Chem.* **2002**, 67, 7631.
- [81] J. M. Cary, J. S. Moore, *J. Org. Chem.* **2002**, 4, 4663.
- [82] T. C. Bedard, J. S. Moore, *J. Am. Chem. Soc.* **1995**, 117, 10662.
- [83] T. Kawase, Y. Seirai, H. R. Darabi, M. Oda, Y. Sarakai, K. Tashiro, *Angew. Chem. Int. Ed. Engl.* **2003**, 42, 1621.
- [84] J. Kim, D. T. McQuade, A. Rose, Z. Zhu, T. M. Swager, *J. Am. Chem. Soc.* **2001**, 123, 11488.
- [85] P. Nguyen, S. Todd, D. Van den Biggelaar, N. J. Taylor, T. B. Marder, F. Wittmann, R. H. Friend, *Synlett.* **1994**, 299.
- [86] M. S. Khan, M. R. A. Al-Mandhary, S. Al-Saadi, P. R. Raithby, A. Köhler, S. J. Teat, *Dalton Trans.* **2004**, 2377.
- [87] D. P. Lydon, L. Porres, A. Beeby, T. B. Marder, P. J. Low, *New J. Chem.* **2005**, 29, 972.
- [88] W. Ried, W. Donner, W. Schlegelmich, *Chem. Ber.* **1961**, 94, 1051.
- [89] M. Sundahl, O. Wennerström, *Tetrahedron Letters.* **1989**, 30, 1429.
- [90] J. H. Geiger, K. Mislow, *J. Org. Chem.* **1986**, 51, 5472.
- [91] K. Müllen, H. Unterberg, W. Huber, O. Wennerström, U. Norinder, D. Tanner, B. Thulin, *J. Am. Chem. Soc.* **1984**, 106, 7514.
- [92] K. Wolinski, J. F. Hilton, P. J. Pulay, *J. Am. Chem. Soc.* **1990**, 112, 8251.
- [93] H. R. Darabi, K. Jadidi, A. R. Mohebbi, L. Faraji, K. Aghapoor, S. Shahbazian, M. Azimzadeh, S. M. Nasser, *Supramolecular Chemistry.* **2008**, 20, 327.
- [94] E. Heilbronner, *Tetrahedron Lett.* **1964**, 29, 1923-1928.
- [95] D. Ajami, O. Oeckler, A. Simon, R. Herges, *Nature* **2003**, 426, 819-821.
- [96] M. Stepien, L. Latos-Grazynski, N. Sprutta, P. Chwalisz, L. Szterenber, *Angew. Chem. Int. Ed. Engl.* **2007**, 46, 7869-7873.
- [97] a) J. Sankar, S. Mori, S. Saito, H. Rath, M. Suzuki, A. Osuka, *J. Am. Chem. Soc.* **2008**, 130, 13568-13579; Y. Tanaka, S. Saito, S. Mori, A. Osuka, *Angew. Chem. Int. Ed. Engl.* **2008**, 47, 2543-

- 2546; J. K. Park, Z. S. Yoon, M. C. Yoon, K. S. Kim, S. Mori, A. osuka. *J. Am. Chem. Soc.* **2008**, *130*, 1824-1825.
- [98] R. Herges, *Chem. Rev.* **2006**, *106*, 4820-4842.
- [99] R. Herges, D. Geuenich, *J. Phys. Chem. A.* **2001**, *105*, 3214.
- [100] D. Geuenich, K. Hess, F. Köhler, R. Herges, *Chem. Rev.* **2005**, *105*, 3758.
- [101] P. V. R. Schleyer, C. Maerker, A. Dransfeld, H. Jiao, N. J. Hommes, *J. Am. Chem. Soc.* **1996**, *118*, 6317.
- [102] For more information, see chapter one.
- [103] D. J. Cram, *Nature.* **1992**, *356*, 29.
- [104] M. Baure, M. Nieger, F. Vögtle, *Chem. Ber.* **1992**, *125*, 2533.
- [105] H. R. Darabi, dissertation, department of chemistry, faculty of science, Osaka University, Japan, **1997**.
- [106] T. Kawase, N. Ueda, H. R. Darabi, M. Oda, *Angew. Chem. Int. Ed. Engl.* **1996**, *108*, 1658.
- [107] C. Glueck, V. Poignee, H. Schwager, *Synthesis.* **1987**, *3*, 260.
- [108] O. Cakmak, I. Demirtas, H. T. Balaydin, *Tetrahedron.* **2002**, *58*, 5603.
- [109] O. Cakmak, R. Erenler, A. Tutar, N. Celik, *J. Org. Chem.* **2006**, *71*, 1795.
- [110] S. Duan, J. Turk, J. Speigle, J. Corbin, J. Masnovi, R. J. Baker, *J. Org. Chem.* **2000**, *56*, 3005.
- [111] M. S. Khan, M. R. A. Al-Mandhary, M. K. Al-Suti, *Dalton Trans.* **2004**, 2377.

Lebenslauf

Persönliche Daten

Name: Ali Reza Mohebbi
Geburtsdatum: 12. 10. 1975, Amol, Iran

Schulbildung

1982-1987 Grundschole Amol, Iran
1987-1990 Orientierungsstufe, Amol, Iran
1990-1994 Gymnasium, Amol, Iran

Hochschulstudium

1995-1999 B.Sc. (Chemie)
Isfahan University, Isfahan, Iran

2000-2002 M.Sc. (Organische Chemie)
Chemistry and Chemical Engineering Research
Center of Iran, Tehran, Iran
Betreuer: Dr. H.R.Darabi and M.S.Abaee

2002-2005 Chemistry & Chemical Engineering Research Center of
Iran (CCERCI), P.O.Box: 14335-186, Tehran, Iran
Research Associate. (Organic Chemistry)

Seit Feb. 2005 Promotionsarbeit an Otto-Diels-Institut für Organische
Chemie Christian-Albrecht-Universität zu Kiel in der
arbeitsgruppe von Prof. Dr. Rainer Herges